Mag.rer.nat. Peter Leitner

Impact of Energy and Momentum Conservation on Fluid Resonances in the Kinetic Modelling of the Interaction of Resonant Magnetic Perturbations with a Tokamak Plasma

DOCTORAL THESIS

For obtaining the academic degree of

Doktor der Naturwissenschaften

Doctoral Programme of Natural Sciences
Technical Physics

Graz University of Technology

Supervisor:

Ao.Univ.-Prof. Dipl.-Ing. Dr.phil. Martin F. Heyn

Institute of Theoretical and Computational Physics

Graz, May 2015

Abstract

Resonant magnetic perturbations (RMPs) are realised to effectively mitigate edge localised modes (ELMs) in tokamak H-regimes. Linear theory however predicts that RMPs are strongly shielded at the mode-specific resonant surfaces. In this thesis, the penetration of RMPs into a tokamak plasma with JET-like parameters is modelled in kinetic approximation. The quasilinear evolution of the plasma parameters and their sensitivity to the RMP field is studied self-consistently by a linear wave code and a 1-D balance code. Model results show that the perpendicular electron fluid velocity becomes zero around the resonant surface and shielding is modified but not removed. In a separate study, the impact of momentum and energy conservation of the collision operator on the plasma shielding is studied by a linear model of plasma shielding using ASDEX-Upgrade parameters for the tokamak plasma. For this purpose a particle conserving Fokker-Planck collision operator in Ornstein-Uhlenbeck approximation is supplemented by two separate integral collision operators ensuring the conservation of energy and momentum, respectively. It is shown how to solve the resulting integro-differential kinetic equation in terms of linear combinations of moments of the Green's function of the purely differential problem. Two recursions relating moments of the Green's function are derived. By application of one of these recursions, the diffusion matrix of the generalised model is analytically shown to be Onsager symmetric. At the electron fluid resonance and the electric resonance, respectively shielding is found to be strongly reduced or even made void, i.e. an amplification of the radial magnetic field perturbation relative to its vacuum value is observed. It is shown that energy conservation in the electron collision operator is important for the quantitative descrition of plasma shielding effects at the resonant surface, while the results are not considerably modified by momentum conservation in the ion collision operator.

Acknowledgments

Most notably, I want to thank my supervisor Martin Heyn for his guidance during my Ph.D. studies. I owe him a lot of the skills and knowledge I gained in the course of this work, that would not have been possible without his constant and diligent support. I also thank him for his lasting patience as the final completion of this thesis was delayed. Furthermore I want to express my gratitude to Winfried Kernbichler, who promoted the progress of this work at all stages and on whose support I could always rely on. I also gained a lot from the experiences I made due to his endeavours to send me on conferences and summer schools. I owe Sergei Kasilov a debt of gratitude for giving this work a sensible direction and thereby enabling its successful completion as well as for sharing his expertise and knowledge with me. I also want to thank Ivan Ivanov for helping me to gain ground on the new field of research during my time as a freshman and his keen and well-intentioned encouragement. I am grateful to Andreas Hirczy for always instantly having taken care of any arisen IT-problem and the many physics or computing related discussions. I also thank the members of our work group, Miran Mulec, Bernhard Seiwald, Andreas Martitsch, Gernot Kapper and Christopher Albert for the good team spirit as well as my further colleagues Faruk Geles, Thomas Rotter, Christof Weber, and Jürgen Waxenegger for the many scientific discussions.

I finally thank my parents for their moral support and confidence in all my endeavours.

I am grateful for the funding by the Austrian OEAW-EURATOM Association.

AFFIDAVIT

I declare that I have authored this thesis independently, that I have not used other than the declared sources/resources, and that I have explicitly indicated all material which has been quoted either literally or by content from the sources used. The text document uploaded to TUGRAZonline is identical to the present doctoral thesis.

May 25, 2015

Date

Signature

Publications

Peer reviewed journal articles

- P. Leitner, M. F. Heyn, I. B. Ivanov, S. V. Kasilov, and W. Kernbichler: *Effect of energy and momentum conservation on fluid resonances for resonant magnetic perturbations in a tokamak.* Physics of Plasmas **21**, 062508 (2014)

  Lead author publication. Notes on authorship: Analytical and numerical results have been obtained by the lead author. Contribution of co-authors: This work was supervised by M. F. Heyn, S. V. Kasilov and W. Kernbichler. The final phrasing was done to a considerable extent by my supervisor Martin Heyn. Some numeric estimates, Eq. (30) to (32) have been derived by Sergei Kasilov. The physical model applied herein is based on the kinetic model by I. B. Ivanov *et al.* (2011) [33] and M. F. Heyn *et al.* (2014) [30] but extended w.r.t. an integral, momentum conserving collision operator.

- M. F. Heyn, I. B. Ivanov, S. V. Kasilov, W. Kernbichler, P. Leitner, V. V. Nemov, W. Suttrop, and the ASDEX Upgrade Team: *Quasilinear modelling of RMP interaction with a tokamak plasma: application to ASDEX Upgrade ELM mitigation experiments.* Nuclear Fusion **54**, 064005 (2014)

  Co-author publication. My contribution was to numerically and finally even analytically check whether or not the transport matrix resulting from the integro-differential collision model was Onsager symmetric. The Onsager symmetry proofs were not discussed in-depth in the publication, yet a full derivation can be found in the Section 3.5.2 of this thesis.

- M. F. Heyn, I. B. Ivanov, S. V. Kasilov, W. Kernbichler, and P. Leitner: *Quasilinear Modelling of RMP Penetration into a Tokamak Plasma.* Problems of atomic science and technology/Series Plasma Physics (2012)

  Lead author conference proceeding in peer-reviewed Ukrainian journal Problems of atomic science and technology/Series Plasma Physics. Remarks on authorship: The model is again based on Ivanov *et al.* (2011) [33]. Here, it was extended by an integral energy conserving collision operator. The model generalisation and results concerning the diffusion matrix and the response current density have been obtained by Martin Heyn and Sergei Kasilov. My contributions pertain to the derivation of recursive relations between the moments of the Green's function associated with the extended collision operator as well as explicit Onsager symmetry proofs.

This work was supervised by Martin Heyn, Sergei Kasilov, and Winfried Kernbichler.

Conference Proceedings

- M. F. Heyn, I. B. Ivanov, S. V. Kasilov, W. Kernbichler, and P. Leitner: *Quasilinear Response to Resonant Magnetic Field Perturbations in a Tokamak*, 39th EPS Conference on Plasma Physics (2012)

- M. F. Heyn, I. B. Ivanov, S. V. Kasilov, W. Kernbichler, and P. Leitner: *Resonant magnetic field perturbations and the quasilinear response of the tokamak plasma*, 38th EPS Conference on Plasma Physics (2011)

Poster Presentations

- P. Leitner, M. F. Heyn, I. B. Ivanov, S. V. Kasilov, and W. Kernbichler: *Kinetic estimate of the shielding of resonant magnetic field perturbations by the plasma in ITER scenario 2.* Culham Plasma Physics Summer School (2010)

- M. F. Heyn, I. B. Ivanov, S. V. Kasilov, W. Kernbichler, and P. Leitner: *Quasilinear Modelling of RMP penetration into a Tokamak*, International Conference and School on Plasma Physics and Controlled Fusion, Alushta (2012)

The results discussed in Chapter 3 have been published for the most part in the two lead-author articles referenced above. This being said, references to those two articles are only given again for literal quotations, inclusion of contributions of the co-authors with an appropriate indication, and reproduction of figures published therein. This procedure is in accordance with the guidelines given by the rectorship of TU Graz for proper quotation practice.[1] Permission for reproduction of contents and figures of the lead-author paper was granted by Physics of Plasmas.

[1] Richtlinie des Rektorates der Technischen Universität Graz zur Sicherung guter wissenschaftlicher Praxis und zur Vermeidung von Fehlverhalten in der Wissenschaft, 25.11.2009

Contents

Conventions and Notation

Throughout this thesis Gaussian CGS-units are used. One exception is the thermal energy denoted by temperature T, Boltzmann's constant being absorbed into T, which is common practice in plasma physics. Consequently T has the dimension of energy and is measured in $[T] = \mathrm{eV}$.

Abstract, i.e. non-projected vectors and tensors are printed boldface, tensors being indicated by sans serif fonts in addition. This convention however does not apply to the matrix representation of a tensor, which e.g. in the case of the diffusion tensor D here is simply written as $D = (D_{ij})$. Variables are printed italic, no matter which rank (scalar, vector, tensor-rank 2, etc.) they have.

It is unavoidable that some quantities share the same symbol, however, whenever possible, subscripts or a direct explanation in the text help to distinguish their meaning. E.g. the symbol p is mostly used for the canonical momentum and p_{kin} for the kinematic momentum apart from few situations, where this notation is unusual, while capitalised P denotes macroscopic pressure and power in the context of reactor physics, respectively.

Unit vectors and normalised basis vectors are indicated by a hat on top as in $\hat{\boldsymbol{h}}$, $\hat{\boldsymbol{e}}_r$, $\hat{\boldsymbol{e}}_\vartheta$, ..., while a hat on top of vector components, e.g. $\hat{A}_r$, $\hat{A}_\vartheta$, $\hat{A}_z$ indicates that they represent physical coordinates in order to distinguish them from covariant ones. Covariant and contravariant basis vectors are either indicated by $\boldsymbol{e}_i$ and $\boldsymbol{e}^i$, respectively or by their direct definitions as tangent and reciprocal basis vectors as $\partial \boldsymbol{r}/\partial u^i$ and ∇u^i, respectively.

Introduction

From the early second half of the last century the achievement of controlled thermonuclear fusion has been considered a valuable aim in the need of covering the world's growing energy demands and has been pursued with great efforts ever since. Physical and technological issues have however been underestimated in the beginning and it was soon recognised that research results had to be declassified and that only by joint efforts further milestones towards a commercial fusion reactor could be achieved.

Several confinement concepts have been considered, from inertial fusion to diverse magnetic confinement geometries. Of the latter, the tokamak is at present the best understood and has been intensely studied theoretically and experimentally, the Joint European Torus (JET) located in Abingdon, UK being the largest scale experiment at the present moment. JET has been operating since 1983, having been the first reactor ever to produce a fusion plasma delivering D-T fusion energy in 1991, see e.g. [71, p. 579ff]. High expectations are raised for the International Thermonuclear Experimental Reactor (ITER) which is aimed at achieving a gain factor of $Q \approx 10$, i.e. providing 10 times the net thermal output power of the input power that is consumed for heating the plasma.

Towards that goal several issues concerning the plasma confinement and its stabilisation are addressed in transport simulations and experiments like JET, ASDEX-Upgrade in Garching, Germany and DIII-D in San Diego in the United States. Experiments at JET and ASDEX-Upgrade provide valuable fundamental research for the design of ITER. One key aspect is the mitigation of type-I edge localised modes (ELMs) that, if left uncontrolled, are a source of possible damage to the first wall and to the divertor by giving rise to rapid radial transport of particles and heat. On the other hand, high confinement modes without ELM-activity were found to return to low-confinement regimes [54], since the occurring steep edge gradients are not flattened out by a moderate release of particles [71, p. 382ff]. In addition, helium ash from nuclear reactions and ions resulting from sputtering at the wall accumulate in the plasma that not only dilute the D-T fuel but also lead to radiative energy loss [54]. In order to control ELMs, resonant magnetic perturbations (RMPs) are presently considered as an effective means to ergodize the edge layer at specifically chosen resonant surfaces and thereby making it possible to influence the plasma edge transport at will. ELM mitigation by RMPs was accomplished in experiments like DIII-D [12], JET [42], ASDEX-Upgrade [30] and is considered also for ITER [4].

The interaction of RMPs with a plasma is an extensive area of research. In a layer around the surfaces where the magnetic perturbations resonate, plasma response currents are excited that, due to the diamagnetic nature of the plasma,

have a tendency to shield the plasma from the perturbation field, see e.g. [70]. For the mitigation of ELMs it is therefore a major concern to find conditions that suppress shielding and allow the penetration of RMPs into the plasma.

The thesis at hand is intended to further investigate such operational limits with the help of a wave-code [33] and a balance code [26, 30] that have been developed in the plasma physics division at the Institute of Theoretical and Computational Physics at TU Graz, simulating linear and quasilinear RMP-driven transport. In contrast to previous studies conducted by our work group, this thesis is intended to generalise the RMP-plasma interaction model by considering an integro-differential collision operator that remedies the fact that the differential Fokker-Planck collision operator in the Ornstein-Uhlenbeck approximation alone ensures the conservation of particles only but does not account for momentum and energy conservation of the plasma species. We will see that energy conservation – once implemented in the code – is mandatory for further studies suppressing fake heat fluxes in our model, while momentum conservation serves the purpose of making the model directly comparable to MHD models neglecting toroidal effects or shear viscosity. If, on the other hand, only energy but not momentum conservation is enforced, the model effectively simulates the momentum loss to the trapped particles.

The structure of this thesis is as follows: Chapter 1 is intended to give a brief overview of fundamental topics of plasma physics research, listing the fundamental thermonuclear reactions in a burning plasma as well as the key requirements that have to be met to start ignition and to finally achieve the desired break-even condition. Subsequently, the tokamak device is introduced without going into whatsoever of the vast engineering details as they will not be of concern in what is following. Finally, an important means for plasma stabilisation and confinement – the mitigation of ELMs by RMPs, is discussed.

Chapter 2 on Methods sets the framework for the studies conducted in course of this thesis. The kinetic equation of plasma physics as well as one of its most important approximations – the guiding centre approximation – is derived in detail. This effort is warranted by the fact that the whole wave-plasma interaction model used here is based on the gyrokinetic equation, so that its origin and the assumptions it is based upon are of relevance for the comprehension of the analysis to follow. The quasilinear model of perturbation-induced transport presented here also in its Hamiltonian form, together with the linear wave-model [25, 26, 33, 27, 30] provides the basis for the investigations undertaken in this work. The chapter concludes with a presentation of the quasilinear balance equations in toroidal geometry and the necessary relations for conversion of the RMP field evaluated in cylindrical geometry to a real tokamak geometry. Fi-

nally, shielding factors are introduced, which are an effective measure for to what extent the perturbation field may penetrate or is shielded from the plasma.

In the final Chapter 3 on Results, first an application of quasilinear modelling with a JET-like tokamak plasma is presented and the sensitivity of the plasma profiles on the RMP-field in the quasilinear evolution is discussed. Furthermore, RMP penetration for various amplitudes of the perturbation field is studied. Secondly, an integro-differential collision operator is introduced and shown to fulfil the desired conservation properties of energy and momentum of the particle species. It will be demonstrated how to solve the linearised integro-differential gyrokinetic equation by constructing a Green's function of moments of the Green's function of the original, purely differential problem. In the following section two formulæ are derived that allow to recursively relate moments of the generalised Green's function. They are used to almost effortlessly numerically evaluate higher moments needed for the computation of transport coefficients. It is further shown that the collisionless limit of the moments coincides with the results obtained by application of the Green's function in the collisionless limit case. From the solution of the kinetic equation the transport matrix is obtained for the general collisional case and the collisional limit and shown to be Onsager symmetric. For both, the check of the collisionless limit of the moments as well as the Onsager proofs, use is made of the second recursion formula. Finally, a numerical model of the linear response of a plasma with ASDEX-Upgrade parameters to a single perturbation mode is presented and various combinations of collision models for the electron and ion component are studied.

In Appendix A, the purely differential kinetic equation with Ornstein-Uhlenbeck Fokker-Planck operator is solved by the method of characteristics. The solution represents no new finding, being presented with by far less details concerning the solution method already in [33]. Nonetheless, due to its huge significance also for the generalised model studied here, it is included so that the model calculations may be fully retraceable from first principles. Appendix B contains some intermediate calculations provided for the diligent reader wishing to follow the various steps needed for the construction of a momentum conserving collision operator. These are migrated from Chapter 3 such that the reading flow is not impeded. In Appendix C explicit evaluations of the diffusion coefficients in the collisional case as well as in the collisionless limit can be found. Finally, in Appendix D it is shown how to determine the plasma response current density in lowest order FLRE.

Chapter 1

Basics

The following sections are intended to set the framework for the investigations carried out in course of this thesis. They cover aspects of thermonuclear fusion, a survey of the structure of a tokamak, the geometry of the tokamak vacuum field and finally some remarks on confinement as well as the role of Resonant Magnetic Perturbations (RMPs) in influencing the plasma edge transport. This introductory part outlining the necessary fundamentals for what follows is based fully on meanwhile well-established textbook knowledge for which I refer to Chapter 1, p. 1–31 and Chapter 3, p. 105–142 of the standard handbook *Tokamaks* by J. Wesson [71] in the contexts of fusion power and the tokamak equilibrium magnetic field, respectively, Chapter 4, p. 55–99, on "Magnetic-Field-Structure related Concepts" of *Flux Coordinates and Magnetic Field Structure* by W. D. d'Haeseleer *et al.* [10], as well as *Plasma Physics* edited by R. Dendy and the handbook *Fusion Physics* edited by M. Kikuchi *et al.* [36], for which separate references to the relevant chapters are given. For the case of RMPs which represent an up-to-date area of research, original literature has been used.

Contents

1.1 Thermonuclear Fusion

The world energy consumption by the year 2100 is expected to be at least twice the present usage [22]. The challenging problem of covering the fast-growing energy demands along with the necessity of reducing the release of greenhouse gases is omnipresent in the media. It is the present belief that such ambitious goals can only be achieved by large investments in renewable energy sources along with overcoming the many remaining engineering and scientific issues still unsolved for a steady-state fusion power plant operation. At present, due to – though not exclusively – various plasma instabilities, only a short-term, pulsed operation is possible and only a fraction of the input power is regained. Not surprisingly, a big part of research activity is devoted to plasma confinement and macroscopic stability of tokamak plasmas. Only recently a record was set at the JET[1] experiment in Abingdon, UK, where a stabilisation of the fusion plasma was achieved for 15 minutes [3, p. 96].

In order for a nuclear reaction to take place two light nuclei have to overcome the electrostatic repulsion of their positive charges. If the relative velocity of the nuclei is low, the particles suffer a deflection from their orbits and are hindered to approach each other closely. With increasing kinetic energy the particles spend less time within the interaction region and thus get diverted from their paths to a lesser extent. Increasing the kinetic energy even further, at some point the nuclei can either overcome the Coulomb barrier or become ever more likely to penetrate that barrier due to quantum mechanical tunnelling, given that impact parameters are small enough. From there the short range, attractive nuclear strong force is dominant and a fusion reaction is initiated. For light element fusion, the mass of the resultant nucleus is less than the masses of the separate nuclei, resulting in a release of binding energy in form of kinetic energy of the reaction products. In case of the deuterium-tritium reaction this energy is $E = \Delta m\, c^2 \approx 0.01875\, m_\mathrm{p}\, c^2 \approx 17.59\,\mathrm{MeV}$, see e.g. [71], where m_p denotes a proton mass.

Several fusion reactions are being considered feasible for energy production in a fusion reactor, the by far most promising reaction being the fusion of a ${}^{2}_{1}\mathrm{D}$ deuterium with a ${}^{3}_{1}\mathrm{T}$ tritium nucleus, Eq. (1.3). This is due to D-T having the highest cross section σ at the lowest energies [71] as is shown in Fig. 1.1. The

[1] Joint European Torus at the Culham Centre for Fusion Energy

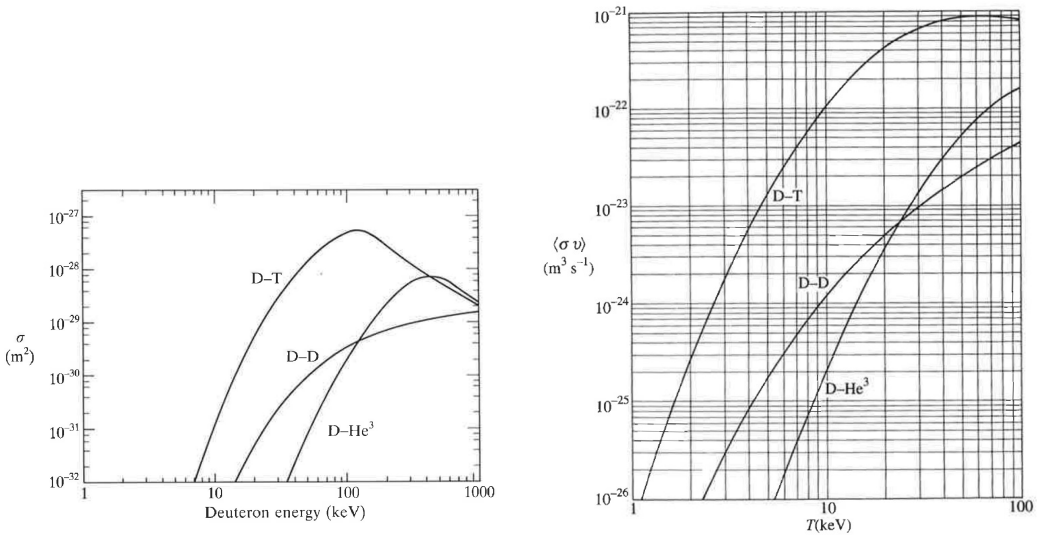

Figure 1.1: Cross section σ (left) and $\langle \sigma v \rangle$ (right) for the reactions given in (1.3) to (1.5). Source: Wesson, *Tokamaks* [71].

total thermal energy content in the plasma of volume $\mathcal{V}$ is by definition

$$W = 3 \int_{\mathcal{V}} \mathrm{d}^3 r \, nT = 3\overline{nT}\mathcal{V}, \tag{1.1}$$

assuming an equal number of electrons and ions $n_\mathrm{e} = n_\mathrm{i} = n/2$, each species holding an average kinetic energy of $T/2$ per degree of freedom and so in total $3nT$ per unit volume [71]. The actually relevant measure is the *total reaction rate*, given by the integral of $\sigma(v')v' f_1(\boldsymbol{v}_1) f_2(\boldsymbol{v}_2)$ over both particles' velocity space [71],

$$\mathcal{R} = \int_{\mathbb{R}^3} \mathrm{d}^3 v_1 \int_{\mathbb{R}^3} \mathrm{d}^3 v_2 \, \sigma(\|\boldsymbol{v}'\|) \, \|\boldsymbol{v}'\| \, f_1(\boldsymbol{v}_1) f_2(\boldsymbol{v}_2) \overset{(\mathrm{D-T})}{=} n_\mathrm{D} n_\mathrm{T} \langle \sigma v \rangle, \tag{1.2}$$

which in the case of a D-T reaction can be shown to give the right-hand side of Eq. (1.2). Here $\boldsymbol{v}' = \boldsymbol{v}_1 - \boldsymbol{v}_2$ is the relative velocity and $f_i(\boldsymbol{v}_i)$ is the distribution function of the particular particle species. This rate reaches its maximum value if the ion particle densities are equal, $n_\mathrm{D} = n_\mathrm{T}$ [71]. The product $\langle \sigma v \rangle$ for the D-T, D-D, and D-$^3_2$He reaction respectively is shown on the right graph of Fig. 1.1.

In the following, the three most important reactions for controlled fusion are listed, see e.g. [71, 35]:

$$^2_1\mathrm{D} + {}^3_1\mathrm{T} \rightarrow {}^4_2\mathrm{He} + {}^1_0\mathrm{n} \tag{1.3}$$

$$ {}^{2}_{1}\mathrm{D} + {}^{2}_{1}\mathrm{D} \rightarrow \begin{cases} {}^{3}_{1}\mathrm{T} + {}^{1}_{1}\mathrm{p} \\ {}^{3}_{2}\mathrm{He} + {}^{1}_{0}\mathrm{n} \end{cases} \tag{1.4} $$

$$ {}^{2}_{1}\mathrm{D} + {}^{3}_{2}\mathrm{He} \rightarrow {}^{4}_{2}\mathrm{He} + {}^{1}_{1}\mathrm{p} \tag{1.5} $$

When, as shown in (1.3), the hydrogen isotopes deuterium and tritium are brought to react with each other, an α-particle and a neutron are produced, their kinetic energies being distributed as follows: 3.5 MeV ($^{4}_{2}$He) and 14.1 MeV ($^{1}_{0}$n) [71, 35], thus yielding in total 17.6 MeV per reaction. The neutron that carries approximately 4/5 of the released energy leaves the plasma without interaction. It is intended to become absorbed in the blanket such that its kinetic energy can be converted into heat and conducted outside by means of a coolant generating electric power in a conventional way [71]. The charged α-particle on the other hand, which is confined by the magnetic field only receives the small remaining fifth part of the reaction energy. This small energy fraction then contributes mainly to sustain the plasma at a high enough temperature to allow for further nuclear reactions to occur. The thermonuclear power per unit volume p_{tn} is directly proportional to the species' particle densities, the product $\langle\sigma v\rangle$ and the energy release per single reaction $\mathcal{E}$ [71],

$$ p_{\mathrm{tn}} = n_{\mathrm{D}} n_{\mathrm{T}} \langle\sigma v\rangle \mathcal{E} \tag{1.6} $$

and, in the optimum case where $n_{\mathrm{D}} = n_{\mathrm{T}} = n/2$, gives for the α-particle heating per unit volume $p_\alpha = {}^{1}\!/_{4}\, n^2 \langle\sigma v\rangle \mathcal{E}_\alpha$ or, in total [71],

$$ P_\alpha = \int_{\mathcal{V}} \mathrm{d}^3 r\, p_\alpha = \frac{1}{4} \overline{n^2 \langle\sigma v\rangle} \mathcal{E}_\alpha \mathcal{V}. \tag{1.7} $$

Deuterium is plentifully available in form of heavy water D_2O [35], while tritium does not occur naturally being unstable to β-decay [35]. It has to be bred from Lithium according to one of the two following reactions of a neutron, which is generated in a fusion process, together with one of the two lithium isotopes $^{6}_{3}$Li and $^{7}_{3}$Li with substantial occurrence in the Earth's crust and in the oceans [35],

$$ {}^{6}_{3}\mathrm{Li} + {}^{1}_{0}\mathrm{n} \rightarrow {}^{4}_{2}\mathrm{He} + {}^{3}_{1}\mathrm{T}, \tag{1.8} $$

$$ {}^{7}_{3}\mathrm{Li} + {}^{1}_{0}\mathrm{n} \rightarrow {}^{3}_{1}\mathrm{T} + {}^{4}_{2}\mathrm{He} + {}^{1}_{0}\mathrm{n}. \tag{1.9} $$

The first reaction releases 4.8 MeV and requires a slow neutron for the reaction to occur, while the second consumes 2.5 MeV and a fast neutron [22]. While breeding tritium in a lithium-blanket is considered for the first generation fusion reactors, the focus for the second generation reactors will also be laid on the D-D reaction [35], which requires substantially higher energies as can be seen

from Fig. 1.1.

In order for a net positive energy balance to occur, the nuclei have to react before they lose their energy due to bremsstrahlung on occasion of electron-electron and electron-ion encounters, synchrotron radiation due to the confinement of the plasma by a magnetic field and various transport processes. The power loss P_{L} defined by means of the energy confinement time τ_{E} as $P_L = W/\tau_{\mathrm{E}}$ [71] has to be balanced by external heating of the fusion plasma and the intrinsic α-particle heating, $P_{\mathrm{H}} + P_\alpha = P_{\mathrm{L}}$, giving the power balance equation [71]

$$P_{\mathrm{H}} + \frac{1}{4}\overline{n^2\langle\sigma v\rangle}\mathcal{E}_\alpha\mathcal{V} = \frac{3\overline{nT}}{\tau_{\mathrm{E}}}\mathcal{V}. \tag{1.10}$$

The so called *power gain*, defined by $Q = P_{\mathrm{out}}/P_{\mathrm{in}} = P_{\mathrm{fusion}}/P_{\mathrm{aux}}$ apparently has to exceed one, the minimum criterion $Q = 1$ being called "break-even condition" [35]. For this purpose a D-T plasma has to be heated to $\sim 10\,\mathrm{keV}$ [35] corresponding to $\sim 10^8\,\mathrm{K}$. At so high a temperature the plasma can be considered completely ionised. Furthermore it is then the high-energy tail of the Maxwellian-distributed assumed reactants, i.e.

$$f_i(v_i) = n_i\left(\frac{m_i}{2\pi T}\right)^{3/2}\exp\left(-\frac{m_i v_i^2}{2T}\right) \tag{1.11}$$

that contributes most to the nuclear reactions [71].

When the burning process becomes self-sustaining and no further energy has to be supplied for further fusion reactions to occur, ignition is reached. In order for ignition to set in, the so called "triple product" of electron density and temperature and energy confinement time has to exceed a threshold value, see e.g. [71, 35],

$$n_{\mathrm{e}}\tau_{\mathrm{E}}T_{\mathrm{e}} > 1.5\times 10^{15}\,\mathrm{cm}^{-3}\,\mathrm{s}\,\mathrm{keV}, \tag{1.12}$$

this criterion being based on the original work by Lawson [39]. The energy confinement time τ_{E} in steady-state is often obtained experimentally from $\tau_{\mathrm{E}} = W/P_{\mathrm{H}}$ [71], i.e. the the ratio of the total energy content in the plasma W and the power supplied by heating, assuming that the thermonuclear power in present day experiments is low and thus external heating balances energy losses in steady state, i.e. $P_{\mathrm{H}} \approx P_{\mathrm{L}}$ [71].

Most importantly, fusion power is considered safe: in contrast to nuclear reactions in a fission power plant the operation is bound to cease without a continuous supply of fuel, while the mass of fuel at any instant of time in a reactor corresponds to no more than "the weight of several postage stamps" [22]. In case of an accident, the fusion material would allow energy production to continue for no more than a few seconds [35].

1.2 The Tokamak

In contrast to inertial confinement, where high density plasmas are generated during very short nanosecond time intervals, magnetic confinement is aimed at constraining a low density plasma to closed magnetic field lines for much longer time scales. Since the threshold value for self-sustaining burning scales with both the density and temperature, Eq. (1.12), there must be a strong enough magnetic field present to counteract the required plasma pressure in a reactor. Present technological limits allow the generation of magnetic fields of about $1.2 \times 10^5\,\mathrm{G}$, while it seems likely that coils generating a $\sim 1.6 \times 10^5\,\mathrm{G}$ field are engineered in the future [71]. Considering the inverse radial dependence of the toroidal field on the major radius R, this corresponds to a field strength of $(6 \ldots 8) \times 10^4\,\mathrm{G}$ at the plasma centre [71].

Being originally developed in the Soviet Union in the late 1950s, today's largest scale tokamak experiment is the Joint European Torus located at Culham Laboratory in Abingdon, UK which started operation in 1983. Tokamak performance has improved significantly over the last decades, the first devices featuring a confinement time of no more than few milliseconds [71]. With heating methods such as neutral beam injection and RF heating at the ion cyclotron resonance, ion temperatures could be improved from originally several hundreds of eV to a few keV in the 1980s [71]. While JET holds the world record for fusion power, in recent years it also served in carrying out experiments specifically aimed at design studies for the next larger-scale experiment, the International Thermonuclear Experimental Reactor (ITER) to be built in Cadarache, France.

The tokamak plasma is surrounded by a blanket, a shield, and finally the coils generating the toroidal field. A significant role is played by the blanket, which

- absorbs neutrons from the D-T reaction whose thermal energy of 14.1 MeV is removed by a liquid or gaseous coolant and transformed to electrical power in the conventional way by a turbine and a generator
- shields the superconducting coils, which have to be protected from damage and kept at very low temperatures
- provides the conditions for the breeding of tritium according to either of the processes (1.8) or (1.9).

While most of the neutrons are absorbed in the blanket, the energy flux of the remaining neutrons is still by a factor of $10^6 \ldots 10^7$ too high to be let pass to the superconducting coils; a further reduction is accomplished by a roughly 1 m shield of material with high atomic number Z, such as steel [71].

1.2.1 Magnetic Field Geometry

Before discussing the magnetic field geometry, a few remarks on the coordinates used are indicated. While R is used to measure the distance of a particular point from the major axis, R_0 is the radius of the magnetic axis (also minor axis) which lies at the centre of the set of nested flux surfaces. Here, the plasma pressure P and the current density $\boldsymbol{j}$ reach their maximum values. The distance of an arbitrary point $\boldsymbol{r} = (x, y, z)$ under consideration from that axis is given by the radial coordinate r, that together with the poloidal angle θ and toroidal angle ϕ form the set of toroidal coordinates $(u^1, u^2, u^3) = (r, \theta, \phi)$ linked to Cartesian coordinates by the relations, see e.g. [10],

$$\begin{aligned} x &= (R_0 + r\cos\theta)\sin\phi, \\ y &= (R_0 + r\cos\theta)\cos\phi, \\ z &= r\sin\theta, \end{aligned} \tag{1.13}$$

where $r \in \mathbb{R}^+$ and $\theta, \phi \in [0, 2\pi)$. For $(\hat{\boldsymbol{e}}_r, \hat{\boldsymbol{e}}_\theta, \hat{\boldsymbol{e}}_\phi)$ to form a right-handed system, the toroidal angle ϕ has to be measured clockwise as opposed to the usual convention, see Fig. 1.2.

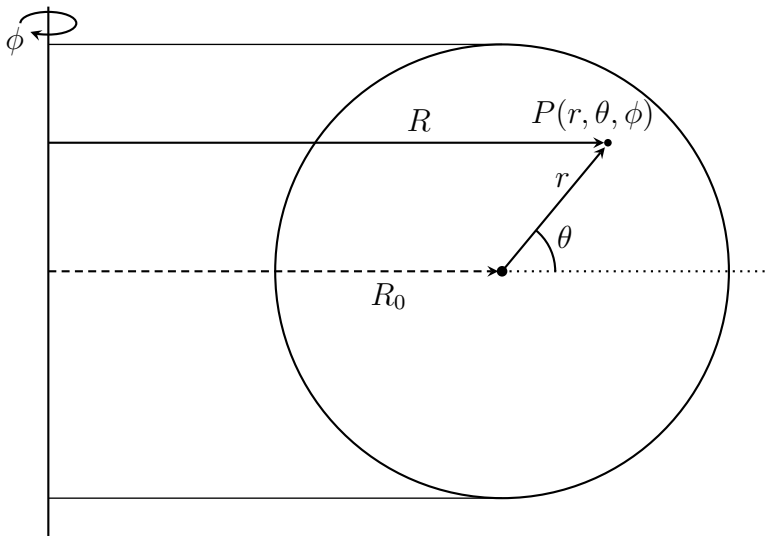

Figure 1.2: Toroidal coordinates for the tokamak geometry.

In a tokamak, the toroidal magnetic field B_ϕ is generated by external superconducting field coils. As already mentioned before, the toroidal field strength varies characteristically with $1/R$ in radial direction. This is easily realised by applying Ampère's law to a circular toroidal path inside the toroidal field coils,

neglecting the small contribution from the poloidal plasma current [71],

$$\int_{\mathcal{S}} \mathrm{d}\boldsymbol{S} \cdot \nabla \times \boldsymbol{B} = \oint_{\partial\mathcal{S}} \mathrm{d}\boldsymbol{r} \cdot \boldsymbol{B} \approx 2\pi R B_\phi = \frac{4\pi}{c} \int_{\mathcal{S}} \mathrm{d}\boldsymbol{S} \cdot \boldsymbol{j} = \frac{4\pi}{c} I_{\mathrm{coil}}, \tag{1.14}$$

and hence, $B_\phi \propto 1/R$. In toroidal direction, the ideally constant field strength is slightly rippled due to the field coils being placed at discrete angles around the torus. In a purely toroidal magnetic field electrons and ions would drift apart vertically in opposite directions, giving rise to a vertical electric field and hence an undesired radial $\boldsymbol{E} \times \boldsymbol{B}$-motion. For this purpose a weaker poloidal field B_θ is put in place by a transformer action inducing a toroidal electric field and hence a toroidal plasma current[2]. The toroidal together with the poloidal field forms a helically wound magnetic field geometry as depicted in Fig. 1.3. The tokamak vacuum field can be approximated as follows [54],

$$\boldsymbol{B} = (0, B_\theta(r), B_0)^{\mathrm{T}} \left(1 - \frac{r}{R_0} \cos\theta\right). \tag{1.15}$$

The poloidal field leads to particle trajectories that prevent the formation of such a vertical electric field, allowing for particle orbits constrained to magnetic flux surfaces albeit small deviations are inherent due to ∇B- and magnetic curvature drifts.

An infinite set of nested flux surfaces is traced out by a series of magnetic field lines. In equilibrium, the plasma pressure is exactly balanced by the magnetic force, $\boldsymbol{j} \times \boldsymbol{B} = \nabla P$, a relation often referred to as "magnetostatic equation"[3] [38]. Hence it follows that the current flows within the flux surface, $\boldsymbol{j} \cdot \nabla P = 0$ and pressure is a constant on a flux surface, $\boldsymbol{B} \cdot \nabla P = 0$. In this simple picture neither of effects like resistivity, viscosity, finite flow velocities or finite Larmor radius are considered [10]. The variation of the gradient of the filed lines as one traverses the flux surfaces radially leads to global magnetic shear [41],

$$s = \frac{r}{q} \frac{\mathrm{d}q}{\mathrm{d}r}, \tag{1.16}$$

the pitch of the field line being measured by the safety factor $q(r)$. Marking the point in an arbitrary poloidal cross section where the field lines pierces the plane and measuring the toroidal angle $\Delta\phi$ covered until it will return to that

[2] In contrast to the tokamak, in a stellerator the poloidal field is generated by helical field coils.

[3] together with the further field equations $\nabla \times \boldsymbol{B} = 4\pi\boldsymbol{j}/c$ and $\nabla \cdot \boldsymbol{B} = 0$.

position provides another way of defining the safety factor as [71]

$$q = \frac{\Delta\phi}{2\pi}. \tag{1.17}$$

Especially for the case of rational surfaces $q \in \mathbb{Q}$, i.e. m, $n \in \mathbb{Z}$, the field line closes upon itself having helically traversed the flux surface m times in toroidal and n times in poloidal direction. In all other cases of irrational surfaces where $q \in \mathbb{R}\backslash\mathbb{Q}$, the field line traces out the whole surface. The safety factor derives its name from the fact that plasma stability improves with higher q-values [71].

If one considers the field line equation, see e.g. [10]

$$\boldsymbol{B} \times \mathrm{d}\boldsymbol{r} = \boldsymbol{0} \Rightarrow \frac{B_\phi}{R\,\mathrm{d}\phi} = \frac{B_\theta}{\mathrm{d}s} = \text{const}, \tag{1.18}$$

where $\mathrm{d}s$ is an infinitesimal path element in poloidal direction, isolates $\mathrm{d}\phi$ and substitutes the expression to the definition of q in Eq. (1.17) one obtains [71]

$$q = \frac{1}{2\pi}\oint_{\mathcal{C}} \mathrm{d}s\,\frac{1}{R}\frac{B_\phi}{B_\theta} \approx \frac{r}{R_0}\frac{B_\phi}{B_\theta} \tag{1.19}$$

as an approximation for the safety factor for large aspect ratio R/r and circular cross section. In the so-far considered case of circular poloidal cross-sections and large aspect-ratio, one can further find an expression for the radial q-profile by applying Ampère's law again, this time considering a poloidal cross-section $\mathcal{S}_{\text{tor}}$ of a flux surface at r and its boundary $\partial\mathcal{S}_{\text{tor}}$, respectively [71],

$$\oint_{\partial\mathcal{S}_{\text{tor}}} \mathrm{d}\boldsymbol{r}\cdot\boldsymbol{B} = 2\pi r B_\theta = \frac{8\pi^2}{c}\int_0^r \mathrm{d}r'\,r' j(r'). \tag{1.20}$$

For non specified current density profile $j(r)$ the current flowing within $0 \leq r' \leq r$ is $I(r) = 2\pi\int_0^r \mathrm{d}r'\,r' j(r')$ and from (1.19) the radial q-dependence is obtained as

$$q(r) \approx \frac{c r^2 B_\phi}{2R_0 I(r)}, \tag{1.21}$$

giving $q(a) \approx c a^2 B_\phi / 2R_0 I_{\text{tor}}$ at the plasma edge and $q(0) \approx c B_\phi / 2R_0 \pi j(0)$ at the magnetic axis, having used $\lim_{r\to 0} I(r) = \lim_{r\to 0} r^2 \pi j(0)$ [71]. The simple approximation for q at the plasma edge is no longer valid in the case of a divertor due to the domination of contributions coming from the vicinity of the X-point, q being $\propto 1/B_\theta$, see Eq. (1.19), since there the poloidal field is zero.

Density (cm^{-3})	Ion temperature (keV)	$B_\phi\,(10^4\,\mathrm{G})$	R/a
$\sim 10^{13}\ldots10^{14}$	$\sim 10\ldots30$	$\sim 1\ldots5$	~ 4

Table 1.1: Typical tokamak plasma parameters. Data from O'Brien, M. R. and Robinson, D. C.: *Plasma Physics* [54, Chapter 8: Tokamak experiments, p. 189ff].

1.2.2 Particle Orbits

Particle orbits in a tokamak will be studied in great detail in Sect. 2.2 on the guiding centre approximation. However some general remarks on the orbits of two classes of particles, namely the trapped and passing particles, are indicated here. While particles with a sufficiently large parallel velocity component traverse the whole torus and hence are called passing, a fraction of the particles cannot circle the whole flux surface but is trapped to the low field region. A particle's adiabatic moment $\mu = mv_\perp^2/2B$ and kinetic energy $K = m(v_\perp^2 + v_\parallel^2)/2$ being constant, the perpendicular velocity is bound to rise as the particle moves into regions with higher magnetic field strength. Consequently $v_\parallel$ decreases accordingly until, for the trapped particle species, the whole momentum is transferred to the perpendicular motion and the particle is mirrored at a particular poloidal angle θ_c while precessing toroidally [23]. Projecting the gyromotion to a poloidal cross section shows the typical shape of a banana orbit. In a collisional plasma trapped particles are scattered out of the trapping cone in velocity space. For the electrons such a collision typically leads to a displacement of the order of the electron banana width. The essential point here is that this length is larger than the electron Larmor radius ϱ_e. Although only a fraction of particles is trapped, these dominate the transport, their associated random-walk step size exceeding the length scale for classical diffusion [71]. For an isotropic distribution, the velocity space geometry determines the ratio of trapped to passing particles being $\sim (2r/R)^{1/2}$ on any magnetic surface [23]. It considerably influences the transport e.g. by affecting the plasma conductivity and pressure-driven currents [54].

1.2.3 Plasma Confinement

A deliberate induction of radial electric fields at the edge plasma gives rise to an abrupt transition from a low (L-mode) to a high confinement regime (H-mode) associated with considerably better confinement times. This coincidence was first observed at the ASDEX tokamak featuring a divertor to separate the plasma from the first wall and operating at high temperature. With the H-mode plasma edge confinement improved and steep gradients of density and temperature were

Plasma/Device Parameters	
n_e	$(1 \ldots 4) \times 10^{13}\,\mathrm{cm}^{-3}$
T_e	$\lesssim 5$ keV
T_i	$\lesssim 3$ keV
B_ϕ	$(1.3 \ldots 3.4) \times 10^4$ G
R	296 cm
a	125 cm
R/a	2.38
q	$2.3 \ldots 10$
I_ϕ	$\sim 2 \times 10^{16}\,\mathrm{statA}$

Table 1.2: Parameters of the Joint European Torus. Data from Rebut, P. H. *et al.* (1985) [57] and Wesson, J.: *Tokamaks* [71, p. 581ff]

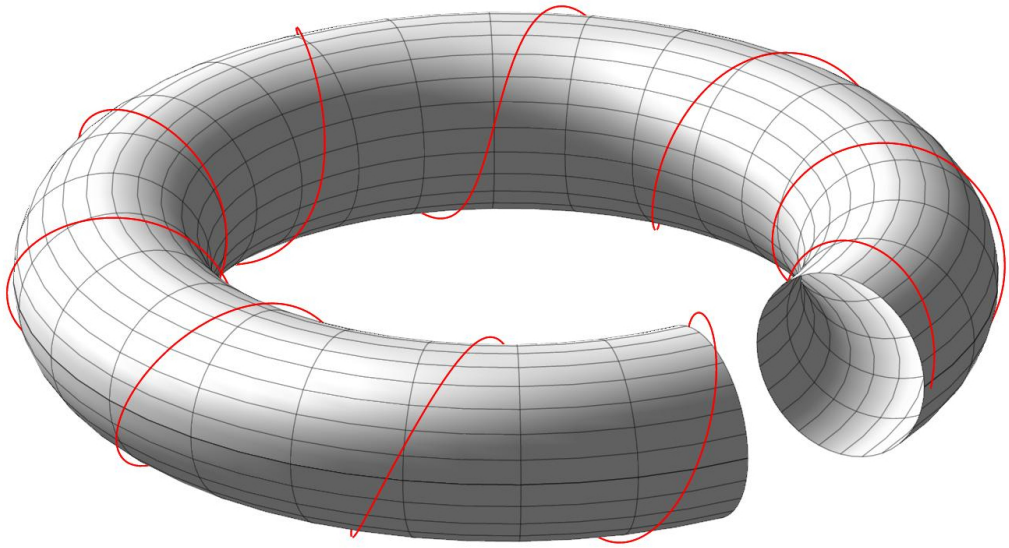

Figure 1.3: Idealised Tokamak geometry: Flux surface with circular cross-section. A helical magnetic field (indicated here by a red field line) is accomplished by exterior superconducting coils generating a toroidal field and the toroidal plasma current I_ϕ superimposing a poloidal field.

found to occur at the separatrix [54]. Many an H-mode is accompanied by edge localised modes (ELMs) which, being a burst of MHD activity degrade energy and particle confinement. If on the other hand an H-mode lacks ELM-activity, the density rises until a transition back to the L-mode is triggered. In order to stabilise the density it is therefore desired to control ELMs and thereby transport characteristics at the plasma edge. Local studies of particle-, momentum- and energy transport have shown that transport coefficients, e.g. thermal diffusivities are low, e.g. $D \sim 3 \times 10^3\,\mathrm{cm}^2/\mathrm{s}$ for $q \lesssim 1$, rising gradually until $r \approx 0.8\,a$, while at the edge with increasing turbulent characteristics, a strong increase up to $D \sim 10^4\,\mathrm{cm}^2/\mathrm{s}$ is observed [54].

While increasing the energy confinement time is a core technological issue for the plasma centre, this is not true for the outer layer where impurities resulting from material sputtering of the first wall and helium ash have to be constantly removed. Ion impurities reduce the performance already in small concentration due to the radiative power loss being $\propto Z_\mathrm{i}^2$, while alpha particles resulting from either the D-T or the D-He reaction quickly dilute the plasma. A measure for the acceptable impurity content is the effective charge $Z_\mathrm{eff} = \sum_i n_i Z_i^2/n_\mathrm{e}$ which must be kept low, $Z_\mathrm{eff} \lesssim 2$ in order not to critically reduce the fusion power density [54].

One way to get rid of impurities resulting from plasma-wall interactions are magnetic divertors which, at the plasma edge divert magnetic field lines and thus also the charged particles that follow them to an external chamber, where they are neutralised and extracted.

1.2.4 Resonant Magnetic Perturbations

An important means to increase the radial transport at specifically chosen layers of the edge plasma is to intentionally perturb the equilibrium magnetic flux surfaces by imposing a perturbation field that is resonant at flux surfaces such that the ratio of toroidal to poloidal wave number coincides with the safety factor at the particular plasma radius, i.e. $q(r) = {}^m\!/_n$. For this purpose an antenna current exciting the perturbations is induced parallel to the field lines on the resonant equilibrium flux surface. Resonant magnetic perturbations (RMPs) interacting with a static plasma lead to the formation of magnetic islands by affecting the magnetic field topology and giving rise to magnetic reconnection [58]. Thereby transport is enhanced as particles move around the islands following the perturbed field lines and steep gradients at the plasma edge are flattened. Hence undesirable type-I ELMs that cause a substantial heat load on the wall and the divertor, thereby stressing the material can be mitigated by RMPs. Besides externally applied magnetic field perturbations a typical tokamak suffers from

non-axisymmetric resonant field errors of the order $\delta B/B \sim 10^{-4}$ [58]. Analogous to RMPs also these non-purposed aberrations from axisymmetry lead to pronounced island formation of widths $w \propto \sqrt{|B_r(r_{\mathrm{res}})|}$ as is shown by Reiman and Monticello [58]. Their numerical studies [58] have shown that those island widths scale as $\sqrt{\delta B/B}$. With increasing size islands start to overlap, thereby forming ergodic regions that enable fast radial transport. The formation process, however was found to be suppressed when the plasma is rotating [15, 17] in which case the perturbation decelerates the plasma rotation by exertion of a braking force. This effect of plasma shielding is not desirable if one deliberately wants to ergodize the plasma edge for ELM mitigation. It has been shown that RMPs may be shielded by the plasma response currents flowing in a thin layer at the resonant surfaces and are reduced by several orders of magnitude [25, 26, 33]. Waelbroeck [70] studied the effect of diamagnetic drifts on the shielding of RMPs by plasma rotation. He showed that the force exerted by the perturbations affects the electrons such that they are brought to rest in the frame of the perturbation. In [70] it is also shown that the force induced by the perturbations at the resonant layer as a function of the rotation frequency has three minima and that between these minima there are two so-called locked states where the force is resonant. In Heyn *et al.* [30] yet another resonance associated with the equilibrium field reversal point $E_r = 0$ is studied, which is shown to even possibly amplify the perturbation field. Here the shielding is suppressed, allowing the formation of magnetic islands.

Chapter 2

Methods

The study at hand is based on a linear and quasilinear, respectively kinetic model of the interaction of resonant magnetic perturbations (RMPs) with a tokamak plasma, described as a straight cylinder with rotational transform [25]. In Sections 2.2 to 2.3 a detailed derivation of the gyrokinetic model of RMP-driven transport is given. When discussing the guiding centre approximation in Section 2.2, an analysis of the motion of a single charged particle in prescribed electromagnetic fields is developed. Taylor-expanding fields and potentials in small gyroradii, one finally obtains the drift equations of motion, thereby limiting oneself to gyro-averaged orbits. The connection between the orbit of such a test particle and its associated guiding centre velocity with the dynamics of average properties of the whole plasma is manifested in the kinetic equation, which is the subject of the following Section 2.1. Sections 2.4 to 2.5 are devoted to the derivation of the plasma response to the perturbation field. In Sections 2.6 and 2.7, the key equations underlying the linear model and the quasilinear balance code, respectively are presented.

As in the preceding chapter, the contents presented here do not represent original research by the author but theoretical fundamentals derived here in great detail as well as a description of the transport model that was developed in our work group at the ITP/CP at TU Graz. Nonetheless, the methods introduced here provide the framework in which the original results, obtained in course of this thesis and discussed in Chapter 3, are embedded.

Contents

2.1 Plasma Kinetic Equation

In plasma kinetic theory the motions of all the particles which make up the plasma are considered, though not necessarily by an exact description of all the particles' orbits in phase space but by a statistical description of these which still enables one to determine average properties of the plasma. Although not of direct value for the computational modelling of a plasma, Klimontovich's exact equation of the spatial and temporal evolution of a plasma is one possible starting point for the derivation of the kinetic equation. A detailed derivation of the kinetic equation based on either the Klimontovich or the Liouville equation can be found in Nicholson's "Introduction to plasma theory" [51], chapters 3 to 5, while here only a sketch of the derivation of the probably most fundamental equation of plasma physics pursuant to [51] is given.

The density of particles of a two-component plasma, made up by N electrons and ions, each in 6-D phase space $\mathbb{P}$ with coordinates $(\boldsymbol{r}, \boldsymbol{v})$ is [51]

$$n(\boldsymbol{r}, \boldsymbol{v}, t) = \sum_{\sigma=\mathrm{e,i}} \sum_{i=1}^{N} \delta(\boldsymbol{r} - \boldsymbol{R}_i(t)) \delta(\boldsymbol{v} - \boldsymbol{V}_i(t)), \tag{2.1}$$

with $\boldsymbol{R}_i(t)$ and $\boldsymbol{V}_i(t)$ denoting the actual particle position and velocity, respectively. One should mention here that while the Klimontovich equation is an exact description of a particle ensemble in the sense that no statistical averages over particle trajectories are applied, already in this first step, Eq. (2.1) a simplification has been made in that the particles have been assumed point-like. For a plasma made up by electrons and protons this assumption does not seem to be

severe, while for complex dusty plasmas such an ansatz would be questionable. The trajectories and velocities of each particle obey equations of motion,

$$\dot{\boldsymbol{R}}_i(t) = \boldsymbol{V}_i(t), \tag{2.2}$$

$$\dot{\boldsymbol{V}}_i(t) = \frac{q_\sigma}{m_\sigma}\left\{\boldsymbol{E}^{\mathrm{m}}[\boldsymbol{R}_i(t),t] + \frac{\boldsymbol{V}_i(t)}{c}\times\boldsymbol{B}^{\mathrm{m}}[\boldsymbol{R}_i(t),t)]\right\}, \tag{2.3}$$

$\boldsymbol{E}^{\mathrm{m}}$ and $\boldsymbol{B}^{\mathrm{m}}$ being the self-consistent microscopic fields that include externally applied fields as well as the fields that originate from the particles themselves. The particles' charge and current densities are sources

$$\varrho^{\mathrm{m}}(\boldsymbol{r},t) = \sum_{\sigma=\mathrm{e,i}} q_\sigma \int_{\mathbb{R}^3} \mathrm{d}^3v\, n_\sigma(\boldsymbol{r},\boldsymbol{v},t), \tag{2.4}$$

$$\boldsymbol{j}^{\mathrm{m}}(\boldsymbol{r},t) = \sum_{\sigma=\mathrm{e,i}} q_\sigma \int_{\mathbb{R}^3} \mathrm{d}^3v\, \boldsymbol{v}\, n_\sigma(\boldsymbol{r},\boldsymbol{v},t) \tag{2.5}$$

of the electromagnetic field. Together with Maxwell's equations

$$\nabla\cdot\boldsymbol{E}^{\mathrm{m}}(\boldsymbol{r},t) = 4\pi\varrho(\boldsymbol{r},t), \tag{2.6}$$

$$\nabla\cdot\boldsymbol{B}^{\mathrm{m}}(\boldsymbol{r},t) = 0, \tag{2.7}$$

$$\nabla\times\boldsymbol{E}^{\mathrm{m}}(\boldsymbol{r},t) = -\frac{1}{c}\frac{\partial\boldsymbol{B}^{\mathrm{m}}(\boldsymbol{r},t)}{\partial t} \tag{2.8}$$

$$\nabla\times\boldsymbol{B}^{\mathrm{m}}(\boldsymbol{r},t) = \frac{4\pi}{c}\boldsymbol{j}(\boldsymbol{r},t) + \frac{1}{c}\frac{\partial\boldsymbol{E}^{\mathrm{m}}(\boldsymbol{r},t)}{\partial t}, \tag{2.9}$$

the equations of motion form a closed set of equations, meaning that provided initial conditions for particle positions and velocities are given, the complete state of all particles in phase space, i.e. $\boldsymbol{r}_i(t)$ and $\boldsymbol{v}_i(t)$ $(i = 1,\ldots,N)$ can be determined along with the fields that couple with the equations of motion via Eq. (2.3).

The Klimontovich equation is obtained by taking the time derivative of the density of particles in phase space, Eq. (2.1),

$$\begin{aligned}\frac{\partial n_\sigma(\boldsymbol{r},\boldsymbol{v},t)}{\partial t} &= -\sum_{i=1}^{N}\dot{\boldsymbol{R}}_i\cdot\nabla_{\boldsymbol{R}}\,\delta(\boldsymbol{r}-\boldsymbol{R}_i(t))\delta(\boldsymbol{v}-\boldsymbol{V}_i(t))\\ &\quad -\sum_{i=1}^{N}\dot{\boldsymbol{V}}_i\cdot\nabla_{\boldsymbol{V}}\,\delta(\boldsymbol{r}-\boldsymbol{R}_i(t))\delta(\boldsymbol{v}-\boldsymbol{V}_i(t))\\ &= -\sum_{i=1}^{N}\boldsymbol{V}_i\cdot\nabla_{\boldsymbol{R}}\,\delta(\boldsymbol{r}-\boldsymbol{R}_i(t))\delta(\boldsymbol{v}-\boldsymbol{V}_i(t))\end{aligned}$$

$$-\sum_{i=1}^{N}\frac{q_\sigma}{m_\sigma}\left\{\boldsymbol{E}^{\mathrm{m}}[\boldsymbol{R}_i(t),t]+\frac{\boldsymbol{V}_i}{c}\times\boldsymbol{B}^{\mathrm{m}}[\boldsymbol{R}_i(t),t]\right\}$$
$$\cdot\nabla_{\boldsymbol{V}}\delta(\boldsymbol{r}-\boldsymbol{R}_i(t))\delta(\boldsymbol{v}-\boldsymbol{V}_i(t)) \tag{2.10}$$

Due to property $a\delta(a-b)=b\delta(a-b)$ of the delta function, one can replace $\boldsymbol{R}_i(t)$ by $\boldsymbol{r}$ and $\boldsymbol{V}_i(t)$ by $\boldsymbol{v}$. Also $\sum_{i=1}^{N}\delta(\boldsymbol{r}-\boldsymbol{R}_i(t))\delta(\boldsymbol{v}-\boldsymbol{V}_i(t))$ can again be identified as $n_\sigma(\boldsymbol{r},\boldsymbol{v},t)$, Eq. (2.1), so that (2.10) can be written further as

$$\boxed{\frac{\partial n_\sigma(\boldsymbol{r},\boldsymbol{v},t)}{\partial t}+\boldsymbol{v}\cdot\nabla_{\boldsymbol{r}}n_\sigma+\frac{q_\sigma}{m_\sigma}\left(\boldsymbol{E}^{\mathrm{m}}(\boldsymbol{r},t)+\frac{\boldsymbol{v}}{c}\times\boldsymbol{B}^{\mathrm{m}}(\boldsymbol{r},t)\right)\cdot\nabla_{\boldsymbol{v}}n_\sigma=0,} \tag{2.11}$$

which is the famous Klimontovich equation, see e.g. [37, 11, 51]. This equation describes the exact orbits of each and every particle in the plasma. Provided given initial conditions and initial fields, together with Maxwell's equations (2.6) to (2.9) the set of equations is closed and in principle allows the evaluation of densities and fields indefinitely in a deterministic way. Making use of the convective derivative in phase space

$$\frac{\mathrm{D}}{\mathrm{D}t}=\partial t+\left.\frac{\mathrm{d}\boldsymbol{r}}{\mathrm{d}t}\right|_{\mathrm{orbit}}\cdot\nabla_{\boldsymbol{r}}+\left.\frac{\mathrm{d}\boldsymbol{v}}{\mathrm{d}t}\right|_{\mathrm{orbit}}\cdot\nabla_{\boldsymbol{v}}, \tag{2.12}$$

the Klimontovich equation can be written compactly as [51]

$$\frac{\mathrm{D}n_\sigma(\boldsymbol{r},\boldsymbol{v},t)}{\mathrm{D}t}=0. \tag{2.13}$$

From a practical computational point of view one can neither process these equations which are by far too detailed, nor is it necessary to obtain the information of each and every particle orbit for the description of the evolution of a plasma. From here, the much more useful kinetic equation is obtained by taking an ensemble average of the Klimontovich equation.

The ensemble average $\langle\ldots\rangle$ over the possible realisations of a plasma is a means of replacing the spiky functions $n_\sigma(\boldsymbol{r},\boldsymbol{v},t)$ by smooth distribution function $f_\sigma(\boldsymbol{r},\boldsymbol{v},t)\equiv\langle n_\sigma(\boldsymbol{r},\boldsymbol{v},t)\rangle$, being the number of particles of plasma species σ per unit configuration space and unit velocity space [51]. Letting $\delta n_\sigma(\boldsymbol{r},\boldsymbol{v},t)$, $\delta\boldsymbol{E}(\boldsymbol{r},\boldsymbol{v},t)$ and $\delta\boldsymbol{B}(\boldsymbol{r},\boldsymbol{v},t)$ be the deviation from the ensemble averaged particle density and electromagnetic fields, respectively,

$$n_\sigma(\boldsymbol{r},\boldsymbol{v},t)=f_\sigma(\boldsymbol{r},\boldsymbol{v},t)+\delta n_\sigma(\boldsymbol{r},\boldsymbol{v},t), \tag{2.14}$$
$$\boldsymbol{E}^{\mathrm{m}}(\boldsymbol{r},\boldsymbol{v},t)=\boldsymbol{E}(\boldsymbol{r},\boldsymbol{v},t)+\delta\boldsymbol{E}^{\mathrm{m}}(\boldsymbol{r},\boldsymbol{v},t), \tag{2.15}$$
$$\boldsymbol{B}^{\mathrm{m}}(\boldsymbol{r},\boldsymbol{v},t)=\boldsymbol{B}(\boldsymbol{r},\boldsymbol{v},t)+\delta\boldsymbol{B}^{\mathrm{m}}(\boldsymbol{r},\boldsymbol{v},t), \tag{2.16}$$

so that by definition $\langle \delta n_\sigma \rangle = \langle \delta \boldsymbol{E}^{\mathrm{m}} \rangle = \langle \delta \boldsymbol{B}^{\mathrm{m}} \rangle = 0$, substituting (2.14) to (2.16) into (2.11) and taking the ensemble average, the plasma kinetic equation [51]

$$\boxed{\frac{\partial f_\sigma(\boldsymbol{r},\boldsymbol{v},t)}{\partial t} + \boldsymbol{v}\cdot\nabla_{\boldsymbol{r}} f_\sigma + \frac{q_\sigma}{m_\sigma}\left(\boldsymbol{E} + \frac{\boldsymbol{v}}{c}\times\boldsymbol{B}\right)\cdot\nabla_{\boldsymbol{v}} f_\sigma = Q_\sigma} \tag{2.17}$$

with source term

$$Q_\sigma = -\frac{q_\sigma}{m_\sigma}\left\langle \left(\delta\boldsymbol{E} + \frac{\boldsymbol{v}}{c}\times\delta\boldsymbol{B}\right)\cdot\nabla_{\boldsymbol{v}}\delta n_\sigma \right\rangle, \tag{2.18}$$

describing the discrete particle effects of the plasma, i.e. the collisions, is obtained. The ensemble averaged fields $\boldsymbol{E}$ and $\boldsymbol{B}$ again satisfy Maxwell's equations (2.6) to (2.9), where due to the linearity of the equations, one can simply replace the microscopic fields by the ensemble averaged fields. Taking velocity space moments of the ensemble averaged distribution function f_σ instead of the spiky density function n_σ, one obtains the ensemble averaged density and current [51],

$$\varrho(\boldsymbol{r},t) = \langle \varrho^{\mathrm{m}} \rangle = \sum_{\sigma=\mathrm{e,i}} q_\sigma \int_{\mathbb{R}^3} \mathrm{d}^3 v\, f_\sigma(\boldsymbol{r},\boldsymbol{v},t), \tag{2.19}$$

$$\boldsymbol{j}(\boldsymbol{r},t) = \langle \boldsymbol{j}^{\mathrm{m}} \rangle = \sum_{\sigma=\mathrm{e,i}} q_\sigma \int_{\mathbb{R}^3} \mathrm{d}^3 v\, \boldsymbol{v} f_\sigma(\boldsymbol{r},\boldsymbol{v},t). \tag{2.20}$$

Again, the set of equations is closed.

At this point it is apparent how single particle orbits enter the statistical description of a whole plasma species. This motivates the close examination of particle orbits and drifts in a prescribed electromagnetic field in the next section. The description of the motion of charged particles due to the Lorentz force will be shown to be somewhat simplified by the so-called guiding centre or adiabatic approximation. The guiding centre drift velocity $\dot{\boldsymbol{R}}$ could be obtained by gyro-averaging of the equations of motion in such a way that the system of second order equations is transformed to a first order system with separate parts for the slow drift motion and the fast oscillatory gyromotion [63]. An alternative systematic approach is a coordinate transformation to guiding centre coordinates in the single particle Lagrangian and expanding fields and potentials in the small parameter $\epsilon \sim \varrho/L$ [44], L representing the scale length of the magnetic field. Drifts to various orders of ϵ are obtained from the Euler-Lagrange equations of the expanded Lagrangian. The guiding centre drift velocity finally enters the kinetic equation as the configuration space part of the phase space velocity $\dot{z}^i$, giving the gyrokinetic equation. The kinetic equation is simplified substantially by introducing phase space coordinates that are invariants of the

motion. Finally, the kinetic equation is formulated for phase space coordinates made up of velocity components parallel and perpendicular to the magnetic field, which are the appropriate coordinates for the collision operator. It will be shown how to solve the linearised gyrokinetic equation by the method of characteristics [33] for a 1-D Galilean-invariant, hence charge conserving collision operator in Appendix A.

2.2 Guiding centre Approximation

2.2.1 Single Particle Motion in an Electromagnetic Field

Newton's equation of motion for a particle with charge q and mass m in an electromagnetic field is given by

$$\frac{\mathrm{d}\boldsymbol{p}}{\mathrm{d}t} = q\left(\boldsymbol{E}(\boldsymbol{r},t) + \frac{\dot{\boldsymbol{r}}}{c}\times\boldsymbol{B}(\boldsymbol{r},t)\right). \tag{2.21}$$

It follows from the non-relativistic limit of the exact Lagrangian of a charged particle in an electromagnetic field, see e.g. [20, p. 179],

$$\mathcal{L}(\boldsymbol{r},\boldsymbol{v},t) = -mc^2\sqrt{1-\frac{v(t)^2}{c^2}} - q\,\Phi(\boldsymbol{r},t) + \frac{q}{c}\,\boldsymbol{v}\cdot\boldsymbol{A}(\boldsymbol{r},t), \tag{2.22}$$

which, except for an additive constant $-mc^2$, is, e.g. [18, p. 73],

$$\mathcal{L}(\boldsymbol{r},\dot{\boldsymbol{r}},t) \overset{(v\ll c)}{=} \frac{m}{2}\dot{\boldsymbol{r}}^2 - q\,\Phi(\boldsymbol{r},t) + \frac{q}{c}\,\dot{\boldsymbol{r}}\cdot\boldsymbol{A}(\boldsymbol{r},t). \tag{2.23}$$

The particle's equation of motion is Euler-Lagrange's equation $\mathrm{d}(\partial\mathcal{L}/\partial\dot{\boldsymbol{r}})/\,\mathrm{d}t = \partial\mathcal{L}/\partial\boldsymbol{r}$, following from Hamilton's principle,

$$\delta\int_{t_1}^{t_2}\mathrm{d}t\,\mathcal{L}(\boldsymbol{r},\dot{\boldsymbol{r}},t) = 0. \tag{2.24}$$

Evaluated explicitly, the left and right hand sides are

$$\frac{\mathrm{d}}{\mathrm{d}t}\frac{\partial\mathcal{L}}{\partial\dot{\boldsymbol{r}}} = m\ddot{\boldsymbol{r}} + \frac{q}{c}\frac{\mathrm{d}}{\mathrm{d}t}\boldsymbol{A}(\boldsymbol{r},t) = m\ddot{\boldsymbol{r}} + (\dot{\boldsymbol{r}}\cdot\nabla)\boldsymbol{A}(\boldsymbol{r},t) + \frac{\partial}{\partial t}\boldsymbol{A}(\boldsymbol{r},t),$$

$$\nabla\mathcal{L} = -q\nabla\Phi(\boldsymbol{r},t) + \frac{q}{c}\nabla(\dot{\boldsymbol{r}}\cdot\boldsymbol{A}(\boldsymbol{r},t)).$$

Expressing the fields by their potentials $\boldsymbol{E}(\boldsymbol{r},t) = -\nabla\Phi(\boldsymbol{r},t) - (\partial\boldsymbol{A}/\partial t)/c$ and $\boldsymbol{B}(\boldsymbol{r},t) = \nabla\times\boldsymbol{A}(\boldsymbol{r},t)$, it immediately follows that the terms where the del operator acts on the vector potential give the magnetic component of the Lorentz-

force,

$$\frac{q}{c}\left[\nabla\left(\dot{\boldsymbol{r}}\cdot\boldsymbol{A}\right)-\left(\dot{\boldsymbol{r}}\cdot\nabla\right)\boldsymbol{A}\right]=\frac{q}{c}\dot{\boldsymbol{r}}\times\left(\nabla\times\boldsymbol{A}\right)=\frac{q}{c}\dot{\boldsymbol{r}}\times\boldsymbol{B},$$

so that the equations of motion are as expected given by the Lorentz force law,

$$m\ddot{\boldsymbol{r}}=q\left(\boldsymbol{E}(\boldsymbol{r},t)+\frac{\dot{\boldsymbol{r}}}{c}\times\boldsymbol{B}(\boldsymbol{r},t)\right). \tag{2.25}$$

Integrals of motion can be found if the potentials have symmetries. In cylindrical geometry $(x^1,x^2,x^3)=(r,\vartheta,z)$, the Lagrangian (2.23) becomes

$$\begin{aligned}\mathcal{L}(r,z,\dot{r},\dot{\vartheta},\dot{z},t)&=\frac{m}{2}g_{ij}\dot{x}^i\dot{x}^j-e\,\Phi(x^i,t)+\frac{e}{c}g_{ij}\dot{x}^iA^j(x^i,t)\\&=\frac{m}{2}\left(\dot{r}^2+r^2\dot{\vartheta}^2+\dot{z}^2\right)-e\,\Phi(x^i,t)+\frac{e}{c}\left(\dot{r}A^r+r^2\dot{\vartheta}A^\vartheta+\dot{z}A^z\right)\\&=\frac{m}{2}\left(\dot{r}^2+r^2\dot{\vartheta}^2+\dot{z}^2\right)-e\,\Phi(r,\vartheta,z,t)+\frac{e}{c}\left(\dot{r}\hat{A}_r+r\dot{\vartheta}\hat{A}_\vartheta+\dot{z}\hat{A}_z\right),\end{aligned} \tag{2.26}$$

where the over-hat denotes the physical vector components of the vector potential. If the system has axial symmetry, i.e. $\Phi=\Phi(r,z,t)$ and $\boldsymbol{A}=\boldsymbol{A}(r,z,t)$, the azimuth ϑ is a cyclic coordinate and the corresponding canonical momentum is invariant,

$$p_\vartheta=\frac{\partial\mathcal{L}}{\partial\dot{\vartheta}}=mr^2\dot{\vartheta}+\frac{e}{c}r\hat{A}_\vartheta=\text{const.} \tag{2.27}$$

If the potentials have no explicit dependency on time, neither has the Lagrangian, in which case the energy is conserved,

$$\begin{aligned}\mathcal{H}&=\sum_i\frac{\partial\mathcal{L}}{\partial\dot{x}^i}\dot{x}^i-\mathcal{L}=E\\&=\frac{m}{2}\left(\dot{r}^2+r^2\dot{\vartheta}^2+\dot{z}^2\right)+e\,\Phi(r,\vartheta,z)=\text{const.}\end{aligned} \tag{2.28}$$

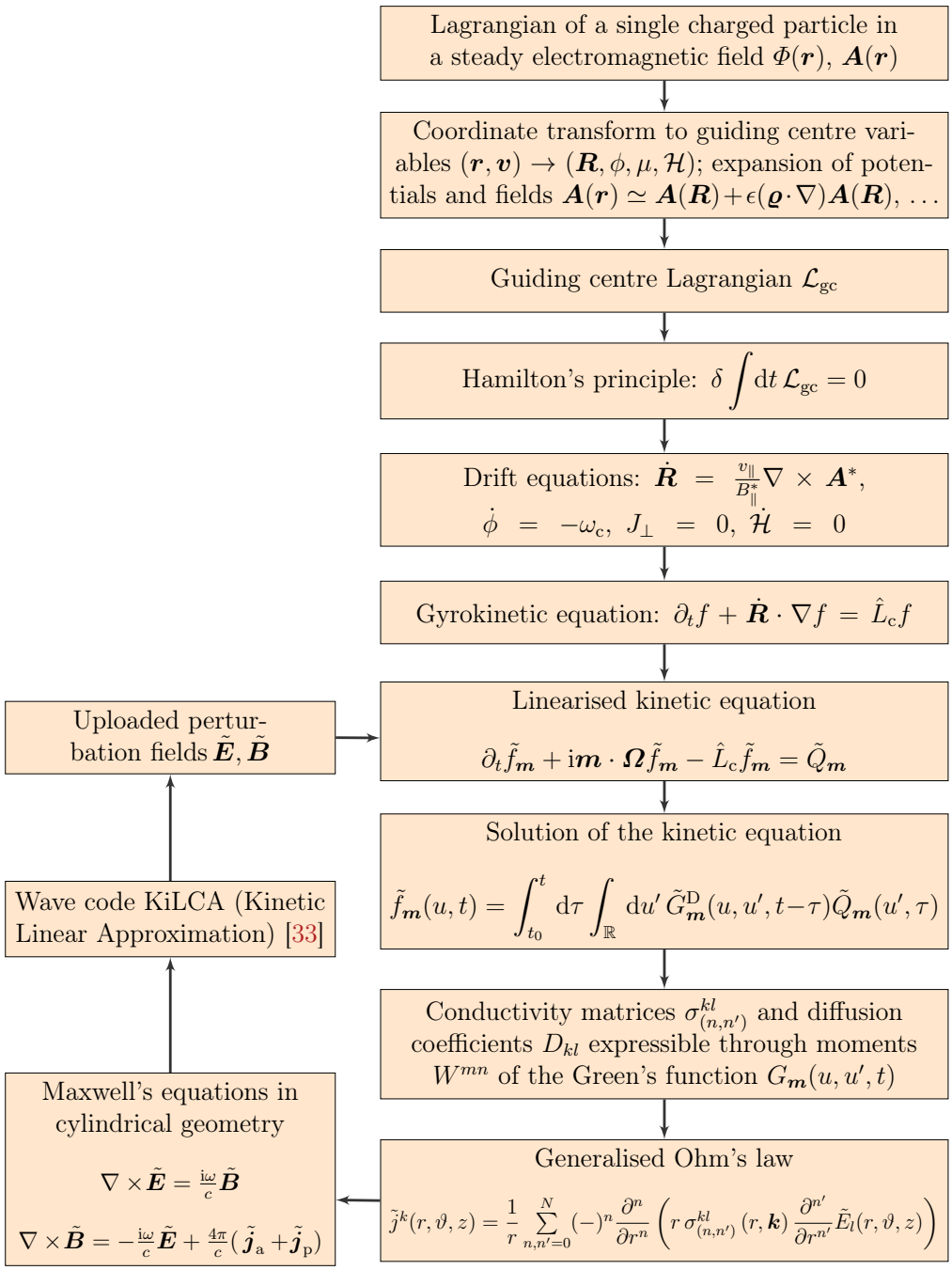

Figure 2.1: Schematic diagram of the quasilinear plasma-RMP interaction model

2.2.2 Guiding centre Lagrangian

The equation of motion for a charged particle in an electromagnetic field (2.25) can only be solved analytically if the field possesses symmetries or is static [47]. In the general case of an arbitrarily complicated field geometry, approximations to the exact integrals of motion have to be found.

If the electromagnetic fields vary slowly and have weak variations in space, or to be more precise, if time scales are large compared to a gyroperiod $2\pi/\omega_c$ and in addition perpendicular length scales are large compared to a gyroradius $\varrho = v_\perp/\omega_c$, the necessary conditions for the guiding-centre approximation are met. In principle, a guiding centre approximation is a method to average out the fast gyromotion of the equations of motion. What remains are the drift equations describing the gyroaveraged motion of a single charged particle in prescribed fields. In order to derive these drifts one can either heuristically study the equations of motion resulting from the Lorentz force law for various field configurations separately, i.e. for a solely homogeneous magnetic field, an additional electric field, for curved field lines, inhomogeneous fields, fields varying in time, etc., separate the slowly varying drift from the fast oscillatory gyromotion and finally put the parts together. Another approach is to gyroaverage the exact second order system of equations of motion to a system of first order equations with a clear separation of drift and oscillatory parts [63, 47]. Alternatively, one may start from the Lagrangian of a single charged particle, Eq. (2.23), which is transformed to guiding centre variables and expanded to several orders in the small parameter $\epsilon = \varrho/L$. The differences in the methods are subtle and vary e.g. in the application of Hamiltonian [43] and non-Hamiltonian formulations, see e.g. the Northrop Lagrangian formulation [52, 9]. In addition, the methodology of the separation of the guiding centre motion from the actual particle motion differs from the application of averaging techniques for second order differential equations developed by Bogolyubov, see e.g. [6] or Appendix 1 of [47], to a variational approach for a guiding centre Lagrangian [44], which relies on fundamental and well known principles from the study of Theoretical Mechanics. To explain the method, in the following the guiding centre Lagrangian and the corresponding Euler-Lagrange equations of motion, i.e. the drift motion is derived, in close accordance to Littlejohn's work [44] but for a different set of generalised coordinates. Here, a complete derivation is given and a lot more intermediate steps than in the original paper [44] are shown to ease the reproduction.

In the following we focus on the particle motion in a steady electromagnetic field. The canonical Hamiltonian of a particle in a steady electromagnetic field

follows from the Lagrangian (2.23) by the Legendre transformation

$$\mathcal{H}(\boldsymbol{r},\boldsymbol{p},t)=\sum_{i=1}^{3}p_i\dot{r}_i(\boldsymbol{r},\boldsymbol{p},t)-\mathcal{L}(\boldsymbol{r},\dot{\boldsymbol{r}}(\boldsymbol{r},\boldsymbol{p},t),t), \tag{2.29}$$

where $\boldsymbol{p}$ is the canonical momentum

$$\boldsymbol{p}=\frac{\partial\mathcal{L}}{\partial\dot{\boldsymbol{r}}}=m\dot{\boldsymbol{r}}+\frac{e}{c}\boldsymbol{A}(\boldsymbol{r}) \tag{2.30}$$

being related to the kinematic momentum by

$$\boldsymbol{p}_{\text{kin}}=m\dot{\boldsymbol{r}}=\boldsymbol{p}-\frac{e}{c}\boldsymbol{A}. \tag{2.31}$$

Thus it follows for the Hamiltonian of a charged particle, see e.g. [61],

$$\begin{aligned}\mathcal{H}&=\sum_{i=1}^{3}\frac{p_i}{m}\left(p_i-\frac{e}{c}A_i\right)-\frac{1}{2m}\left(p_i-\frac{e}{c}A_i\right)^2+e\,\Phi-\frac{e}{mc}\sum_{i=1}^{3}\left(p_i-\frac{e}{c}A_i\right)A_i\\&=\frac{1}{2m}\left(\boldsymbol{p}-\frac{e}{c}\boldsymbol{A}(\boldsymbol{r})\right)^2+e\,\Phi(\boldsymbol{r}),\end{aligned} \tag{2.32}$$

which in this case is simply the total energy $E=m\dot{\boldsymbol{r}}^2/2+e\,\Phi=\text{const}$ that in the case of time-independent fields, i.e. $\boldsymbol{A}=\boldsymbol{A}(\boldsymbol{r})$ and $\Phi=\Phi(\boldsymbol{r})$ is a constant of motion [47]. In the following, the phase space Lagrangian is introduced from which result the equations of motion in phase space by a variation over all phase space coordinates and which equals the Lagrangian (2.23) of the configuration-space variables in value [9],

$$\mathcal{L}(\boldsymbol{r},\boldsymbol{v},\dot{\boldsymbol{r}},\dot{\boldsymbol{v}},t)=\boldsymbol{p}(\boldsymbol{r},\boldsymbol{v},t)\cdot\dot{\boldsymbol{r}}-\mathcal{H}(\boldsymbol{r},\boldsymbol{p}(\boldsymbol{r},\boldsymbol{v},t),t). \tag{2.33}$$

Here, no new symbol for this Lagrangian has been introduced, and in the following $\mathcal{L}$ shall denote the phase space Lagrangian, if not explicitly said otherwise. For this choice of non-canonical phase space coordinates $(\boldsymbol{r},\boldsymbol{v})$, the phase space Lagrangian consequently is [44]

$$\mathcal{L}(\boldsymbol{r},\dot{\boldsymbol{r}},\boldsymbol{v})=\left(m\boldsymbol{v}+\frac{e}{\epsilon c}\boldsymbol{A}(\boldsymbol{r})\right)\cdot\dot{\boldsymbol{r}}-\left(\frac{m\boldsymbol{v}^2}{2}+e\,\Phi(\boldsymbol{r})\right), \tag{2.34}$$

where an adiabatic ordering parameter ϵ has been introduced for the electromagnetic potential. At this point one should not identify $\dot{\boldsymbol{r}}$ by $\boldsymbol{v}$, coordinates and velocities being independent of each other.[1]

[1] "This is because the variational principle selects the physical motion, out of all conceivable

In the following, the particle velocity is decomposed into its components parallel and perpendicular to the magnetic field $\boldsymbol{v} = v_\parallel \hat{\boldsymbol{h}} + v_\perp \hat{\boldsymbol{c}}$ and a transformation to guiding centre variables is performed [44],

$$\boldsymbol{r} = \boldsymbol{R} + \boldsymbol{\varrho} = \boldsymbol{R} + \epsilon \frac{v_\perp}{\omega_\mathrm{c}} \hat{\boldsymbol{a}}. \tag{2.35}$$

Here, $(v_\perp/\omega_\mathrm{c})\,\hat{\boldsymbol{a}}$ is the gyroradius $\boldsymbol{\varrho}$, i.e. the particle position relative to the guiding centre $\boldsymbol{R}$ and $\hat{\boldsymbol{h}} = \boldsymbol{B}/\left\|\boldsymbol{B}\right\|$ is a unit vector along the magnetic field line. The unit vectors $\hat{\boldsymbol{a}}$, $\hat{\boldsymbol{h}}$ and $\hat{\boldsymbol{c}}$ form an orthonormal basis, $\hat{\boldsymbol{a}} = \hat{\boldsymbol{h}} \times \hat{\boldsymbol{c}}$ rotating relative to a fixed orthonormal basis $\hat{\boldsymbol{e}}_1 \times \hat{\boldsymbol{e}}_2 = \hat{\boldsymbol{h}}$, see Fig. 2.2, where one can read off the relation between the bases depending on the gyrophase ϕ:

$$\hat{\boldsymbol{a}} = \cos\phi\, \hat{\boldsymbol{e}}_1 - \sin\phi\, \hat{\boldsymbol{e}}_2, \tag{2.36}$$

$$\hat{\boldsymbol{c}} = -\sin\phi\, \hat{\boldsymbol{e}}_1 - \cos\phi\, \hat{\boldsymbol{e}}_2. \tag{2.37}$$

The gyrofrequency $\omega_\mathrm{c}(\boldsymbol{r})$, being itself a function of coordinates through the magnetic field thus has an implicit time dependence and is expanded also in small gyroradii, though, for readability, this functionality is suppressed in the following.

Here, $z = (\boldsymbol{R}, \phi, J_\perp, \mathcal{H})$ are chosen as phase space coordinates, differing from Littlejohn's phase space coordinates in so far that not the Hamiltonian but the parallel velocity is used as an independent variable. By substitution of Eq. (2.35) into the phase space Lagrangian one obtains[2]

$$\begin{aligned}\mathcal{L}(\boldsymbol{R}, \dot{\boldsymbol{R}}, \phi, J_\perp, \mathcal{H}) = &\left[m\left(v_\parallel \hat{\boldsymbol{h}} + v_\perp \hat{\boldsymbol{c}}\right) + \frac{e}{\epsilon c}\boldsymbol{A}\left(\boldsymbol{R} + \epsilon \frac{v_\perp}{\omega_\mathrm{c}}\hat{\boldsymbol{a}}\right)\right] \\ &\cdot \left(\dot{\boldsymbol{R}} + \epsilon \frac{\mathrm{d}}{\mathrm{d}t}\frac{v_\perp}{\omega_\mathrm{c}}\hat{\boldsymbol{a}}\right) - \mathcal{H}.\end{aligned} \tag{2.38}$$

The potentials are expanded around the guiding centre in small Larmor radii using $\|\boldsymbol{\varrho}\| \ll \|\boldsymbol{R}\|$,

$$\begin{aligned}\boldsymbol{A}\left(\boldsymbol{R} + \epsilon \frac{v_\perp}{\omega_\mathrm{c}}\hat{\boldsymbol{a}}\right) &= \sum_{n=0}^{\infty} \left(\epsilon \frac{v_\perp}{\omega_\mathrm{c}}\hat{\boldsymbol{a}} \cdot \nabla\right)^n \boldsymbol{A}(\boldsymbol{R}) \\ &= \boldsymbol{A}(\boldsymbol{R}) + \left(\epsilon \frac{v_\perp}{\omega_\mathrm{c}}\hat{\boldsymbol{a}} \cdot \nabla\right)\boldsymbol{A}(\boldsymbol{R}) + \mathcal{O}(\epsilon^2),\end{aligned} \tag{2.39}$$

motions, as the one to make its action integral stationary. Although $\boldsymbol{v} = \dot{\boldsymbol{x}}$ on the physical motion, this will not be true along all conceivable paths through $(\boldsymbol{x}, \boldsymbol{v})$ space." [44]

[2] Here the invariance of the Lagrangian under reversible coordinate transformations is used, which is discussed in detail below.

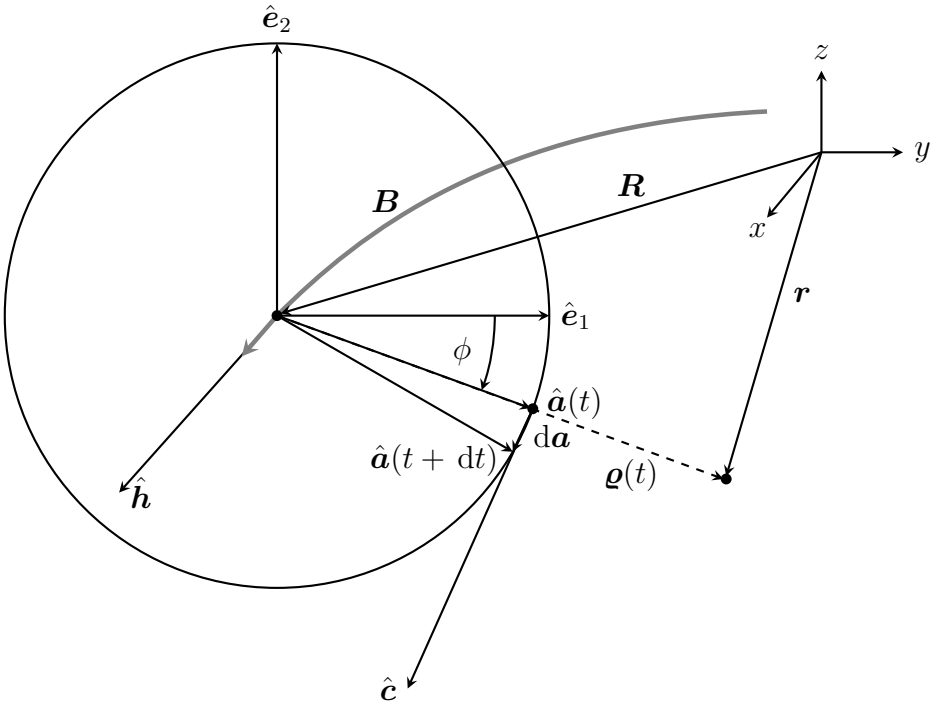

Figure 2.2: Geometry of the gyromotion. Particle position $\boldsymbol{r}$, guiding centre position $\boldsymbol{R}$ and local orthonormal field-aligned bases $(\hat{\boldsymbol{e}}_1, \hat{\boldsymbol{e}}_2, \hat{\boldsymbol{h}})$, the fixed frame, and $(\hat{\boldsymbol{a}}, \hat{\boldsymbol{h}}, \hat{\boldsymbol{c}})$. The gyration is clockwise (so in the mathematical negative sense), giving $\mathrm{d}\boldsymbol{a} = \dot{\phi}\,\hat{\boldsymbol{c}}\,\mathrm{d}t$ and for the pseudo-vector $\mathrm{d}\boldsymbol{\phi}/\,\mathrm{d}t = \boldsymbol{\omega}_\mathrm{c} \propto -\boldsymbol{B}$, wherefrom follows $\boldsymbol{\omega}_\mathrm{c} = -e\boldsymbol{B}/mc$.

$$\Phi\left(\boldsymbol{R}+\epsilon\frac{v_\perp}{\omega_\mathrm{c}}\hat{\boldsymbol{a}}\right)=\Phi(\boldsymbol{R})+\epsilon\frac{v_\perp}{\omega_\mathrm{c}}(\hat{\boldsymbol{a}}\cdot\nabla)\Phi(\boldsymbol{R})+\mathcal{O}(\epsilon^2). \tag{2.40}$$

Inserting the expanded potentials into (2.38) gives

$$\begin{aligned}\mathcal{L}(\boldsymbol{R},\dot{\boldsymbol{R}},\phi,J_\perp,\mathcal{H})=\Bigg[&m\left(v_\parallel\hat{\boldsymbol{h}}+v_\perp\hat{\boldsymbol{c}}\right)+\frac{e}{\epsilon c}\boldsymbol{A}(\boldsymbol{R})+\left(\frac{v_\perp}{\omega_\mathrm{c}}\hat{\boldsymbol{a}}\cdot\nabla\right)\frac{e}{c}\boldsymbol{A}(\boldsymbol{R})\\&+\mathcal{O}(\epsilon)\Bigg]\cdot\left(\dot{\boldsymbol{R}}+\epsilon\frac{\mathrm{d}}{\mathrm{d}t}\frac{v_\perp}{\omega_\mathrm{c}}\hat{\boldsymbol{a}}+\mathcal{O}(\epsilon^2)\right)-\mathcal{H}.\end{aligned} \tag{2.41}$$

One should note that for $\mathcal{O}(\epsilon)$ terms also $B=B(\boldsymbol{R}+\epsilon\boldsymbol{\varrho})$ as well as $v_\parallel(\boldsymbol{R}+\epsilon\boldsymbol{\varrho})$ is expanded, which for the sake of clarity is suppressed in the notation. Since for the choice of guiding centre variables $z=(\boldsymbol{R},\phi,J_\perp,\mathcal{H})$ the Hamiltonian is considered an independent variable as indicated in Eq. (2.41) but the parallel velocity is not, one has to consider

$$\begin{aligned}v_\parallel=\pm\Bigg\{\frac{2}{m}\Bigg[&\mathcal{H}-\mu B(\boldsymbol{R})-\mu\epsilon\frac{v_\perp}{\omega_\mathrm{c}}(\hat{\boldsymbol{a}}\cdot\nabla)B(\boldsymbol{R})\\&-e\Phi(\boldsymbol{R})-e\epsilon\frac{v_\perp}{\omega_\mathrm{c}}\hat{\boldsymbol{a}}\cdot\nabla\Phi(\boldsymbol{R})+\mathcal{O}(\epsilon^2)\Bigg]\Bigg\}^{1/2}.\end{aligned} \tag{2.42}$$

To lowest order ϵ^{-1}, the guiding centre Lagrangian is simply

$$\mathcal{L}_{\epsilon^{-1}}=\frac{e}{c\epsilon}\boldsymbol{A}(\boldsymbol{R})\cdot\dot{\boldsymbol{R}}. \tag{2.43}$$

The $\mathcal{O}(1)$ Lagrangian, according to Eq. (2.41) is

$$\begin{aligned}\mathcal{L}_{\epsilon^0}=&\left[m\left(v_\parallel\hat{\boldsymbol{h}}+v_\perp\hat{\boldsymbol{c}}\right)+\frac{mv_\perp}{B}\hat{\boldsymbol{a}}\cdot\nabla\boldsymbol{A}(\boldsymbol{R})\right]\cdot\dot{\boldsymbol{R}}\\&+\frac{\mathrm{d}}{\mathrm{d}t}\left(\frac{mv_\perp}{B}\hat{\boldsymbol{a}}\right)\cdot\boldsymbol{A}(\boldsymbol{R})-\mathcal{H}.\end{aligned} \tag{2.44}$$

The equations of motion are invariant under gauge transformations which mediate between equivalent Lagrangians,

$$\mathcal{L}^*=\mathcal{L}+\frac{\mathrm{d}f(z,t)}{\mathrm{d}t}. \tag{2.45}$$

In fact, the transformed Lagrangian does not leave the action functional $S[z]=\int_{t_1}^{t_2}\mathrm{d}t\,\mathcal{L}(z,\dot{z},t)$ invariant,

$$\begin{aligned}S^*[z]&=\int_{t_1}^{t_2}\mathrm{d}t\,\mathcal{L}^*(z,\dot{z},t)=\int_{t_1}^{t_2}\mathrm{d}t\,\mathcal{L}(z,\dot{z},t)+f(z(t_2),t_2)-f(z(t_1),t_1)\\&=S[z]+f(z(t_2),t_2)-f(z(t_1),t_1)\neq S[z],\end{aligned} \tag{2.46}$$

but its variation with the phase space trajectory $z(t)$, e.g. [18, p. 119],

$$\delta S^* = \delta S + \sum_{i=1}^{f} \left(\frac{\partial f}{\partial z_i}\right)_{t_2} \delta z_i(t_2) - \sum_{i=1}^{f} \left(\frac{\partial f}{\partial z_i}\right)_{t_1} \delta z_i(t_1) = \delta S, \tag{2.47}$$

where $\delta z_i(t_1) = \varepsilon\eta_i(t_1) = 0$ and $\delta z_i(t_2) = \varepsilon\eta_i(t_2) = 0$ has been used since the boundaries are held fixed during the variation. Such a total derivative of an arbitrary function of phase space variables and time, $f(z,t)$ can be identified in (2.44) as

$$f(z,t) = -\frac{mv_\perp}{B}\hat{\boldsymbol{a}} \cdot \boldsymbol{A}(\boldsymbol{R}), \tag{2.48}$$

see [44], so that adding the terms

$$\begin{aligned}\frac{\mathrm{d}f(z,t)}{\mathrm{d}t} &= -\frac{\mathrm{d}}{\mathrm{d}t}\left(\frac{mv_\perp}{B}\hat{\boldsymbol{a}}\right) \cdot \boldsymbol{A}(\boldsymbol{R}) - \frac{mv_\perp}{B}\hat{\boldsymbol{a}} \cdot (\dot{\boldsymbol{R}} \cdot \nabla)\boldsymbol{A}(\boldsymbol{R}) \\ &= -\frac{\mathrm{d}}{\mathrm{d}t}\left(\frac{mv_\perp}{B}\hat{\boldsymbol{a}}\right) \cdot \boldsymbol{A}(\boldsymbol{R}) - \frac{mv_\perp}{B}\hat{\boldsymbol{a}} \cdot \Big[(\nabla \boldsymbol{A}) \cdot \dot{\boldsymbol{R}} - \dot{\boldsymbol{R}} \times (\nabla \times \boldsymbol{A})\Big]\end{aligned} \tag{2.49}$$

to the $\mathcal{O}(1)$ Lagrangian leaves the equations of motion invariant. The last term of (2.49) can be identified with

$$\frac{mv_\perp}{B}\hat{\boldsymbol{a}} \cdot \dot{\boldsymbol{R}} \times \boldsymbol{B} = mv_\perp \hat{\boldsymbol{a}} \cdot \dot{\boldsymbol{R}} \times \hat{\boldsymbol{h}} = -mv_\perp \dot{\boldsymbol{R}} \cdot \hat{\boldsymbol{c}}, \tag{2.50}$$

i.e. the second term of Eq. (2.44). Thus, the $\mathcal{O}(1)$ Lagrangian simplifies to

$$\mathcal{L}_{\epsilon^0} = mv_\parallel \hat{\boldsymbol{h}} \cdot \dot{\boldsymbol{R}} - \mathcal{H}. \tag{2.51}$$

To $\mathcal{O}(\epsilon)$ the guiding centre Lagrangian is

$$\begin{aligned}\mathcal{L}_\epsilon = \epsilon \Bigg\{ &\left[-\frac{mv_\perp^2}{\omega_\mathrm{c} B^2}\nabla B(\hat{\boldsymbol{a}} \cdot \nabla)\boldsymbol{A}(\boldsymbol{R}) \cdot \hat{\boldsymbol{a}}\right] \cdot \dot{\boldsymbol{R}} + \left(\frac{mv_\perp^2}{\omega_\mathrm{c} B}\hat{\boldsymbol{a}} \cdot \nabla \boldsymbol{A} \cdot \hat{\boldsymbol{c}} + \frac{mv_\perp^2}{\omega_\mathrm{c}}\right)\dot{\phi} \\ &+ \left(\frac{mv_\perp}{\omega_\mathrm{c} B}\hat{\boldsymbol{a}} \cdot \nabla \boldsymbol{A} \cdot \hat{\boldsymbol{a}}\right) \dot{v}_\perp \Bigg\},\end{aligned} \tag{2.52}$$

where use has been made of $\dot{\hat{\boldsymbol{a}}} = \dot{\phi}\,\hat{\boldsymbol{c}}$, see Fig. 2.2. For this order also a total derivative $\mathrm{d}f(z,t)/\,\mathrm{d}t$ can be found [44],

$$f(z,t) = -\epsilon\frac{mv_\perp^2}{2\omega_\mathrm{c} B}\hat{\boldsymbol{a}} \cdot \nabla \boldsymbol{A} \cdot \hat{\boldsymbol{a}} \tag{2.53}$$

with

$$\frac{\mathrm{d}f(z,t)}{\mathrm{d}t} = -\epsilon\frac{mv_\perp\dot{v}_\perp}{\omega_\mathrm{c}B}\hat{\boldsymbol{a}}\cdot\nabla\boldsymbol{A}\cdot\hat{\boldsymbol{a}} + \epsilon\frac{mv_\perp^2}{\omega_\mathrm{c}B^2}(\nabla B\cdot\dot{\boldsymbol{R}})\hat{\boldsymbol{a}}\cdot\nabla\boldsymbol{A}\cdot\hat{\boldsymbol{a}} - \epsilon\frac{mv_\perp^2\dot{\phi}}{2\omega_\mathrm{c}B}\hat{\boldsymbol{c}}\cdot\nabla\boldsymbol{A}\cdot\hat{\boldsymbol{a}} - \epsilon\frac{mv_\perp^2\dot{\phi}}{2\omega_\mathrm{c}B}\hat{\boldsymbol{a}}\cdot\nabla\boldsymbol{A}\cdot\hat{\boldsymbol{c}} + \mathcal{O}(\epsilon^2) \tag{2.54}$$

Expanding the third term on the right hand side of Eq. (2.54) by using the dyadic identity $\boldsymbol{A}\cdot\nabla\boldsymbol{B}\cdot\boldsymbol{C} - \boldsymbol{C}\cdot\nabla\boldsymbol{B}\cdot\boldsymbol{A} = (\boldsymbol{A}\times\boldsymbol{C})\cdot(\nabla\times\boldsymbol{B})$, see e.g. [10], this term is rearranged to

$$\hat{\boldsymbol{c}}\cdot\nabla\boldsymbol{A}\cdot\hat{\boldsymbol{a}} = \hat{\boldsymbol{a}}\cdot\nabla\boldsymbol{A}\cdot\hat{\boldsymbol{c}} + \hat{\boldsymbol{h}}\cdot\boldsymbol{B}. \tag{2.55}$$

Altogether, the gauge transformation leaves only the term

$$\mathcal{L}_\epsilon = \frac{mv_\perp^2}{2\omega_\mathrm{c}}\dot{\phi} = J_\perp\dot{\phi}, \tag{2.56}$$

where the perpendicular adiabatic invariant $J_\perp = mv_\perp^2/2\omega_\mathrm{c}$ has been introduced. It is a result of the resulting Euler Lagrange equations that $J_\perp$, at least within this $\mathcal{O}(\epsilon)$ approximation, is an invariant. Of course, doing the expansion up to higher orders this invariance is no longer exact, yet still very accurate, being adiabatic.

Terms which result from the expansion of $v_\parallel(\boldsymbol{R}+\epsilon(v_\perp/\omega_\mathrm{c})\hat{\boldsymbol{a}})$, i.e.

$$\epsilon\frac{v_\perp}{\omega_\mathrm{c}v_\parallel}\hat{\boldsymbol{a}}\cdot[\mu\nabla B(\boldsymbol{R}) + e\nabla\Phi(\boldsymbol{R})]\hat{\boldsymbol{h}}\cdot\dot{\boldsymbol{R}} + \mathcal{O}(\epsilon^2) \tag{2.57}$$

have been intentionally left out since they lead to second order drifts only, see [44]. Collecting all orders from $\mathcal{O}(\epsilon^{-1})$ to $\mathcal{O}(\epsilon)$, one obtains the guiding centre Lagrangian (to order ϵ) [9],

$$\boxed{\mathcal{L}_\mathrm{gc}(\boldsymbol{R},\dot{\boldsymbol{R}},\phi,J_\perp,\mathcal{H}) = \left[mv_\parallel\hat{\boldsymbol{h}} + \frac{e}{c}\boldsymbol{A}(\boldsymbol{R})\right]\cdot\dot{\boldsymbol{R}} + J_\perp\dot{\phi} - \mathcal{H}} \tag{2.58}$$

At this point it is advantageous to notice that this Lagrangian, which followed from the transformation to guiding centre variables in the phase space Lagrangian (without the need of calculating a single explicit gyroaverage) is not a completely new result, if one compares this expression with the Lagrangian for the drift approximation of Morozov and Solev'ev [47], which has already been found in 1966 by the method of averaging,

$$\mathcal{L}_\mathrm{Mor} = \frac{e}{c}\dot{\boldsymbol{R}}\cdot\boldsymbol{A}^*, \quad \boldsymbol{A}^* = \boldsymbol{A} + \frac{mcv_\parallel}{eB}\boldsymbol{B}. \tag{2.59}$$

Evidently,

$$\mathcal{L}_{\mathrm{gc}}(\boldsymbol{R}, \dot{\boldsymbol{R}}, \phi, J_\perp, \mathcal{H}) = \mathcal{L}_{\mathrm{Mor}}(\boldsymbol{R}, \dot{\boldsymbol{R}}) + J_\perp \dot{\phi} - \mathcal{H}, \tag{2.60}$$

$\mathcal{L}_{\mathrm{Mor}}(\boldsymbol{R}, \dot{\boldsymbol{R}})$ being the configuration space part of the phase space Lagrangian $\mathcal{L}_{\mathrm{gc}}$, already yields the drift equations, see next section, apart from the conservation law for $J_\perp$, which in principle can also be found by considering separately the constancy of the magnetic moment of a current loop $\mu = IS/c = (e\omega_{\mathrm{c}})/(2\pi c) \cdot \pi\varrho^2 = (e\omega_{\mathrm{c}})/(2\pi c) \cdot \pi v_\perp^2/\omega_{\mathrm{c}}^2 = e v_\perp^2/(2c\omega_{\mathrm{c}}) = m v_\perp^2/2B$ for a gyrating particle with charge e (or the constancy of magnetic flux $\Phi_B = \int \boldsymbol{B} \cdot \mathrm{d}\boldsymbol{S} = \pi\varrho^2 B = \pi m^2 v_\perp^2 c^2/(e^2 B)$ through a gyrocircle). Such a separation of Lagrangians as in (2.60) is always possible if all terms of the full (in this case the phase space) Lagrangian are either dependent on the one or the other set of variables but no terms mixing these sets are present, see e.g. [18, p. 132].

Symbol	Physical Quantity/Function
$\boldsymbol{r} = \boldsymbol{R} + \boldsymbol{\varrho}$	Particle position
$\boldsymbol{\varrho}$	Gyroradius
$\boldsymbol{R}$	Guiding centre position
$\dot{\boldsymbol{R}}$	Guiding centre velocity
ϕ	Gyrophase
$J_\perp = m v_\perp^2/2\omega_{\mathrm{c}}$	Perp. adiabatic invariant
$\mathcal{L}_{\mathrm{gc}}(\boldsymbol{R}, \dot{\boldsymbol{R}}, \phi, J_\perp, \mathscr{H})$	Guiding centre Lagrangian
$\mathcal{L}_{\mathrm{Mor}}(\boldsymbol{R}, \dot{\boldsymbol{R}})$	Drift Lagrangian [47]
$S[\boldsymbol{R}] = \int \mathrm{d}t\, \mathcal{L}_{\mathrm{gc}}$	Guiding centre action functional
$\mathcal{H}(\boldsymbol{r}, \boldsymbol{p}, t)$	Charged-particle Hamiltonian
$\Phi^* = \Phi + (\mu/e)B$	Effective scalar potential
$\boldsymbol{A}^* = \boldsymbol{A} + (c/e) m v_\parallel \hat{\boldsymbol{h}}$	Effective vector potential

Table 2.1: Symbols used for the description of the guiding centre motion.

2.2.3 Drift Equations

The drift equations are the Euler-Lagrange equations of the guiding centre Lagrangian $\mathcal{L}_{\mathrm{gc}}(\boldsymbol{R}, \dot{\boldsymbol{R}}, t)$. Formally, Fréchet's functional derivative of the action functional w.r.t. variations of the guiding centre coordinates $\boldsymbol{R}$ has to vanish for the action $S[\boldsymbol{R}]$ to be stationary,

$$\frac{\delta S[\boldsymbol{R}]}{\delta \boldsymbol{R}(t)} \equiv \frac{\partial \mathcal{L}_{\mathrm{gc}}}{\partial \boldsymbol{R}} - \frac{\mathrm{d}}{\mathrm{d}t} \frac{\partial \mathcal{L}_{\mathrm{gc}}}{\partial \dot{\boldsymbol{R}}} = 0. \tag{2.61}$$

The derivation of the guiding centre drift equation is straight forward if one considers that the potentials and fields are now evaluated at the guiding centre position $\boldsymbol{R}$, not at the particle position $\boldsymbol{r}$, and that the nabla-operator also acts on this coordinate, $\nabla \equiv \nabla_{\boldsymbol{R}}$. Evaluating explicitly the left and right hand sides of the Euler-Lagrange equation, gives

$$\frac{\partial \mathcal{L}_{\mathrm{gc}}}{\partial \boldsymbol{R}} = m(\nabla v_\parallel)\hat{\boldsymbol{h}} \cdot \dot{\boldsymbol{R}} + m v_\parallel \nabla(\hat{\boldsymbol{h}} \cdot \dot{\boldsymbol{R}}) + \frac{e}{c}\nabla(\boldsymbol{A} \cdot \dot{\boldsymbol{R}}), \tag{2.62}$$

$$\frac{\mathrm{d}}{\mathrm{d}t}\frac{\partial \mathcal{L}_{\mathrm{gc}}}{\partial \dot{\boldsymbol{R}}} = \frac{\mathrm{d}}{\mathrm{d}t}\left(m v_\parallel \hat{\boldsymbol{h}} + \frac{e}{c}\boldsymbol{A}\right) = m\dot{v}_\parallel \hat{\boldsymbol{h}} + m v_\parallel (\dot{\boldsymbol{R}} \cdot \nabla)\hat{\boldsymbol{h}} + \frac{e}{c}(\dot{\boldsymbol{R}} \cdot \nabla)\boldsymbol{A}. \tag{2.63}$$

Since in the second and third term of (2.62) ∇ acts on $\hat{\boldsymbol{h}}$ and $\boldsymbol{A}$, respectively (and not on $\dot{\boldsymbol{R}}$) one can simply apply the BAC-CAB rule here giving $-e/c\dot{\boldsymbol{R}}\times(\nabla\times\boldsymbol{A})$ in the first case and an analogous term in the second, so that one obtains the Euler-Lagrange equation of motion for the guiding centre variable $\boldsymbol{R}$,

$$m\dot{v}_\parallel \hat{\boldsymbol{h}} - m v_\parallel \dot{\boldsymbol{R}} \times (\nabla \times \hat{\boldsymbol{h}}) - \frac{e}{c}\dot{\boldsymbol{R}} \times (\nabla \times \boldsymbol{A}) - m(\nabla v_\parallel)\hat{\boldsymbol{h}} \cdot \dot{\boldsymbol{R}} = \boldsymbol{0}. \tag{2.64}$$

Anticipating that $\hat{\boldsymbol{h}} \cdot \dot{\boldsymbol{R}} = v_\parallel$ (this will be shown below) and explicitly evaluating the gradient of the parallel velocity Eq. (2.42),

$$\nabla v_\parallel = -\frac{1}{m v_\parallel}(\mu \nabla B + e\nabla \Phi), \tag{2.65}$$

the Lagrange equation for $\boldsymbol{R}$ is simplified to

$$m\dot{v}_\parallel \hat{\boldsymbol{h}} - m v_\parallel \dot{\boldsymbol{R}} \times (\nabla \times \hat{\boldsymbol{h}}) - \frac{e}{c}\dot{\boldsymbol{R}} \times (\nabla \times \boldsymbol{A}) + \mu \nabla B + e\nabla \Phi = \boldsymbol{0}. \tag{2.66}$$

The guiding centre velocity $\dot{\boldsymbol{R}}$ can be isolated from this equation by taking the vector product with $\hat{\boldsymbol{h}}$ [9], giving

$$m v_\parallel \hat{\boldsymbol{h}} \times \left[\dot{\boldsymbol{R}} \times (\nabla \times \hat{\boldsymbol{h}})\right] + \frac{e}{c}\hat{\boldsymbol{h}} \times \left[\dot{\boldsymbol{R}} \times (\nabla \times \boldsymbol{A})\right] + (\mu \nabla B + e\nabla \Phi) \times \hat{\boldsymbol{h}} = \boldsymbol{0}. \tag{2.67}$$

Again using $v_\parallel = \hat{\boldsymbol{h}} \cdot \dot{\boldsymbol{R}}$ and expanding the double-vector products yields

$$\begin{aligned} m v_\parallel \dot{\boldsymbol{R}}\left[\hat{\boldsymbol{h}} \cdot (\nabla \times \hat{\boldsymbol{h}})\right] - m v_\parallel^2 \nabla \times \hat{\boldsymbol{h}} + \frac{e}{c}\dot{\boldsymbol{R}}\left[\hat{\boldsymbol{h}} \cdot (\nabla \times \boldsymbol{A})\right] - v_\parallel \frac{e}{c}(\nabla \times \boldsymbol{A}) \\ + (\mu \nabla B + e\nabla \Phi) \times \hat{\boldsymbol{h}} = \boldsymbol{0}, \end{aligned} \tag{2.68}$$

wherefrom $\dot{\boldsymbol{R}}$ can be isolated,

$$\dot{\boldsymbol{R}} = v_\parallel \frac{\nabla \times \boldsymbol{A} + \frac{c}{e} m v_\parallel \nabla \times \hat{\boldsymbol{h}} - \frac{1}{v_\parallel}\frac{c}{e}\nabla(\mu B + e\Phi) \times \hat{\boldsymbol{h}}}{\frac{c}{e} m v_\parallel \hat{\boldsymbol{h}} \cdot (\nabla \times \hat{\boldsymbol{h}}) + \hat{\boldsymbol{h}} \cdot (\nabla \times \boldsymbol{A})}. \tag{2.69}$$

The second and third term in the numerator can be combined as follows

$$\frac{c}{e} m v_\parallel \nabla \times \hat{\boldsymbol{h}} - \frac{1}{v_\parallel}\frac{c}{e}\nabla(\mu B + e\Phi) \times \hat{\boldsymbol{h}} = \nabla \times \left(\frac{c}{e} m v_\parallel(\boldsymbol{R})\hat{\boldsymbol{h}}(\boldsymbol{R})\right) \tag{2.70}$$

due to vector identity $\nabla \times (f\boldsymbol{A}) = f\nabla \times \boldsymbol{A} + \nabla f \times \boldsymbol{A}$ [10] and analogously the first term in the denominator can be expanded as follows,

$$\begin{aligned} \frac{c}{e} m v_\parallel (\nabla \times \hat{\boldsymbol{h}}) \cdot \hat{\boldsymbol{h}} &= \left\{ \nabla \times \left[\frac{c}{e} m v_\parallel(\boldsymbol{R})\hat{\boldsymbol{h}}(\boldsymbol{R})\right] + \frac{1}{v_\parallel}\frac{c}{e}\nabla(\mu B + e\Phi) \times \hat{\boldsymbol{h}} \right\} \cdot \hat{\boldsymbol{h}} \\ &= \nabla \times \left(\frac{c}{e} m v_\parallel \hat{\boldsymbol{h}}\right) \cdot \hat{\boldsymbol{h}}. \end{aligned} \tag{2.71}$$

Substituting these simplifications into the expression for $\dot{\boldsymbol{R}}$, Eq. (2.69) yields

$$\boxed{\dot{\boldsymbol{R}} = v_\parallel \frac{\nabla \times \left(\boldsymbol{A} + \frac{c}{e} m v_\parallel \hat{\boldsymbol{h}}\right)}{\nabla \times \left(\boldsymbol{A} + \frac{c}{e} m v_\parallel \hat{\boldsymbol{h}}\right) \cdot \hat{\boldsymbol{h}}} = v_\parallel \frac{\nabla \times \boldsymbol{A}^*}{\nabla \times \boldsymbol{A}^* \cdot \hat{\boldsymbol{h}}} = v_\parallel \frac{\boldsymbol{B}^*}{B_\parallel^*}} \tag{2.72}$$

This famous result can be found in [47, 44] and (similarly) in [9][3]. Here, the "effective electromagnetic fields"

$$\boldsymbol{E}^* = -\nabla \Phi^*, \qquad \boldsymbol{B}^* = \nabla \times \boldsymbol{A}^* \tag{2.73}$$

and "effective electromagnetic potentials"

$$e\Phi^* = e\Phi + \mu B, \qquad \boldsymbol{A}^* = \boldsymbol{A} + \frac{c}{e} m v_\parallel \hat{\boldsymbol{h}}, \tag{2.74}$$

first introduced by Morozov and Solev'ev in 1966 [47] have been used, which allow to write the equation of motion in a very compact form. One should note however, that all relevant drifts (apart from the polarisation drift since steady-state fields have been assumed from the very beginning) are contained in $\dot{\boldsymbol{R}} = v_\parallel \boldsymbol{B}^*/B_\parallel^*$, being hidden in the effective electromagnetic fields and potentials.

Up to here, the guiding centre velocity is exact to $\mathcal{O}(\epsilon)$ of the adiabatic ordering parameter. However at this point a subtlety arises if one compares this

[3] There, a local frame of reference was chosen moving with $\boldsymbol{V}_E = c\boldsymbol{E} \times \boldsymbol{B}/B^2$ giving an additional term $c\boldsymbol{E}^* \times \hat{\boldsymbol{h}}/B_\parallel^*$ in the expression for $\dot{\boldsymbol{R}}$.

expression with the expression for the guiding centre velocity most commonly used, namely $v_\parallel \boldsymbol{B}^*/B$. In the original paper of Morozov and Solev'ev [47] the authors claim that the drift equations are found if they limit themselves to the case $\hat{\boldsymbol{h}} \cdot (\nabla \times \hat{\boldsymbol{h}}) = 0$ without giving physical reasoning for this step, while obviously the guiding centre velocity becomes a lot simpler to handle by omitting the projection of curl $\hat{\boldsymbol{h}}$ onto the field line itself. Also Boozer shows in his famous paper on guiding centre drifts of 1980 [7], how one can arrive from the elementary expressions for single particle drifts in a plasma at the much more elegant $\boldsymbol{v}_{\mathrm{gc}} = (v_\parallel/B)[\boldsymbol{B} + \nabla \times (v_\parallel/\omega_{\mathrm{c}})\boldsymbol{B}]$, yet pointing out that neglecting the first order term in the averaged Jacobian J from the transformation $\mathrm{d}^3v = J\,\mathrm{d}E\,\mathrm{d}\mu\,\mathrm{d}\phi$, $\langle J \rangle = (B/m^2 v_\parallel)(1+(v_\parallel/\omega_{\mathrm{c}})\hat{\boldsymbol{h}}\cdot\nabla\times\hat{\boldsymbol{h}})$ results in an incorrect first order correction to $\boldsymbol{v}_{\mathrm{gc}} \cdot \hat{\boldsymbol{h}}$. In this context Boozer also refers to the result for the guiding centre velocity of Northrop and Rome on "Extensions of guiding centre motion to higher order" [53], which is equivalent to Eq. (2.72) and Littlejohn's Eq. (11) in [44], given there without derivation for the special choice of generalised coordinates $(\boldsymbol{R}, \mathcal{H}, \phi, \mu)$. This gives at least some insight that the neglect of $\hat{\boldsymbol{h}} \cdot (\nabla \times \hat{\boldsymbol{h}})$ is equivalent to neglecting a first order Larmor radius correction in the Jacobian from Cartesian velocity coordinates to the generalised coordinates E (or equivalently $\mathcal{H}$), μ (or $J_\perp$) and ϕ. In our model $B^*_\parallel$ is also simplified in favour of B because in transport theory, corrections to the parallel velocity of the order of the guiding centre drift should be ignored [30].

The drifts are now obtained straight forward

$$\dot{\boldsymbol{R}} = \frac{v_\parallel}{B^*_\parallel}\nabla \times \boldsymbol{A}^* \approx \frac{v_\parallel}{B}\nabla \times \left(\boldsymbol{A} + \frac{v_\parallel}{\omega_{\mathrm{c}}}\boldsymbol{B}\right) = \underbrace{\frac{v_\parallel}{B}\boldsymbol{B}}_{=\dot{\boldsymbol{R}}_\parallel} + \underbrace{\frac{v_\parallel}{B}\nabla \times \frac{mcv_\parallel}{e}\hat{\boldsymbol{h}}}_{=\dot{\boldsymbol{R}}_\perp} \tag{2.75}$$

with the cross field drifts

$$\begin{aligned}\dot{\boldsymbol{R}}_\perp &= \frac{v_\parallel}{\omega_{\mathrm{c}}}\nabla \times (v_\parallel \hat{\boldsymbol{h}}) = \frac{v_\parallel}{\omega_{\mathrm{c}}}\left(v_\parallel \nabla \times \hat{\boldsymbol{h}} + \nabla v_\parallel \times \hat{\boldsymbol{h}}\right) \\ &= \frac{v_\parallel^2}{\omega_{\mathrm{c}}}\nabla \times \hat{\boldsymbol{h}} + \frac{c\boldsymbol{B}}{eB^2} \times (\mu \nabla B + e\nabla \Phi),\end{aligned} \tag{2.76}$$

the second and third term on the right hand side being obviously the ∇B and $\boldsymbol{V}_E = c(\boldsymbol{E} \times \boldsymbol{B})/B^2$ drifts, while the first term needs some further manipulation to show that it is the curvature drift. For this purpose, two vector identities for unit vectors are given,

$$\hat{\boldsymbol{h}} \cdot \nabla \hat{\boldsymbol{h}} = -\hat{\boldsymbol{h}} \times (\nabla \times \hat{\boldsymbol{h}}) \quad \text{and} \quad \nabla \times \boldsymbol{B} = B\nabla \times \hat{\boldsymbol{h}} - \hat{\boldsymbol{h}} \times \nabla B, \tag{2.77}$$

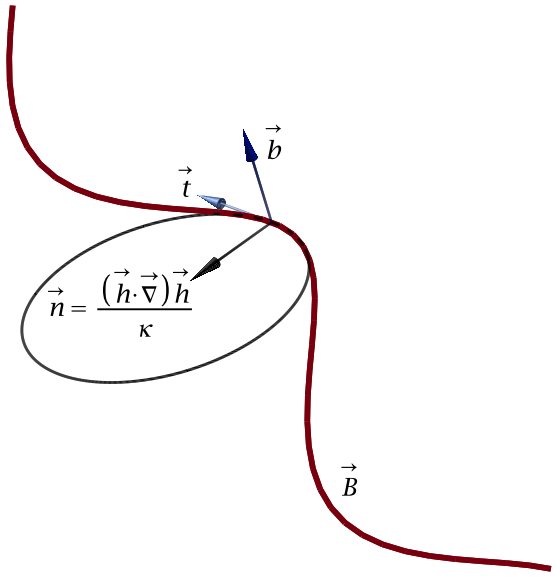

Figure 2.3: Particle comoving Frenet-Serret frame and osculating circle with tangent normal vector $\hat{\boldsymbol{t}} = \hat{\boldsymbol{h}}$, $\hat{\boldsymbol{n}} \propto \boldsymbol{\kappa}$ and $\boldsymbol{v}_\mathrm{d} \propto \hat{\boldsymbol{b}}$ for helically wound $\boldsymbol{B}$-field.

which together give [7]

$$\hat{\boldsymbol{h}} \times (\hat{\boldsymbol{h}} \cdot \nabla \hat{\boldsymbol{h}}) = \frac{\hat{\boldsymbol{h}} \times \nabla B + \nabla \times \boldsymbol{B}}{B}. \tag{2.78}$$

So the first drift on the right hand side of (2.76) can be written as

$$\begin{aligned} \frac{v_\parallel^2}{\omega_\mathrm{c}} \nabla \times \hat{\boldsymbol{h}} &= \frac{mcv_\parallel^2}{eB} \nabla \times \hat{\boldsymbol{h}} \overset{(2.77)}{=} \frac{mcv_\parallel^2}{eB^2} \left(\nabla \times \boldsymbol{B} + \hat{\boldsymbol{h}} \times \nabla B \right) \\ &= \frac{c\boldsymbol{B}}{eB^2} \times m v_\parallel^2 \hat{\boldsymbol{h}} \cdot \nabla \hat{\boldsymbol{h}} = \frac{c\boldsymbol{B}}{eB^2} \times m v_\parallel^2 \boldsymbol{\kappa}, \end{aligned} \tag{2.79}$$

being the curvature drift. In the last line it was used that the curvature $\boldsymbol{\kappa}$, according to the first of Frenet-Serret's formulas, is given by

$$\left. \frac{\mathrm{d}\hat{\boldsymbol{t}}}{\mathrm{d}s} \right|_{\text{along } \hat{\boldsymbol{t}}} = \kappa \hat{\boldsymbol{n}} = \boldsymbol{\kappa} = \left. \frac{\mathrm{d}\hat{\boldsymbol{h}}}{\mathrm{d}s} \right|_{\text{along } \hat{\boldsymbol{h}}}, \tag{2.80}$$

where $\hat{\boldsymbol{t}}$ is the tangent vector to the curve corresponding to $\hat{\boldsymbol{h}}$ in the case of our

magnetic field line and s is the arc length, measured along the curve. $\mathrm{d}/\,\mathrm{d}s|_{\text{along }\hat{\boldsymbol{h}}}$ is the directional derivative, i.e. the projection of the del operator onto $\hat{\boldsymbol{h}}$ [10]

$$\hat{\boldsymbol{h}} \cdot \nabla = \frac{\partial}{\partial s} = \left.\frac{\mathrm{d}}{\mathrm{d}s}\right|_{\text{along }\hat{\boldsymbol{h}}} \tag{2.81}$$

and thus $\boldsymbol{\kappa} = (\hat{\boldsymbol{h}} \cdot \nabla)\hat{\boldsymbol{h}} = \hat{\boldsymbol{h}} \cdot \nabla\hat{\boldsymbol{h}}$, which was used in (2.79). The radius of curvature $\boldsymbol{R}_\mathrm{c}$ is by definition [10] $\boldsymbol{\kappa} = -\boldsymbol{R}_\mathrm{c}/R_\mathrm{c}^2$ pointing from the local centre of curvature to the field line. In terms of $\boldsymbol{R}_\mathrm{c}$, the curvature drift is given by the more familiar expression

$$\boldsymbol{v}_\mathrm{d} = \frac{c\boldsymbol{B}}{eB^2} \times m v_\parallel^2 \hat{\boldsymbol{h}} \cdot \nabla\hat{\boldsymbol{h}} = \frac{c m v_\parallel^2}{\|\boldsymbol{R}_\mathrm{c}\|\, eB^2} \hat{\boldsymbol{R}}_\mathrm{c} \times \boldsymbol{B}. \tag{2.82}$$

Altogether it has been shown that Littlejohn's expression for the guiding centre velocity, resulting from the guiding centre Lagrangian to $\mathcal{O}(\epsilon)$ is equivalent to Morozov and Solev'ev's formulation of the drift equations resulting from an averaging procedure, which upon approximating $v_\parallel \boldsymbol{B}^*/B_\parallel^* \approx v_\parallel \boldsymbol{B}^*/B$ simplifies to the standard expression for the guiding centre drifts, which can be found in any introductory plasma physics text book, e.g. [5, p. 96],

$$\boxed{\dot{\boldsymbol{R}} = v_\parallel \frac{\boldsymbol{B}}{B} + \frac{c\boldsymbol{B}}{eB^2} \times \left(\mu \nabla B + e\nabla\Phi + m v_\parallel^2 \hat{\boldsymbol{h}} \cdot \nabla\hat{\boldsymbol{h}}\right),} \tag{2.83}$$

the terms on the right hand side describing (i) the parallel motion and the perpendicular drifts, namely (ii) the grad-B drift, (iii) the $\boldsymbol{E} \times \boldsymbol{B}$ drift, and (iv) the curvature drift.[4]

2.2.4 Symmetries of the Guiding centre Lagrangian

The guiding centre Lagrangian possesses symmetries, from which follow conservation properties. First, obviously the gyrophase is a cyclic coordinate so that the associated canonical momentum p_ϕ is a constant of motion,

$$p_\phi = \frac{\partial \mathcal{L}_\mathrm{gc}}{\partial \dot{\phi}} = J_\perp \overset{(2.56)}{=} \frac{m v_\perp^2}{2\omega_\mathrm{c}} = \text{const.} \tag{2.84}$$

[4] Having assumed a steady electromagnetic field from the very beginning of the derivation no polarisation drift is present here.

The canonical momentum of the azimuth angle ϕ is obviously connected to the constant angular momentum of the gyromotion, being

$$\boldsymbol{\ell} = \varrho\,\hat{\boldsymbol{e}}_\varrho \times m\varrho\dot{\phi}\,\hat{\boldsymbol{e}}_\phi = -m\varrho v_\perp \hat{\boldsymbol{h}} \tag{2.85}$$

and $p_\phi = m\varrho v_\perp/2 = \|\boldsymbol{\ell}\|/2$. The adiabatic invariant $J_\perp$ is the action integral [61] evaluated along a closed gyroorbit:

$$\begin{aligned} J_\perp &= \frac{1}{2\pi}\oint \boldsymbol{p}\cdot \mathrm{d}\boldsymbol{q} = \frac{1}{2\pi}\oint (m\boldsymbol{v} + \frac{e}{c}\boldsymbol{A})\cdot \mathrm{d}\boldsymbol{r} \\ &= \frac{1}{2\pi}\int_0^{2\pi} m\boldsymbol{v}\cdot\frac{\partial \boldsymbol{\varrho}}{\partial\phi}\,\mathrm{d}\phi + \frac{e}{c}\frac{1}{2\pi}\oiint \nabla\times\boldsymbol{A}\cdot\mathrm{d}\boldsymbol{S}. \end{aligned} \tag{2.86}$$

Decomposing the velocity $\boldsymbol{v}$ into its parallel and phase-dependent perpendicular part, $\boldsymbol{v} = v_\parallel\,\hat{\boldsymbol{h}} + v_\perp\,\hat{\boldsymbol{c}}$ and using Eqns. (2.36) and (2.37)

$$\boldsymbol{v}\cdot\frac{\partial\boldsymbol{\varrho}}{\partial\phi} = \Big[v_\parallel\,\hat{\boldsymbol{h}} + v_\perp(-\sin\phi\,\hat{\boldsymbol{e}}_1 - \cos\phi\,\hat{\boldsymbol{e}}_2)\Big]\cdot\frac{v_\perp}{\omega_\mathrm{c}}\,(-\sin\phi\,\hat{\boldsymbol{e}}_1 - \cos\phi\,\hat{\boldsymbol{e}}_2) = \frac{v_\perp^2}{\omega_\mathrm{c}}$$

and considering the surface normal directed in the mathematical positive sense, so that $\mathrm{d}\boldsymbol{S} = -\,\mathrm{d}S\,\hat{\boldsymbol{h}}$, one gets

$$J_\perp = m\frac{v_\perp^2}{\omega_\mathrm{c}} - \frac{e}{c}\frac{1}{2\pi}\boldsymbol{B}\cdot\hat{\boldsymbol{h}}\,\varrho^2\pi = m\frac{v_\perp^2}{\omega_\mathrm{c}} - \frac{m}{2}\frac{v_\perp^2}{\omega_\mathrm{c}} = \frac{mv_\perp^2}{2\omega_\mathrm{c}}. \tag{2.87}$$

This invariant is equivalent to the magnetic moment $\mu = mv_\perp^2/2B$ and to the magnetic flux through a gyroorbit Φ_B within a constant: $J_\perp = (mc/e)\cdot\mu = e/(2\pi c)\cdot\Phi_B$. Here, a remark is indicated, that the constancy of the first adiabatic invariant is strictly valid only in first order of the gyromotion. An expansion of the adiabatic invariant to higher orders can be found e.g. in [47] and is a central issue in Northrop's paper of the extension of the guiding centre motion to higher orders [53].

Secondly, there is no explicit time dependency in the Lagrangian $\mathcal{L}_\mathrm{gc}$, wherefrom follows that the Hamiltonian function also is time independent,

$$-\frac{\partial\mathcal{L}_\mathrm{gc}}{\partial t} = \frac{\mathrm{d}}{\mathrm{d}t}\left(\sum_{i=1}^{6}\frac{\partial\mathcal{L}_\mathrm{gc}}{\partial\dot{z}^i}\cdot\dot{z}^i - \mathcal{L}_\mathrm{gc}\right) = \frac{\mathrm{d}\mathcal{H}}{\mathrm{d}t} = 0. \tag{2.88}$$

Finally, the already used relation $v_\parallel = \hat{\boldsymbol{h}}\cdot\dot{\boldsymbol{R}}$ shall be shown. For this purpose a theorem for Lagrangians is applied, see e.g. [61, p. 95], which says that if $z^i(t)$ is a solution of the Lagrange equations for the Lagrangian $\mathcal{L}(z^i,\ldots,z^f,\dot{z}^i,\ldots\dot{z}^f,t)$, then a diffeomorphism $G: z^i \to \tilde{z}^i : z^i = g_i(\tilde{z}^1,\ldots,\tilde{z}^f,t),\ i = 1,\ldots,f$ with

$g = G^{-1}$ and f, the number of degrees of freedom, which is at least $\mathcal{C}^2$ differentiable and has a non-singular Jacobian determinant $\det(\partial g_l/\partial \tilde{z}_k) \neq 0$ gives a transformed Lagrangian $\tilde{\mathcal{L}}$

$$\begin{aligned}\tilde{\mathcal{L}} &= \mathcal{L} \circ G^{-1} \\ &= \mathcal{L}\left(g_1(\tilde{z},t), \ldots, g_f(\tilde{z},t), \sum_{k=1}^{f} \frac{\partial g_1}{\partial \tilde{z}^k}\dot{\tilde{z}}^k + \frac{\partial g_1}{\partial t}, \ldots, \sum_{k=1}^{f} \frac{\partial g_f}{\partial \tilde{z}^k}\dot{\tilde{z}}^k + \frac{\partial g_f}{\partial t}, t\right)\end{aligned}$$

for which $\delta\mathcal{L}/\delta z^k = 0$ is equivalent to $\delta\tilde{\mathcal{L}}/\delta\tilde{z}^k = 0$. The proof of this theorem can be found e.g. in [61, p. 96]. To put it in simple words, the coordinate independence of the Lagrangian allows to transform the Lagrangian by carrying out the substitutions $z(\tilde{z},t)$ and $\dot{z} = \partial_t z + \sum_i \dot{\tilde{z}}^i \partial z/\partial \tilde{z}^i$ [9]. In contrast, in Hamiltonian mechanics coordinate transformations are restricted to the class of canonical transformations $z^i \to \tilde{z}^i$, which require the Jacobian $J^\beta_\alpha = \partial\tilde{z}^\beta/\partial z^\alpha$ to be symplectic, i.e. the Jacobian has to satisfy the relation $\boldsymbol{J}\cdot\boldsymbol{\sigma}\cdot\boldsymbol{J}^\dagger = \boldsymbol{\sigma}$ with the fundamental symplectic matrix [9]

$$\sigma = \begin{pmatrix} 0 & \delta^{ij} \\ -\delta^{ij} & 0 \end{pmatrix}. \tag{2.89}$$

From the trivial coordinate transform $\mathcal{H} \mapsto v_\parallel$ follows the equivalent guiding centre Lagrangian

$$\tilde{\mathcal{L}}_{\mathrm{gc}}(\boldsymbol{R}, \dot{\boldsymbol{R}}, \phi, J_\perp, v_\parallel) = \left(m v_\parallel \hat{\boldsymbol{h}} + \frac{e}{c}\boldsymbol{A}\right)\cdot\dot{\boldsymbol{R}} - \frac{m}{2}v_\parallel^2 - e\,\Phi, \tag{2.90}$$

which allows to formulate the Euler Lagrange equation for the parallel velocity,

$$\frac{\mathrm{d}}{\mathrm{d}t}\frac{\partial\tilde{\mathcal{L}}_{\mathrm{gc}}}{\partial\dot{v}_\parallel} = 0 = \frac{\partial\tilde{\mathcal{L}}_{\mathrm{gc}}}{\partial v_\parallel} = m\hat{\boldsymbol{h}}\cdot\dot{\boldsymbol{R}} - m v_\parallel, \tag{2.91}$$

confirming $v_\parallel = \dot{\boldsymbol{R}}\cdot\hat{\boldsymbol{h}}$, which "dictates that $v_\parallel$ is the velocity of the guiding centre in the direction of the magnetic field at the guiding centre" [9] rather than being a mere definition of $v_\parallel$.

In the following, the equations of motion for the parallel and perpendicular velocity shall be derived. Returning to the Euler-Lagrange equation for the guiding centre coordinate $\boldsymbol{R}$, Eq. (2.66) and taking the projection onto $\dot{\boldsymbol{R}}$ yields

$$m\dot{v}_\parallel v_\parallel + e\dot{\boldsymbol{R}}\cdot\nabla\Phi + \mu\dot{\boldsymbol{R}}\cdot\nabla B = 0$$

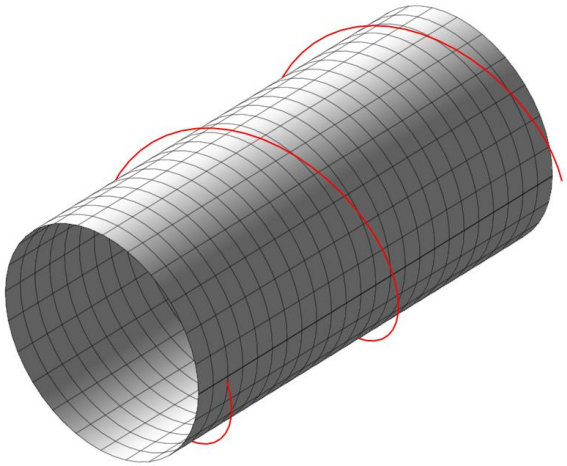

Figure 2.4: Cylindrical model with rotational transform of a tokamak with azimuthal symmetry and radial inhomogeneity. The relation to the toroidal angle φ is given by $z = R\,\varphi$ with R the major radius of the torus. The cylindrical and toroidal wave number of the perturbation field is linked by $k_z = m/R$. Likewise, the poloidal background field is related to the z-component by $B_0^\vartheta = B_0^z/qR$. Here $q = q(r) = m/n$ is the safety factor or winding number, i.e. the ratio of the toroidal to poloidal winding, which e.g. in the case of the above sketch equals $1/2$.

and thus [30]

$$\boxed{\dot{v}_\parallel = -\frac{e}{mv_\parallel}\dot{\boldsymbol{R}}\cdot\nabla\Phi - \frac{v_\perp^2}{2v_\parallel B}\dot{\boldsymbol{R}}\cdot\nabla B.} \tag{2.92}$$

The equation of motion for $v_\parallel$ is obtained by isolating $v_\perp^2$ from the perpendicular kinetic energy

$$K_\perp = \frac{mv_\perp^2}{2} = \omega_c J_\perp \tag{2.93}$$

and taking the total time derivative. One obtains [30]

$$\boxed{\dot{v}_\perp = \frac{eJ_\perp}{m^2 v_\perp c}\dot{B} = \frac{v_\perp}{2B}\dot{\boldsymbol{R}}\cdot\nabla B.} \tag{2.94}$$

2.3 The Gyrokinetic Equation

Recapitulating the last section, by Hamilton's principle the guiding centre Lagrangian leads to the drift equations, which in compact notation are

$$\dot{\boldsymbol{R}} \approx v_\parallel \frac{\boldsymbol{B}^*}{B}, \quad \dot{\phi} = -\omega_\mathrm{c}, \quad \dot{J}_\perp = 0, \quad \dot{\mathcal{H}} = 0.$$

In addition, the equations of motion for the parallel and perpendicular velocity have been found in Eqns. (2.92) and (2.94).

Now, the kinetic equation (2.17) is formulated for the guiding centre variables $z = (\boldsymbol{R}, \phi, J_\perp, \mathcal{H})$,

$$\partial_t f_\sigma + \dot{z}^i \frac{\partial f_\sigma}{\partial z^i} = \hat{L}_\mathrm{c} f_\sigma \quad (i = 1, \dots 6), \tag{2.95}$$

where in the following the plasma species index σ is dropped. Due to z^4, z^5 and z^6 being integrals of the motion, the kinetic equation simplifies to the gyrokinetic equation, see e.g. [30],

$$\boxed{\partial_t f + \dot{\boldsymbol{R}} \cdot \nabla f = \hat{L}_\mathrm{c} f.} \tag{2.96}$$

The collision operator is an integro-differential operator,

$$\hat{L}_\mathrm{cp} = \hat{L}_\mathrm{cD} + \hat{L}^\mathrm{E}_\mathrm{cI}, \tag{2.97}$$

where the differential part, $\hat{L}_\mathrm{cD}$ is a 1-D Fokker-Planck collision operator in the so-called Ornstein-Uhlenbeck approximation [69],

$$\hat{L}_\mathrm{cD} f = \frac{\partial}{\partial u} D \left(\frac{\partial}{\partial u} + \frac{u}{v_T^2} \right) f, \tag{2.98}$$

with $u = v_\parallel - V_{\parallel 0}$ a, by the bulk parallel velocity shifted, parallel velocity, $v_T = \sqrt{T_0/m}$ the thermal velocity and $D = \nu v_T^2$, a constant diffusion coefficient in velocity space. While this collision operator ensures Galilean invariance and thus conserves the number of particles (and hence, the charge), it does not conserve momentum and energy of the plasma species. Together with the integral operator [30]

$$\hat{L}^\mathrm{E}_\mathrm{cI} f(v_\perp, u) = \frac{\nu}{\sqrt{2\pi} v_T} \exp\left(-\frac{u^2}{2v_T^2}\right) \left(\frac{u^2}{v_T^2} - 1\right) \int_\mathbb{R} \mathrm{d}u' \left(\frac{u'^2}{v_T^2} - 1\right) f(v_\perp, u') \tag{2.99}$$

also the conservation of energy for each particle species is ensured. This issue will be dealt with in detail in Section 3.2.

2.4 Quasilinear Response Model

Since the collision operator is preferably formulated in the $v_\parallel$ and $v_\perp$ variables, we introduce a phase space coordinate transformation $z = (\boldsymbol{R}, \phi, J_\perp, \mathcal{H}) \mapsto \tilde{z} = (\boldsymbol{R}, \phi, v_\parallel, v_\perp)$, such that $v_\parallel$ and $v_\perp$ are now independent variables, and expand the drift velocity and the distribution function to first order of an externally applied perturbation field[5]

$$\dot{\boldsymbol{R}} = \dot{\boldsymbol{R}}_0 + \dot{\boldsymbol{R}}_1 + \ldots, \quad \dot{v}_\parallel = \dot{v}_{\parallel 0} + \dot{v}_{\parallel 1} + \ldots, \quad \dot{v}_\perp = \dot{v}_{\perp 0} + \dot{v}_{\perp 1} + \ldots, \tag{2.100}$$

$$f = f_0 + f_1 + \ldots, \tag{2.101}$$

with f_0, the distribution function of the unperturbed system being an inhomogeneous drifting Maxwellian normalised to momentum space [33, 30]

$$f_0(r, v_\parallel, v_\perp) = \frac{n_0(r)}{(2\pi m T_0(r))^{3/2}} \exp\left\{ -\frac{m\left[v_\perp^2 + (v_\parallel - V_{\parallel 0})^2\right]}{2T_0(r)} \right\}. \tag{2.102}$$

The parameters n_0, T_0, and $V_{\parallel 0}$ for each plasma species, as well as the equilibrium electrostatic potential Φ_0 are computed from given radial input profiles of the unperturbed density, temperature, parallel fluid velocity and safety factor $q(r)$, so that to first order Larmor radius expansion the quasi-neutrality condition is satisfied and the parameters differ from the actual equilibrium profiles only by first order Larmor radius corrections [25, 33]. The kinetic equation formulated for phase space coordinates $\tilde{z}^i$ in steady-state is [30],

$$\dot{\boldsymbol{R}} \cdot \nabla f + \dot{v}_\parallel \frac{\partial f}{\partial v_\parallel} + \dot{v}_\perp \frac{\partial f}{\partial v_\perp} = \hat{L}_c f. \tag{2.103}$$

Substituting the expansions (2.100) and (2.101), the following hierarchy of equations (0th and 1st order in the perturbation field) is obtained [30],

$$\dot{\boldsymbol{R}}_0 \cdot \nabla f_0 + \dot{v}_{\parallel 0} \frac{\partial f_0}{\partial v_\parallel} + \dot{v}_{\perp 0} \frac{\partial f_0}{\partial v_\perp} - \hat{L}_c f_0 = 0, \tag{2.104}$$

$$\dot{\boldsymbol{R}}_0 \cdot \nabla f_1 + \dot{v}_{\parallel 0} \frac{\partial f_1}{\partial v_\parallel} + \dot{v}_{\perp 0} \frac{\partial f_1}{\partial v_\perp} - \hat{L}_c f_1 = -\dot{\boldsymbol{R}}_1 \cdot \nabla f_0 - \dot{v}_{\parallel 1} \frac{\partial f_0}{\partial v_\parallel} - \dot{v}_{\perp 1} \frac{\partial f_0}{\partial v_\perp}, \tag{2.105}$$

[5] This is in contrast to neoclassical theory, where instead of the perturbation field the radial drift velocity plays the role of the expansion parameter [30]. Compared to the neoclassical toroidal viscosity theory (NTV) this expansion is carried out w.r.t. the unperturbed magnetic surfaces [30, 62, 56] .

where the sources (thermodynamic driving terms towards the equilibrium as will become apparent below) have been put on the right hand side of the above equation, constituting the inhomogeneity of the partial differential equation.

The solution of the 0th-order equation is given by the drifting Maxwellian (3.88) with [30]

$$\dot{\boldsymbol{R}}_0 = v_\parallel \hat{\boldsymbol{h}}_0 + \boldsymbol{V}_E, \quad \dot{v}_{\parallel 0} = 0, \quad \dot{v}_{\perp 0} = 0, \tag{2.106}$$

where $\hat{\boldsymbol{h}}_0 = \boldsymbol{B}_0/B_0$ is the unit vector of the unperturbed magnetic field and the $\boldsymbol{E} \times \boldsymbol{B}$-drift velocity $\boldsymbol{V}_E$ as already specified before in Eq. (2.76) in Sect. 2.2.3,

$$\boldsymbol{V}_E = c\frac{\boldsymbol{B}_0 \times \nabla \Phi_0}{B_0^2}. \tag{2.107}$$

In order to rearrange the first order kinetic equation (2.105), the terms on the right hand side are explicitly evaluated. Taking the gradient of the equilibrium distribution function $\nabla f_0 = \partial_r f_0 \nabla r$ with $\nabla r = \boldsymbol{e}^r = \hat{\boldsymbol{n}}_\psi$, the contravariant radial basis vector and also the normal unit vector $\hat{\boldsymbol{n}}_\psi$ of an undistorted nested flux surface ψ, one obtains

$$\nabla f_0 = \left\{ \frac{1}{n_0}\frac{\partial n_0}{\partial r} - \frac{3}{2T}\frac{\partial T}{\partial r} + \frac{m\left[v_\perp^2 + (v_\parallel - V_{\parallel 0})^2\right]}{2T^2}\frac{\partial T}{\partial r} \right\} f_0 \nabla r. \tag{2.108}$$

Introducing the thermodynamic forces [24]

$$\mathscr{A}_1 = \frac{1}{n_0}\frac{\partial n_0}{\partial r} + \frac{e}{T}\frac{\partial \Phi_0}{\partial r} - \frac{3}{2T}\frac{\partial T}{\partial r}, \quad \mathscr{A}_2 = \frac{1}{T}\frac{\partial T}{\partial r}, \tag{2.109}$$

∇f_0 can now be written compactly as

$$\nabla f_0 = \left(a_1 \mathscr{A}_1 + a_2 \mathscr{A}_2\right) f_0 \nabla r - \frac{e}{T} f_0 \nabla \Phi_0 \tag{2.110}$$

with coefficients [30]

$$a_1 = 1, \quad a_2 = \frac{m}{2T}\left[v_\perp^2 + (v_\parallel - V_{\parallel 0})^2\right]. \tag{2.111}$$

For the second and third term on the right hand side of the first order kinetic equation (2.105) one is referred to the expressions (2.92) and (2.94), that have been obtained in course of the derivation of the drift equations from the guiding centre Lagrangian. By referring to a system moving with parallel fluid velocity $V_{\parallel 0}$, one has to replace $v_\parallel \to v_\parallel - V_{\parallel 0} =: u$ in the expression for $\dot{v}_\parallel$. Expanding

the expressions to first order in the in the perturbation field, one obtains

$$\dot{v}_{\parallel 1} = -\frac{e}{mu}\left(\dot{\boldsymbol{R}}_0 \cdot \nabla\tilde{\Phi}_1 + \dot{\boldsymbol{R}}_1 \cdot \nabla\Phi_0\right) - \frac{v_\perp^2}{2uB}\left(\dot{\boldsymbol{R}}_0 \cdot \nabla\tilde{B}_1 + \dot{\boldsymbol{R}}_1 \cdot \nabla B_0\right), \quad (2.112)$$

$$\dot{v}_{\perp 1} = \frac{v_\perp}{2B}\left(\dot{\boldsymbol{R}}_0 \cdot \nabla\tilde{B}_1 + \dot{\boldsymbol{R}}_1 \cdot \nabla B_0\right). \quad (2.113)$$

Evaluating the second and third term on the r.h.s. of Eq. (2.105), the four terms containing either $\dot{\boldsymbol{R}}_0 \cdot \nabla\tilde{B}_1$ or $\dot{\boldsymbol{R}}_1 \cdot \nabla B_0$ cancel each other, leaving

$$\dot{v}_{\parallel 1}\frac{\partial f_0}{\partial v_\parallel} + \dot{v}_{\perp 1}\frac{\partial f_0}{\partial v_\perp} = \frac{e f_0}{T}\left(\dot{\boldsymbol{R}}_0 \cdot \nabla\tilde{\Phi}_1 + \dot{\boldsymbol{R}}_1 \cdot \nabla\Phi_0\right). \quad (2.114)$$

Thus one can write the first order steady-state kinetic equation as

$$\dot{\boldsymbol{R}}_0 \cdot \nabla f_1 - \hat{L}_c f_1 = -\left(a_1\mathscr{A}_1 + a_2\mathscr{A}_2\right) f_0 \dot{\boldsymbol{R}}_1 \cdot \nabla r - \frac{e f_0}{T}\dot{\boldsymbol{R}}_0 \cdot \nabla\tilde{\Phi}_1. \quad (2.115)$$

By denoting the perturbation distribution function [30]

$$\tilde{f} = f_1 + f_0\frac{e\tilde{\Phi}_1}{T}, \quad (2.116)$$

the second term of the first order kinetic equation becomes

$$\begin{aligned}\dot{\boldsymbol{R}}_0 \cdot \nabla f_1 &= \dot{\boldsymbol{R}}_0 \cdot \left(\nabla\tilde{f} - \frac{e\tilde{\Phi}_1}{T}\nabla f_0 - \frac{e f_0}{T}\nabla\tilde{\Phi}_1 + \frac{e f_0\tilde{\Phi}_1}{T^2}\nabla T\right) \\ &= \dot{\boldsymbol{R}}_0 \cdot \nabla\tilde{f} - \frac{e f_0}{T}\dot{\boldsymbol{R}}_0 \cdot \nabla\tilde{\Phi}_1. \end{aligned} \quad (2.117)$$

Here, it has been used that the directional derivative $\dot{\boldsymbol{R}}_0 \cdot \nabla$ is a derivative within a constant flux surface, perpendicular to $\hat{\boldsymbol{h}}$ and so gives zero acting on f_0 or T, which are axial symmetric and have concentric cylinders as equipotential surfaces $f_0(r_0)$, $T(r_0)$.

For the perturbation distribution function $\tilde{f}$ the first order steady-state kinetic equation is thus [30]

$$\dot{\boldsymbol{R}}_0 \cdot \nabla\tilde{f} - \hat{L}_c\tilde{f} = -\left[\mathscr{A}_1 + \frac{m\left(v_\perp^2 + u^2\right)}{2T}\mathscr{A}_2\right] f_0\, \dot{\boldsymbol{R}}_1 \cdot \nabla r. \quad (2.118)$$

In the following, the contravariant radial component $\dot{\boldsymbol{R}}_1 \cdot \nabla r = \dot{R}_{i,1}\nabla x^i \cdot \nabla r = \dot{R}_{r,1}g^{rr} = \dot{R}_1^r$ of the first order drift velocity, arising in (2.118) is further evaluated in cylindrical coordinates $(x^1, x^2, x^3) = (r, \vartheta, z)$. Note that subscript "1" refers to the first order in the perturbation field, while i and r are co- and contravariant

indices, respectively. Here, expression (2.75), already obtained in Sect. 2.2.3 for the guiding centre drift velocity is applied,

$$\begin{aligned}\dot{R}_1^r = \dot{\boldsymbol{R}}_1 \cdot \nabla r &= \left[\frac{v_\parallel}{B}\nabla \times \left(\boldsymbol{A} + \frac{v_\parallel}{\omega_\mathrm{c}}\boldsymbol{B}\right)\right]_1 \cdot \nabla r \\ &= \left[\frac{v_\parallel}{B}\boldsymbol{B}\cdot\nabla r + \frac{v_\parallel^2}{\omega_\mathrm{c}B}\nabla\times\boldsymbol{B}\cdot\nabla r + \frac{v_\parallel}{B}\nabla\left(\frac{v_\parallel}{\omega_\mathrm{c}}\right)\times\boldsymbol{B}\right]_1 . \end{aligned} \tag{2.119}$$

The three terms are evaluated separately in the following,

$$\frac{v_\parallel}{B}\boldsymbol{B}\cdot\nabla r = \frac{v_\parallel}{B}B_i\nabla x^i\cdot\nabla r = \frac{v_\parallel}{B}B^r, \tag{2.120}$$

$$\begin{aligned}\frac{v_\parallel^2}{\omega_\mathrm{c}B}\nabla\times\boldsymbol{B}\cdot\nabla r &= \frac{v_\parallel^2}{\omega_\mathrm{c}B}\frac{\epsilon^{ijk}}{\sqrt{g}}\partial_i B_j \boldsymbol{e}_k\cdot\nabla r = \frac{v_\parallel^2}{\omega_\mathrm{c}B}\frac{\epsilon^{ijk}}{\sqrt{g}}\partial_i B_j g_{kk}\nabla x^k\cdot\nabla r \\ &= \frac{v_\parallel^2}{\omega_\mathrm{c}Br}\left(\partial_\vartheta B_z - \partial_z B_\vartheta\right), \end{aligned} \tag{2.121}$$

$$\begin{aligned}\frac{v_\parallel}{B}\nabla\left(\frac{v_\parallel}{\omega_\mathrm{c}}\right)\times\boldsymbol{B}\cdot\nabla r &= \frac{v_\parallel}{B}\nabla\left(\frac{\sigma\sqrt{\frac{2}{m}\left(\mathcal{H} - e\Phi(\boldsymbol{r}) - \omega_\mathrm{c}J_\perp\right)}}{\omega_\mathrm{c}(\boldsymbol{r})}\right)\times\boldsymbol{B}\cdot\nabla r \\ &= -\frac{1}{B}\left(c\nabla\Phi + \frac{v_\perp^2}{2\omega_\mathrm{c}}\nabla B + \frac{mv_\parallel^2 c}{eB}\nabla B\right)\times\hat{\boldsymbol{h}}\cdot\nabla r \\ &= -\frac{1}{B}\left(c\frac{\epsilon^{ijk}}{\sqrt{g}}\partial_i\Phi h_j\frac{\partial\boldsymbol{r}}{\partial x^k} + \frac{v_\perp^2 + 2v_\parallel^2}{2\omega_\mathrm{c}}\frac{\epsilon^{ijk}}{\sqrt{g}}\partial_i B h_j\frac{\partial\boldsymbol{r}}{\partial x^k}\right)\cdot g^{rr}\frac{\partial\boldsymbol{r}}{\partial x^r} \\ &= -\frac{c}{Br}\epsilon^{ijk}\partial_i\Phi h_j\delta_k^r - \frac{v_\perp^2 + 2v_\parallel^2}{2\omega_\mathrm{c}Br}\epsilon^{ijk}\partial_i B h_j\delta_k^r \\ &= -\frac{c}{Br}\epsilon^{ijr}h_j\partial_i\Phi - \frac{v_\perp^2 + 2v_\parallel^2}{2\omega_\mathrm{c}Br}\epsilon^{ijr}h_j\partial_i\boldsymbol{h}\cdot\boldsymbol{B} \\ &= -\frac{c}{Br}\left(h_z\frac{\partial\Phi}{\partial\vartheta} - h_\vartheta\frac{\partial\Phi}{\partial z}\right) \\ &\quad - \frac{v_\perp^2 + 2v_\parallel^2}{2\omega_\mathrm{c}Br}\left(h_z\frac{\partial}{\partial\vartheta}\boldsymbol{h}\cdot\boldsymbol{B} - h_\vartheta\frac{\partial}{\partial z}\boldsymbol{h}\cdot\boldsymbol{B}\right). \end{aligned} \tag{2.122}$$

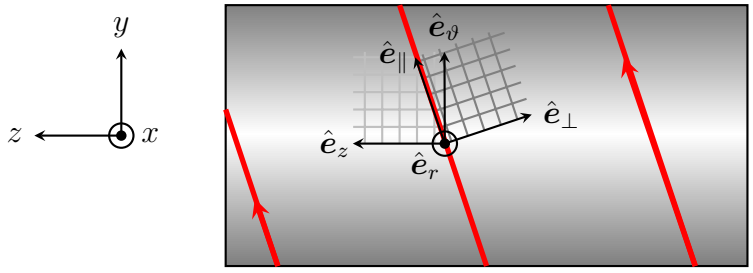

Figure 2.5: Field-aligned local orthonormal basis $(\hat{\boldsymbol{e}}_\parallel, \hat{\boldsymbol{e}}_r, \hat{\boldsymbol{e}}_\perp)$ and local cylindrical basis $(\hat{\boldsymbol{e}}_r, \hat{\boldsymbol{e}}_\vartheta, \hat{\boldsymbol{e}}_z)$. The perpendicular direction $\hat{\boldsymbol{e}}_\perp = \hat{\boldsymbol{h}}_0 \times \hat{\boldsymbol{e}}_r = \hat{\boldsymbol{e}}_\parallel \times \hat{\boldsymbol{e}}_r$ lies per definition within an unperturbed flux surface spanning a tangent plane together with $\hat{\boldsymbol{e}}_\parallel$ at the point in consideration.

Thus, the first order radial drift velocity is [30]

$$\dot{R}_1^r = \frac{v_\parallel}{B_0}\tilde{B}_1^r + \frac{v_\parallel^2}{\omega_{c0}B_0 r}\left(\frac{\partial \tilde{B}_{1z}}{\partial \vartheta} - \frac{\partial \tilde{B}_{1\vartheta}}{\partial z}\right) - \frac{c}{B_0 r}\left(h_z\frac{\partial \tilde{\Phi}_1}{\partial \vartheta} - h_\vartheta \frac{\partial \tilde{\Phi}_1}{\partial z}\right) - \frac{v_\perp^2 + 2v_\parallel^2}{\omega_{c0}B_0 r}\left(h_z\frac{\partial \boldsymbol{h}\cdot\tilde{\boldsymbol{B}}_1}{\partial \vartheta} - h_\vartheta \frac{\partial \boldsymbol{h}\cdot\tilde{\boldsymbol{B}}_1}{\partial z}\right). \tag{2.123}$$

In the following, the perturbation fields, the perturbed distribution function and the radial contravariant component of the radial drift velocity are expanded in Fourier series,

$$\tilde{\boldsymbol{B}}_1 = \Re\sum_{\boldsymbol{m}} \tilde{\boldsymbol{B}}_{\boldsymbol{m}} \mathrm{e}^{\mathrm{i}(m_\vartheta \vartheta + k_z z)}, \qquad \tilde{\Phi}_1 = \Re\sum_{\boldsymbol{m}} \tilde{\Phi}_{\boldsymbol{m}} \mathrm{e}^{\mathrm{i}(m_\vartheta \vartheta + k_z z)}, \tag{2.124}$$

$$\tilde{f} = \Re\sum_{\boldsymbol{m}} \tilde{f}_{\boldsymbol{m}} \mathrm{e}^{\mathrm{i}(m_\vartheta \vartheta + k_z z)}, \qquad \dot{R}_1^r = \Re\sum_{\boldsymbol{m}} v_{\boldsymbol{m}}^r \mathrm{e}^{\mathrm{i}(m_\vartheta \vartheta + k_z z)}. \tag{2.125}$$

By evaluating the perpendicular and parallel components of the wave vector $\boldsymbol{k}$ and of the Fourier amplitude of the perturbed magnetic field $\boldsymbol{B}_{\boldsymbol{m}}$, the Fourier amplitudes $v_{\boldsymbol{m}}^r$ can be expressed in terms of perpendicular and parallel field amplitudes.

$$k_\parallel = g_{ij}k^i h^j = g_{\vartheta\vartheta}m^\vartheta h^\vartheta + g_{zz}k^z h^z = m_\vartheta h^\vartheta + k_z h^z, \tag{2.126}$$

$$\begin{aligned} k_\perp &= \boldsymbol{k}\times\hat{\boldsymbol{h}}\cdot\nabla r = k_i \nabla x^i \times h_j \nabla x^j \cdot \nabla r \\ &= \nabla r \cdot \nabla\vartheta \times \nabla z \left(h_z m_\vartheta - h_\vartheta k_z\right) \\ &= \frac{1}{r}\left(h_z m_\vartheta - h_\vartheta k_z\right), \end{aligned} \tag{2.127}$$

where it has been used that $\hat{\boldsymbol{h}}$ has no radial component and $\nabla r \cdot \nabla\vartheta \times \nabla z = 1/J = 1/\sqrt{g}$. The components of the field amplitudes are obtained analogously,

$$\tilde{B}_{\boldsymbol{m}\parallel} = \boldsymbol{h} \cdot \tilde{\boldsymbol{B}}_{\boldsymbol{m}} = \tilde{B}_{\boldsymbol{m}\vartheta} h^{\vartheta} + \tilde{B}_{\boldsymbol{m}z} h^{z}, \tag{2.128}$$

$$\tilde{B}_{\boldsymbol{m}\perp} = \tilde{\boldsymbol{B}}_{\boldsymbol{m}} \times \hat{\boldsymbol{h}} \cdot \nabla r = \frac{1}{r}\left(h_z \tilde{B}_{\boldsymbol{m}\vartheta} - h_{\vartheta} \tilde{B}_{\boldsymbol{m}z}\right). \tag{2.129}$$

Finally, explicit expressions for the covariant ϑ and z-components of the wave vector and field amplitude are needed for the evaluation of $v^r_{\boldsymbol{m}}$. In order to get an expression for m_{ϑ}, Eq. (2.127), multiplied by rh^z and Eq. (2.126), multiplied by h_{ϑ} are added,

$$rh^z k_{\perp} + h_{\vartheta} k_{\parallel} = m_{\vartheta}(h_{\vartheta} h^{\vartheta} + h_z h^z) = m_{\vartheta}. \tag{2.130}$$

k_z is obtained by multiplying (2.127) by $-rh^{\vartheta}$ and (2.126) by h_z and adding them up,

$$-rh^{\vartheta} k_{\perp} + h_z k_{\parallel} = k_z(h_{\vartheta} h^{\vartheta} + h_z h^z) = k_z, \tag{2.131}$$

and analogously for the perpendicular and parallel components of $\tilde{B}_{\boldsymbol{m}}$,

$$rh^z \tilde{B}_{\boldsymbol{m}\perp} + h_{\vartheta} \tilde{B}_{\boldsymbol{m}\parallel} = \tilde{B}_{\boldsymbol{m}\vartheta}(h_{\vartheta} h^{\vartheta} + h_z h^z) = \tilde{B}_{\boldsymbol{m}\vartheta}, \tag{2.132}$$

$$-rh^{\vartheta} \tilde{B}_{\boldsymbol{m}\perp} + h_z \tilde{B}_{\boldsymbol{m}\parallel} = \tilde{B}_{\boldsymbol{m}z}(h_{\vartheta} h^{\vartheta} + h_z h^z) = \tilde{B}_{\boldsymbol{m}z}. \tag{2.133}$$

Having expressed the cylindrical covariant components through the field-aligned and perpendicular components, all preliminaries are set to determine $v^r_{\boldsymbol{m}}$. First, the Fourier expanded field and electrostatic potential is substituted in Eq. (2.123),

$$\begin{aligned}
\dot{R}^r_1 &= \Re \sum_{\boldsymbol{m}} v^r_{\boldsymbol{m}} \mathrm{e}^{\mathrm{i}(m_{\vartheta}\vartheta + k_z z)} \\
&= \frac{v_{\parallel}}{B_0} \Re \sum_{\boldsymbol{m}} \tilde{B}_{\boldsymbol{m}} \mathrm{e}^{\mathrm{i}(m_{\vartheta}\vartheta + k_z z)} \cdot \nabla r \\
&\quad + \frac{v_{\parallel}^2}{\omega_{\mathrm{c}0} B_0 r} \left(\mathrm{i} m_{\vartheta} \frac{\partial \boldsymbol{r}}{\partial x^z} - \mathrm{i} k_z \frac{\partial \boldsymbol{r}}{\partial x^{\vartheta}}\right) \cdot \Re \sum_{\boldsymbol{m}} \tilde{\boldsymbol{B}}_{\boldsymbol{m}} \mathrm{e}^{\mathrm{i}(m_{\vartheta}\vartheta + k_z z)} \\
&\quad - \frac{c}{B_0 r} \left(\mathrm{i} m_{\vartheta} h_z - \mathrm{i} k_z h_{\vartheta}\right) \Re \sum_{\boldsymbol{m}} \tilde{\Phi}_{\boldsymbol{m}} \mathrm{e}^{\mathrm{i}(m_{\vartheta}\vartheta + k_z z)} \\
&\quad - \frac{v_{\perp}^2 + 2v_{\parallel}^2}{2\omega_{\mathrm{c}0} B_0 r} \left(\mathrm{i} m_{\vartheta} h_z - \mathrm{i} k_z h_{\vartheta}\right) \hat{\boldsymbol{h}} \cdot \Re \sum_{\boldsymbol{m}} \tilde{\boldsymbol{B}}_{\boldsymbol{m}} \mathrm{e}^{\mathrm{i}(m_{\vartheta}\vartheta + k_z z)},
\end{aligned} \tag{2.134}$$

so that for the Fourier amplitude one obtains

$$v^r_{\boldsymbol{m}} = \frac{v_\parallel}{B_0}\tilde{B}^r_{\boldsymbol{m}} + \frac{\mathrm{i}v_\parallel^2}{\omega_{\mathrm{c}0}B_0 r}\left(m_\vartheta \tilde{B}_{\boldsymbol{m}z} - k_z \tilde{B}_{\boldsymbol{m}\vartheta}\right) - \frac{\mathrm{i}c}{B_0 r}\left(m_\vartheta h_z - k_z h_\vartheta\right)\tilde{\Phi}_{\boldsymbol{m}} - \mathrm{i}\frac{v_\perp^2 + 2v_\parallel^2}{2\omega_{\mathrm{c}0}B_0 r}\left(m_\vartheta h_z - k_z h_\vartheta\right)\tilde{B}_{\boldsymbol{m}\parallel}.$$

After substitution for m_ϑ, k_z, $\tilde{B}_{\boldsymbol{m},\vartheta}$, and $\tilde{B}_{\boldsymbol{m},z}$, the Fourier amplitude of the radial drift velocity reads [30]

$$\boxed{v^r_{\boldsymbol{m}} = \frac{v_\parallel}{B_0}\tilde{B}^r_{\boldsymbol{m}} - \frac{\mathrm{i}ck_\perp}{B_0}\tilde{\Phi}_{\boldsymbol{m}} - \frac{\mathrm{i}k_\perp v_\perp^2}{2\omega_{\mathrm{c}0}B_0}\tilde{B}_{\boldsymbol{m}\parallel} - \frac{\mathrm{i}k_\parallel v_\parallel^2}{\omega_{\mathrm{c}0}B_0}\tilde{B}_{\boldsymbol{m}\perp}.} \tag{2.135}$$

The first term describes the parallel motion of particles along perturbed magnetic field lines. The second term is the $\boldsymbol{E}\times\boldsymbol{B}$-drift due to the violation of equipotentiality on the unperturbed flux surface. These two terms have an effect only in the resonance layer, where ideal MHD is not valid. The third and fourth term are magnetic drifts, or to be more precise, the gradient B and curvature drift, respectively.[6] They are small in the resonant layer where [30]

$$k_\parallel v_T \lesssim k_\perp V_E \tag{2.136}$$

due to

$$k_\parallel = \frac{m_\vartheta + m_\varphi q}{qR} \ll k_\perp \sim \frac{m_\vartheta}{R}. \tag{2.137}$$

In the following magnetic drifts are no longer considered being smaller than the $\boldsymbol{E}\times\boldsymbol{B}$ drift by a factor of the order of the aspect ratio [30].

The Fourier expansion of the directional derivative $\dot{\boldsymbol{R}}_0\cdot\nabla$ gives $(v_\parallel\hat{\boldsymbol{h}}_0 + \boldsymbol{V}_E)\cdot\nabla = \mathrm{i}v_\parallel\hat{\boldsymbol{h}}_0\cdot\boldsymbol{k} + \mathrm{i}c(\boldsymbol{E}\times\boldsymbol{B}_0\cdot\boldsymbol{k})/B_0^2 = \mathrm{i}v_\parallel k_\parallel + \mathrm{i}V_{E\perp}k_\perp$, i.e.

$$\mathscr{F}\left\{\dot{\boldsymbol{R}}_0\cdot\nabla\right\} = \mathrm{i}(k_\parallel v_\parallel + \omega_E) \tag{2.138}$$

with

$$\omega_E = k_\perp V_{E\perp} = \frac{ck_\perp}{B_0}\frac{\partial\Phi_0}{\partial r}. \tag{2.139}$$

Referring again to a system moving with velocity parallel fluid velocity $V_{\parallel 0}$, the

[6] It is discussed in [30] that this results agrees with the canonical Hamiltonian formalism in action-angle variables, where the first three terms correspond to the first order perturbed Hamiltonian $\tilde{\mathcal{H}} = -e/c\,\boldsymbol{v}_0\cdot\tilde{\boldsymbol{A}} = \mathrm{i}e/\omega\,\boldsymbol{v}_0\cdot\tilde{\boldsymbol{E}} = \mathrm{i}e/\omega\,\Omega^i\mathcal{E}_i$ [25, 32], valid in the radiation gauge $\Phi_1 = 0$ via $v^r_{\boldsymbol{m}}|_{v_\parallel=-\omega_E/k_\parallel} = -\mathrm{i}ck_\perp/eB_0\,\mathcal{H}_{\boldsymbol{m}}$, while the fourth term, i.e. the curvature drift belongs to the second order Hamiltonian $e^2/2mc^2\,\tilde{\boldsymbol{A}}^2$.

Fourier expansion of the first order kinetic equation (2.118) hence is [30]

$$\boxed{\hat{L}\tilde{f}_{\boldsymbol{m}} = \mathrm{i}\left(k_{\parallel}u + \omega_E\right)\tilde{f}_{\boldsymbol{m}} - \hat{L}_{\mathrm{c}}\tilde{f}_{\boldsymbol{m}} = \tilde{Q}_{\boldsymbol{m}},} \tag{2.140}$$

where the inhomogeneity, the transport driving gradients are combined to the source term

$$\tilde{Q}_{\boldsymbol{m}} = -\left[\mathscr{A}_1 + \frac{m\left(v_\perp^2 + u^2\right)}{2T}\mathscr{A}_2\right] f_0 v^r_{\boldsymbol{m}}. \tag{2.141}$$

2.4.1 Fluxes and the Diffusion Tensor

In the following fluxes of particles and heat through a flux surface S are determined from the perturbed distribution function $\tilde{f}$ as follows [30],

$$\Gamma \approx \frac{1}{S}\int_S \mathrm{d}S \int_{\mathbb{R}^3} \mathrm{d}^3p\, \tilde{f}\, \dot{\boldsymbol{R}}_1 \cdot \nabla r, \tag{2.142}$$

$$Q \approx \frac{1}{S}\int_S \mathrm{d}S \int_{\mathbb{R}^3} \mathrm{d}^3p\, (\mathcal{H} - e\Phi)\tilde{f}\, \dot{\boldsymbol{R}}_1 \cdot \nabla r. \tag{2.143}$$

In this approximation, by substituting the Fourier series one obtains

$$\begin{aligned}\Gamma &= \frac{1}{2\pi r L} r \int_{-\pi}^{\pi}\mathrm{d}\vartheta \int_0^L \mathrm{d}z \int_{\mathbb{R}^3}\mathrm{d}^3p\, \Re\sum_{\boldsymbol{m}} \tilde{f}_{\boldsymbol{m}} \mathrm{e}^{\mathrm{i}m_\vartheta\vartheta + \mathrm{i}k_z z}\, \Re\sum_{\boldsymbol{m}'} v^r_{\boldsymbol{m}'}\mathrm{e}^{\mathrm{i}m'_\vartheta\vartheta + \mathrm{i}k'_z z} \\ &= \frac{1}{2}\Re\sum_{\boldsymbol{m}}\int_{\mathbb{R}^3}\mathrm{d}^3p\, \tilde{f}_{\boldsymbol{m}} v^{r*}_{\boldsymbol{m}}\end{aligned} \tag{2.144}$$

and analogously for the heat flux

$$Q = \frac{1}{2}\Re\sum_{\boldsymbol{m}}\int_{\mathbb{R}^3}\mathrm{d}^3p\, \frac{m}{2}\left(v_\perp^2 + u^2\right)\tilde{f}_{\boldsymbol{m}} v^{r*}_{\boldsymbol{m}}, \tag{2.145}$$

as is shown in [30].

2.4.2 The Collisionless Limit

In the collisionless limit, formally $\hat{L}_{\mathrm{c}} \to 0$ and the linearised, Fourier expanded kinetic equation (2.140) becomes algebraic and one obtains [30]

$$\boxed{\tilde{f}_{\boldsymbol{m}} = \frac{\mathrm{i}v^r_{\boldsymbol{m}}}{k_{\parallel}u + \omega_E - \mathrm{i}0^+}\left[\mathscr{A}_1 + \frac{m}{2T}\left(v_\perp^2 + u^2\right)\mathscr{A}_2\right] f_0.} \tag{2.146}$$

The solution $\tilde{f}_{\boldsymbol{m}}$ of the kinetic equation is substituted into the expressions for the particle and heat fluxes (2.144) and (2.145), again shown here explicitly

for the particle flux,

$$\begin{aligned}\Gamma &= \frac{1}{2}\,\Re\sum_{\boldsymbol{m}}\int_{\mathbb{R}^3}\mathrm{d}^3p\,f_0\frac{\mathrm{i}\,|v^r_{\boldsymbol{m}}|^2}{k_\parallel u+\omega_E-\mathrm{i}0^+}\sum_{i=1}^{2}a_i\mathscr{A}_i\\ &= -\frac{\pi}{2}\sum_{\boldsymbol{m}}\int_{\mathbb{R}^3}\mathrm{d}^3p\,f_0\,\delta(k_\parallel u+\omega_E)|v^r_{\boldsymbol{m}}|^2\sum_{i=1}^{2}a_i\mathscr{A}_i,\end{aligned}\tag{2.147}$$

where Plemelj's formula has been applied. From the fluxes Γ and Q the diffusion tensor $\boldsymbol{D}$ is obtained, whose coefficients are related to the fluxes via the thermodynamic forces, see [24], as follows,

$$\begin{aligned}\Gamma &= -n_0(D_{11}\mathscr{A}_1+D_{12}\mathscr{A}_2),\\ Q &= -n_0T(D_{21}\mathscr{A}_1+D_{22}\mathscr{A}_2).\end{aligned}$$

By comparison with the computed fluxes, the matrix elements of the diffusion tensor $\boldsymbol{D}$ are seen to be [30]

$$D_{kl}=\frac{\pi}{2n_0}\sum_{\boldsymbol{m}}\int_{\mathbb{R}^3}\mathrm{d}^3p\;\delta(k_\parallel u+\omega_E)\,|v^r_{\boldsymbol{m}}|^2\,a_ka_lf_0,\tag{2.148}$$

with the coefficients $a_k(v_\perp,u)$ being

$$a_1=1,\qquad a_2=\frac{m}{2T}\left(v_\perp^2+u^2\right).\tag{2.149}$$

In the following, the diffusion coefficients are evaluated explicitly according to Eq. (2.148). Since the integrand is expressed in parallel and perpendicular velocity components, the integrals are evaluated over velocity space in cylindrical coordinates,

$$\mathrm{d}^3p=2\pi m^3v_\perp\,\mathrm{d}v_\perp\,\mathrm{d}u$$

with

$$\int_{\mathbb{R}^3}\mathrm{d}^3p=2\pi\,m^3\int_{-\infty}^{\infty}\mathrm{d}u\int_0^{\infty}v_\perp\,\mathrm{d}v_\perp,\tag{2.150}$$

see Fig. (2.6). Explicit evaluation of e.g. coefficient D_{12} gives

$$\begin{aligned}D_{12} &= \frac{\pi}{2n_0}\sum_{\boldsymbol{m}}\int_{\mathbb{R}^3}\mathrm{d}^3p\,\delta(k_\parallel u+\omega_E)|v^r_{\boldsymbol{m}}|^2\frac{m}{2T}(v_\perp^2+u^2)f_0\\ &= \frac{\pi m^3}{4n_0v_T^2}\sum_{\boldsymbol{m}}\int_{\mathbb{R}}\mathrm{d}u\,\mathrm{e}^{-\frac{mu^2}{2T}}\,|v^r_{\boldsymbol{m}}|^2\,\frac{\delta(u+\omega_E/k_\parallel)}{k_\parallel}\int_0^{\infty}2\pi v_\perp\,\mathrm{d}v_\perp\frac{n_0(v_\perp^2+u^2)}{(2\pi mT)^{3/2}}\mathrm{e}^{-\frac{mv_\perp^2}{2T}}\end{aligned}$$

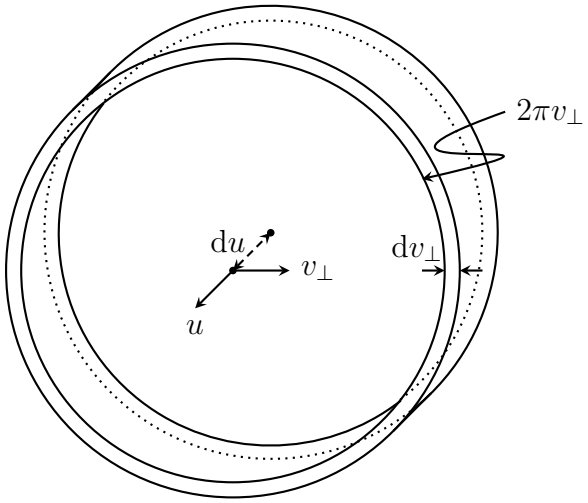

Figure 2.6: Momentum space volume element $\mathrm{d}^3p = 2\pi m^3 v_\perp \, \mathrm{d}v_\perp \, \mathrm{d}u$

$$
\begin{aligned}
&= \frac{\sqrt{\pi}}{2^{5/2} k_\parallel v_T^5} \sum_{\boldsymbol{m}} |v_{\boldsymbol{m}}^r|^2_{u=-\omega_E/k_\parallel} \mathrm{e}^{-\omega_E^2/2k_\parallel^2 v_T^2} \\
&\quad \times \left(\int_0^\infty \mathrm{d}v_\perp \, v_\perp^3 \mathrm{e}^{-mv_\perp^2/2T} + \left(\frac{\omega_E}{k_\parallel}\right)^2 \int_0^\infty \mathrm{d}v_\perp \, v_\perp \mathrm{e}^{-mv_\perp^2/2T} \right) \\
&= \frac{\sqrt{\pi}|Z|}{4|\omega_E|} \mathrm{e}^{-Z^2} |v_{\boldsymbol{m}}^r|^2_{u=-\omega_E/k_\parallel} \left(2 + \frac{1}{v_T^2} \frac{\omega_E^2}{k_\parallel^2} \right)
\end{aligned}
\tag{2.151}
$$

with $Z = -\omega_E/\sqrt{2}k_\parallel v_T$. From analogous calculations for the remaining coefficients the symmetric diffusion matrix for particle and heat flux is obtained,

$$
\begin{aligned}
D = \frac{\sqrt{\pi}|Z|}{2|\omega_E|} \mathrm{e}^{-Z^2} &\sum_{\boldsymbol{m}} |v_{\boldsymbol{m}}^r|^2_{u=-\omega_E/k_\parallel} \\
&\cdot \begin{pmatrix} 1 & \frac{1}{2}\left(2 + \frac{1}{v_T^2}\frac{\omega_E^2}{k_\parallel^2}\right) \\ \frac{1}{2}\left(2 + \frac{1}{v_T^2}\frac{\omega_E^2}{k_\parallel^2}\right) & \frac{2}{v_T^5}\left(v_T^5 + \frac{\omega_E^2 v_T^3}{2k_\parallel^2} + \frac{v_T \omega_E^4}{8k_\parallel^4}\right) \end{pmatrix}.
\end{aligned}
\tag{2.152}
$$

2.4.3 The General Collisional Case

Considering now the collisional case, the solution of the linearised kinetic equation (2.140) with the purely differential collision operator $\hat{L}_\mathrm{c} = \hat{L}_\mathrm{cD}$ for $t > t_0$

can be written as [33]

$$\tilde{f}_{\boldsymbol{m}}(u,t) = \int_{t_0}^{t} \mathrm{d}\tau \int_{\mathbb{R}} \mathrm{d}u'\, \tilde{G}^{\mathrm{D}}_{\boldsymbol{m}}(u,u',t-\tau)\tilde{Q}_{\boldsymbol{m}}(u',\tau) \tag{2.153}$$

with $\tilde{G}^{\mathrm{D}}_{\boldsymbol{m}}(u,u',t)$, the Green's function for the purely differential problem that is given by [33]

$$\tilde{G}^{\mathrm{D}}_{\boldsymbol{m}}(u,u',t) = \begin{cases} 0 & t \leq 0 \\ \dfrac{1}{\sqrt{4\pi\tilde{a}}} \exp\left[\mathrm{i}\dfrac{k_\parallel}{\nu}(u-u') - c - \dfrac{1}{4\tilde{a}}(u-u'\mathrm{e}^{-\nu t} + \mathrm{i}\tilde{b})^2\right] & t > 0 \end{cases} \tag{2.154}$$

with

$$\tilde{a}(t) = \frac{v_T^2}{2}\left(1-\mathrm{e}^{-2\nu t}\right), \quad \tilde{b}(t) = \frac{2k_\parallel v_T^2}{\nu}\left(1-\mathrm{e}^{-\nu t}\right), \quad c(t) = \left(\mathrm{i}\omega_\ell + \frac{k_\parallel v_T^2}{\nu}\right)t. \tag{2.155}$$

The Green's function $\tilde{G}^{\mathrm{D}}_{\boldsymbol{m}}(u,u',t)$, being the inverse operator of $\hat{L}$ has to satisfy the relation

$$\hat{L}\tilde{G}^{\mathrm{D}}_{\boldsymbol{m}} = \delta(t-t_0)\delta(u-u'). \tag{2.156}$$

A complete derivation of the Green's function by the method of characteristics is presented in Appendix A. In the following mainly its temporal Fourier transform

$$\tilde{G}^{\mathrm{D}}_{\omega\boldsymbol{m}}(u,u') = \int_0^\infty \mathrm{d}t\, \mathrm{e}^{\mathrm{i}\omega t}\tilde{G}^{\mathrm{D}}_{\boldsymbol{m}}(u,u',t) \tag{2.157}$$

is used.

Now the solution of the full integro-differential problem, i.e. the linearised kinetic equation with right hand side $\hat{L}_{\mathrm{c}}\tilde{f}_{\boldsymbol{m}} = \hat{L}_{\mathrm{cD}}\tilde{f}_{\boldsymbol{m}} + \hat{L}^{\mathrm{E}}_{\mathrm{cI}}\tilde{f}_{\boldsymbol{m}}$ is [30]

$$\begin{aligned} \tilde{f}_{\boldsymbol{m}}(u) &= \int_{\mathbb{R}} \mathrm{d}u'\, \tilde{G}_{\omega\boldsymbol{m}}(u,u')\tilde{Q}_{\boldsymbol{m}}(v_\perp,u') \\ &= -\int_{\mathbb{R}} \mathrm{d}u'\, \tilde{G}_{\omega\boldsymbol{m}}(u,u')\left[\mathscr{A}_1 + a_2(v_\perp,u')\mathscr{A}_2\right] f_0(v_\perp,u')v^r_{\boldsymbol{m}}(v_\perp,u'), \end{aligned} \tag{2.158}$$

where the new Green's function $\tilde{G}_{\omega\boldsymbol{m}}(u,u')$ is given in terms of moments of the original Ornstein-Uhlenbeck Green's function $\tilde{G}^{\mathrm{D}}_{\omega\boldsymbol{m}}(u,u')$ as follows [30]

$$\begin{aligned} \tilde{G}_{\omega\boldsymbol{m}}(u,u') = \tilde{G}^{\mathrm{D}}_{\omega\boldsymbol{m}}(u,u') &+ \frac{\nu C^{-1}_{\boldsymbol{m}}}{\sqrt{2\pi}v_T} \\ &\times \int_{\mathbb{R}} \mathrm{d}u'''\, \tilde{G}^{\mathrm{D}}_{\omega\boldsymbol{m}}(u,u''') \exp\left(-\frac{u'''^2}{2v_T^2}\right)\left(\frac{u'''^2}{v_T^2} - 1\right) \end{aligned}$$

$$\times \int_{\mathbb{R}} \mathrm{d}u'' \left(\frac{u''^2}{v_T^2} - 1 \right) \tilde{G}^{\mathrm{D}}_{\omega \boldsymbol{m}}(u'', u') \tag{2.159}$$

with constant $C_{\boldsymbol{m}}$ being

$$C_{\boldsymbol{m}} = 1 - \frac{\nu}{\sqrt{2\pi} v_T} \int_{\mathbb{R}} \mathrm{d}u'' \left(\frac{u''^2}{v_T^2} - 1 \right) \times \int_{\mathbb{R}} \mathrm{d}u' \, \tilde{G}^{\mathrm{D}}_{\omega \boldsymbol{m}}(u'', u') \exp\left(-\frac{u'^2}{2v_T^2} \right) \left(\frac{u'^2}{v_T^2} - 1 \right). \tag{2.160}$$

The details of obtaining the solution of the integro-differential equation is deferred to Chapter 3, where the solution of the kinetic equation with an even more extended collision operator, additionally conserving momentum for each species is discussed. Since the purely energy conserving calculation on which we focus here is a special case of the solution with the full integro-differential operator, the results presented here will be derived as limit cases of the more general calculation presented later.

Substitution of the formal solution (2.158) into the formulas for the particle (2.144) and energy fluxes (2.145) gives the diffusion coefficients formally as [30]

$$D_{kl} = \frac{\pi m^3}{n_0} \Re \sum_{\boldsymbol{m}} \int_0^\infty \mathrm{d}v_\perp \, v_\perp \int_{\mathbb{R}} \mathrm{d}u \int_{\mathbb{R}} \mathrm{d}u' \, \tilde{G}_{\omega \boldsymbol{m}}(u, u') \times v^{r*}_{\boldsymbol{m}}(v_\perp, u) v^r_{\omega \boldsymbol{m}}(v_\perp, u') a_k(v_\perp, u) a_l(v_\perp, u') f_0(v_\perp, u'). \tag{2.161}$$

If one evaluates the integral over perpendicular velocity, one can express the diffusion coefficients in terms of moments I^{mn} of the Green's function, defined by [30]

$$I^{mn}(x_1, x_2) \stackrel{\mathrm{def}}{=} \frac{\nu}{\sqrt{2\pi} v_T^{m+n+1}} \int_{\mathbb{R}} \mathrm{d}u \int_{\mathbb{R}} \mathrm{d}u' \, \tilde{G}_{\omega \boldsymbol{m}}(u, u') \exp\left(-\frac{u'^2}{2v_T^2} \right) u^m u'^n \tag{2.162}$$

with the dimensionless parameters

$$x_1 = \frac{k_\parallel v_T}{\nu} \qquad \text{and} \qquad x_2 = -\frac{\omega_E}{\nu} \tag{2.163}$$

as follows [30],

$$D_{11} = \frac{1}{2\nu B_0^2} \sum_{\boldsymbol{m}} \Big[c^2 |\tilde{E}_{\boldsymbol{m}\perp}|^2 \, \Re(I^{00}) + 2cv_T \, \Re(\tilde{E}^*_{\boldsymbol{m}\perp} \tilde{B}^r_{\boldsymbol{m}}) \times \Re(I^{10}) + v_T^2 |\tilde{B}^r_{\boldsymbol{m}}|^2 \, \Re(I^{11}) \Big], \tag{2.164}$$

$$D_{12} = D_{21} = \frac{1}{2\nu B_0^2} \sum_{\boldsymbol{m}} \Big[c^2 |\tilde{E}_{\boldsymbol{m}\perp}|^2 \, \Re(I^{00} + {}^1\!/_2 I^{20}) + 2cv_T \, \Re(\tilde{E}^*_{\boldsymbol{m}\perp} \tilde{B}^r_{\boldsymbol{m}}) \, \Re(I^{10} + {}^1\!/_4 I^{30} + {}^1\!/_4 I^{21}) + v_T^2 |\tilde{B}^r_{\boldsymbol{m}}|^2 \, \Re(I^{11} + {}^1\!/_2 I^{31}) \Big], \tag{2.165}$$

$$D_{22} = \frac{1}{2\nu B_0^2} \sum_{\boldsymbol{m}} \Big[c^2 |\tilde{E}_{\boldsymbol{m}\perp}|^2 \, \Re(2I^{00} + I^{20} + {}^1\!/_4 I^{22}) + 2cv_T \, \Re(\tilde{E}^*_{\boldsymbol{m}\perp} \tilde{B}^r_{\boldsymbol{m}}) \, \Re(2I^{10} + {}^1\!/_2 I^{30} + {}^1\!/_2 I^{21} + {}^1\!/_4 I^{32}) + v_T^2 |\tilde{B}^r_{\boldsymbol{m}}|^2 \, \Re(2I^{11} + I^{31} + {}^1\!/_4 I^{32}) \Big]. \tag{2.166}$$

The moments for the full integro-differential problem, I^{mn} are related to the moments of the Ornstein-Uhlenbeck Green's function via [30]

$$I^{mn} = I_{\mathrm{D}}^{mn} + \frac{(I_{\mathrm{D}}^{m0} - I_{\mathrm{D}}^{m2})\,(I_{\mathrm{D}}^{n0} - I_{\mathrm{D}}^{n2})}{1 - I_{\mathrm{D}}^{00} + 2I_{\mathrm{D}}^{20} - I_{\mathrm{D}}^{22}}, \tag{2.167}$$

where I_{D}^{mn} can be explicitly derived from [33, 30]

$$I_{\mathrm{D}}^{mn}(x_1, x_2) = \left\{ \frac{\partial^{m+n}}{\partial\alpha^m \partial\beta^n} \int_0^\infty \mathrm{d}\tau \, \exp\left[(\mathrm{i}x_2 - x_1^2)\tau + (\alpha + \mathrm{i}x_1)(\beta + \mathrm{i}x_1)(\mathrm{e}^{-\tau} - 1) + \frac{(\alpha+\beta)^2}{2} \right] \right\}_{\alpha,\beta=0}. \tag{2.168}$$

With the solution (2.158) one can finally determine the parallel linear response current density in terms of the thermodynamic forces and moments of the Green's function [30]

$$\begin{aligned} \tilde{j}_{\boldsymbol{m}\parallel} &= e \int_{\mathbb{R}^3} \mathrm{d}^3 p \, u \tilde{f}_{\boldsymbol{m}} \\ &= -em^3 \int_0^\infty 2\pi v_\perp \, \mathrm{d}v_\perp \int_{\mathbb{R}} \mathrm{d}u \, u \int_{\mathbb{R}} \mathrm{d}u' \, G_{\omega\boldsymbol{m}}(u, u') \, [\mathscr{A}_1 + a_2(v_\perp, u')\mathscr{A}_2] \\ &\quad \times f_0(v_\perp, u') v^r_{\boldsymbol{m}}(v_\perp, u') \\ &= -\frac{n_0 e v_T}{\nu B_0} \Big\{ \left[(\mathscr{A}_1 + \mathscr{A}_2)\, I^{10} + {}^1\!/_2 \mathscr{A}_2 I^{21} \right] c\tilde{E}_{\boldsymbol{m}\perp} \\ &\quad + \left[(\mathscr{A}_1 + \mathscr{A}_2)\, I^{11} + {}^1\!/_2 \mathscr{A}_2 I^{31} \right] v_T \tilde{B}^r_{\boldsymbol{m}} \Big\}. \end{aligned} \tag{2.169}$$

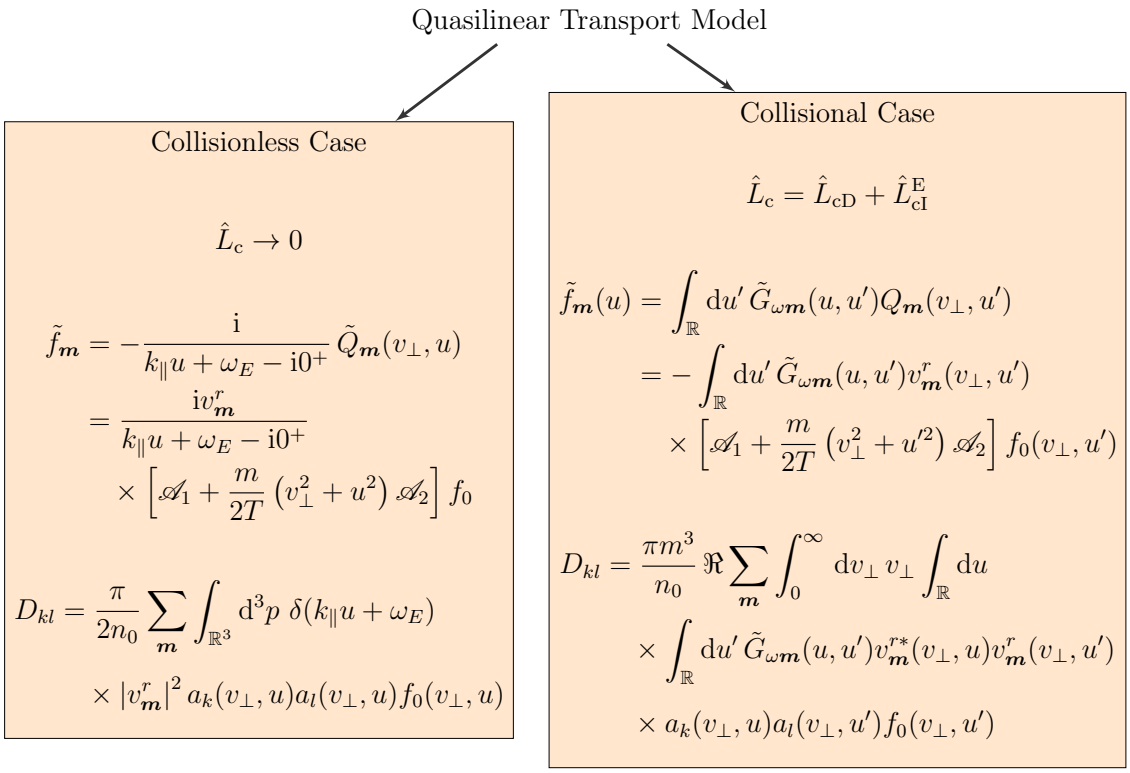

Figure 2.7: Comparison of the collisional case and the collisionless limit case of the quasilinear model.

2.5 Hamiltonian Quasilinear Model of RMP-driven Transport

Formulation of the Kinetic Equation in Action-Angle Variables

Kinetic theory in action-angle variables has been introduced in the 1960's by Kaufmann [34] and later by Mahajan and Chen [45]. Our model of RMP-plasma interaction has been formulated with action-angle variables by Heyn *et al.* (2006) [25] and improved w.r.t. a Galilean invariant collision operator by Ivanov *et al.* (2011) [33]. Action variables are defined by, see e.g. [61, p. 153],

$$J(E) \stackrel{\text{def}}{=} \frac{1}{2\pi} \oint_{\Gamma_E} p \, \mathrm{d}q, \tag{2.170}$$

where Γ_E is a periodic orbit corresponding to energy E. If a canonical transformation $G_2(\boldsymbol{q}, \boldsymbol{J}, t)$ from the original phase space coordinates $(\boldsymbol{p}, \boldsymbol{q})$ to coordinates $(\boldsymbol{J}, \boldsymbol{\Theta})$ is found, such that the new Hamiltonian

$$\mathcal{H}' = \mathcal{H} + \frac{\partial G_2(\boldsymbol{q}, \boldsymbol{J}, t)}{\partial t} \tag{2.171}$$

is independent of $\boldsymbol{\Theta}$, the new variables are denoted action $\boldsymbol{J}$ and angle $\boldsymbol{\Theta}$ variables[7]. An integrable system for which action-angle variables have been found is described by a Hamiltonian $\mathcal{H}_0(\boldsymbol{J})$. Hamilton's equations of motion for the canonical variables $\boldsymbol{J}$ and $\boldsymbol{\Theta}$ are

$$\dot{\boldsymbol{\Theta}} = \boldsymbol{\Omega} = \frac{\partial \mathcal{H}_0(\boldsymbol{J})}{\partial \boldsymbol{J}}, \qquad \dot{\boldsymbol{J}} = -\frac{\partial \mathcal{H}_0(\boldsymbol{J})}{\partial \boldsymbol{\Theta}} = \boldsymbol{0}. \tag{2.172}$$

The independence of the unperturbed (background) Hamiltonian of $\boldsymbol{\Theta}$ and thus the constancy of $\boldsymbol{J}$ is the main motivation for the coordinate transformation to action-angle variables. The Hamiltonian of a charged particle in the background field, expressed by its potentials is given by [33]

$$\mathcal{H}_0(\boldsymbol{r}, \boldsymbol{p}) = \frac{1}{2m} \left(\boldsymbol{p} - \frac{e}{c} \boldsymbol{A}_0(\boldsymbol{r}) \right)^2 + e\Phi_0(\boldsymbol{r}).$$

By the application of perturbations, the Hamiltonian of the perturbed system

[7] The index "2" refers to the special class of generating functions that depend on the old configuration space variables $\boldsymbol{q}$ and the new momenta $\boldsymbol{J}$, e.g. [18].

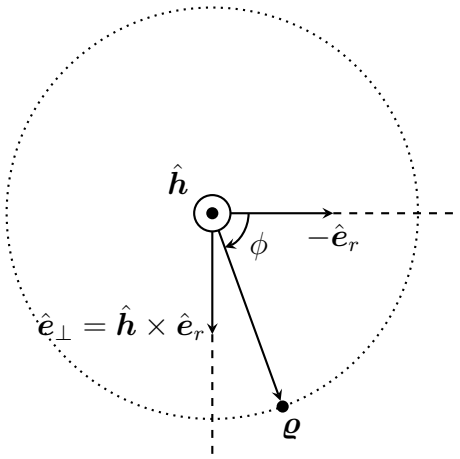

Figure 2.8: Gyroorbit in frame positioned at $\boldsymbol{R}(t)$ and spanned by $\hat{\boldsymbol{e}}_r$ and $\hat{\boldsymbol{h}} \times \hat{\boldsymbol{e}}_r$.

is given by, see e.g. [61],

$$\mathcal{H}(\boldsymbol{J}, \boldsymbol{\Theta}, \epsilon) = \mathcal{H}_0(\boldsymbol{J}) + \epsilon \mathcal{H}_1(\boldsymbol{J}, \boldsymbol{\Theta}, \epsilon), \tag{2.173}$$

where ϵ is a measure for the strength of the perturbation.

The unperturbed motion is an integrable system with orbits $\boldsymbol{r} = \boldsymbol{R} + \boldsymbol{\varrho}$, or expressed in contravariant components

$$x^i_{\mathrm{c}}(\boldsymbol{J}, \boldsymbol{\Theta}) = x^i_{\mathrm{gc}}(\boldsymbol{J}) + \varrho^i(\boldsymbol{J}, \boldsymbol{\Theta}), \tag{2.174}$$

where the guiding centre coordinates are independent of the gyrophase [25] and the index "c" denotes "curvilinear". The gyroorbit is given by

$$\boldsymbol{\varrho} = \|\boldsymbol{\varrho}\| \left(\sin\phi\, \hat{\boldsymbol{h}} \times \hat{\boldsymbol{e}}_r - \cos\phi\, \hat{\boldsymbol{e}}_r \right), \tag{2.175}$$

see Fig. (2.5), where $\|\boldsymbol{\varrho}\| = \varrho = \sqrt{2J_\perp / m\omega_{\mathrm{c}}}$. Considering $\hat{\boldsymbol{h}} \perp \hat{\boldsymbol{e}}_r$, one can evaluate (2.175) in contravariant cylindrical coordinates,

$$\begin{aligned}
\boldsymbol{\varrho} &= \varrho \left[\sin\phi \left(\hat{h}_\vartheta \hat{\boldsymbol{e}}_\vartheta + \hat{h}_z \hat{\boldsymbol{e}}_z \right) \times \hat{\boldsymbol{e}}_r - \cos\phi\, \hat{\boldsymbol{e}}_r \right] \\
&= \varrho \left[\sin\phi \left(\hat{h}_z \hat{\boldsymbol{e}}_\vartheta - \hat{h}_\vartheta\, \hat{\boldsymbol{e}}_z \right) - \cos\phi\, \hat{\boldsymbol{e}}_r \right] \\
&= \varrho \left[\sin\phi \left(h_z \frac{\boldsymbol{e}_\vartheta}{\sqrt{g_{\vartheta\vartheta}}} - \frac{h_\vartheta}{\sqrt{g_{\vartheta\vartheta}}} \boldsymbol{e}_z \right) - \cos\phi\, \boldsymbol{e}_r \right],
\end{aligned}$$

so that [33]

$$\varrho^r = -\varrho\cos\phi, \quad \varrho^\vartheta = \frac{\varrho}{r}h_z\sin\phi, \quad \varrho^z = -\frac{\varrho}{r}h_\vartheta\sin\phi. \tag{2.176}$$

Having obtained the orbit of a particle in the unperturbed system, the next task is to formulate the kinetic equation for the background distribution function f_0 in action-angle variables. For Cartesian phase-space variables $\boldsymbol{p}_0$ and $\boldsymbol{r}$, where $\boldsymbol{p}_0$ denotes the canonical momentum of the unperturbed system, i.e. $\boldsymbol{p}_0 = m\boldsymbol{v} + (e/c)\boldsymbol{A}_0$ and $\boldsymbol{r}$ is the Cartesian configuration space vector, it is [33]

$$\boldsymbol{v}\cdot\frac{\partial f_0}{\partial \boldsymbol{r}} + \boldsymbol{F}_0\cdot\frac{\partial f_0}{\partial \boldsymbol{p}_0} = \hat{L}_\mathrm{c} f_0 + S, \tag{2.177}$$

where internal sources and sinks are considered in the source term S and $\boldsymbol{F}_0$ is the zeroth-order Lorentz force $\boldsymbol{F}_0 = e\boldsymbol{E}_0 + (e/c)\boldsymbol{v}\times\boldsymbol{B}_0$. The kinetic equation is covariant under the transformation $(\boldsymbol{p}_0, \boldsymbol{r}) \to (\boldsymbol{J}, \boldsymbol{\Theta})$, so that for the new velocities $\mathcal{V}_0^i$ and forces $\mathcal{F}_{0i}$ it reads [33]

$$\mathcal{V}_0^i\frac{\partial f_0}{\partial \Theta^i} + \mathcal{F}_{0i}\frac{\partial f_0}{\partial J_i} = \hat{L}_\mathrm{c} f_0 + S. \tag{2.178}$$

In the following, the velocities and forces for the background system in the new action-angle phase space are determined. First we consider that substituting $K = p_j$ and $K = x^j$ into the expression for a Poisson bracket of two arbitrary observables,

$$\{F, K\} = \sum_{i=1}^{f}\left(\frac{\partial F}{\partial x^i}\frac{\partial K}{\partial p_i} - \frac{\partial F}{\partial p_i}\frac{\partial K}{\partial x^i}\right) \tag{2.179}$$

where the index $f = 3$ is the number of degrees of freedom of our particle, gives

$$\{F, p_j\} = \frac{\partial F}{\partial x^i}\delta_i^j = \frac{\partial F}{\partial x^j}, \qquad \{F, x^j\} = -\frac{\partial F}{\partial p_i}\frac{\partial x^j}{\partial x^i} = -\frac{\partial F}{\partial p_i}\delta_i^j = -\frac{\partial F}{\partial p_j}, \tag{2.180}$$

so that $\nabla_{\boldsymbol{r}} F = \{f, \boldsymbol{p}\}$ and $\nabla_{\boldsymbol{p}} F = \{\boldsymbol{r}, F\} = -\{F, \boldsymbol{r}\}$. We will also make use of the Poisson brackets

$$\frac{\partial \Theta^i}{\partial \boldsymbol{r}} = \{\Theta^i, \boldsymbol{p}_0\} = \frac{\partial \Theta^i}{\partial \Theta^j}\frac{\partial \boldsymbol{p}_0}{\partial J_j} - \frac{\partial \Theta^i}{\partial J_j}\frac{\partial \boldsymbol{p}_0}{\partial \Theta^j} = \frac{\partial \boldsymbol{p}_0}{\partial J_i}, \tag{2.181}$$

$$\frac{\partial \Theta^i}{\partial \boldsymbol{p}_0} = \{\boldsymbol{r}, \Theta^i\} = \frac{\partial \boldsymbol{r}}{\partial \Theta^j}\frac{\partial \Theta^i}{\partial J_j} - \frac{\partial \Theta^i}{\partial \Theta^j}\frac{\partial \boldsymbol{r}}{\partial J_j} = -\frac{\partial \boldsymbol{r}}{\partial J_i}. \tag{2.182}$$

Now the left hand side of the kinetic equation in its original form (2.177) can

be written

$$\frac{\mathrm{d}f_0}{\mathrm{d}t} = \dot{\boldsymbol{r}} \cdot \{f_0, \boldsymbol{p}_0\} + \dot{\boldsymbol{p}}_0 \cdot \{\boldsymbol{r}, f_0\}, \tag{2.183}$$

and due to the invariance of Poisson-brackets under canonical transformations also as

$$\frac{\mathrm{d}f_0}{\mathrm{d}t} = \{\boldsymbol{r}, \mathcal{H}_0\} \cdot \left(\frac{\partial f_0}{\partial \Theta^i} \frac{\partial \boldsymbol{p}_0}{\partial J_i} - \frac{\partial f}{\partial J_i} \frac{\partial \boldsymbol{p}_0}{\partial \Theta^i} \right) + \{\boldsymbol{p}_0, \mathcal{H}_0\} \cdot \left(\frac{\partial \boldsymbol{r}}{\partial \Theta^i} \frac{\partial f_0}{\partial J_i} - \frac{\partial \boldsymbol{r}}{\partial J_i} \frac{\partial f_0}{\partial \Theta^i} \right). \tag{2.184}$$

Since in the action-angle formalism $\mathcal{H}_0 = \mathcal{H}_0(\boldsymbol{J})$ only, the special Poisson-brackets for $\dot{\boldsymbol{r}}$ and $\dot{\boldsymbol{p}}_0$ simplify as follows,

$$\dot{\boldsymbol{r}} = \{\boldsymbol{r}, \mathcal{H}_0\} = \frac{\partial \boldsymbol{r}}{\partial \Theta^i} \frac{\partial \mathcal{H}_0}{\partial J_i} - \frac{\partial \boldsymbol{r}}{\partial J_i} \frac{\partial \mathcal{H}_0}{\partial \Theta^i} = \Omega^i \frac{\partial \boldsymbol{r}}{\partial \Theta^i}, \tag{2.185}$$

$$\dot{\boldsymbol{p}}_0 = \{\boldsymbol{p}_0, \mathcal{H}_0\} = \frac{\partial \boldsymbol{p}_0}{\partial \Theta^i} \frac{\partial \mathcal{H}_0}{\partial J_i} - \frac{\partial \boldsymbol{p}_0}{\partial J_i} \frac{\partial \mathcal{H}_0}{\partial \Theta^i} = \Omega^i \frac{\partial \boldsymbol{p}_0}{\partial \Theta^i}. \tag{2.186}$$

Substituting these two expressions into (2.184), reordering terms and considering (2.181) and (2.182) shows that the left hand side of the kinetic equation simplifies considerably,

$$\begin{aligned} \frac{\mathrm{d}f_0}{\mathrm{d}t} &= \frac{\partial f_0}{\partial \Theta^i} \left(\frac{\partial \boldsymbol{p}_0}{\partial J_i} \frac{\partial \boldsymbol{r}}{\partial \Theta^j} \Omega^j - \frac{\partial \boldsymbol{r}}{\partial J_i} \frac{\partial \boldsymbol{p}_0}{\partial \Theta^j} \Omega^j \right) \\ &\quad + \frac{\partial f_0}{\partial J_i} \left(\frac{\partial \boldsymbol{r}}{\partial \Theta^i} \frac{\partial \boldsymbol{p}_0}{\partial \Theta^j} \Omega^j - \frac{\partial \boldsymbol{p}_0}{\partial \Theta^i} \frac{\partial \boldsymbol{r}}{\partial \Theta^j} \Omega^j \right) \\ &= \frac{\partial f_0}{\partial \Theta^i} \delta^i_j \Omega^j = \frac{\partial f_0}{\partial \Theta^i} \Omega^i, \end{aligned} \tag{2.187}$$

where it has been used that the Jacobian determinant of a canonical transformation $|\partial(\boldsymbol{p}_0, \boldsymbol{r})/\partial(\boldsymbol{J}, \boldsymbol{\Theta})| \equiv 1$. The left hand side of the kinetic equation (2.177) can also be written as

$$\begin{aligned} \frac{\mathrm{d}f_0}{\mathrm{d}t} &= \boldsymbol{v} \cdot \left(\frac{\partial f_0(\boldsymbol{J}, \boldsymbol{\Theta})}{\partial J_i} \frac{\partial J_i}{\partial \boldsymbol{r}} + \frac{\partial f_0(\boldsymbol{J}, \boldsymbol{\Theta})}{\partial \Theta^i} \frac{\partial \Theta^i}{\partial \boldsymbol{r}} \right) \\ &\quad + \boldsymbol{F}_0 \cdot \left(\frac{\partial f_0(\boldsymbol{J}, \boldsymbol{\Theta})}{\partial J_i} \frac{\partial J_i}{\partial \boldsymbol{p}_0} + \frac{\partial f_0(\boldsymbol{J}, \boldsymbol{\Theta})}{\partial \Theta^i} \frac{\partial \Theta^i}{\partial \boldsymbol{p}_0} \right) \\ &= \left(\boldsymbol{v} \cdot \frac{\partial \Theta^i}{\partial \boldsymbol{r}} + \boldsymbol{F}_0 \cdot \frac{\partial \Theta^i}{\partial \boldsymbol{p}_0} \right) \frac{\partial f_0}{\partial \Theta^i} + \left(\boldsymbol{v} \cdot \frac{\partial J_i}{\partial \boldsymbol{r}} + \boldsymbol{F}_0 \cdot \frac{\partial J_i}{\partial \boldsymbol{p}_0} \right) \frac{\partial f_0}{\partial J_i} \\ &= \left(\boldsymbol{v} \cdot \frac{\partial \boldsymbol{p}_0}{\partial J_i} - \boldsymbol{F}_0 \cdot \frac{\partial \boldsymbol{r}}{\partial J_i} \right) \frac{\partial f_0}{\partial \Theta^i} + \left(-\boldsymbol{v} \cdot \frac{\partial \boldsymbol{p}_0}{\partial \Theta^i} + \boldsymbol{F}_0 \cdot \frac{\partial \boldsymbol{r}}{\partial \Theta^i} \right) \frac{\partial f_0}{\partial J_i} \end{aligned} \tag{2.188}$$

so that by comparison with (2.178) one can identify $\mathcal{V}_0^i$ and $\mathcal{F}_{0i}$ as the coefficients

of $\partial f_0/\partial\Theta^i$ and $\partial f_0/\partial J_i$,

$$\mathcal{V}_0^i = \boldsymbol{v}\cdot\frac{\partial \boldsymbol{p}_0}{\partial J_i} - \boldsymbol{F}_0\cdot\frac{\partial \boldsymbol{r}}{\partial J_i} \quad \text{and} \quad \mathcal{F}_{0i} = -\boldsymbol{v}\cdot\frac{\partial \boldsymbol{p}_0}{\partial \Theta^i} + \boldsymbol{F}_0\cdot\frac{\partial \boldsymbol{r}}{\partial \Theta^i}, \tag{2.189}$$

cf. [33]. But in the Hamiltonian formulation it is also true that

$$\frac{\mathrm{d}f_0}{\mathrm{d}t} = \frac{\partial f_0}{\partial t} + \{f_0, \mathcal{H}_0\} = \frac{\partial f_0}{\partial \Theta^i}\frac{\partial \mathcal{H}_0}{\partial J_i} - \frac{\partial \mathcal{H}_0}{\partial \Theta^i}\frac{\partial f_0}{\partial J_i} = \Omega^i\frac{\partial f_0}{\partial \Theta^i} \tag{2.190}$$

and by comparison with (2.178) again one finds that [33]

$$\mathcal{V}_0^i = \frac{\partial \mathcal{H}_0}{\partial J_i} = \Omega^i, \qquad \mathcal{F}_{0i} = -\frac{\partial \mathcal{H}_0}{\partial \Theta^i} = 0. \tag{2.191}$$

If we consider f_0 Maxwellian, such that $\hat{L}_\mathrm{c} f_0 = 0$ and ignore the source term S, $\Omega^i\partial f_0/\partial\Theta^i = 0$ implies that $f_0 = f_0(\boldsymbol{J})$ [33].

Let us now consider the full kinetic equation for the perturbed motion in action-angle variables as given in [33],

$$\frac{\partial f}{\partial t} + \mathcal{V}^i\frac{\partial f}{\partial \Theta^i} + \mathcal{F}_i\frac{\partial f}{\partial J_i} = \hat{L}_\mathrm{c} f. \tag{2.192}$$

For this purpose the distribution function, the fields and their potentials, respectively are expanded as follows,

$$f = f_0 + \tilde{f}, \tag{2.193}$$

$$\Phi(\boldsymbol{r},t) = \Phi_0(\boldsymbol{r}) + \tilde{\Phi}(\boldsymbol{r},t), \qquad \boldsymbol{A}(\boldsymbol{r},t) = \boldsymbol{A}_0(\boldsymbol{r}) + \tilde{\boldsymbol{A}}(\boldsymbol{r},t) \tag{2.194}$$

$$\boldsymbol{E}(\boldsymbol{r},t) = \boldsymbol{E}_0(\boldsymbol{r}) + \tilde{\boldsymbol{E}}(\boldsymbol{r},t), \qquad \boldsymbol{B}(\boldsymbol{r},t) = \boldsymbol{B}_0(\boldsymbol{r}) + \tilde{\boldsymbol{B}}(\boldsymbol{r},t), \tag{2.195}$$

where $\tilde{\boldsymbol{E}} = -\nabla\tilde{\Phi} - (1/c)\partial\tilde{\boldsymbol{A}}/\partial t$, $\tilde{\boldsymbol{B}} = \nabla\times\tilde{\boldsymbol{A}}$ and $\tilde{\boldsymbol{F}} = e[\tilde{\boldsymbol{E}} + (1/c)\boldsymbol{v}\times\tilde{\boldsymbol{B}}]$ is the Lorentz force, first order in the perturbation. We can reuse (2.188) by substituting f for f_0 and $\boldsymbol{F} = \boldsymbol{F}_0 + \tilde{\boldsymbol{F}}$ for $\boldsymbol{F}_0$ to determine velocities and forces in action-angle variables, being

$$\mathcal{V}^i = \mathcal{V}_0^i - \tilde{\boldsymbol{F}}\cdot\frac{\partial \boldsymbol{r}}{\partial J_i}, \qquad \mathcal{F}_i = \mathcal{F}_{0i} + \tilde{\boldsymbol{F}}\cdot\frac{\partial \boldsymbol{r}}{\partial \Theta^i}. \tag{2.196}$$

In order to obtain the linearised kinetic equation, the expansions in background and perturbation parts are substituted into the kinetic equation (2.192) and the background kinetic equation (2.178) is subtracted, giving

$$\frac{\partial \tilde{f}}{\partial t} + \tilde{\boldsymbol{F}}\cdot\frac{\partial \boldsymbol{r}}{\partial J_i}\frac{\partial f_0}{\partial \Theta^i} + \mathcal{V}_0^i\frac{\partial \tilde{f}}{\partial \Theta^i} - \tilde{\boldsymbol{F}}\cdot\frac{\partial \boldsymbol{r}}{\partial J_i}\frac{\partial \tilde{f}}{\partial \Theta^i} + \tilde{\boldsymbol{F}}\cdot\frac{\partial \boldsymbol{r}}{\partial \Theta^i}\frac{\partial f_0}{\partial J_i} + \mathcal{F}_{0i}\frac{\partial \tilde{f}}{\partial J_i} = \hat{L}_\mathrm{c}\tilde{f}. \tag{2.197}$$

Neglecting terms quadratic in perturbed quantities and considering $f_0 = f_0(\boldsymbol{J})$, $\mathcal{F}_{0\alpha} = 0$ and $\mathcal{V}_0^i = \Omega^i$, as was found earlier, the linearised kinetic equation as formulated in [33] is obtained,

$$\boxed{\frac{\partial \tilde{f}}{\partial t} + \Omega^i \frac{\partial \tilde{f}}{\partial \Theta^i} + \dot{J}_i \frac{\partial f_0}{\partial J_i} = \hat{L}_{\mathrm{c}} \tilde{f},} \tag{2.198}$$

where $\dot{J}_i$ is the perturbation force in action-angle variables, which is obtained from the force in curvilinear coordinates by the transformation $\dot{J}_i = \tilde{\boldsymbol{F}} \cdot \partial \boldsymbol{r} / \partial \Theta^i$, considering that $\dot{J}_i$ transforms like a covariant vector,

$$\begin{aligned} \dot{J}_i = e\tilde{\mathcal{E}}_i^{\mathrm{t}} &= e\left[\tilde{\boldsymbol{E}} + \frac{\boldsymbol{v}}{c} \times (\nabla \times \tilde{\boldsymbol{A}})\right] \cdot \frac{\partial \boldsymbol{r}}{\partial \Theta^i} \\ &= e\tilde{\mathcal{E}}_i - \frac{e}{c} \Omega^j \left(\frac{\partial \tilde{\mathcal{A}}_i}{\partial \Theta^j} - \frac{\partial \tilde{\mathcal{A}}_j}{\partial \Theta^i} \right). \end{aligned} \tag{2.199}$$

Here

$$\tilde{\mathcal{E}}_i = -\frac{\partial \tilde{\Phi}}{\partial \Theta^i} - \frac{1}{c} \frac{\partial \tilde{\mathcal{A}}_i}{\partial t} \tag{2.200}$$

and the second line in (2.199) follows from the first by considering

$$\begin{aligned} \Omega^j \left(\frac{\partial \tilde{\mathcal{A}}_i}{\partial \Theta^j} - \frac{\partial \tilde{\mathcal{A}}_j}{\partial \Theta^i} \right) &= \Omega^j \frac{\partial \tilde{A}_k}{\partial x_{\mathrm{c}}^l} \left(\frac{\partial x_{\mathrm{c}}^l}{\partial \Theta^j} \frac{\partial x_{\mathrm{c}}^k}{\partial \Theta^i} - \frac{\partial x_{\mathrm{c}}^l}{\partial \Theta^i} \frac{\partial x_{\mathrm{c}}^k}{\partial \Theta^j} \right) \\ &= \frac{\partial \tilde{A}_k}{\partial x_{\mathrm{c}}^l} \left(v_{\mathrm{c}}^l \frac{\partial x_{\mathrm{c}}^k}{\partial \Theta^i} - v_{\mathrm{c}}^k \frac{\partial x_{\mathrm{c}}^l}{\partial \Theta^i} \right) \\ &\overset{k \leftrightarrow l}{=} \left(v_{\mathrm{c}}^l \frac{\partial \tilde{A}_k}{\partial x_{\mathrm{c}}^l} - v_{\mathrm{c}}^l \frac{\partial \tilde{A}_l}{\partial x_{\mathrm{c}}^k} \right) \frac{\partial x_{\mathrm{c}}^k}{\partial \Theta^i} \\ &= \sqrt{g} \epsilon_{lmk} v_{\mathrm{c}}^l \left(\frac{\epsilon^{mnp}}{\sqrt{g}} \frac{\partial \tilde{A}_n}{\partial x_{\mathrm{c}}^p} \right) \frac{\partial x_{\mathrm{c}}^k}{\partial \Theta^i} \\ &= \left(\delta_k^n \delta_l^p - \delta_l^n \delta_k^p \right) v_{\mathrm{c}}^l \frac{\partial \tilde{A}_n}{\partial x_{\mathrm{c}}^p} \frac{\partial x_{\mathrm{c}}^k}{\partial \Theta^i} \\ &= \left(v_{\mathrm{c}}^p \frac{\partial \tilde{A}_k}{\partial x_{\mathrm{c}}^p} - v_{\mathrm{c}}^n \frac{\partial \tilde{A}_n}{\partial x_{\mathrm{c}}^k} \right) \frac{\partial x_{\mathrm{c}}^k}{\partial \Theta^i} \\ &= -\left(\boldsymbol{v}_{\mathrm{c}} \times (\nabla \times \tilde{\boldsymbol{A}}) \right)_k \frac{\partial x_{\mathrm{c}}^k}{\partial \Theta^i}, \end{aligned} \tag{2.201}$$

where the index "c" denotes "curvilinear" in this context. Here, the coordinate

transformations

$$\tilde{\mathcal{A}}_i = \frac{\partial x_{\rm c}^k}{\partial \Theta^i}\tilde{A}_k \qquad \text{and} \qquad v_{\rm c}^l = \frac{\partial x_{\rm c}^l}{\partial \Theta^j}\Omega^j \tag{2.202}$$

have been considered in lines 1 and 2, summation dummy indices have been renamed in the second term in parenthesis in the second line and use has been made of the identity $(\boldsymbol{v}\times(\nabla\times\boldsymbol{E}))_i = v_j\partial_i E_j - v_j\partial_j E_i$. Thus, the total force in action-angle variables, as specified in [33], is given by

$$\mathcal{F}_i = \dot{J}_i = -e\frac{\partial\tilde{\Phi}}{\partial\Theta^i} - \frac{e}{c}\left[\frac{\partial\tilde{A}_i}{\partial t} + \Omega^j\left(\frac{\partial\tilde{A}_i}{\partial\Theta^j} - \frac{\partial\tilde{A}_j}{\partial\Theta^i}\right)\right]. \tag{2.203}$$

Now expanding the perturbed quantities in Fourier series as follows,

$$\tilde{f}(\boldsymbol{J},\boldsymbol{\Theta},t) = \sum_{\boldsymbol{m}}\tilde{f}_{\boldsymbol{m}}(\boldsymbol{J},t)\,\mathrm{e}^{\mathrm{i}\boldsymbol{m}\cdot\boldsymbol{\Theta}}, \tag{2.204}$$

$$\tilde{\Phi}(\boldsymbol{J},\boldsymbol{\Theta},t) = \sum_{\boldsymbol{m}}\tilde{\Phi}_{\boldsymbol{m}}(\boldsymbol{J},t)\,\mathrm{e}^{\mathrm{i}\boldsymbol{m}\cdot\boldsymbol{\Theta}}, \tag{2.205}$$

$$\tilde{\boldsymbol{A}}(\boldsymbol{J},\boldsymbol{\Theta},t) = \sum_{\boldsymbol{m}}\tilde{\boldsymbol{A}}_{\boldsymbol{m}}(\boldsymbol{J},t)\,\mathrm{e}^{\mathrm{i}\boldsymbol{m}\cdot\boldsymbol{\Theta}}, \tag{2.206}$$

$$\vdots$$

and substituting the expansions into the linearised kinetic equation (2.198), the linear kinetic equation for the Fourier amplitudes $\tilde{f}_{\boldsymbol{m}}$ is obtained [33],

$$\boxed{\frac{\partial\tilde{f}_{\boldsymbol{m}}}{\partial t} + \mathrm{i}\boldsymbol{m}\cdot\boldsymbol{\Omega}\tilde{f}_{\boldsymbol{m}} - \hat{L}_{\rm c}\tilde{f}_{\boldsymbol{m}} = \tilde{Q}_{\boldsymbol{m}}} \tag{2.207}$$

with the Fourier amplitudes of the source term being given by

$$\tilde{Q}_{\boldsymbol{m}}(\boldsymbol{J},t) = e\frac{\partial f_0}{\partial J_i}\left\{\mathrm{i}m_i\tilde{\Phi}_{\boldsymbol{m}} + \frac{1}{c}\left[\frac{\partial(\tilde{\mathcal{A}}_i)_{\boldsymbol{m}}}{\partial t} + \mathrm{i}\Omega^j\left(m_j(\tilde{\mathcal{A}}_i)_{\boldsymbol{m}} - m_i(\tilde{\mathcal{A}}_j)_{\boldsymbol{m}}\right)\right]\right\}. \tag{2.208}$$

In this model a 1-D Fokker-Planck collision operator in the Ornstein-Uhlenbeck approximation [69, 33] is considered,

$$\hat{L}_{\rm c}\tilde{f}_{\boldsymbol{m}}(\boldsymbol{J}) = \frac{\partial}{\partial u}D\left(\frac{\partial}{\partial u} + \frac{u}{v_T^2}\right)\tilde{f}_{\boldsymbol{m}}(\boldsymbol{J}). \tag{2.209}$$

With the frequencies [25, 32]

$$\Omega^{\phi} = \omega_{\mathrm{c}}, \quad \Omega^{\vartheta} = h^{\vartheta} v_{\parallel} + \frac{c h_z}{r_0 B_0} \frac{\mathrm{d}\Phi_0}{\mathrm{d}r_0}, \quad \Omega^{z} = h^{z} v_{\parallel} - \frac{c h_{\vartheta}}{r_0 B_0} \frac{\mathrm{d}\Phi_0}{\mathrm{d}r_0} \tag{2.210}$$

and the modes numbers $\boldsymbol{m} = (\ell, k_{\vartheta}, k_z)$, one obtains

$$\begin{aligned} \boldsymbol{m} \cdot \boldsymbol{\Omega} &= \ell\omega_{\mathrm{c}} + k_{\vartheta}\left(h^{\vartheta} v_{\parallel} + \frac{c h_z}{r_0 B_0} \frac{\mathrm{d}\Phi_0}{\mathrm{d}r_0}\right) + k_z \left(h^{z} v_{\parallel} - \frac{c h_{\vartheta}}{r_0 B_0} \frac{\mathrm{d}\Phi_0}{\mathrm{d}r_0}\right) \\ &= \ell\omega_{\mathrm{c}} + k_{\parallel} v_{\parallel} + k_{\perp} V_{E\perp}, \end{aligned} \tag{2.211}$$

using the already derived relations for the parallel and perpendicular wave numbers $k_{\parallel} = k_{\vartheta} h^{\vartheta} + k_z h^{z}$ and $k_{\perp} = (h_z k_{\vartheta} - h_{\vartheta} k_z)/r_0$. Using the definition of the electrical particle drift frequency $\omega_E = k_{\perp} V_{E\perp}$ and defining the Doppler-shifted frequency $\omega_{\ell} = \ell\omega_{\mathrm{c}} + \boldsymbol{k} \cdot \boldsymbol{V} = \ell\omega_{\mathrm{c}} + \omega_E + k_{\parallel} V_{\parallel}$ as the cyclotron frequency plus electric particle drift frequency, the kinetic equation can be written explicitly as [33]

$$\left[\frac{\partial}{\partial t} + \mathrm{i}(\omega_{\ell} + k_{\parallel} u) - D \frac{\partial}{\partial u}\left(\frac{\partial}{\partial u} + \frac{u}{v_T^2}\right)\right] \tilde{f}_{\boldsymbol{m}}(u, t) = \tilde{Q}_{\boldsymbol{m}}(u, t), \tag{2.212}$$

where the shifted parallel velocity $u = v_{\parallel} - V_{\parallel}$ and the constant diffusion coefficient $D = \nu v_T^2$ have been introduced. A formal solution of this equation in terms of a Green's function was obtained by Ivanov *et al*, 2011 [33],

$$\boxed{\tilde{f}_{\boldsymbol{m}}(u, t) = \int_0^{t-t_0} \mathrm{d}\tau \int_{\mathbb{R}} \mathrm{d}u' \, \tilde{G}^{\mathrm{D}}_{\boldsymbol{m}}(u, u', \tau) \tilde{Q}_{\boldsymbol{m}}(u', t - \tau)} \tag{2.213}$$

where the Green's function is given by

$$\tilde{G}^{\mathrm{D}}_{\boldsymbol{m}}(u, u', t) = \begin{cases} 0 & t \leq 0 \\ \dfrac{1}{\sqrt{4\pi\tilde{a}}} \exp\left[\mathrm{i}\dfrac{k_{\parallel}}{\nu}(u - u') - c - \dfrac{1}{4\tilde{a}}(u - u'\mathrm{e}^{-\nu t} + \mathrm{i}\tilde{b})^2\right] & t > 0 \end{cases} \tag{2.214}$$

with

$$\tilde{a}(t) = \frac{v_T^2}{2}\left(1 - \mathrm{e}^{-2\nu t}\right), \quad \tilde{b}(t) = \frac{2 k_{\parallel} v_T^2}{\nu}\left(1 - \mathrm{e}^{-\nu t}\right), \quad c(t) = \left(\mathrm{i}\omega_{\ell} + \frac{k_{\parallel} v_T^2}{\nu}\right) t. \tag{2.215}$$

Since this Green's function plays an essential role in determining the solution of the linearised kinetic equation with the more complicated energy and momentum conserving, integro-differential collision operator studied in detail in Chapter 3, its derivation is given in detail in Appendix A.

Coordinate transformations	
Curvilinear coordinates	Action-angle coordinates
$\dot{x}^i_{\rm c} = \frac{\partial x^i_{\rm c}}{\partial \Theta^j}\dot{\Theta}^j = \frac{\partial x^i_{\rm c}}{\partial \Theta^j}\Omega^j$	$\dot{\Theta}^i = \Omega^i = \frac{\partial \Theta^i}{\partial x^j_{\rm c}}\dot{x}^j_{\rm c} = \dot{\boldsymbol{r}}\cdot\frac{\partial \Theta^i}{\partial \boldsymbol{r}}$
$\dot{x}_{{\rm c}i} = \frac{\partial \Theta^j}{\partial x^i_{\rm c}}\Omega_j = \boldsymbol{\Omega}\cdot\frac{\partial \boldsymbol{\Theta}}{\partial x^i_{\rm c}}$	$\Omega_i = \frac{\partial x^j_{\rm c}}{\partial \Theta^i}\dot{x}_{{\rm c}j} = \dot{\boldsymbol{r}}\cdot\frac{\partial \boldsymbol{r}}{\partial \Theta^i}$
$\tilde{F}_i = \frac{\partial \Theta^j}{\partial x^i_{\rm c}}\dot{J}_j = \dot{\boldsymbol{J}}\cdot\frac{\partial \boldsymbol{\Theta}}{\partial x^i_{\rm c}}$	$\dot{J}_i = \frac{\partial x^j_{\rm c}}{\partial \Theta^i}\tilde{F}_j = \tilde{\boldsymbol{F}}\cdot\frac{\partial \boldsymbol{r}}{\partial \Theta^i} = \tilde{\boldsymbol{F}}\cdot\frac{\partial J_i}{\partial \boldsymbol{p}}$
$\tilde{E}_i = \frac{\partial \Theta^j}{\partial x^i_{\rm c}}\tilde{\mathcal{E}}_j = \tilde{\boldsymbol{\mathcal{E}}}\cdot\frac{\partial \boldsymbol{\Theta}}{\partial x^i_{\rm c}}$	$\tilde{\mathcal{E}}_i = \frac{\partial x^j_{\rm c}}{\partial \Theta^i}\tilde{E}_j = \tilde{\boldsymbol{E}}\cdot\frac{\partial \boldsymbol{r}}{\partial \Theta^i} = \tilde{\boldsymbol{E}}\cdot\frac{\partial J_i}{\partial \boldsymbol{p}}$
$\tilde{E}^i = \frac{\partial x^i_{\rm c}}{\partial \Theta^j}\tilde{\mathcal{E}}^j = \tilde{\boldsymbol{\mathcal{E}}}\cdot\frac{\partial x^i_{\rm c}}{\partial \boldsymbol{\Theta}}$	$\mathcal{E}^i = \frac{\partial \Theta^i}{\partial x^j_{\rm c}}\tilde{E}^j = \tilde{\boldsymbol{E}}\cdot\frac{\partial \Theta^i}{\partial \boldsymbol{r}}$
$\frac{\partial \tilde{\Phi}}{\partial x^i_{\rm c}} = \frac{\partial \Theta^j}{\partial x^i_{\rm c}}\frac{\partial \tilde{\Phi}}{\partial \Theta^j}$	$\frac{\partial \tilde{\Phi}}{\partial \Theta^i} = \frac{\partial \tilde{\Phi}}{\partial x^j_{\rm c}}\frac{\partial x^j_{\rm c}}{\partial \Theta^i} = \nabla\tilde{\Phi}\cdot\frac{\partial \boldsymbol{r}}{\partial \Theta^i}$
$\tilde{A}_i = \frac{\partial \Theta^j}{\partial x^i_{\rm c}}\tilde{\mathcal{A}}_j = \tilde{\boldsymbol{\mathcal{A}}}\cdot\frac{\partial \boldsymbol{\Theta}}{\partial x^i_{\rm c}}$	$\tilde{\mathcal{A}}_i = \frac{\partial x^j_{\rm c}}{\partial \Theta^i}\tilde{A}_j = \tilde{\boldsymbol{A}}\cdot\frac{\partial \boldsymbol{r}}{\partial \Theta^i} = \tilde{\boldsymbol{A}}\cdot\frac{\partial J_i}{\partial \boldsymbol{p}}$
$\frac{\partial \tilde{E}_i}{\partial x^j_{\rm c}}$	$\frac{\partial \mathcal{E}_i}{\partial \Theta^j} = \frac{\partial x^k_{\rm c}}{\partial \Theta^i}\frac{\partial x^m_{\rm c}}{\partial \Theta^j}\frac{\partial \tilde{E}_k}{\partial x^m_{\rm c}} + \tilde{E}^k\frac{\partial^2 x^k_{\rm c}}{\partial \Theta^i \partial \Theta^j}$
$\left[\boldsymbol{v}_{\rm c}\times(\nabla\times\tilde{\boldsymbol{E}})\right]_i$	$\Omega^j\left(\frac{\partial \mathcal{E}_i}{\partial \Theta^j} - \frac{\partial \mathcal{E}_j}{\partial \Theta^i}\right) = -\frac{{\rm i}\omega}{c}(\boldsymbol{v}_{\rm c}\times(\nabla\times\tilde{\boldsymbol{E}}))_j\frac{\partial x^j_{\rm c}}{\partial \Theta^i}$
$v^i_{\rm c0}$	$\mathcal{V}^i_0 = \boldsymbol{v}\cdot\frac{\partial \boldsymbol{p}_0}{\partial J_i} - \boldsymbol{F}_0\cdot\frac{\partial \boldsymbol{r}}{\partial J_i}$
F_{0i}	$\mathcal{F}_{0i} = -\boldsymbol{v}\cdot\frac{\partial \boldsymbol{p}_0}{\partial \Theta^i} + \boldsymbol{F}_0\cdot\frac{\partial \boldsymbol{r}}{\partial \Theta^i}$
$v^i_{\rm c}$	$\mathcal{V}^i = \mathcal{V}^i_0 - \tilde{\boldsymbol{F}}\cdot\frac{\partial \boldsymbol{r}}{\partial J_i} = \mathcal{V}^i_0 + \tilde{\boldsymbol{F}}\cdot\frac{\partial \Theta^i}{\partial \boldsymbol{p}}$
F_i	$\mathcal{F}_i = \mathcal{F}_{0i} + \tilde{\boldsymbol{F}}\cdot\frac{\partial \boldsymbol{r}}{\partial \Theta^i} = \mathcal{F}_{0i}\cdot\frac{\partial J_i}{\partial \boldsymbol{p}}$
Invariants	
$\tilde{\mathcal{H}} = \frac{{\rm i}e}{\omega}\boldsymbol{v}_{\rm c}\cdot\tilde{\boldsymbol{E}}$	$\tilde{\mathcal{H}} = \frac{{\rm i}e}{\omega}\Omega^i\mathcal{E}_i$
$\tilde{E}_i\{x^i_{\rm c}, f_0\} = \tilde{\boldsymbol{E}}\cdot\{\boldsymbol{r}, f_0\}$	$\tilde{\mathcal{E}}_i\{\Theta^i, f_0\} = \tilde{\boldsymbol{\mathcal{E}}}\cdot\{\boldsymbol{\Theta}, f_0\}$

Table 2.2: Relations between covariant and contravariant indexed quantities in curvilinear and action-angle variables.

2.6 Linear Model

2.6.1 Maxwell's Equations in Cylindrical Geometry

We consider Maxwell's equations

$$\nabla \cdot \tilde{\boldsymbol{E}}(\boldsymbol{r},t) = 4\pi\rho(\boldsymbol{r},t), \qquad \nabla \times \tilde{\boldsymbol{E}}(\boldsymbol{r},t) = -\frac{1}{c}\frac{\partial \tilde{\boldsymbol{B}}(\boldsymbol{r},t)}{\partial t}, \tag{2.216}$$

$$\nabla \times \tilde{\boldsymbol{B}}(\boldsymbol{r},t) = \frac{4\pi}{c}\boldsymbol{j}(\boldsymbol{r},t) + \frac{1}{c}\frac{\partial \tilde{\boldsymbol{E}}(\boldsymbol{r},t)}{\partial t}, \qquad \nabla \cdot \tilde{\boldsymbol{B}}(\boldsymbol{r},t) = 0, \tag{2.217}$$

where for a plasma the induced contribution of the plasma particles of the two species as well as external sources have to be considered for the sources ρ and $\boldsymbol{j}$. In the case of the linear response model the current density in Ampère's law consists of the antenna current at $r = r_\mathrm{a}$ plus the response current obtained from kinetic theory, $\boldsymbol{j} = \boldsymbol{j}_\mathrm{ant} + \tilde{\boldsymbol{j}}(\tilde{\boldsymbol{E}})$. In tensor index notation, the divergence equations follow from index contraction of the covariant derivatives of the fields,

$$\mathscr{D}_k \tilde{E}^k = \tilde{E}^k_{\|k} = \tilde{E}^k_{|k} + \Gamma^k_{ik}\tilde{E}^i = 4\pi\rho, \qquad \mathscr{D}_k \tilde{B}^k = 0, \tag{2.218}$$

and the curl equations are

$$E^{ijk}\partial_i \tilde{B}_j = \frac{\epsilon^{ijk}}{\sqrt{g}}\partial_i \tilde{B}_j = \frac{4\pi}{c}j^k + \frac{1}{c}\partial_t \tilde{E}^k, \qquad \frac{\epsilon^{ijk}}{\sqrt{g}}\partial_i \tilde{E}_j = -\frac{1}{c}\partial_t \tilde{B}^k, \tag{2.219}$$

where E^{ijk}, the permutation tensor for the non-Galilean case, i.e. the generalisation of the Galilean case to curvilinear coordinates, is connected with the antisymmetric Levi-Civita pseudo-tensor by $E^{ijk} = (1/\sqrt{g})\epsilon^{ijk}$. The Christoffel symbols for cylindrical coordinates are

$$(\Gamma^r_{ij}) = \begin{pmatrix} 0 & 0 & 0 \\ 0 & -r & 0 \\ 0 & 0 & 0 \end{pmatrix}, \quad (\Gamma^\vartheta_{ij}) = \begin{pmatrix} 0 & 1/r & 0 \\ 1/r & 0 & 0 \\ 0 & 0 & 0 \end{pmatrix}, \quad (\Gamma^z_{ij}) = \begin{pmatrix} 0 & 0 & 0 \\ 0 & 0 & 0 \\ 0 & 0 & 0 \end{pmatrix}, \tag{2.220}$$

with $i,j \in \{r,\vartheta,z\}$, which are, see e.g. [21], obtained from

$$\begin{aligned} \Gamma^r_{\vartheta\vartheta} &= \boldsymbol{e}^r \cdot \frac{\partial \boldsymbol{e}_\vartheta}{\partial \vartheta} = \frac{1}{2}g^{rn}\left(2\frac{\partial g_{n\vartheta}}{\partial \vartheta} - \frac{\partial g_{\vartheta\vartheta}}{\partial x^n}\right) \\ &= -\frac{1}{2}g^{rr}\frac{\partial g_{\vartheta\vartheta}}{\partial r} = \frac{1}{2}(-2r) = -r, \end{aligned} \tag{2.221}$$

$$\Gamma^\vartheta_{r\vartheta} = \Gamma^\vartheta_{\vartheta r} = \boldsymbol{e}^\vartheta \cdot \frac{\partial \boldsymbol{e}_r}{\partial \vartheta} = \frac{1}{2}g^{\vartheta n}\left(\frac{\partial g_{nr}}{\partial \vartheta} + \frac{\partial g_{n\vartheta}}{\partial r} - \frac{\partial g_{r\vartheta}}{\partial x^n}\right)$$

$$= \frac{1}{2} g^{\vartheta\vartheta} \frac{\partial g_{\vartheta\vartheta}}{\partial r} = \frac{1}{2} \frac{2r}{r^2} = \frac{1}{r}. \tag{2.222}$$

Hence, the divergence of the vector field $\tilde{E}^k$ is given by

$$\mathscr{D}_k \tilde{E}^k = \partial_k \tilde{E}^k + \Gamma^{\vartheta}_{r\vartheta} \tilde{E}^r = \partial_r \tilde{E}^r + \partial_\vartheta \tilde{E}^\vartheta + \partial_z \tilde{E}^z + \frac{1}{r} \tilde{E}^r \tag{2.223}$$

and the divergence equations become

$$\frac{1}{r} \frac{\partial (r \hat{\tilde{E}}_r)}{\partial r} + \frac{1}{r} \frac{\partial \hat{\tilde{E}}_\vartheta}{\partial \vartheta} + \frac{\partial \hat{\tilde{E}}_z}{\partial z} = 4\pi\rho, \tag{2.224}$$

$$\frac{1}{r} \frac{\partial (r \hat{\tilde{B}}_r)}{\partial r} + \frac{1}{r} \frac{\partial \hat{\tilde{B}}_\vartheta}{\partial \vartheta} + \frac{\partial \hat{\tilde{B}}_z}{\partial z} = 0, \tag{2.225}$$

where only the physical ϑ-vector component $\hat{\tilde{E}}_\vartheta = \sqrt{g_{\vartheta\vartheta}} \tilde{E}^\vartheta = \tilde{E}_\vartheta / \sqrt{g_{\vartheta\vartheta}}$ differs from the contravariant and covariant one, respectively. The curl equations are

$$\frac{1}{r} \frac{\partial \hat{\tilde{B}}_z}{\partial \vartheta} - \frac{\partial \hat{\tilde{B}}_\vartheta}{\partial z} = \frac{4\pi}{c} \hat{j}_r + \frac{1}{c} \frac{\partial \hat{\tilde{E}}_r}{\partial t}, \tag{2.226}$$

$$\frac{\partial \hat{\tilde{B}}_r}{\partial z} - \frac{\partial \hat{\tilde{B}}_z}{\partial r} = \frac{4\pi}{c} \hat{j}_\vartheta + \frac{1}{c} \frac{\partial \hat{\tilde{E}}_\vartheta}{\partial t}, \tag{2.227}$$

$$\frac{1}{r} \frac{\partial (r \hat{\tilde{B}}_\vartheta)}{\partial r} - \frac{1}{r} \frac{\partial \hat{\tilde{B}}_r}{\partial \vartheta} = \frac{4\pi}{c} \hat{j}_z + \frac{1}{c} \frac{\partial \hat{\tilde{E}}_z}{\partial t} \tag{2.228}$$

and

$$\frac{1}{r} \frac{\partial \hat{\tilde{E}}_z}{\partial \vartheta} - \frac{\partial \hat{\tilde{E}}_\vartheta}{\partial z} = -\frac{1}{c} \frac{\partial \hat{\tilde{B}}_r}{\partial t}, \tag{2.229}$$

$$\frac{\partial \hat{\tilde{E}}_r}{\partial z} - \frac{\partial \hat{\tilde{E}}_z}{\partial r} = -\frac{1}{c} \frac{\partial \hat{\tilde{B}}_\vartheta}{\partial t}, \tag{2.230}$$

$$\frac{1}{r} \frac{\partial (r \hat{\tilde{E}}_\vartheta)}{\partial r} - \frac{1}{r} \frac{\partial \hat{\tilde{E}}_r}{\partial \vartheta} = -\frac{1}{c} \frac{\partial \hat{\tilde{B}}_z}{\partial t}. \tag{2.231}$$

Considering wave solutions of the form $\propto \exp(\mathrm{i}\hat{k}_\vartheta \vartheta + \mathrm{i}\hat{k}_z z - \mathrm{i}\omega t)$, Maxwell's equations become

$$\boxed{\begin{aligned} &\frac{1}{r} \frac{\partial (r \hat{\tilde{E}}_r)}{\partial r} + \frac{\mathrm{i}\hat{k}_\vartheta}{r} \hat{\tilde{E}}_\vartheta + \mathrm{i}\hat{k}_z \hat{\tilde{E}}_z = 4\pi\rho, \\ &\frac{1}{r} \frac{\partial (r \hat{\tilde{B}}_r)}{\partial r} + \frac{\mathrm{i}\hat{k}_\vartheta}{r} \hat{\tilde{B}}_\vartheta + \mathrm{i}\hat{k}_z \hat{\tilde{B}}_z = 0, \end{aligned}} \tag{2.232}$$

$$\begin{aligned}
\frac{\mathrm{i}\hat{k}_\vartheta}{r}\hat{\tilde{B}}_z - \mathrm{i}\hat{k}_z\hat{\tilde{B}}_\vartheta &= \frac{4\pi}{c}\hat{j}_r - \frac{\mathrm{i}\omega}{c}\hat{\tilde{E}}_r,\\
\mathrm{i}\hat{k}_z\hat{\tilde{B}}_r - \frac{\partial}{\partial r}\hat{\tilde{B}}_z &= \frac{4\pi}{c}\hat{j}_\vartheta - \frac{\mathrm{i}\omega}{c}\hat{\tilde{E}}_\vartheta,\\
\frac{1}{r}\frac{\partial(r\hat{\tilde{B}}_\vartheta)}{\partial r} - \frac{\mathrm{i}\hat{k}_\vartheta}{r}\hat{\tilde{B}}_r &= \frac{4\pi}{c}\hat{j}_z - \frac{\mathrm{i}\omega}{c}\hat{\tilde{E}}_z,
\end{aligned} \tag{2.233}$$

and

$$\begin{aligned}
\frac{\mathrm{i}\hat{k}_\vartheta}{r}\hat{\tilde{E}}_z - \mathrm{i}\hat{k}_z\hat{\tilde{E}}_\vartheta &= \frac{\mathrm{i}\omega}{c}\hat{\tilde{B}}_r,\\
\mathrm{i}\hat{k}_z\hat{\tilde{E}}_r - \frac{\partial}{\partial r}\hat{\tilde{E}}_z &= \frac{\mathrm{i}\omega}{c}\hat{\tilde{B}}_\vartheta,\\
\frac{1}{r}\frac{\partial(r\hat{\tilde{E}}_\vartheta)}{\partial r} - \frac{\mathrm{i}\hat{k}_\vartheta}{r}\hat{\tilde{E}}_r &= \frac{\mathrm{i}\omega}{c}\hat{\tilde{B}}_z.
\end{aligned} \tag{2.234}$$

Equations (2.233) to (2.234) are integrated numerically w.r.t. radius as a set of ordinary differential equations for the RMP field by the kinetic wave code KiLCA (Kinetic Linear Cylindrical Approximation), developed by Ivanov *et al*, 2011 [33, 25, 26] for a straight periodic cylinder under the assumption that the plasma equilibrium parameters are known. Although the geometry is simplified, the kinetic physical model is accurate. Appropriate boundary conditions at the magnetic axis and at the ideally conducting outer wall have to be satisfied. The plasma and vacuum solutions, respectively, obtained inside and outside of the antenna have to be matched at the antenna position. This turns out to be complicated because due to the stiffness of the problem the initially orthogonal chosen state vectors for individual modes become collinear, so that a Gram-Schmidt procedure has to be executed after a certain number of steps to re-orthogonalise the state vectors. The final solution is obtained by a linear combination of the individual modes. The coefficients have to be rescaled radially backwards according to the information that has been stored during the re-orthogonalisation procedure. It has been found that the solutions are insensitive to the variation of the positions of the antenna and the ideal wall, increasing only the perturbation amplitude, which is a free parameter of the linear problem. Considering a finite conductivity instead of the ideal wall also has no implications on the results [49].

For a single spatial harmonic of the perturbation field the perturbation current density is linked to the perturbation electric field by a differential conductivity operator, which results from carrying out a finite Larmor radius (FLR) expansion of the exact integral conductivity operator. In order to obtain the conductivity operator, the linearised kinetic equation has to be solved. The details of the derivation of the conductivity operator can be found in [33, 32], here only the relation between the perturbed current density $\tilde{j}^i \propto \exp(\mathrm{i}m_\vartheta\vartheta + \mathrm{i}k_z z)$

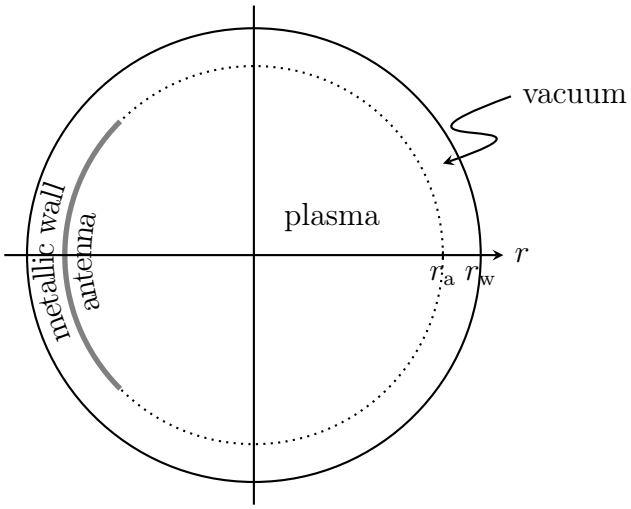

Figure 2.9: Poloidal cross section showing plasma and vacuum regions matched at $r = r_a$.

and the perturbation electric field is shown,

$$\tilde{j}^k(r,\vartheta,z) = \frac{1}{r}\sum_{n,n'=0}^{N}(-)^n\frac{\partial^n}{\partial r^n}\left(r\sigma^{kl}_{(n,n')}(r,\boldsymbol{k})\frac{\partial^n}{\partial r^{n'}}\tilde{E}_l(r,\vartheta,z)\right), \tag{2.235}$$

the derivatives occurring due to the FLRE of the exact integral conductivity operator. It is based on the full kinetic equation and thus also the gyromotion and polarisation currents are taken into account, reproducing all kinds of plasma oscillations, as e.g. resistive wall modes that have been obtained from this model [49, 48].

The conductivity operator elements $\sigma^{kl}_{(n,n')}$ were first derived by Heyn *et al.*, (2006) [25] from the collisionless and the Krook collision model. In a later study based on the improved Ornstein-Uhlenbeck Fokker-Planck operator ensuring Galilean invariance for a transformation to a moving frame the elements were re-evaluated also w.r.t. a more compact FLR expansion. The equations connecting the the moments of the Green's function with the elements of the conductivity operator are not altered by the improved collision operators ensuring also energy and momentum conservation, derived and applied in the most recent studies [30, 40]. The linear model has also been used to study the influence of RMPs on the α-particle confinement in ITER, Heyn *et al.* [28].

2.7 The Quasilinear Balance Equations

The equilibrium plasma parameters are computed within the quasilinear model. The slow evolution of the electron density n_e, the flux surface averaged ion toroidal rotation frequency V_i^φ and thermal energy densities $^3/_2\, n_{\mathrm{e,i}} T_{\mathrm{e,i}}$ under the action of the RMP field are described by the electron continuity equation (2.236), the toroidal momentum balance (2.237) and the respective species' heat balance equation (2.238), formulated here in toroidal geometry [26, 30],

$$\frac{\partial n_\mathrm{e}}{\partial t} + \frac{1}{S}\frac{\partial}{\partial r} S \left(\Gamma_\mathrm{e}^\mathrm{EM} + \Gamma_\mathrm{e}^\mathrm{A} \right) = S_{n_\mathrm{e}}^\mathrm{AUX}, \tag{2.236}$$

$$\begin{aligned} & m_\mathrm{i} n_\mathrm{i} \left\langle g_{\varphi\varphi} \right\rangle \frac{\partial V_\mathrm{i}^\varphi}{\partial t} - \frac{1}{S}\frac{\partial}{\partial r} S m_\mathrm{i} n_\mathrm{i} \left\langle g_{\varphi\varphi} \right\rangle \mu_\varphi^\mathrm{A} \frac{\partial V_\mathrm{i}^\varphi}{\partial r} \\ & \quad + \frac{1}{c} \sqrt{g} B_0^\vartheta \sum_{\sigma=\mathrm{e,i}} e_\sigma \left(\Gamma_\sigma^\mathrm{EM} + \Gamma_\sigma^\mathrm{A} \right) = S_{p_\varphi}^\mathrm{AUX}, \end{aligned} \tag{2.237}$$

$$\frac{\partial}{\partial t}\frac{3}{2} n_{\mathrm{e,i}} T_{\mathrm{e,i}} + \frac{1}{S}\frac{\partial}{\partial r} S \left(Q_{\mathrm{e,i}}^\mathrm{EM} + Q_{\mathrm{e,i}}^\mathrm{A} + Q_\mathrm{i}^\mathrm{NEO} \right) = -e_{\mathrm{e,i}} \Gamma_{\mathrm{e,i}}^\mathrm{EM} + S_{nT;\,\mathrm{e,i}}^\mathrm{A} + S_{nT;\,\mathrm{e,i}}^\mathrm{AUX}, \tag{2.238}$$

where S is the flux surface area and $\langle g_{\varphi\varphi} \rangle \propto R^2$ is the flux surface averaged covariant toroidal component of the metric tensor for symmetry flux coordinates and μ_φ^A is the anomalous shear viscosity coefficient. The fluxes denoted by index "EM" are the electron and ion particle and heat fluxes, which are driven by the perturbation field, i.e.

$$\begin{aligned} \Gamma_{\mathrm{e,i}}^\mathrm{EM} &= -n_{\mathrm{e,i}} (D_{11} \mathscr{A}_1 + D_{12} \mathscr{A}_2), \\ Q_{\mathrm{e,i}}^\mathrm{EM} &= -n_{\mathrm{e,i}} T_{\mathrm{e,i}} (D_{21} \mathscr{A}_1 + D_{22} \mathscr{A}_2), \end{aligned}$$

repeated here for convenience, with the diffusion coefficients given in (2.164) to (2.166) in Sect. 2.4.3. The sum over species in the toroidal momentum balance equation (2.237) is the toroidal torque density T_φ^EM of electrons and ions, for each species given by [30]

$$T_{\varphi;\,\mathrm{e,i}}^\mathrm{EM} = -\frac{e_{\mathrm{e,i}}}{c} \sqrt{g} B_0^\vartheta \Gamma_{\mathrm{e,i}}^\mathrm{EM}. \tag{2.239}$$

The upper index A denotes anomalous particle and heat fluxes, modelled by

$$\Gamma_{\mathrm{e,i}}^\mathrm{A} = -D_\perp \frac{\partial n_{\mathrm{e,i}}}{\partial r}, \qquad Q_{\mathrm{e,i}}^\mathrm{A} = -\frac{3}{2} D_\perp \frac{\partial n_{\mathrm{e,i}} T_{\mathrm{e,i}}}{\partial r}, \tag{2.240}$$

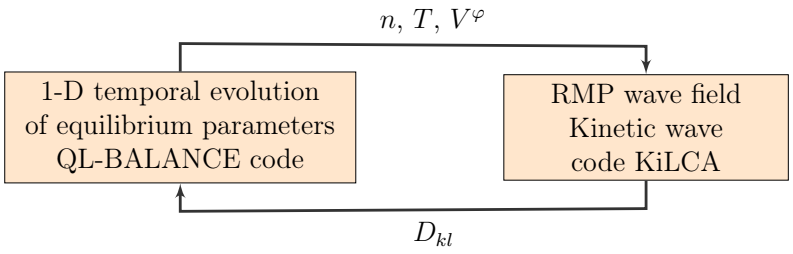

Figure 2.10: Self-consistent model consisting of equilibrium and wave code.

which is described in detail in [26]. The ion neoclassical heat flux appearing in Eq. (2.238) is given by the low-collisionality limit of Eq. (6.131) of [31],

$$Q_{\mathrm{i}}^{\mathrm{NEO}} = -1.32\, n_{\mathrm{i}} \left(\frac{R}{r}\right)^{3/2} \frac{q^2 v_{T_{\mathrm{i}}}^2}{\omega_{\mathrm{ci}}^2 \tau_{\mathrm{i}}} \frac{\partial T_{\mathrm{i}}}{\partial r}, \tag{2.241}$$

with $\tau_{\mathrm{i}} = 3\sqrt{m_{\mathrm{i}}} T_{\mathrm{i}}^{3/2} / (4\sqrt{\pi} e_{\mathrm{i}}^4 n_{\mathrm{i}} \Lambda)$ and Λ, the Coulomb logarithm.

The particle and energy sources $S_{n_{\mathrm{e}}}^{\mathrm{AUX}}$, $S_{nT;\mathrm{e,i}}^{\mathrm{AUX}}$ and the equilibrium torque density $S_{p_\varphi}^{\mathrm{AUX}}$ are chosen such that a steady state for the equilibrium parameters[8] is achieved in the absence of the perturbation field [50, 26].

Finally, a comment concerning the equilibrium radial electric field E_{0r} is indicated, since it enters the balance equations at the right hand sides of (2.237) and (2.238) and also the thermodynamic force $\mathscr{A}_1$. Its value is determined such that the poloidal ion velocity $V_{\mathrm{i}}^{\vartheta}$ coincides with the equilibrium neoclassical velocity [24],

$$V_{\mathrm{i}}^{\vartheta} = \frac{ckB_{0\varphi}}{e\sqrt{g}\langle B_0^2 \rangle} \frac{\partial T_{\mathrm{i}}}{\partial r}, \tag{2.242}$$

with a coefficient k computed by the code NEO-2. According to this condition, it is given by [30]

$$E_{0r} = -\frac{\partial \Phi_0}{\partial r} = \frac{\sqrt{g} B_0^{\vartheta}}{c} \left(V_{\mathrm{i}}^{\varphi} - q V_{\mathrm{i}}^{\vartheta}\right) + \frac{1}{n_{\mathrm{i}} e_{\mathrm{i}}} \frac{\partial n_{\mathrm{i}} T_{\mathrm{i}}}{\partial r}.$$

The balance equations (2.236) to (2.238) are solved by the FORTRAN code QL-BALANCE [26, 30] by tracing the time evolution of the background parameters. The code is based on a conservative finite difference scheme. The model is self-consistent insofar that the RMP-field is updated at each time step by the wave code KiLCA, see Fig. 2.10.

[8] corresponding to experimental profiles that serve as an input to the self-consistent modelling

2.7.1 Tokamak Geometry

In order to convert the RMP field to a real tokamak geometry, the total magnetic field $\boldsymbol{B} = \boldsymbol{B}_0 + \tilde{\boldsymbol{B}}_1$ is expressed through the vector potential in symmetry flux coordinates $(x^1, x^2, x^3) = (\psi_{\mathrm{tor}}, \vartheta, \varphi)$ [26, 32, 28, 30],

$$\boldsymbol{B}_0 = \nabla\psi_{\mathrm{pol}} \times \nabla\varphi + B_{0\varphi}\nabla\varphi, \tag{2.243}$$

$$\tilde{\boldsymbol{B}}_1 = \nabla\tilde{A}_{1\psi} \times \nabla\psi_{\mathrm{tor}} + \nabla\tilde{A}_{1\vartheta} \times \nabla\vartheta, \tag{2.244}$$

where ψ_{tor} and ψ_{pol} are, within a factor of 2π, the toroidal and poloidal magnetic fluxes of the axisymmetric background magnetic field $\boldsymbol{B}_0$. Only the covariant ϑ-component of the perturbed magnetic potential determines the magnetic field topology and quasilinear effects in the resonant layer [30]. This component is expanded in a Fourier series over angles,

$$\tilde{A}_{1\vartheta} = 2\,\Re\sum_{n=1}^{\infty}\sum_{m=-\infty}^{\infty}\tilde{A}_{\vartheta;\,m,n}(\psi_{\mathrm{tor}})\mathrm{e}^{\mathrm{i}m\vartheta+\mathrm{i}n\varphi}, \tag{2.245}$$

where $m = m_\vartheta$ and $n = n_\varphi$. In this expansion, the Fourier amplitudes in vacuum, which are determined by Biot-Savart's law from the coil currents are replaced by shielded amplitudes [26, 30]

$$\tilde{A}_{\vartheta;\,m,n}(\psi_{\mathrm{tor}}) = \tilde{A}^{\mathrm{vac}}_{\vartheta;\,m,n}(\psi_{\mathrm{tor}})T_{m,n}(\psi_{\mathrm{tor}}), \tag{2.246}$$

which for each mode m, n and effective radius r (or the corresponding flux surface ψ_{tor}) are obtained from the linear model in terms of form factors $T_{m,n}$, given by the ratio of the Fourier amplitudes of the radial magnetic field component in plasma and in vacuum, respectively [26, 32, 33, 30],

$$T_{m,n}(\psi_{\mathrm{tor}}) = \frac{\tilde{B}^{r\,(\mathrm{plas})}_{\boldsymbol{m}}(r)}{\tilde{B}^{r\,(\mathrm{vac})}_{\boldsymbol{m}}(r)}. \tag{2.247}$$

The shielding factors introduced already in [26] and used further in [28, 30, 40] are a measure of the shielding of the magnetic field by the perturbation field.

The transport coefficients in the tokamak geometry are gained for each separate mode $\boldsymbol{m}$ by affixing spectral weights [30]

$$W_{\boldsymbol{m}} = \left|\frac{k_z\tilde{A}^{\mathrm{vac}}_{\vartheta\,m,n}}{r\tilde{B}^{r\,(\mathrm{vac})}_{\boldsymbol{m}}}\right|^2 \tag{2.248}$$

during the summation. Here, the cylindrical wave number k_z is related to the toroidal wave number by m_φ/R.

Chapter 3

Analytical and Numerical Results

The results presented here have been published for the most part in either of the two lead-author articles:

- P. Leitner, M. F. Heyn, I. B. Ivanov, S. V. Kasilov, and W. Kernbichler: *Effect of energy and momentum conservation on fluid resonances for resonant magnetic perturbations in a tokamak.* Physics of Plasmas **21**, 062508 (2014)

- M. F. Heyn, I. B. Ivanov, S. V. Kasilov, W. Kernbichler, and P. Leitner: *Quasilinear Modelling of RMP Penetration into a Tokamak Plasma.* Problems of atomic science and technology/Series Plasma Physics (2013)

Section 3.1 on quasilinear kinetic modelling of RMP penetration with energy conserving collision operator covers results published in the latter proceeding report [29], while the remaining sections 3.2 to 3.6 refer to the publication in Physics of Plasmas [40]. Permission for inclusion of this article in this dissertation was granted by Physics of Plasmas. This said, references to those two articles are given again only for reproduction of figures and literal quotations, thereby following the guidelines for proper quotation practice of the TU Graz.

Contents

3.1 Quasilinear Kinetic Modelling of RMP Penetration into a Tokamak Plasma

RMPs are nowadays realised an effective remedy for uncontrolled ELM activity in tokamak H-regimes. Especially type-I ELMs that represent short bursts of large-amplitude activity release high-pulsed heat load on the divertor plates and are therefore to be avoided [22, p. 504ff]. On the other end of the ELM classification scheme are type-III ELMs that continuously release pressure at the edge thereby however undermining the advantages of H-mode confinement [22]. Type-II ELMs are considered an acceptable compromise allowing for a moderate removal of impurities and guaranteeing confinement times well above L-mode operation [22]. RMPs have proven to successfully mitigate ELMs in tokamak experiments like DIII-D in San Diego in the United States [12], JET in the UK [42], and ASDEX-Upgrade in Garching, Germany [30].

A strong shielding of RMPs, however, is predicted by linear theory [16, 25]. From MHD theory it is known that shielding can be circumvented by adjusting the RMP amplitude to a certain threshold value; the RMP driven plasma torque effectively slows down the electron fluid motion across the magnetic field lines and the penetration of RMPs becomes possible [15]. Here, the penetration of RMPs was studied within quasilinear theory in the kinetic approximation. An energy conserving collision operator (2.99) is used to avoid the occurrence of artefacts such as fake heat fluxes in the limit of ideal MHD. The resulting transport matrix was shown to be Onsager symmetric, the proof being deferred to Section 3.5.2, where Onsager symmetry is studied for the even more general model with additional momentum conserving collision operator. The basic equations of this quasilinear modelling as well as the linear wave code KiLCA [33] and the balance code [30] used for the computation of the evolution of the plasma background are discussed in detail in the preceding chapter on Methods, leaving the focus on the application of the model to a numerical experiment for a single perturbation with JET-like plasma parameters.

From the solution of the kinetic equation particle and heat fluxes were determined[1]. This allowed for the further computation of the quasilinear evolution

[1]This quasilinear transport was realised to be attributed to the mismatch between perturbed magnetic flux surfaces and perturbed equipotential surfaces [30].

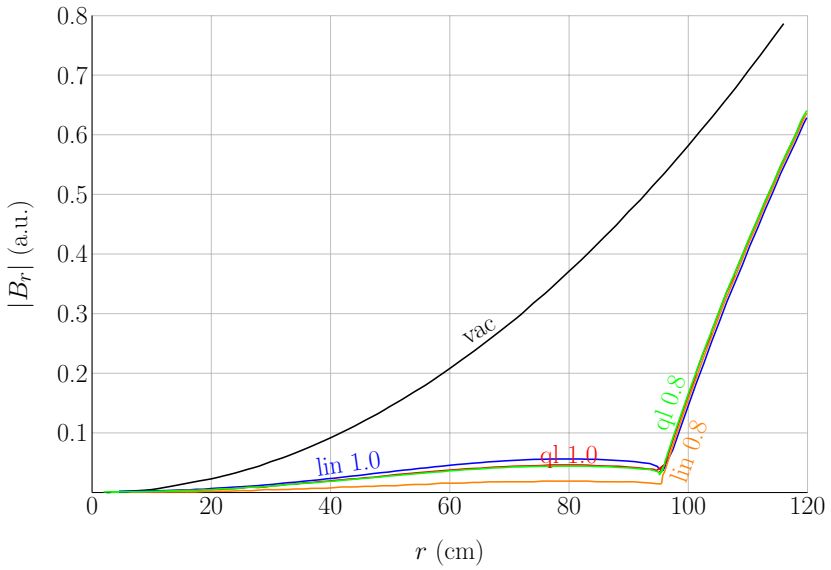

Figure 3.1: Profile of $|B_r|$ for linear and quasilinear evolution and two scaling factors, 0.8 and 1.0 of the toroidal rotation velocity. Source: [29].

of the following plasma parameters: electron density n_e, toroidal ion rotation velocity V_i^ϕ, and electron and ion temperatures $T_{e,i}$ according to the balance equations (2.236) [26, 30]. The modelling was done for the single perturbation mode $(-3, 1)$ of the C-coil spectrum and two values for the anomalous diffusion coefficient, namely 10^4 and $5 \times 10^3\,\mathrm{cm}^2/\mathrm{s}$.

The radial profiles of $|B_r|$ obtained before and after quasilinear relaxation, see Fig. 3.1, show that quasilinear effects do not necessarily reduce the shielding but may even increase it, although the parallel electron current in the resonant zone is reduced, see Fig. 3.2. The profiles that were found to be affected by the perturbations are the electron temperature, Fig. 3.3, and, to a lesser extent, the toroidal rotation velocity, Fig. 3.4, in contrast to earlier MHD theories [33]. The electron density- and ion temperature profiles however were not altered by the RMP-field. At the resonant surface, the perpendicular electron fluid velocity was found to become zero, which, as can be seen from the bottom of Fig. 3.2, is mostly due to the effect of RMPs on the electron diamagnetic velocity. This agrees with a quasilinear modelling based on Drift-MHD theory [50], where the electron diamagnetic velocity was also observed to be the most affected quantity. A zero perpendicular electron fluid velocity as found here for all cases would lead to field penetration according to MHD theory. In kinetic theory however, the radii of maximum radial magnetic field and zero toroidal torque do not coincide as can be seen in Fig. 3.5, why the plasma shielding is not necessarily reduced. The results were found to be insensitive to the chosen values of the anomalous diffusion coefficient.

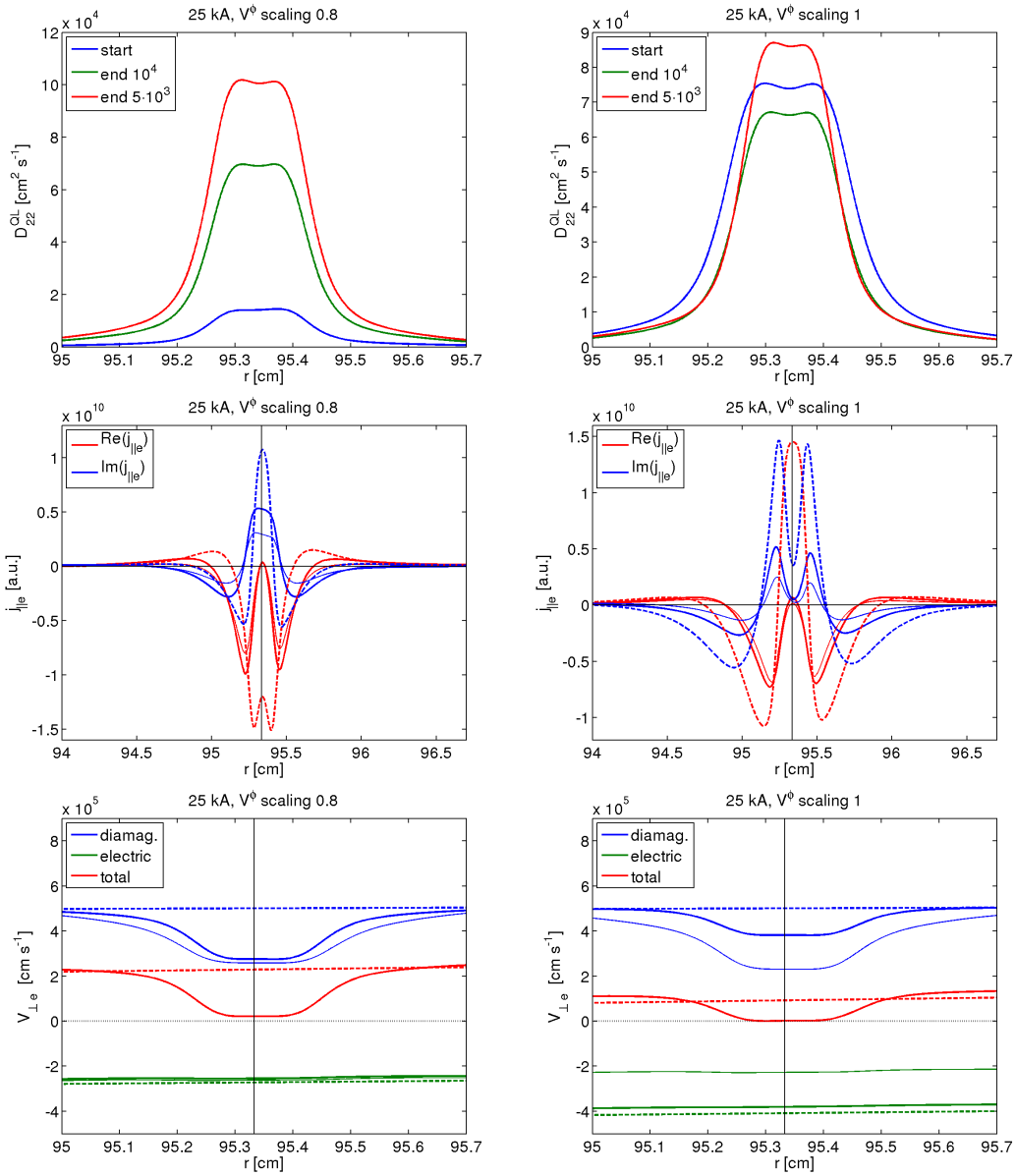

Figure 3.2: Evolution of the quasilinear heat conductivity (top panel), parallel electron current density (middle), and components of the perpendicular electron fluid velocity (bottom). Solid lines for the current and perpendicular velocity show the profiles after quasilinear evolution, dashed lines represent initial profiles. The thin lines show results for the reduced value of the anomalous diffusion coefficient. Source: [29].

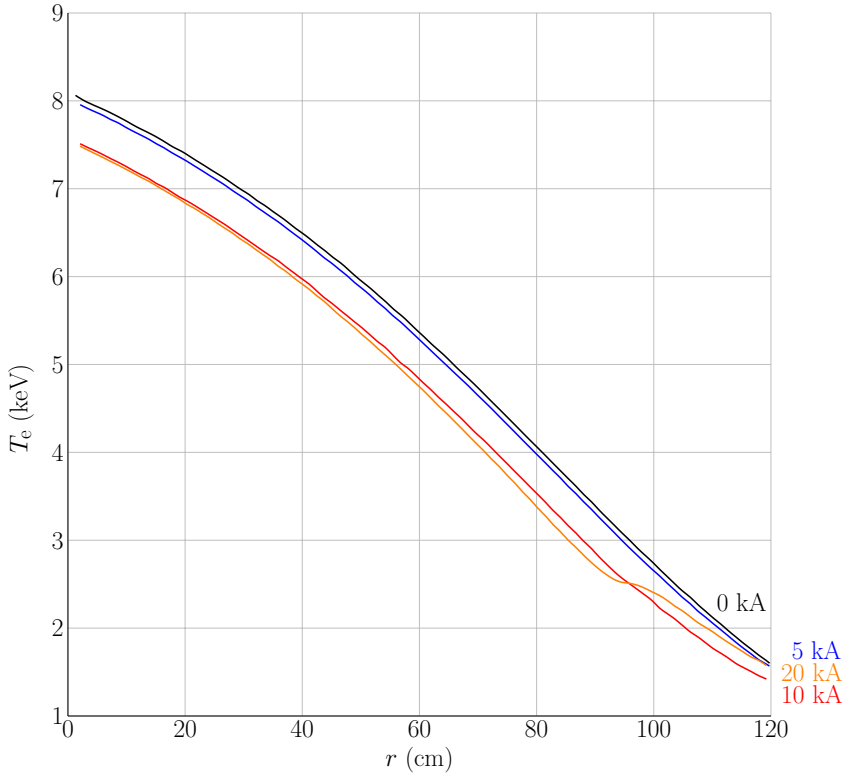

Figure 3.3: Quasilinear evolution for different RMP amplitudes of mode $(-3, 1)$.

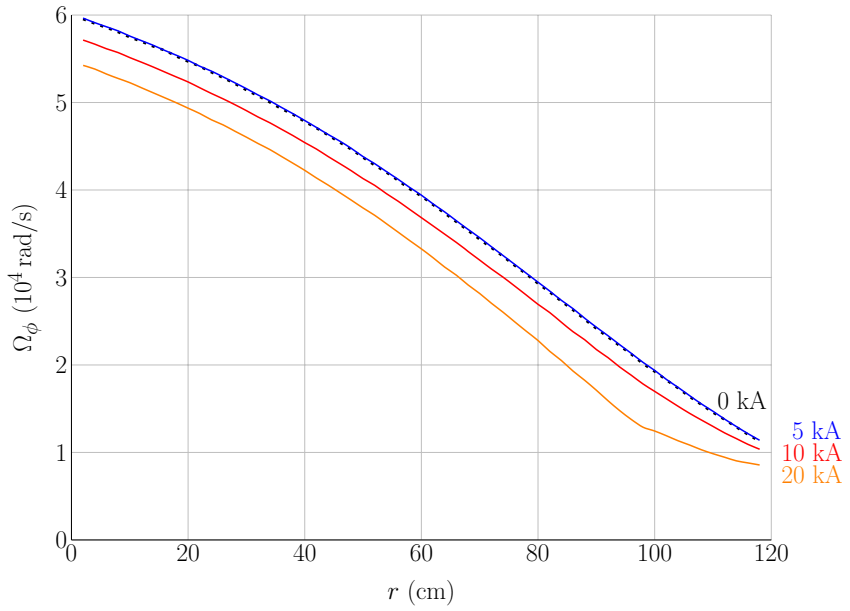

Figure 3.4: Toroidal rotation velocity for different amplitudes of RMP mode $(-3, 1)$. The dashed black line represents the unperturbed toroidal rotation profile.

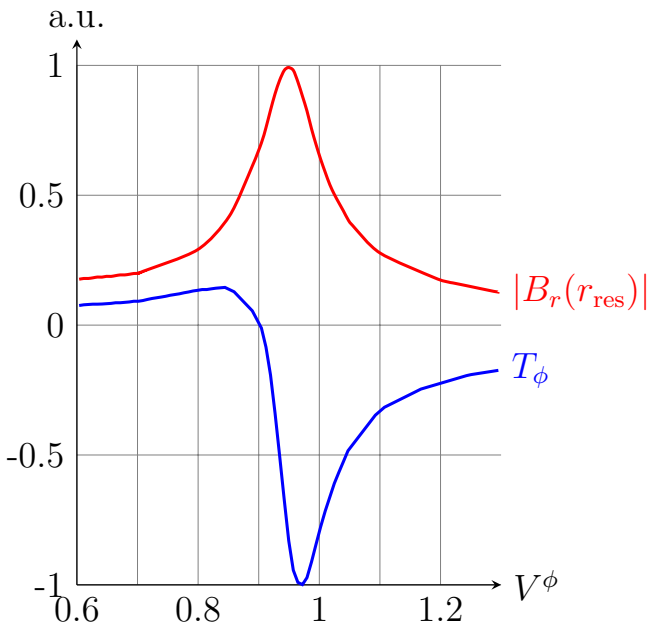

Figure 3.5: Modulus of the radial magnetic field at the resonant surface and toroidal torque T_ϕ as a function of the toroidal velocity scaling factor. Source: [29].

3.2 Momentum Conserving Collision Operator

In Heyn *et al.* (2014) [30] the kinetic model of RMP-plasma interaction has been extended by an advanced collision operator with an integral part that in addition to particle- and thus charge conservation also ensures the conservation of energy, see Sect. 2.4.3. In the following it will be shown how to further extend this operator by an additional integral part, so that for the plasma species considered, particles, energy and momentum are conserved. While, due to the mass ratio of protons to electrons of $m_\mathrm{p}/m_\mathrm{e} \approx 1\,836.2$ the energy transfer during a single Coulomb collision from the electron to the ion or vice versa is only $\sim \mathcal{O}(m_\mathrm{e}/m_\mathrm{i})$ and so energy conservation of both plasma species should be considered, that argument does not apply to the momentum transfer of electrons colliding with ions.

Keeping the overall electron momentum artificially at a constant value obviously is not justified on physical grounds, therefore for electrons the same collision operator as in Ref. [30] is used in the modelling. For the ions however a closer examination is indicated: In contrast to our cylindrical model, where the equilibrium parallel ion flow is a free parameter[2], in a tokamak, due to poloidal viscosity, the equilibrium parallel ion flow is restricted to a neoclassical value and momentum is transferred to the trapped particles. In MHD models [4] this effect is considered by taking parallel viscosity into account. The flow braking is described in terms of parallel viscosity in the long mean free path regime and as the product of collision frequency and the fraction of trapped particles for a kinetic estimate, the former overestimating the flow braking rate. The loss of momentum to the trapped particles is simulated in our model, when we restrict the collision operator to conserve particles and energy only. If, on the other hand, momentum conservation on the ion component is enforced, the model results are comparable to MHD model results neglecting toroidal effects and shear viscosity, since parallel momentum conservation in a cylinder model is incompatible with parallel flow braking due to the toroidicity of real tokamaks.

For the details of our linear and quasilinear model, the reader is referred to Chapter 2, while here the focus is laid on the differences that arise when a momentum conserving collision operator is applied regarding the solution of the kinetic equation and derived quantities such as diffusion coefficients and the linear response current. Starting point of the discussion of the response model is the kinetic equation linearised w.r.t. an equilibrium described by a distribution function f_0, an electrostatic field $\boldsymbol{E}_0$ and a magnetic field $\boldsymbol{B}_0$, formulated here

[2] when neglecting radial transport or shear viscosity

in action-angle variables $(\boldsymbol{\Theta}, \boldsymbol{J})$ and repeated here for convenience [33],

$$\frac{\partial \tilde{f}}{\partial t} + \Omega^i \frac{\partial \tilde{f}}{\partial \Theta^i} - \hat{L}_\mathrm{c} \tilde{f} = \tilde{Q}(t, \boldsymbol{\Theta}, \boldsymbol{J})$$

with source term

$$\tilde{Q}(t, \boldsymbol{\Theta}, \boldsymbol{J}) = -e \left(\tilde{\boldsymbol{E}} + \frac{1}{c} \boldsymbol{v} \times \tilde{\boldsymbol{B}} \right) \cdot \frac{\partial \boldsymbol{r}}{\partial \Theta^i} \frac{\partial f_0(\boldsymbol{J})}{\partial J_i}.$$

As was explained in detail in Section 2.5, the equilibrium is an integrable Hamiltonian system, see Eqns. (2.172), with distribution function $f_0(\boldsymbol{J})$ satisfying the steady state kinetic equation. Action-angle variables in the straight periodic cylinder with length $L = 2\pi R$ were chosen $\boldsymbol{\Theta} = (\phi, \theta_\mathrm{gc}, z_\mathrm{gc})$ and $\boldsymbol{J} = (J_\perp, p_\vartheta, p_z)$. The generalised momenta, however are not used directly but re-expressed through more physical variables $(r_0, v_\parallel, v_\perp)$ as follows,

$$p_{\vartheta,z} = \left(m\boldsymbol{h}(r_0) v_\parallel + m\boldsymbol{V}_E(r_0) + \frac{e}{c} \boldsymbol{A}_0(r_0) \right)_{\vartheta,z}. \tag{3.1}$$

A basis aligned to the local equilibrium field composed of $(\boldsymbol{e}_r, \boldsymbol{h} = \boldsymbol{B}_0/B_0, \boldsymbol{e}_\perp = \boldsymbol{h} \times \boldsymbol{e}_r)$, as introduced in Section 2.5 and depicted in Fig. 2.8 is used. By Fourier-series expansion of the perturbed quantities in the angle variable, e.g.

$$\tilde{f}(t, \boldsymbol{\Theta}, \boldsymbol{J}) = \sum_{\boldsymbol{m}} \tilde{f}_{\boldsymbol{m}}(t, \boldsymbol{J}) \mathrm{e}^{\mathrm{i}\boldsymbol{m}\cdot\boldsymbol{\Theta}},$$

the linear kinetic equation for the Fourier amplitude $f_{\boldsymbol{m}}(t, \boldsymbol{J})$ is obtained [33],

$$\frac{\partial \tilde{f}_{\boldsymbol{m}}}{\partial t} + \mathrm{i}\boldsymbol{m} \cdot \boldsymbol{\Omega} \tilde{f}_{\boldsymbol{m}} - \hat{L}_\mathrm{c} \tilde{f}_{\boldsymbol{m}} = \tilde{Q}_{\boldsymbol{m}}. \tag{3.2}$$

In previous studies, the collision term was modelled by a Krook term [25],

$$\hat{L}_\mathrm{c} f = \nu \left[f_0 \left(\boldsymbol{r}, \boldsymbol{p} - \frac{e}{c} \tilde{\boldsymbol{A}}_1 \right) - f(t, \boldsymbol{r}, \boldsymbol{p}) \right], \tag{3.3}$$

being a crude approximation for the collision integral based on the assumption that since $\hat{L}_\mathrm{c} f$ is vanishing for $f \equiv f_0$, the collision term for small deviations of the distribution from the equilibrium $f = f_0 + \delta f$ should be proportional to $-\delta f$, see e.g. [19].

Later, it had been substituted by an improved Galilean invariant Fokker-Planck collision operator [33]

$$\hat{L}_\mathrm{cD} f = \frac{\partial}{\partial u} D \left(\frac{\partial}{\partial u} + \frac{u}{v_T^2} \right) f. \tag{3.4}$$

Just recently, the operator has been further extended to an integro-differential, energy conserving operator in 2014 [30],

$$\hat{L}_{\mathrm{cp}} f(v_\perp, u) = \hat{L}_{\mathrm{cD}} f(v_\perp, u) + \frac{\nu}{\sqrt{2\pi} v_T} \exp\left(-\frac{u^2}{2v_T^2}\right)\left(\frac{u^2}{v_T^2} - 1\right) \times \int_{\mathbb{R}} \mathrm{d}u' \left(\frac{u'^2}{v_T^2} - 1\right) f(v_\perp, u'). \tag{3.5}$$

Missing is still the derivation of the solution of the linearised kinetic equation with integro-differential collision operator $\hat{L}_{\mathrm{c}} = \hat{L}_{\mathrm{cD}} + \hat{L}_{\mathrm{cI}}^{\mathrm{E}} + \hat{L}_{\mathrm{cI}}^{\mathrm{M}}$, which includes the solution to the case with energy conservation only as a limit case.

Construction of a Momentum Conserving Collision Operator

For the equilibrium distribution function f_0 a local drifting Maxwellian normalised to momentum space,

$$f_0(r, v_\parallel, v_\perp) = \frac{n_0(r)}{(2\pi m T_0(r))^{3/2}} \exp\left\{-\frac{m\left[v_\perp^2 + (v_\parallel - V_{\parallel 0}(r))^2\right]}{2T_0(r)}\right\}$$

is chosen with the density n_0, the temperature T_0 and the parallel flow velocity $V_{\parallel 0}$ being free parameters of the model describing parallel (but ignoring radial) transport as a consequence of the respective particle, energy, and momentum conservation in collisions. The freedom in parameters results in a linearly modified Maxwellian δf_{M} for the equilibrium solution of the unperturbed kinetic equation with linearised Coulomb collision operator, given by

$$\delta f_{\mathrm{M}} = C_n f_{\mathrm{M}} + C_v f_{\mathrm{M}} v_\parallel + C_T f_{\mathrm{M}} v^2, \tag{3.6}$$

with C_n, C_v, and C_T being arbitrary functions of r_0, describing infinitesimal changes in density, flow velocity, and temperature, respectively. In this study collisions are not modelled by the exact linearised Coulomb collision operator but by a simple model collision operator simulating collisional scattering over the parallel velocity component that keeps the equilibrium solution (3.6) intact, thereby conserving particles, parallel momentum, and parallel energy.

Integration of f_0 over momentum space using (2.150) again should give the equilibrium density distribution, which can be easily shown,

$$\int_{\mathbb{R}^3} \mathrm{d}^3 p\, f_0(r, u, v_\perp) = 2\pi m^3 \int_0^\infty \mathrm{d}v_\perp\, v_\perp \int_{\mathbb{R}} \mathrm{d}u\, f_0$$

$$= \frac{n_0}{\sqrt{2\pi}v_T^3} \int_0^\infty \mathrm{d}v_\perp \, v_\perp \mathrm{e}^{-v_\perp^2/2v_T^2} \int_{\mathbb{R}} \mathrm{d}u \, \mathrm{e}^{-u^2/2v_T^2}$$
$$= \frac{n_0}{\sqrt{2\pi}v_T^3} v_T^2 \sqrt{2\pi} v_T = n_0(r). \tag{3.7}$$

In the following, also the parallel component $V_\parallel$ of the flow velocity

$$\boldsymbol{V} = \frac{\int_{\mathbb{R}^3} \mathrm{d}^3 v \, \boldsymbol{v} \, f}{\int_{\mathbb{R}^3} \mathrm{d}^3 v \, f} \tag{3.8}$$

is expanded to first order $V_\parallel = V_{\parallel 0} + V_{\parallel 1}$. Now, the Ornstein-Uhlenbeck Fokker-Planck collision operator $\hat{L}_{\mathrm{cD}}$ acting on $f = f_0 + f_1$ gives

$$\begin{aligned}
\hat{L}_{\mathrm{cD}}(f_0 + f_1) &= \nu v_T^2 \frac{\partial}{\partial v_\parallel} \left[\frac{\partial}{\partial v_\parallel}(f_0 + f_1) + \frac{v_\parallel - (V_{\parallel 0} + V_{\parallel 1})}{v_T^2}(f_0 + f_1) \right] \\
&\approx \nu v_T^2 \frac{\partial^2}{\partial v_\parallel^2} f_0 + \nu v_T^2 \frac{\partial^2}{\partial v_\parallel^2} f_1 \\
&\quad + \nu \frac{\partial}{\partial v_\parallel} \left[(v_\parallel - V_{\parallel 0}) f_0 + (v_\parallel - V_{\parallel 0}) f_1 - V_{\parallel 1} f_0 \right] \\
&= \underbrace{\nu v_T^2 \frac{\partial^2}{\partial v_\parallel^2} f_0 + \nu \frac{\partial}{\partial v_\parallel}(v_\parallel - V_{\parallel 0}) f_0}_{= \hat{L}_{\mathrm{cD}} f_0} + \underbrace{\nu v_T^2 \frac{\partial^2}{\partial v_\parallel^2} f_1 + \nu \frac{\partial}{\partial v_\parallel}(v_\parallel - V_{\parallel 0}) f_1}_{= \hat{L}_{\mathrm{cD}} f_1} \\
&\quad - \nu \frac{\partial}{\partial v_\parallel} V_{\parallel 1} f_0,
\end{aligned}$$

by restricting oneself to the linear order in perturbations. The first two terms on the right hand side are the separate actions of $\hat{L}_{\mathrm{cD}}$ on f_0 and f_1 and the remaining term is now defined as the action of a new collision operator $\hat{L}_{\mathrm{cI}}^{\mathrm{M}}$ on f_1, i.e. $\hat{L}_{\mathrm{cI}}^{\mathrm{M}} f_1 = -\nu V_{\parallel 1} \partial f_0 / \partial v_\parallel$, such that

$$\hat{L}_{\mathrm{cD}}(f_0 + f_1) = \hat{L}_{\mathrm{cD}} f_0 + \hat{L}_{\mathrm{cD}} f_1 + \hat{L}_{\mathrm{cI}}^{\mathrm{M}} f_1 = (\hat{L}_{\mathrm{cD}} + \hat{L}_{\mathrm{cI}}^{\mathrm{M}}) f_1. \tag{3.9}$$

For this operator, the first order parallel bulk velocity has to be obtained by explicitly evaluating this fluid velocity by taking the first moment,

$$V_\parallel = \frac{\int_{\mathbb{R}} \mathrm{d}v_\parallel \, v_\parallel (f_0 + f_1)}{\int_{\mathbb{R}} \mathrm{d}v_\parallel \, (f_0 + f_1)} = \left(1 + \frac{\int_{\mathbb{R}} \mathrm{d}v_\parallel \, f_1}{\int_{\mathbb{R}} \mathrm{d}v_\parallel \, f_0} \right)^{-1} \frac{\int_{\mathbb{R}} \mathrm{d}v_\parallel \, v_\parallel (f_0 + f_1)}{\int_{\mathbb{R}} \mathrm{d}v_\parallel \, f_0}$$

$$\approx \left(1 - \frac{\int_{\mathbb{R}} \mathrm{d}v_\parallel\, f_1}{\int_{\mathbb{R}} \mathrm{d}v_\parallel\, f_0}\right) \frac{\int_{\mathbb{R}} \mathrm{d}v_\parallel\, v_\parallel (f_0 + f_1)}{\int_{\mathbb{R}} \mathrm{d}v_\parallel\, f_0}.$$

Considering the moments n_0 and V_0, zeroth order in the perturbation field,

$$n_0 = \int_{\mathbb{R}} \mathrm{d}v_\parallel\, f_0, \quad V_{\parallel 0} = \frac{1}{n_0} \int_{\mathbb{R}} \mathrm{d}v_\parallel\, v_\parallel f_0 \tag{3.10}$$

$V_\parallel$ can be evaluated further to

$$\begin{aligned} V_\parallel &= V_{\parallel 0} + \frac{1}{n_0} \int_{\mathbb{R}} \mathrm{d}v_\parallel\, v_\parallel f_1 - \frac{1}{n_0^2} \int_{\mathbb{R}} \mathrm{d}v_\parallel\, v_\parallel (f_0 + f_1) \int_{\mathbb{R}} \mathrm{d}v_\parallel\, f_1 \\ &\approx V_{\parallel 0} + \frac{1}{n_0} \int_{\mathbb{R}} \mathrm{d}v_\parallel\, v_\parallel f_1 - \frac{V_{\parallel 0}}{n_0} \int_{\mathbb{R}} \mathrm{d}v_\parallel\, f_1 \\ &= V_{\parallel 0} + \frac{1}{n_0} \int_{\mathbb{R}} \mathrm{d}v_\parallel\, f_1 (v_\parallel - V_{\parallel 0}) = V_{\parallel 0} + V_{\parallel 1} \end{aligned} \tag{3.11}$$

and hence

$$V_{\parallel 1} = \frac{1}{n_0} \int_{\mathbb{R}} \mathrm{d}v_\parallel\, f_1 (v_\parallel - V_{\parallel 0}). \tag{3.12}$$

With determined $V_{\parallel 1}$, the action of operator $\hat{L}_{\mathrm{cI}}^{\mathrm{M}}$ on f_1 is

$$\begin{aligned} \hat{L}_{\mathrm{cI}}^{\mathrm{M}} f_1 &= -\nu \frac{\partial f_0}{\partial v_\parallel} V_{\parallel 1} \\ &= \nu \frac{v_\parallel - V_{\parallel 0}}{v_T^2} f_0 \frac{1}{n_0} \int_{\mathbb{R}} \mathrm{d}v'_\parallel\, (v'_\parallel - V_{\parallel 0}) f_1(v_\perp, v'_\parallel) \\ &= \frac{\nu}{\sqrt{2\pi} v_T} \mathrm{e}^{-u^2/2v_T^2} \frac{u}{v_T} \int_{\mathbb{R}} \mathrm{d}u'\, \frac{u'}{v_T} f_1(v_\perp, v'_\parallel), \end{aligned} \tag{3.13}$$

where the shifted velocity $u = v_\parallel - V_{\parallel 0}$ in the co-moving frame has been substituted. Now it is shown that $\hat{L}_{\mathrm{cD}} f_0$ is indeed zero, which has been used in (3.9):

$$\begin{aligned} \hat{L}_{\mathrm{cD}} f_0 &= \nu v_T^2 \frac{\partial}{\partial v_\parallel} \left(\frac{\partial f_0}{\partial v_\parallel} + \frac{v_\parallel - V_{\parallel 0}}{v_T^2} f_0 \right) \\ &= \nu v_T^2 f_0 \left(\frac{v_\parallel - V_{\parallel 0}}{v_T^2} \right)^2 - \nu f_0 + \nu f_0 \left[1 - \frac{(v_\parallel - V_{\parallel 0})^2}{v_T^2} \right] = 0 \end{aligned} \tag{3.14}$$

Also for the constructed operator $\hat{L}^{\mathrm{M}}_{\mathrm{cI}}$, the condition $\hat{L}^{\mathrm{M}}_{\mathrm{cI}} f_0 = 0$ holds,

$$\hat{L}^{\mathrm{M}}_{\mathrm{cI}} f_0 = -\frac{\nu}{\sqrt{2\pi} v_T} \mathrm{e}^{-u^2/2v_T^2} \frac{u}{v_T} \int_{\mathbb{R}} \mathrm{d}u' \, \frac{u'}{v_T} \frac{n_0}{\sqrt{2\pi} v_T} \mathrm{e}^{-u^2/2v_T^2} = 0,$$

the integrand being an odd function integrated over $\mathbb{R}$. Thus, the total operator $\hat{L}_{\mathrm{cD}} + \hat{L}^{\mathrm{M}}_{\mathrm{cI}}$, denoted $\hat{L}_{\mathrm{cp}}$, acting on f_0 gives zero, thereby conserving the number of particles and hence also the charge,

$$\boxed{\hat{L}_{\mathrm{cp}} f_0 = (\hat{L}_{\mathrm{cD}} + \hat{L}^{\mathrm{M}}_{\mathrm{cI}}) f_0 = 0.} \tag{3.15}$$

For momentum to be conserved, the same argument has to hold for the total operator $\hat{L}_{\mathrm{cD}} + \hat{L}^{\mathrm{M}}_{\mathrm{cI}}$ acting on $u f_0$. The differential Ornstein-Uhlenbeck part gives

$$\hat{L}_{\mathrm{cD}}(u f_0) = -\nu f_0 u, \tag{3.16}$$

see Appendix B, and the remaining part

$$\hat{L}^{\mathrm{M}}_{\mathrm{cI}}(u f_0) = \nu v_T^2 \frac{\partial^2}{\partial u^2}(u f_0) + \frac{\partial}{\partial u}(u^2 f_0).$$

Considering the derivatives

$$\frac{\partial}{\partial u}(u f_0) = \left[1 - \frac{u^2}{v_T^2}\right] f_0 \tag{3.17}$$

$$\frac{\partial}{\partial u}(u^2 f_0) = \left[2 - \frac{u^2}{v_T^2}\right] u f_0 \tag{3.18}$$

$$\frac{\partial^2}{\partial u^2}(u f_0) = \left[\frac{u^2}{v_T^2} - 3\right] \frac{u}{v_T^2} f_0 \tag{3.19}$$

as shown in Appendix B, this gives further by comparison with the first line of Eq. (3.13)

$$\begin{aligned} \hat{L}^{\mathrm{M}}_{\mathrm{cI}}(u f_0) &\overset{(3.13)}{=} -\nu \frac{\partial f_0}{\partial u} \frac{1}{n_0} \int_{\mathbb{R}} \mathrm{d}u \, u^2 f_0 = -\nu \frac{\partial f_0}{\partial u} v_T^2 \\ &= \nu f_0 u. \end{aligned} \tag{3.20}$$

Thus indeed also the total operator $\hat{L}_{\mathrm{c}} + \hat{L}^{\mathrm{M}}_{\mathrm{cI}}$ gives zero acting on $u f_0$,

$$\boxed{\hat{L}_{\mathrm{cp}}(u f_0) = (\hat{L}_{\mathrm{cD}} + \hat{L}^{\mathrm{M}}_{\mathrm{cI}}) f_0 = 0,} \tag{3.21}$$

whereby also the momentum for the respective plasma species under consideration is conserved. The momentum conserving collision operator (3.13) can be

written in a compact form by introducing the functions

$$\alpha^{\mathrm{M}}(u) \overset{\mathrm{def}}{=} \frac{\nu}{\sqrt{2\pi}v_T}\frac{u}{v_T}\mathrm{e}^{-u^2/2v_T^2}, \tag{3.22}$$

$$\beta^{\mathrm{M}}(u) \overset{\mathrm{def}}{=} \frac{u}{v_T}, \tag{3.23}$$

so that

$$\boxed{\hat{L}_{\mathrm{cI}}^{\mathrm{M}} f(v_\perp, u) = \alpha^{\mathrm{M}}(u) \int_{\mathbb{R}} \mathrm{d}u'\, \beta^{\mathrm{M}}(u') f(v_\perp, u').} \tag{3.24}$$

In an analogous way, an energy conserving collision operator can be constructed, which, together with the differential part, satisfies $(\hat{L}_{\mathrm{cD}} + \hat{L}_{\mathrm{cI}}^{\mathrm{E}})u^2 f_0 = 0$. Without repeating the alike derivation, $\hat{L}_{\mathrm{cI}}^{\mathrm{E}}$ is found to be, see [30]

$$\begin{aligned}\hat{L}_{\mathrm{cI}}^{\mathrm{E}} f(v_\perp, u) &= \frac{\nu}{\sqrt{2\pi v_T^2}}\left(\frac{u^2}{v_T^2} - 1\right)\mathrm{e}^{-u^2/2v_T^2}\int_{\mathbb{R}}\mathrm{d}u'\,\left(\frac{u'^2}{v_T^2} - 1\right) f(v_\perp, u') \\ &= \alpha^{\mathrm{E}}(u)\int_{\mathbb{R}}\mathrm{d}u'\,\beta^{\mathrm{E}}(u) f(v_\perp, u'),\end{aligned} \tag{3.25}$$

with functions

$$\alpha^{\mathrm{E}}(u) \overset{\mathrm{def}}{=} \frac{\nu}{\sqrt{2\pi}v_T}\left(\frac{u^2}{v_T^2} - 1\right)\mathrm{e}^{-u^2/2v_T^2}, \tag{3.26}$$

$$\beta^{\mathrm{E}}(u) \overset{\mathrm{def}}{=} \frac{u^2}{v_T^2} - 1, \tag{3.27}$$

defined for convenience. The operators are constructed such that the action of the momentum conserving operator on the phase space energy density gives zero, $\hat{L}_{\mathrm{cI}}^{\mathrm{M}} u^2 f_0 = 0$, and thus also the whole, now integro-differential operator, constituted of the tree parts $\hat{L}_{\mathrm{cp}} = \hat{L}_{\mathrm{cD}} + \hat{L}_{\mathrm{cI}}^{\mathrm{M}} + \hat{L}_{\mathrm{cI}}^{\mathrm{E}}$ gives zero when acting on $u^2 f_0$,

$$\hat{L}_{\mathrm{cp}}\, u^2 f_0 = (\hat{L}_{\mathrm{cD}} + \hat{L}_{\mathrm{cI}}^{\mathrm{M}} + \hat{L}_{\mathrm{cI}}^{\mathrm{E}})\, u^2 f_0 = 0. \tag{3.28}$$

Analogously, since the energy conserving operator acting on $u f_0$ gives zero, $\hat{L}_{\mathrm{cI}}^{\mathrm{E}} u f_0 = 0$, the same applies to the whole operator,

$$\hat{L}_{\mathrm{cp}}\, u f_0 = (\hat{L}_{\mathrm{cD}} + \hat{L}_{\mathrm{cI}}^{\mathrm{M}} + \hat{L}_{\mathrm{cI}}^{\mathrm{E}})\, u f_0 = 0. \tag{3.29}$$

The proof of these relations, in particular the actions of each individual operator on f_0, $u f_0$ and $u^2 f_0$ can be found in Appendix B.

The model operator $\hat{L}_{\mathrm{cp}}$ does not consider the scattering of perpendicular velocity components, which leads to classical cross-field transport. This transport is ignorable in favour of parallel transport and $\boldsymbol{E} \times \boldsymbol{B}$-rotation [30].

Collision operator	Description
$\hat{L}_{\mathrm{cK}} f = -\nu\, \delta f(\boldsymbol{r}, \boldsymbol{p}, t)$	Krook term, e.g. [19]
$\hat{L}_{\mathrm{cD}} f = \nu v_T^2 \partial_u (\partial_u + u/v_T^2) f$	Ornstein-Uhlenbeck operator [33]
$\hat{L}^{\mathrm{E}}_{\mathrm{cI}} f = \alpha^{\mathrm{E}} \int_{\mathbb{R}} \mathrm{d}u'\, \beta^{\mathrm{E}} f$	Energy conserving integral operator [30]
$\hat{L}^{\mathrm{M}}_{\mathrm{cI}} f = \alpha^{\mathrm{M}} \int_{\mathbb{R}} \mathrm{d}u'\, \beta^{\mathrm{M}} f$	Momentum conserving integral operator [40]
$\hat{L}_{\mathrm{cp}} = \begin{cases} \hat{L}_{\mathrm{cD}} + \hat{L}^{\mathrm{E}}_{\mathrm{cI}} \\ \hat{L}_{\mathrm{cD}} + \hat{L}^{\mathrm{M}}_{\mathrm{cI}} \\ \hat{L}_{\mathrm{cD}} + \hat{L}^{\mathrm{E}}_{\mathrm{cI}} + \hat{L}^{\mathrm{M}}_{\mathrm{cI}} \end{cases}$	Integro-differential collision operators [30, 40]
$\hat{L} = \partial_t + \mathrm{i}(\omega_\ell + k_\parallel u) - \hat{L}_{\mathrm{cp}}$	Differential operator of the kinetic eqn. [30]

Table 3.1: Summary of collision operators

The conservation of momentum and energy is valid in zero order w.r.t. Larmor radius, since the distribution function in $\hat{L}^{\mathrm{E}}_{\mathrm{cI}} f$ and $\hat{L}^{\mathrm{M}}_{\mathrm{cI}} f$ is evaluated not at the actual particle position $\boldsymbol{r} = \boldsymbol{R} + \boldsymbol{\varrho}$ but at the guiding centre $\boldsymbol{R}$. However, the error introduced here as compared to the exact Coulomb operator is of the same order as the effects of classical cross-field transport of energy and momentum, which is not taken into account anyway.

3.3 Solution of the Linearised Gyrokinetic Equation

In this section the method for obtaining the analytic solution of the kinetic equation with full integro-differential collision operator is presented. As it was shown in Sect. 2.5, the first order linearised kinetic equation, Fourier transformed w.r.t. canonical angles is given by

$$\left[\frac{\partial}{\partial t} + \mathrm{i}(\omega_\ell + k_\parallel u) - \hat{L}_{\mathrm{cp}}\right] \tilde{f}_{\boldsymbol{m}}(u,t) = \tilde{Q}_{\boldsymbol{m}}(u,t), \tag{3.30}$$

where the purely differential collision operator has now been replaced by the full collision operator $\hat{L}_{\mathrm{cp}} = \hat{L}_{\mathrm{cD}} + \hat{L}^{\mathrm{E}}_{\mathrm{cI}} + \hat{L}^{\mathrm{M}}_{\mathrm{cI}}$. In Ivanov *et al.*, 2011 [33], the solution for the purely differential Fokker-Planck Ornstein-Uhlenbeck operator is given in terms of a Green's function,

$$\tilde{f}_{\boldsymbol{m}}(u,t) = \int_{t_0}^{t} \mathrm{d}\tau \int_{\mathbb{R}} \mathrm{d}u'\, \tilde{G}^{\mathrm{D}}_{\boldsymbol{m}}(u,u',t-\tau) \tilde{Q}_{\boldsymbol{m}}(u',\tau), \quad t > t_0. \tag{3.31}$$

The temporal Fourier transform of the Green's function is denoted

$$\tilde{G}^{\mathrm{D}}_{\omega\boldsymbol{m}}(u,u') = \int_0^\infty \mathrm{d}t\, \tilde{G}^{\mathrm{D}}_{\boldsymbol{m}}(u,u',t)\mathrm{e}^{\mathrm{i}\omega t}. \tag{3.32}$$

The Green's function Fourier-transformed w.r.t. time inherits the adjointness property of $\tilde{G}^{\mathrm{D}}_{\boldsymbol{m}}(u,u',t)$, shown in [33], which shall be used extensively in the following,

$$\tilde{G}^{\mathrm{D}}_{\omega\boldsymbol{m}}(u,u')\exp\left(-\frac{u'^2}{v_T^2}\right) = \tilde{G}^{\mathrm{D}}_{\omega\boldsymbol{m}}(u',u)\exp\left(-\frac{u^2}{v_T^2}\right). \tag{3.33}$$

The solution of the fully integro-differential problem can be constructed in terms of parallel velocity moments of the Green's function $G^{\mathrm{D}}_{\boldsymbol{m}}(u,u',t)$ of the purely differential problem. The solution method is similar yet extended as compared to Ref. [30].

Introducing the the differential operator $\hat{L} = \partial_t + \mathrm{i}(\omega_\ell + k_\parallel u) - \hat{L}_{\mathrm{cD}}$ of the kinetic equation, Eq. (3.30) can be written as

$$\hat{L}\tilde{f}_{\boldsymbol{m}} - \hat{L}^{\mathrm{M}}_{\mathrm{cI}}\tilde{f}_{\boldsymbol{m}} - \hat{L}^{\mathrm{E}}_{\mathrm{cI}}\tilde{f}_{\boldsymbol{m}} = \tilde{Q}_{\boldsymbol{m}}, \tag{3.34}$$

or explicitly

$$\left[\frac{\partial}{\partial t} + \mathrm{i}(\omega_\ell + k_\parallel u) - \nu\frac{\partial}{\partial u}\left(\frac{\partial}{\partial u} + \frac{u}{v_T^2}\right)\right]\tilde{f}_{\boldsymbol{m}}(u) - \alpha^{\mathrm{M}}(u)\int_{\mathbb{R}}\mathrm{d}u'\,\beta^{\mathrm{M}}(u')\tilde{f}_{\boldsymbol{m}}(u') - \alpha^{\mathrm{E}}(u)\int_{\mathbb{R}}\mathrm{d}u'\,\beta^{\mathrm{E}}(u')\tilde{f}_{\boldsymbol{m}}(u') = \tilde{Q}_{\boldsymbol{m}}, \tag{3.35}$$

cf. Eq. (30) of Heyn *et al.* (2014) [30], being extended here by the operator $\hat{L}^{\mathrm{M}}_{\mathrm{cI}}$ (second term on the left hand side) and the thermodynamic force $\mathscr{A}_3 = (1/v_T)\,\partial V_{\parallel 0}/\partial r$ associated with the parallel momentum gradient in the source term $\tilde{Q}_{\boldsymbol{m}}$. Formally, if one applies the inverse operator $\hat{L}^{-1}$ to the kinetic equation one gets

$$\tilde{f}_{\boldsymbol{m}} - \hat{L}^{-1}\hat{L}^{\mathrm{M}}_{\mathrm{cI}}\tilde{f}_{\boldsymbol{m}} - \hat{L}^{-1}\hat{L}^{\mathrm{E}}_{\mathrm{cI}}\tilde{f}_{\boldsymbol{m}} = \hat{L}^{-1}\tilde{Q}_{\boldsymbol{m}} \tag{3.36}$$

or explicitly

$$\tilde{f}_{\boldsymbol{m}} - \hat{L}^{-1}\alpha^{\mathrm{M}}(u)\int_{\mathbb{R}}\mathrm{d}u'\,\beta^{\mathrm{M}}(u')\tilde{f}_{\boldsymbol{m}}(u') - \hat{L}^{-1}\alpha^{\mathrm{E}}(u)\int_{\mathbb{R}}\mathrm{d}u'\,\beta^{\mathrm{E}}(u')\tilde{f}_{\boldsymbol{m}}(u') = \hat{L}^{-1}\tilde{Q}_{\boldsymbol{m}}(u). \tag{3.37}$$

Here, $\tilde{f}_{\boldsymbol{m}}$ in the first term has been expressed explicitly by application of $\hat{L}^{-1}$,

while in the second and third term on the left hand side it is still buried under the integral sign. One can find expressions for $x \equiv \int_{\mathbb{R}} \mathrm{d}u'\, \beta^{\mathrm{E}}(u')\tilde{f}_{\boldsymbol{m}}(u')$ and $y \equiv \int_{\mathbb{R}} \mathrm{d}u\, \beta^{\mathrm{M}}(u')\tilde{f}_{\boldsymbol{m}}(u')$ by multiplying Eq. (3.37) by $\beta^{\mathrm{E}}(u)$ and integrating over u and separately by $\beta^{\mathrm{M}}(u)$ and subsequent integration over u. This gives a set of two linear equations in x and y. Substitution of the solution for x and y back into Eq. (3.37), the solution of the full integro-differential equation (3.35) is obtained. This procedure is demonstrated in detail in the following.

By multiplication by $\beta^{\mathrm{E}}(u)$ and $\beta^{\mathrm{M}}(u)$, respectively and subsequent integration over u, the two equations

$$\begin{aligned}
&\left(1 - \int_{-\infty}^{\infty} \mathrm{d}u\, \beta^{\mathrm{X}}(u)\hat{L}^{-1}\alpha^{\mathrm{E}}(u)\right) \int_{-\infty}^{\infty} \mathrm{d}u' \beta^{\mathrm{E}}(u')\tilde{f}_{\boldsymbol{m}}(u') \\
&- \int_{-\infty}^{\infty} \mathrm{d}u\, \beta^{\mathrm{X}}(u)\hat{L}^{-1}\alpha^{\mathrm{M}}(u) \int_{-\infty}^{\infty} \mathrm{d}u'\, \beta^{\mathrm{M}}(u')\tilde{f}_{\boldsymbol{m}}(u') \\
&= \int_{-\infty}^{\infty} \mathrm{d}u\, \beta^{\mathrm{X}}(u)\hat{L}^{-1}\tilde{Q}_{\boldsymbol{m}}(u),
\end{aligned} \tag{3.38}$$

are obtained, where X denotes either E or M. Now since the Green's function $\tilde{G}^{\mathrm{D}}_{\boldsymbol{m}}$ solves the kinetic equation (3.30) via (3.31), the inverse operator is represented by the integral kernel $(\hat{L}^{-1})_{u,u'} \equiv \tilde{G}^{\mathrm{D}}_{\boldsymbol{m}}(u, u', t)$, which is demonstrated by the identities

$$\hat{L}\tilde{G}^{\mathrm{D}}_{\boldsymbol{m}} = \left[\partial_t + (\mathrm{i}\omega_\ell + k_\parallel u) - \nu\frac{\partial}{\partial u}\left(\frac{\partial}{\partial u} + \frac{u}{v_T^2}\right)\right]\tilde{G}^{\mathrm{D}}_{\boldsymbol{m}} = \delta(t - t_0)\delta(u - u') \tag{3.39}$$

and $[\mathrm{i}(\omega_\ell + k_\parallel u - \omega) - \nu\partial_u(\partial_u + u/v_T^2)]\tilde{G}^{\mathrm{D}}_{\omega\boldsymbol{m}} = \delta(u - u')$, respectively. By introducing the following definitions

$$\mathcal{A} := 1 - \int_{-\infty}^{\infty} \mathrm{d}u\, \beta^{\mathrm{E}}(u) \int_{-\infty}^{\infty} \mathrm{d}u'\, \tilde{G}^{\mathrm{D}}_{\omega\boldsymbol{m}}(u, u')\alpha^{\mathrm{E}}(u'), \tag{3.40}$$

$$\mathcal{B} := \int_{-\infty}^{\infty} \mathrm{d}u\, \beta^{\mathrm{E}}(u) \int_{-\infty}^{\infty} \mathrm{d}u'\, \tilde{G}^{\mathrm{D}}_{\omega\boldsymbol{m}}(u, u')\alpha^{\mathrm{M}}(u'), \tag{3.41}$$

$$\mathcal{C} := \int_{-\infty}^{\infty} \mathrm{d}u\, \beta^{\mathrm{E}}(u) \int_{-\infty}^{\infty} \mathrm{d}u'\, \tilde{G}^{\mathrm{D}}_{\omega\boldsymbol{m}}(u, u')\tilde{Q}_{\boldsymbol{m}}(u'), \tag{3.42}$$

$$\mathcal{A}^{\mathrm{M}} := 1 - \int_{-\infty}^{\infty} \mathrm{d}u\, \beta^{\mathrm{M}}(u) \int_{-\infty}^{\infty} \mathrm{d}u'\, \tilde{G}^{\mathrm{D}}_{\omega\boldsymbol{m}}(u, u')\alpha^{\mathrm{M}}(u'), \tag{3.43}$$

$$\mathcal{B}^{\mathrm{M}} := \int_{-\infty}^{\infty} \mathrm{d}u\, \beta^{\mathrm{M}}(u) \int_{-\infty}^{\infty} \mathrm{d}u'\, \tilde{G}^{\mathrm{D}}_{\omega\boldsymbol{m}}(u, u')\alpha^{\mathrm{E}}(u'), \tag{3.44}$$

$$\mathcal{C}^{\mathrm{M}} := \int_{-\infty}^{\infty} \mathrm{d}u\, \beta^{\mathrm{M}}(u) \int_{-\infty}^{\infty} \mathrm{d}u'\, \tilde{G}^{\mathrm{D}}_{\omega\boldsymbol{m}}(u, u')\tilde{Q}_{\boldsymbol{m}}(u'), \tag{3.45}$$

Eqns. (3.38) can be written compactly as

$$\begin{pmatrix} \mathcal{A} & -\mathcal{B} \\ -\mathcal{B}^{\mathrm{M}} & \mathcal{A}^{\mathrm{M}} \end{pmatrix} \begin{pmatrix} x \\ y \end{pmatrix} = \begin{pmatrix} \mathcal{C} \\ \mathcal{C}^{\mathrm{M}} \end{pmatrix}. \tag{3.46}$$

Eq. (3.46) is solved by

$$x = \frac{1}{\Delta} \left(\mathcal{A}^{\mathrm{M}} \mathcal{C} + \mathcal{B} \mathcal{C}^{\mathrm{M}} \right), \tag{3.47}$$

$$y = \frac{1}{\Delta} \left(\mathcal{B}^{\mathrm{M}} \mathcal{C} + \mathcal{A} \mathcal{C}^{\mathrm{M}} \right) \tag{3.48}$$

with determinant

$$\Delta = \mathcal{A}\mathcal{A}^{\mathrm{M}} - \mathcal{B}\mathcal{B}^{\mathrm{M}}. \tag{3.49}$$

Substitution of this result into (3.37), the Green's function $\tilde{G}_{\omega \boldsymbol{m}}(u, u')$ of the full integro-differential problem is found,

$$\begin{aligned} \tilde{G}_{\omega \boldsymbol{m}}(u, u') = \tilde{G}^{\mathrm{D}}_{\omega \boldsymbol{m}}(u, u') + \frac{1}{\Delta} \int_{\mathbb{R}} \mathrm{d}u'' \int_{\mathbb{R}} \mathrm{d}u''' \, \tilde{G}^{\mathrm{D}}_{\omega \boldsymbol{m}}(u, u'') \, \tilde{G}^{\mathrm{D}}_{\omega \boldsymbol{m}}(u''', u') \\ \times \left[\mathcal{B}^{\mathrm{M}} \alpha^{\mathrm{M}}(u'') \beta^{\mathrm{E}}(u''') + \mathcal{A} \alpha^{\mathrm{M}}(u'') \beta^{\mathrm{M}}(u''') \right. \\ \left. + \mathcal{A}^{\mathrm{M}} \alpha^{\mathrm{E}}(u'') \beta^{\mathrm{E}}(u''') + \mathcal{B} \alpha^{\mathrm{E}}(u'') \beta^{\mathrm{M}}(u''') \right]. \end{aligned} \tag{3.50}$$

Having obtained $\tilde{G}_{\omega \boldsymbol{m}}(u, u')$, the solution of the kinetic equation can be obtained from

$$\boxed{\tilde{f}_{\boldsymbol{m}}(v_\perp, u) = \int_{\mathbb{R}} \mathrm{d}u \, \tilde{G}_{\omega \boldsymbol{m}}(u, u') \tilde{Q}_{\boldsymbol{m}}(v_\perp, u').} \tag{3.51}$$

This solution for the perturbed distribution function will be used for the transport model in Sect. 3.5 to determine mass- and parallel momentum transport as well as the energy flux due to the perturbation field $\tilde{E}_{\omega \boldsymbol{m} \perp}$, $\tilde{B}^r_{\omega \boldsymbol{m}}$.

For the following evaluation of the transport coefficients velocity moments of the Green's function $\tilde{G}_{\omega \boldsymbol{m}}(u, u')$ are defined by multiplication of Eq. (3.50) by $u^m u'^n \exp(-u'^2/2v_T^2)$ and subsequent integration over all possible values of u and u',

$$\begin{aligned} W^{mn} = W^{mn}_{\mathrm{D}} + \frac{\nu}{\sqrt{2\pi v_T^2}} \frac{1}{\Delta} \int_{\mathbb{R}} \mathrm{d}u \int_{\mathbb{R}} \mathrm{d}u' \int_{\mathbb{R}} \mathrm{d}u'' \int_{\mathbb{R}} \mathrm{d}u''' \, \tilde{G}^{\mathrm{D}}_{\omega \boldsymbol{m}}(u, u'') \, \tilde{G}^{\mathrm{D}}_{\omega \boldsymbol{m}}(u', u''') \\ \times \mathrm{e}^{-u''^2/2v_T^2} \mathrm{e}^{-u'''^2/2v_T^2} u^m u'^n \left[\mathcal{B}^{\mathrm{M}} \frac{u''}{v_T} \left(\frac{u'''^2}{v_T^2} - 1 \right) + \mathcal{A} \frac{u''}{v_T} \frac{u'''}{v_T} \right. \\ \left. + \mathcal{A}^{\mathrm{M}} \left(\frac{u''^2}{v_T^2} - 1 \right) \left(\frac{u'''^2}{v_T^2} - 1 \right) + \mathcal{B} \left(\frac{u''^2}{v_T^2} - 1 \right) \frac{u'''}{v_T} \right]. \end{aligned} \tag{3.52}$$

As well as the purely differential Ornstein-Uhlenbeck problem is solved by the Green's function $\tilde{G}^{\mathrm{D}}_{\omega\boldsymbol{m}}(u,u')$, the special functions W^{mn}_{D} are the particular moments in that case, cf. Ivanov *et al.* (2011) [33],

$$W^{mn}_{\mathrm{D}}(k_\parallel,\omega)=\int_{\mathbb{R}}\mathrm{d}u\int_{\mathbb{R}}\mathrm{d}u'\;\tilde{G}^{\mathrm{D}}_{\omega\boldsymbol{m}}(u,u')\exp(-u'^2/2v_T^2)u^m u'^n. \tag{3.53}$$

With the parameters $x_1=k_\parallel v_T/\nu$ and $x_2=(\omega-\omega_\ell)/\nu$ one can also define dimensionless moments,

$$I^{mn}_{\mathrm{D}}(x_1,x_2)=\frac{\nu}{\sqrt{2\pi}v_T^{m+n+1}}W^{mn}_{\mathrm{D}}(\nu x_1/v_T,\nu x_2+\omega_\ell). \tag{3.54}$$

In terms of these moments, Eq. (3.52) becomes

$$\begin{aligned}I^{mn}=I^{mn}_{\mathrm{D}}+\frac{1}{\Delta}\Big[&\mathcal{B}^{\mathrm{M}}I^{m1}_{\mathrm{D}}\left(I^{2n}_{\mathrm{D}}-I^{0n}_{\mathrm{D}}\right)+\mathcal{A}I^{m1}_{\mathrm{D}}I^{n1}_{\mathrm{D}}\\&+\mathcal{A}^{\mathrm{M}}\left(I^{m2}_{\mathrm{D}}-I^{m0}_{\mathrm{D}}\right)\left(I^{2n}_{\mathrm{D}}-I^{0n}_{\mathrm{D}}\right)+\mathcal{B}\left(I^{m2}_{\mathrm{D}}-I^{m0}_{\mathrm{D}}\right)I^{1n}_{\mathrm{D}}\Big],\end{aligned} \tag{3.55}$$

again being constructed by the solution of the purely differential part I^{mn}_{D} and an integral part consisting of particular moments of I^{mn}_{D}. Explicit evaluation of the coefficients $\mathcal{A}$, $\mathcal{A}^{\mathrm{M}}$, $\mathcal{B}$ and $\mathcal{B}^{\mathrm{M}}$ yields

$$\begin{aligned}\mathcal{A}&=1-\int_{\mathbb{R}}\mathrm{d}u\left(\frac{u^2}{v_T^2}-1\right)\int_{\mathbb{R}}\mathrm{d}u'\,\tilde{G}^{\mathrm{D}}_{\omega\boldsymbol{m}}(u,u')\frac{\nu}{\sqrt{2\pi}v_T}\mathrm{e}^{-u'^2/2v_T^2}\left(\frac{u'^2}{v_T^2}-1\right)\\
&=1-\frac{\nu}{\sqrt{2\pi}v_T}\int_{\mathbb{R}}\mathrm{d}u\left(\frac{u}{v_T}\right)^2\int_{\mathbb{R}}\mathrm{d}u'\,\tilde{G}^{\mathrm{D}}_{\omega\boldsymbol{m}}(u,u')\mathrm{e}^{-u'^2/2v_T^2}\left(\frac{u'}{v_T}\right)^2\\
&\quad+\frac{\nu}{\sqrt{2\pi}v_T}\int_{\mathbb{R}}\mathrm{d}u\int_{\mathbb{R}}\mathrm{d}u'\,\tilde{G}^{\mathrm{D}}_{\omega\boldsymbol{m}}(u,u')\mathrm{e}^{-u'^2/2v_T^2}\left(\frac{u'}{v_T}\right)^2\\
&\quad+\frac{\nu}{\sqrt{2\pi}v_T}\int_{\mathbb{R}}\mathrm{d}u\left(\frac{u}{v_T}\right)^2\int_{\mathbb{R}}\mathrm{d}u'\,\tilde{G}^{\mathrm{D}}_{\omega\boldsymbol{m}}(u,u')\mathrm{e}^{-u^2/2v_T^2}\\
&\quad-\frac{\nu}{\sqrt{2\pi}v_T}\int_{\mathbb{R}}\mathrm{d}u\int_{\mathbb{R}}\mathrm{d}u'\,G_{\omega\boldsymbol{m}}(u,u')\mathrm{e}^{-u'^2/2v_T^2}\\
&=1+\frac{\nu}{\sqrt{2\pi}v_T}\left(\frac{1}{v_T^2}W^{02}+\frac{1}{v_T^2}W^{20}-W^{00}-\frac{1}{v_T^4}W^{22}\right)\\
&=1-I^{00}_{\mathrm{D}}+2I^{20}_{\mathrm{D}}-I^{22}_{\mathrm{D}},\end{aligned} \tag{3.56}$$

where the adjointness property of the Greens function $I^{mn}=I^{nm}$ has been used.

Similarly one obtains for the remaining coefficients

$$\begin{aligned}\mathcal{A}^{\mathrm{M}} &= 1 - \int_{\mathbb{R}} \mathrm{d}u\, \frac{u}{v_T} \frac{\nu}{\sqrt{2\pi} v_T} \int_{\mathbb{R}} \mathrm{d}u'\, \tilde{G}^{\mathrm{D}}_{\omega \boldsymbol{m}}(u,u') \mathrm{e}^{-u'^2/2v_T^2} \frac{u'}{v_T} \\ &= 1 - \frac{\nu}{\sqrt{2\pi} v_T} \frac{1}{v_T^2} W^{11} \\ &= 1 - I_{\mathrm{D}}^{11}, \end{aligned} \tag{3.57}$$

$$\begin{aligned}\mathcal{B} &= \int_{\mathbb{R}} \mathrm{d}u\, \left(\frac{u^2}{v_T^2} - 1 \right) \frac{\nu}{\sqrt{2\pi} v_T} \int_{\mathbb{R}} \mathrm{d}u'\, \tilde{G}^{\mathrm{D}}_{\omega \boldsymbol{m}}(u,u') \mathrm{e}^{-u'^2/2v_T^2} \frac{u'}{v_T} \\ &= \frac{\nu}{\sqrt{2\pi} v_T} \left(\frac{1}{v_T^3} W^{21} - \frac{1}{v_T} W^{01} \right) \\ &= I_{\mathrm{D}}^{21} - I_{\mathrm{D}}^{01}, \end{aligned} \tag{3.58}$$

$$\begin{aligned}\mathcal{B}^{\mathrm{M}} &= \frac{\nu}{\sqrt{2\pi} v_T} \int_{\mathbb{R}} \mathrm{d}u\, \frac{u}{v_T} \int_{\mathbb{R}} \mathrm{d}u'\, \tilde{G}^{\mathrm{D}}_{\omega \boldsymbol{m}}((u,u') \mathrm{e}^{-u'^2/2v_T^2} \left(\frac{u'^2}{v_T^2} - 1 \right) \\ &= \frac{\nu}{\sqrt{2\pi} v_T} \left(\frac{1}{v_T^3} W^{12} - \frac{1}{v_T} W^{10} \right) \\ &= I_{\mathrm{D}}^{21} - I_{\mathrm{D}}^{01}, \end{aligned} \tag{3.59}$$

and the determinant

$$\begin{aligned}\Delta = \mathcal{A}\mathcal{A}^{\mathrm{M}} - \mathcal{B}\mathcal{B}^{\mathrm{M}} &= (1 - I_{\mathrm{D}}^{00} + 2I_{\mathrm{D}}^{20} - I_{\mathrm{D}}^{22})(1 - I_{\mathrm{D}}^{11}) - (I_{\mathrm{D}}^{21} - I_{\mathrm{D}}^{01})^2 \\ &= \Delta_1 (1 - I_{\mathrm{D}}^{11}) - \Delta_2^2. \end{aligned} \tag{3.60}$$

From the evaluation of the coefficients in Eqns. (3.58) and (3.59) one immediately sees that $\mathcal{B} \equiv \mathcal{B}^{\mathrm{M}}$.

In the following we consider two important limits, namely the two cases where particles and either momentum or energy are conserved.

- Setting $\beta^{\mathrm{E}} = 0$, we arrive at the limit where the integral collision operator $\hat{L}^{\mathrm{E}}_{\mathrm{cI}}$ in $\hat{L}_{\mathrm{cp}}$ vanishes and only momentum and particles are conserved. From the definitions of the coefficients we see further that in this limit the coefficients reduce to $\mathcal{A} = 1$, $\mathcal{B} = \mathcal{B}^{\mathrm{M}} = 0$ and $\Delta = \mathcal{A}^{\mathrm{M}}$. By substitution in Eq. (3.55) and (3.50), the solution formulated in terms of the moments I^{mn} simplifies considerably,

$$I^{mn} = I^{mn}_{\mathrm{D}} + \frac{1}{\mathcal{A}^{\mathrm{M}}} I^{m1}_{\mathrm{D}} I^{n1}_{\mathrm{D}}. \tag{3.61}$$

- The more important limit case of only energy and particle conservation is obtained by setting $\beta^{\mathrm{M}} = 0$, in which case $\hat{L}^{\mathrm{M}}_{\mathrm{cI}}$ vanishes. Here $\mathcal{A}^{\mathrm{M}} = 1$, $\mathcal{B}^{\mathrm{M}} = \mathcal{B} = 0$ and $\Delta = \mathcal{A}$. Analogous to the prior case it immediately follows that

$$I^{mn} = I^{mn}_{\mathrm{D}} + \frac{1}{\mathcal{A}}(I^{m2}_{\mathrm{D}} - I^{m0}_{\mathrm{D}})(I^{2n}_{\mathrm{D}} - I^{0n}_{\mathrm{D}}). \tag{3.62}$$

  This result reproduces the moment equation already obtained earlier by application of an exclusively energy conserving integral operator by Heyn *et al.* (2014) [30] and Heyn *et al.* (2013) [29].

3.4 Recursion Formulæ

A further relevant part of this thesis has been the derivation of recursion relations between the moments I^{mn}. These relations proved valuable for the numerical evaluation of diffusion coefficients, reducing the computational effort to the evaluation of few lower moments and obtaining higher ones recursively.

As shown in Ref. [33], the moments of the Green's function can be derived from

$$I^{mn}_{\mathrm{D}\,k}(x_1, x_2) = \left[\frac{\partial^m}{\partial \alpha^m} \frac{\partial^n}{\partial \beta^n} \int_0^\infty \mathrm{d}\tau\, \mathrm{e}^{A\tau + B(\alpha,\beta)\mathrm{e}^{-\tau} + C(\alpha,\beta) - k\tau} \right]_{\alpha,\beta=0} \tag{3.63}$$

such that for $k = 0$ the functions I^{mn}_{D} in Eq. (3.54) are recovered. The parameters used above are defined as

$$A = \mathrm{i}x_2 - x_1^2, \tag{3.64}$$

$$B = (\alpha + \mathrm{i}x_1)(\beta + \mathrm{i}x_1), \tag{3.65}$$

$$C = \frac{1}{2}(\alpha^2 + \beta^2) - \mathrm{i}x_1(\alpha + \beta) + x_1^2. \tag{3.66}$$

By explicit evaluation and numerical integration of Eq. (3.63), the moments as functions of $x_1 = k_\parallel v_T/\nu$ and $x_2 = (\omega - \omega_\ell)/\nu$ have been obtained, see Fig. 3.6. It is clear from their definition that the computational effort increases considerably the higher m and n become. The recursions derived below significantly reduce the workload by allowing to compute higher moments practically for free, once a set of lower moments is obtained.

For the sake of notational convenience one can also define the integral part of (3.63) separately as a function

$$J_k(\alpha,\beta) = \int_0^\infty \mathrm{d}\tau\, \exp(A\tau + B(\alpha,\beta)\mathrm{e}^{-\tau} + C(\alpha,\beta) - k\tau). \tag{3.67}$$

This function is the starting point for the derivation of two recursions derived below.

First Recursion

By explicitly evaluating a single derivative w.r.t. β in expression (3.63), one obtains

$$\begin{aligned}
\frac{\partial^m}{\partial\alpha^m}\frac{\partial^n}{\partial\beta^n}J_k(\alpha,\beta) &= \frac{\partial^m}{\partial\alpha^m}\frac{\partial^n}{\partial\beta^n}\int_0^\infty \mathrm{d}\tau\, \exp(A\tau + B\mathrm{e}^{-\tau} + C - k\tau) \\
&= \frac{\partial^m}{\partial\alpha^m}\frac{\partial^{n-1}}{\partial\beta^{n-1}}\int_0^\infty \mathrm{d}\tau\, \exp(A\tau + B\mathrm{e}^{-\tau} + C - k\tau) \\
&\quad \times \left[(\alpha + \mathrm{i}x_1)\mathrm{e}^{-\tau} + (\beta - \mathrm{i}x_1)\right] \\
&= \left[(\alpha + \mathrm{i}x_1)\frac{\partial^m}{\partial\alpha^m}\frac{\partial^{n-1}}{\partial\beta^{n-1}} + m\frac{\partial^{m-1}}{\partial\alpha^{m-1}}\frac{\partial^{n-1}}{\partial\beta^{n-1}}\right] J_{k+1} \\
&\quad + \left[(\beta - \mathrm{i}x_1)\frac{\partial^m}{\partial\alpha^m}\frac{\partial^{n-1}}{\partial\beta^{n-1}} + (n-1)\frac{\partial^m}{\partial\alpha^m}\frac{\partial^{n-2}}{\partial\beta^{n-2}}\right] J_k,
\end{aligned} \tag{3.68}$$

where

$$\frac{\partial^n}{\partial\beta^n}(ab) = \sum_{j=0}^{n}\binom{n}{j}\frac{\partial^j b}{\partial\beta^j}\frac{\partial^{n-j}a}{\partial\beta^{n-j}} \tag{3.69}$$

has been used. In the limit $\alpha, \beta = 0$ this expression reduces to

$$\boxed{I_k^{mn} = \mathrm{i}x_1 I_{k+1}^{m,n-1} + m I_{k+1}^{m-1,n-1} - \mathrm{i}x_1 I_k^{m,n-1} + (n-1) I_k^{m,n-2}.} \tag{3.70}$$

Second Recursion

The obtained recursion (3.70) so far is not of much use, relating moments with different integer values k. It will however be applied in the course of the following

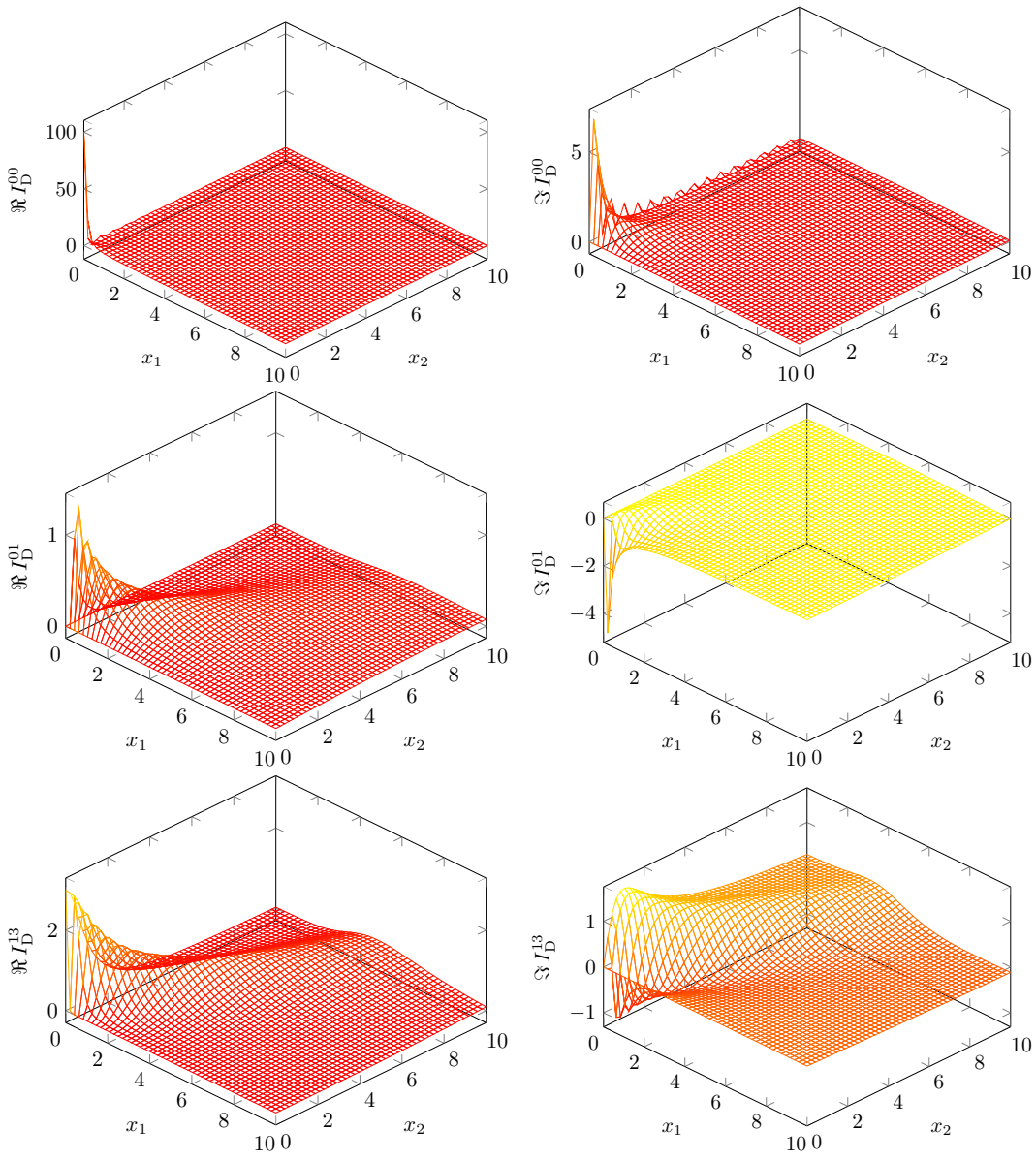

Figure 3.6: Real and imaginary parts of a few representative moments I_{D}^{mn} as obtained by direct numerical integration of Eq. (3.63).

derivation of yet another recursion, allowing the evaluation of I_k^{mn} from the moments $I_k^{m,n-1}$ and $I_k^{m,n-3}$, i.e. independently of index k.

Again expression (3.63) is considered, which shall now be integrated by parts to obtain

$$\begin{aligned}
\frac{\partial^m}{\partial\alpha^m}\frac{\partial^n}{\partial\beta^n}J_k &= \frac{\partial^m}{\partial\alpha^m}\frac{\partial^n}{\partial\beta^n}\left[\frac{B}{A-k}J_{k+1} - \frac{\mathrm{e}^{B+C}}{A-k}\right] \\
&= \frac{1}{A-k}\frac{\partial^m}{\partial\alpha^m}\frac{\partial^n}{\partial\beta^n}\left(BJ_{k+1} - \mathrm{e}^{B+C}\right) \\
&= \frac{1}{A-k}\frac{\partial^m}{\partial\alpha^m}\left(B\frac{\partial^n}{\partial\beta^n}J_{k+1} + n\frac{\partial B}{\partial\beta}\frac{\partial^{n-1}}{\partial\beta^{n-1}}J_{k+1} - \frac{\partial^n}{\partial\beta^n}\mathrm{e}^{B+C}\right) \\
&= \frac{1}{A-k}\left\{B\frac{\partial^m}{\partial\alpha^m}\frac{\partial^n}{\partial\beta^n}J_{k+1} + m\frac{\partial B}{\partial\alpha}\frac{\partial^{m-1}}{\partial\alpha^{m-1}}\frac{\partial^n}{\partial\beta^n}J_{k+1}\right. \\
&\quad + n\frac{\partial B}{\partial\beta}\frac{\partial^m}{\partial\alpha^m}\frac{\partial^{n-1}}{\partial\beta^{n-1}}J_{k+1} + nm\frac{\partial^2 B}{\partial\beta\partial\alpha}\frac{\partial^{n-1}}{\partial\alpha^{n-1}}\frac{\partial^{n-1}}{\partial\beta^{n-1}}J_{k+1} \\
&\quad \left. - \frac{\partial^m}{\partial\alpha^m}\frac{\partial^n}{\partial\beta^n}\exp\left[\frac{(\alpha+\beta)^2}{2}\right]\right\},
\end{aligned} \tag{3.71}$$

Here, rule (3.69) has been applied twice in order to move function $B(\alpha,\beta)$ in front of the derivatives. For the evaluation of the last term in the above expression in the limit of $\alpha,\beta = 0$ another function is defined,

$$H^m \stackrel{\text{def}}{=} \begin{cases} (m-1)!! & m \text{ even} \\ 0 & m \text{ odd} \end{cases} \tag{3.72}$$

or, alternatively

$$H^{2n} = (2n-1)!! = \frac{1}{2^n}\frac{(2n)!}{n!} \qquad n \in \mathbb{N}, \tag{3.73}$$

by which one can write

$$\frac{\partial^m}{\partial\alpha^m}\frac{\partial^n}{\partial\beta^n}\exp\left[\frac{(\alpha+\beta)^2}{2}\right]\Bigg|_{\alpha,\beta=0} = H^{m+n}. \tag{3.74}$$

Thus, in this limit the recursion

$$\begin{aligned}
I_k^{mn} = \frac{1}{A-k}\Big[&\mathrm{i}x_1\left(\mathrm{i}x_1 I_{k+1}^{mn} + mI_{k+1}^{m-1,n}\right) \\
&+ n\left(\mathrm{i}x_1 I_{k+1}^{m,n-1} + mI_{k+1}^{m-1,n-1}\right) - H^{m+n}\Big]
\end{aligned} \tag{3.75}$$

is found. Now recursion (3.70) obtained previously can be rearranged to

$$\mathrm{i}x_1 I_{k+1}^{m,n-1} + m I_{k+1}^{m-1,n-1} = I_k^{mn} + \mathrm{i}x_1 I_k^{m,n-1} - (n-1) I_k^{m,n-2}. \tag{3.76}$$

Using this relation twice in (3.75) yields

$$(A-k) I_k^{mn} = \mathrm{i}x_1 I_k^{m,n+1} + (n - x_1^2) I_k^{mn} - n(n-1) I_k^{m,n-2} - H^{m+n}. \tag{3.77}$$

Replacing n by $n-1$ and $A + x_1^2$ by $\mathrm{i}x_2$, the final recursion formula is obtained

$$\boxed{\begin{aligned} I_k^{mn} = \frac{1}{\mathrm{i}x_1} \big[&(\mathrm{i}x_2 + 1 - n - k) I_k^{m,n-1} \\ &+ (n-1)(n-2) I_k^{m,n-3} + H^{m+n-1} \big], \end{aligned}} \tag{3.78}$$

which is valid for all k and in particular for $k = 0$.

The equivalence of the two expressions (3.72) and (3.73) used for the definition of H^{2n} is a well known identity that is easily verified by taking advantage of the relation $(2n+1)!! = (2n+1)!/(2^n n!)$ between regular and double factorials that can e.g. be found in the standard textbook by Arfken and Weber [2, p. 505] and by setting $n \to n-1$,

$$(2n-1)!! = \frac{(2n-1)!}{2^{n-1}(n-1)!} = \frac{2n(2n-1)!}{2^n n(n-1)!} = \frac{(2n)!}{2^n n!}. \tag{3.79}$$

In Fig. 3.7 the moments I_{D}^{23} and I_{D}^{33}, obtained from the sets of lower moments $\{I_{\mathrm{D}}^{20}, I_{\mathrm{D}}^{22}\}$ and $\{I_{\mathrm{D}}^{30}, I_{\mathrm{D}}^{32}\}$ by application of recursion formula (3.78) are shown.

Collisionless limit

In the following, the obtained recursion formula (3.78) is used to determine the collisional limit of the moments. Returning to their dimensional definition W^{mn} and substituting the actual physical parameters for x_1 and x_2, one obtains

$$\begin{aligned} W^{mn} &= \frac{\nu}{\mathrm{i}k_\parallel v_T} \left[\left(\mathrm{i}\frac{\omega - \omega_\ell}{\nu} + 1 - n \right) v_T W^{m,n-1} + (n-1)(n-2) v_T^3 W^{m,n-3} \right. \\ &\quad \left. + \frac{\sqrt{2\pi}}{\nu} v_T^{m+n+1} H^{m+n-1} \right] \\ &= \frac{\omega - \omega_\ell}{\sqrt{2} k_\parallel v_T} \sqrt{2} v_T W^{m,n-1} + \mathcal{O}(\nu) + \frac{\sqrt{2\pi}}{\mathrm{i}k_\parallel} v_T^{m+n} H^{m+n-1} \end{aligned} \tag{3.80}$$

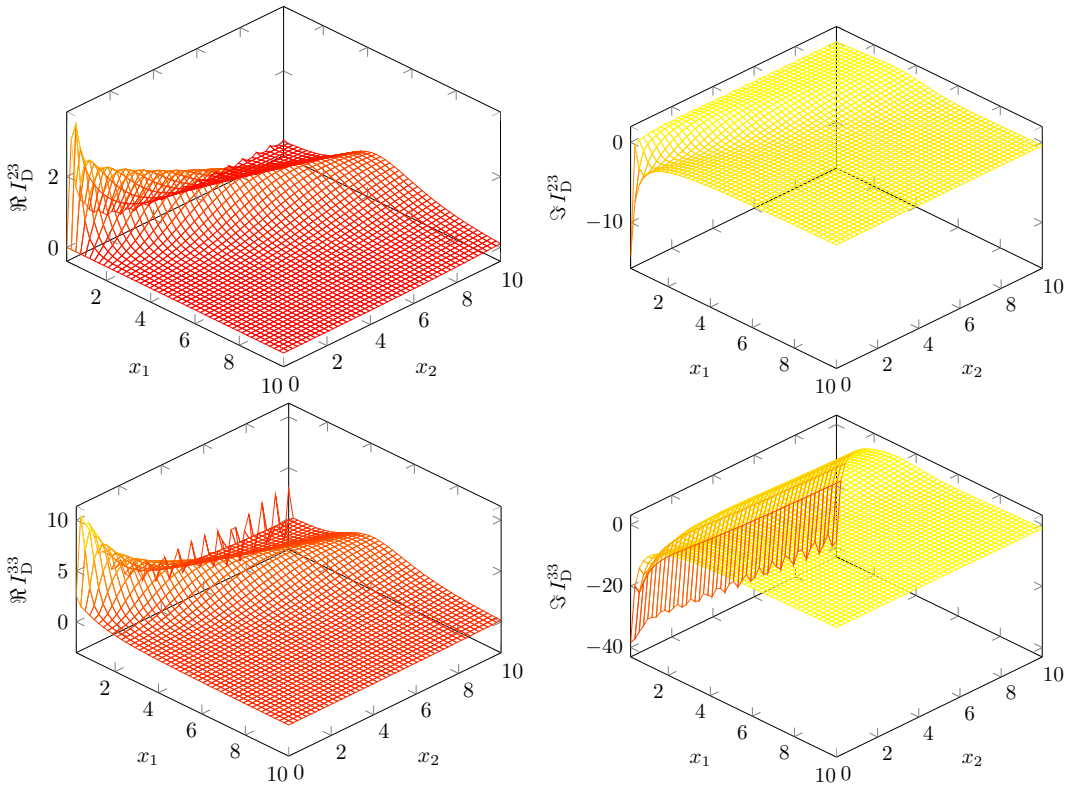

Figure 3.7: Real and imaginary parts of the moments I_{D}^{23} and I_{D}^{33} as obtained from recursion formula (3.78).

In the collisionless case $\nu \to 0$, denoted "nc" (no collisions) in the following, this expression becomes

$$W^{mn}_{\mathrm{nc}} = \lim_{\nu\to 0} W^{mn} = z\sqrt{2}v_T W^{m,n-1}_{\mathrm{nc}} + \frac{\sqrt{2\pi}}{\mathrm{i}k_\parallel} v_T^{m+n} H^{m+n-1}, \tag{3.81}$$

where the dimensionless parameter

$$z = \frac{\omega - \omega_\ell}{\sqrt{2}k_\parallel v_T} \tag{3.82}$$

has been introduced. The same result can be obtained by evaluation of the Green's function (3.32) in the collisionless limit that reduces to

$$\tilde{G}^{\mathrm{D,nc}}_{\omega\boldsymbol{m}}(u,u') = \frac{\mathrm{i}}{\omega - \omega_\ell - k_\parallel u + \mathrm{i}0^+}\delta(u-u') \tag{3.83}$$

and so gives the moments

$$\begin{aligned} W^{mn}_{\mathrm{nc}} &= \int_{\mathbb{R}} \mathrm{d}u \, \frac{\mathrm{i}}{\omega - \omega_\ell - k_\parallel u + \mathrm{i}0^+}\delta(u-u') \exp\left(-\frac{u'^2}{2v_T^2}\right) u^m u'^n \\ &= \int_{\mathbb{R}} \mathrm{d}u \, \frac{\mathrm{i}}{\omega - \omega_\ell - k_\parallel u + \mathrm{i}0^+} \exp\left(-\frac{u^2}{2v_T^2}\right) u^{m+n}. \end{aligned} \tag{3.84}$$

Setting $u/\sqrt{2}v_T^2 = y$, one can evaluate this expression further,

$$\begin{aligned} W^{mn}_{\mathrm{nc}} &= \frac{\pi}{k_\parallel}(\sqrt{2}v_T)^{m+n}\frac{\mathrm{i}}{\pi}\int_{\mathcal{C}} \mathrm{d}y \, \frac{\mathrm{e}^{-y^2}}{z-y} y^{m+n} \\ &= \frac{\mathrm{i}}{k_\parallel}(\sqrt{2}v_T)^{m+n}\int_{\mathcal{C}} \mathrm{d}y \left(\frac{z}{z-y} - 1\right)\mathrm{e}^{-y^2} y^{m+n-1} \\ &= z\sqrt{2}v_T W^{m,n-1}_{\mathrm{nc}} + \frac{\sqrt{2\pi}}{\mathrm{i}k_\parallel} v_T^{m+n} H^{m+n-1}, \end{aligned} \tag{3.85}$$

by considering

$$\int_{\mathbb{R}} \mathrm{d}y \, y^m \frac{\mathrm{e}^{-y^2}}{z-y} = \sqrt{\pi}\frac{H^m}{2^{m/2}}. \tag{3.86}$$

This expression for W^{mn}_{nc} (3.85) is identical to (3.81) obtained above by taking the limit $\nu \to 0$ in the recursion relation. The lowest moment in the collisionless limit is related to the complex probability integral, $(k_\parallel/\pi)W^{00}_{\mathrm{nc}} = w(z)$ that, for instance, is defined in Akhiezer *et al.* (1975) [1],

$$w(z) = \frac{\mathrm{i}}{\pi}\int_{\mathcal{C}} \mathrm{d}y \, \frac{\mathrm{e}^{-y^2}}{z-y} = \mathrm{e}^{-z^2}\left(1 + \frac{2\mathrm{i}}{\sqrt{\pi}}\int_0^z \mathrm{d}y \, \mathrm{e}^{y^2}\right). \tag{3.87}$$

3.5 Transport Model

The model at hand is aimed at describing particle, parallel momentum and energy flux driven by the perturbation field. Simple early transport models assumed a flux of particles being mainly driven by a gradient of the particle density, i.e. $\Gamma \propto -\nabla n$. Similarly, the flow of heat has been attributed to a gradient of the temperature, $Q \propto -(1/T)\nabla T$. If there is more than one transport process taking place at the same time, these processes were realised to affect one another, which lead to phenomenological transport relations of the type $X_i = R_{ij}J_j$, where the X_i are forces that drive current and heat flow J_i, respectively and the coefficients R_{ij} denote electrical and heat resistance. These empirical relations date back to the early findings of W. Thomson on thermoelectric phenomena [55]. Density and temperature gradients drive both, particle and heat fluxes and cross terms are likely to be of comparable importance to the direct terms [8]. Onsager showed in 1931 [55] that whatever the choices for fluxes Γ_i and conjugated thermodynamic forces $\mathscr{A}_i$ are, their product must give the entropy production $\dot{s} = \sum_i \mathscr{A}_i\Gamma_i$ and the resultant transport matrix has to be symmetric. While also Thomson assumed $R_{12} = R_{21}$ to hold, his early assumption was based entirely on experimental data and a rigorous derivation from fundamental principles was left for times to come. It is the following canonical form $\mathscr{A}_1 = (1/n_0)\,\mathrm{d}n_0/\,\mathrm{d}r + (e/T)\,\mathrm{d}\Phi_0/\,\mathrm{d}r - (3/2T)\,\mathrm{d}T/\,\mathrm{d}r$, $\mathscr{A}_2 = (1/T)\,\mathrm{d}T/\,\mathrm{d}r$, and $\mathscr{A}_3 = (1/v_T)\,\mathrm{d}V_{\|0}/\,\mathrm{d}r$ that shall be used for the driving forces due to density, energy, and momentum fluxes in the following. In linear transport theory the fluxes are related to the thermodynamic forces via the transport matrix (D_{ij}): $\Gamma_i = \sum_j D_{ij}\mathscr{A}_j$. Thermodynamic forces $\mathscr{A}_i$ occur whenever a thermodynamic system is out of equilibrium and drive the transport of continuous extensive quantities in order to restore the system to an equilibrium state. Their conjugate fluxes Γ_i are a measure of the rate at which a certain continuous quantity is transported.

The question of the importance of Onsager symmetry of the transport equations has been revived mainly in the 1990's and has been discussed by many authors [59, 46, 65, 68, 60, 66, 67]. It is the general opinion that the violation of Onsager symmetry of the transport matrix strongly indicates an inconsistent theory. In Sec. 3.5.2 Onsager symmetry will be proven for the transport matrix obtained from this model.

3.5.1 Diffusion Matrix

It has already been discussed in detail in Sect. 2.4 how the transport source term $\tilde{Q}_{\boldsymbol{m}}$ is connected to the gradient of the equilibrium distribution and the thermodynamic forces, respectively, see e.g. Eqns. (2.105) and (2.118). For the

extended transport model considering also parallel momentum transport, $\partial_r f_0$ with f_0, the inhomogeneous drifting Maxwellian already introduced earlier,

$$f_0(r, v_\parallel, v_\perp) = \frac{n_0(r)}{(2\pi m T(r))^{3/2}} \exp\left\{ -\frac{m\left[v_\perp^2 + (v_\parallel - V_{\parallel 0}(r))^2\right]}{2T(r)} \right\}, \tag{3.88}$$

is given by a linear combination of the thermodynamic forces extended here by a force $\mathscr{A}_3$,

$$\mathscr{A}_1 = \frac{1}{n_0}\frac{\partial n_0}{\partial r} + \frac{e}{T}\frac{\partial \Phi_0}{\partial r} - \frac{3}{2T}\frac{\partial T}{\partial r}, \quad \mathscr{A}_2 = \frac{1}{T}\frac{\partial T}{\partial r}, \quad \mathscr{A}_3 = \frac{1}{v_T}\frac{\partial V_{\parallel 0}}{\partial r}, \tag{3.89}$$

$$\nabla f_0 = (a_1\mathscr{A}_1 + a_2\mathscr{A}_2 + a_3\mathscr{A}_3) f_0 \nabla r - \frac{e}{T} f_0 \nabla \Phi_0. \tag{3.90}$$

The dimensionless coefficients a_i, needed for the evaluation of the source term are obtained from direct evaluation of

$$\begin{aligned}
\frac{1}{f_0}\frac{\partial f_0}{\partial r} &= \frac{1}{n_0(r)}\frac{\partial n_0(r)}{\partial r} - \frac{3}{2T(r)}\frac{\partial T(r)}{\partial r} + \frac{1}{T^2(r)}\frac{m}{2}\left[v_\perp^2 + (v_\parallel - V_{\parallel 0}(r))^2\right]\frac{\partial T(r)}{\partial r} \\
&\quad + \frac{m}{T(r)}(v_\parallel - V_{\parallel 0}(r))\frac{\partial V_{\parallel 0}(r)}{\partial r} \\
&\overset{!}{=} \left[a_1 \left(\frac{1}{n_0(r)}\frac{\partial n_0(r)}{\partial r} + \frac{e}{T(r)}\frac{\partial \Phi(r)}{\partial r} - \frac{3}{2T(r)}\frac{\partial T(r)}{\partial r} \right) + a_2 \frac{1}{T(r)}\frac{\partial T(r)}{\partial r} \right. \\
&\quad \left. + a_3 \frac{1}{v_T}\frac{\partial V_{\parallel 0}(r)}{\partial r} \right] - \frac{e}{T}\frac{\partial \Phi_0}{\partial r},
\end{aligned} \tag{3.91}$$

$$\Rightarrow \; a_1 = 1, \quad a_2 = \frac{m\left[v_\perp^2 + (v_\parallel - V_{\parallel 0})^2\right]}{2T}, \quad a_3 = \frac{m(v_\parallel - V_{\parallel 0})}{T} v_T. \tag{3.92}$$

In Sect. 2.4.1 it has been shown how to arrive from the general expression for the flux densities, e.g. the particle flux density $\Gamma = (1/S)\int \mathrm{d}S \int \mathrm{d}^3 p\, \tilde{f} \dot{\boldsymbol{R}}_1 \cdot \nabla r$ at the corresponding formula for the Fourier amplitudes, see Eq. (2.142). Having determined the Green's function $\tilde{G}_{\omega \boldsymbol{m}}(u, u')$ for the full integro-differential problem with momentum conservation, the flux densities and the components of the transport matrix can be derived.

From the formal solution of the kinetic equation

$$\begin{aligned}
\tilde{f}_{\boldsymbol{m}}(u) = &- \int_{-\infty}^{\infty} \mathrm{d}u'\, \tilde{G}_{\omega \boldsymbol{m}}(u, u') \left(a_1(v_\perp, u')\mathscr{A}_1 + a_2(v_\perp, u')\mathscr{A}_2 + a_3(v_\perp, u')\mathscr{A}_3\right) \\
&\times f_0(v_\perp, u') v^r_{\boldsymbol{m}}(v_\perp, u')
\end{aligned} \tag{3.93}$$

and the expressions for the flux densities

$$\Gamma = \frac{1}{2}\,\Re \sum_{\boldsymbol{m}} \int \mathrm{d}^3p\, \tilde{f}_{\boldsymbol{m}} v^{r*}_{\boldsymbol{m}}, \tag{3.94}$$

$$Q = \frac{1}{2}\,\Re \sum_{\boldsymbol{m}} \int \mathrm{d}^3p\, \frac{m}{2}\left(v_\perp^2 + u^2\right) \tilde{f}_{\boldsymbol{m}} v^{r*}_{\boldsymbol{m}}, \tag{3.95}$$

$$\Gamma_\parallel = \frac{1}{2}\,\Re \sum_{\boldsymbol{m}} \int \mathrm{d}^3p\, mu \tilde{f}_{\boldsymbol{m}} v^{r*}_{\boldsymbol{m}} \tag{3.96}$$

together with the definition of the diffusion matrix[3]

$$\begin{aligned}
\Gamma &= -n_0(D_{11}\mathscr{A}_1 + D_{12}\mathscr{A}_2 + D_{13}\mathscr{A}_3),\\
Q &= -n_0 T(D_{21}\mathscr{A}_1 + D_{22}\mathscr{A}_2 + D_{23}\mathscr{A}_3),\\
\Gamma_\parallel &= -n_0 mu(D_{31}\mathscr{A}_1 + D_{32}\mathscr{A}_2 + D_{33}\mathscr{A}_3).
\end{aligned} \tag{3.97}$$

the components of the diffusion matrix $D = (D_{ij})$ are obtained [30],

$$\begin{aligned}
D_{ij} = \frac{\pi m^3}{n_0}\,\Re \sum_{\boldsymbol{m}} \int_0^\infty \mathrm{d}v_\perp\, v_\perp \int_{\mathbb{R}} \mathrm{d}u \int_{\mathbb{R}} \mathrm{d}u'\, \tilde{G}_{\omega \boldsymbol{m}}(u,u')\\
\times v^{r*}_{\boldsymbol{m}}(v_\perp,u) v^{r}_{\boldsymbol{m}}(v_\perp,u') a_i(v_\perp,u) a_j(v_\perp,u') f_0(v_\perp,u').
\end{aligned} \tag{3.98}$$

The moments of the Green's function can be expressed through the dimensionless I^{mn} functions defined above. The tedious explicit evaluation of the diffusion coefficients is deferred to Appendix C.1, while here only the results are summarised.

$$\begin{aligned}
D_{11} = \frac{1}{2\nu B_0^2}\,\Re \sum_{\boldsymbol{m}} \Big[& c^2 I^{00} |\tilde{E}_{\boldsymbol{m}\perp}|^2 + c v_T \left(\tilde{B}^{r*}_{\boldsymbol{m}} \tilde{E}_{\boldsymbol{m}\perp} + \tilde{E}^*_{\boldsymbol{m}\perp} \tilde{B}^{r}_{\boldsymbol{m}}\right) I^{10}\\
& + v_T^2 |\tilde{B}^r_{\boldsymbol{m}}|^2 I^{11}\Big],
\end{aligned} \tag{3.99}$$

$$\begin{aligned}
D_{12} = D_{11} + \frac{1}{4\nu B_0^2}\,\Re \sum_{\boldsymbol{m}} \Big[& v_T^2 |\tilde{B}^r_{\boldsymbol{m}}|^2 I^{31} + c v_T (\tilde{E}_{\boldsymbol{m}\perp} \tilde{B}^{r*}_{\boldsymbol{m}} I^{21} + \tilde{E}^*_{\boldsymbol{m}\perp} \tilde{B}^r_{\boldsymbol{m}} I^{30})\\
& + c^2 |\tilde{E}_{\boldsymbol{m}\perp}|^2 I^{20}\Big],
\end{aligned} \tag{3.100}$$

$$D_{13} = \frac{1}{2\nu B_0^2}\,\Re \sum_{\boldsymbol{m}} \Big(v_T^2 |B^r_{\boldsymbol{m}}|^2 I^{21} + c v_T (\tilde{E}_{\boldsymbol{m}\perp} \tilde{B}^{r*}_{\boldsymbol{m}} I^{11} + \tilde{E}^*_{\boldsymbol{m}\perp} \tilde{B}^r_{\boldsymbol{m}} I^{20})$$

[3] It would seem more natural to define the diffusion matrix with its second line containing the coefficients of momentum- instead of heat flux density. The choice with interchanged order of moments is justified by the attempt not to modify the original definitions of the reduced transport model with 2×2 transport matrix.

$$+ c^2|\tilde{E}_{\boldsymbol{m}\perp}|^2 I^{10}\Big)\,, \tag{3.101}$$

$$D_{21} = D_{11} + \frac{1}{4\nu B_0^2}\,\Re\sum_{\boldsymbol{m}}\Big(v_T^2|\tilde{B}^r_{\boldsymbol{m}}|^2 I^{31} + cv_T(\tilde{E}_{\boldsymbol{m}\perp}\tilde{B}^{r*}_{\boldsymbol{m}} I^{30} + \tilde{E}^*_{\boldsymbol{m}\perp}\tilde{B}^r_{\boldsymbol{m}} I^{21})$$
$$+ c^2|\tilde{E}_{\boldsymbol{m}\perp}|^2 I^{20}\Big) = D_{12}, \tag{3.102}$$

$$D_{22} = 2D_{11} + \frac{1}{4\nu B_0^2}\,\Re\sum_{\boldsymbol{m}}\Bigg(2v_T^2|\tilde{B}^r_{\boldsymbol{m}}|^2 I^{31} + cv_T\tilde{E}_{\boldsymbol{m}\perp}\tilde{B}^{r*}_{\boldsymbol{m}}(I^{30} + I^{21})$$
$$+ cv_T\tilde{E}^*_{\boldsymbol{m}\perp}\tilde{B}^r_{\boldsymbol{m}}(I^{21} + I^{30}) + 2c^2|\tilde{E}_{\boldsymbol{m}\perp}|^2 I^{20} + \frac{v_T^2|\tilde{B}^r_{\boldsymbol{m}}|^2}{2} I^{33}$$
$$+ \frac{cv_T}{2} I^{32}(\tilde{E}_{\boldsymbol{m}\perp}\tilde{B}^{r*}_{\boldsymbol{m}} + \tilde{E}^*_{\boldsymbol{m}\perp}\tilde{B}^r_{\boldsymbol{m}}) + \frac{c^2|\tilde{E}_{\boldsymbol{m}\perp}|^2}{2} I^{22}\Bigg)\,, \tag{3.103}$$

$$D_{23} = \frac{1}{2\nu B_0^2}\left[v_T^2|\tilde{B}^r_{\boldsymbol{m}}|^2\left(I^{21} + \frac{I^{32}}{2}\right) + cv_T\tilde{E}_{\boldsymbol{m}\perp}\tilde{B}^{r*}_{\boldsymbol{m}}\left(I^{11} + \frac{I^{31}}{2}\right)\right.$$
$$\left. + cv_T\tilde{E}^*_{\boldsymbol{m}\perp}\tilde{B}^r_{\boldsymbol{m}}\left(I^{20} + \frac{I^{22}}{2}\right) + c^2|\tilde{E}_{\boldsymbol{m}\perp}|^2\left(I^{10} + \frac{I^{21}}{2}\right)\right], \tag{3.104}$$

$$D_{31} = \frac{1}{2\nu B_0^2}\,\Re\sum_{\boldsymbol{m}}\Big[v_T^2|\tilde{B}^r_{\boldsymbol{m}}|^2 I^{21} + cv_T(\tilde{E}_{\boldsymbol{m}\perp}\tilde{B}^{r*}_{\boldsymbol{m}} I^{20} + \tilde{E}_{\boldsymbol{m}\perp}\tilde{B}^r_{\boldsymbol{m}} I^{11})$$
$$+ c^2|\tilde{E}_{\boldsymbol{m}\perp}|^2 I^{10}\Big] = D_{13}, \tag{3.105}$$

$$D_{32} = \frac{1}{2\nu B_0^2}\,\Re\sum_{\boldsymbol{m}}\left[v_T^2|\tilde{B}^r_{\boldsymbol{m}}|^2\left(I^{21} + \frac{I^{23}}{2}\right) + cv_T\tilde{E}_{\boldsymbol{m}\perp}\tilde{B}^{r*}_{\boldsymbol{m}}\left(I^{20} + \frac{I^{22}}{2}\right)\right.$$
$$\left. + cv_T\tilde{E}^*_{\boldsymbol{m}\perp}\tilde{B}^r_{\boldsymbol{m}}\left(I^{11} + \frac{I^{13}}{2}\right) + c^2|\tilde{E}_{\boldsymbol{m}\perp}|^2\left(I^{10} + \frac{I^{12}}{2}\right)\right] = D_{23}, \tag{3.106}$$

$$D_{33} = \frac{1}{2\nu B_0^2}\,\Re\sum_{\boldsymbol{m}}\Big[v_T^2|\tilde{B}^r_{\boldsymbol{m}}|^2 I^{22} + cv_T\left(\tilde{E}_{\boldsymbol{m}\perp}\tilde{B}^{r*}_{\boldsymbol{m}} I^{21} + \tilde{E}^*_{\boldsymbol{m}\perp}\tilde{B}^r_{\boldsymbol{m}} I^{12}\right)$$
$$+ c^2|\tilde{E}_{\boldsymbol{m}\perp}|^2 I^{11}\Big]\,. \tag{3.107}$$

These diffusion coefficients are an extension to the coefficients presented in [30] as also parallel momentum is included in the transport model.

Figures 3.8 and 3.9 show numerically evaluated ion diffusion coefficients obtained from the linear model with and without momentum conservation enforced in the collision operator for two different RMP frequencies close to the electric resonance that is described in detail below. As one can see, tiny structures well below the ion Larmor radius develop as one advances to the electric resonance. Strictly speaking the model leaves its range of validity as one closely approaches this resonance.

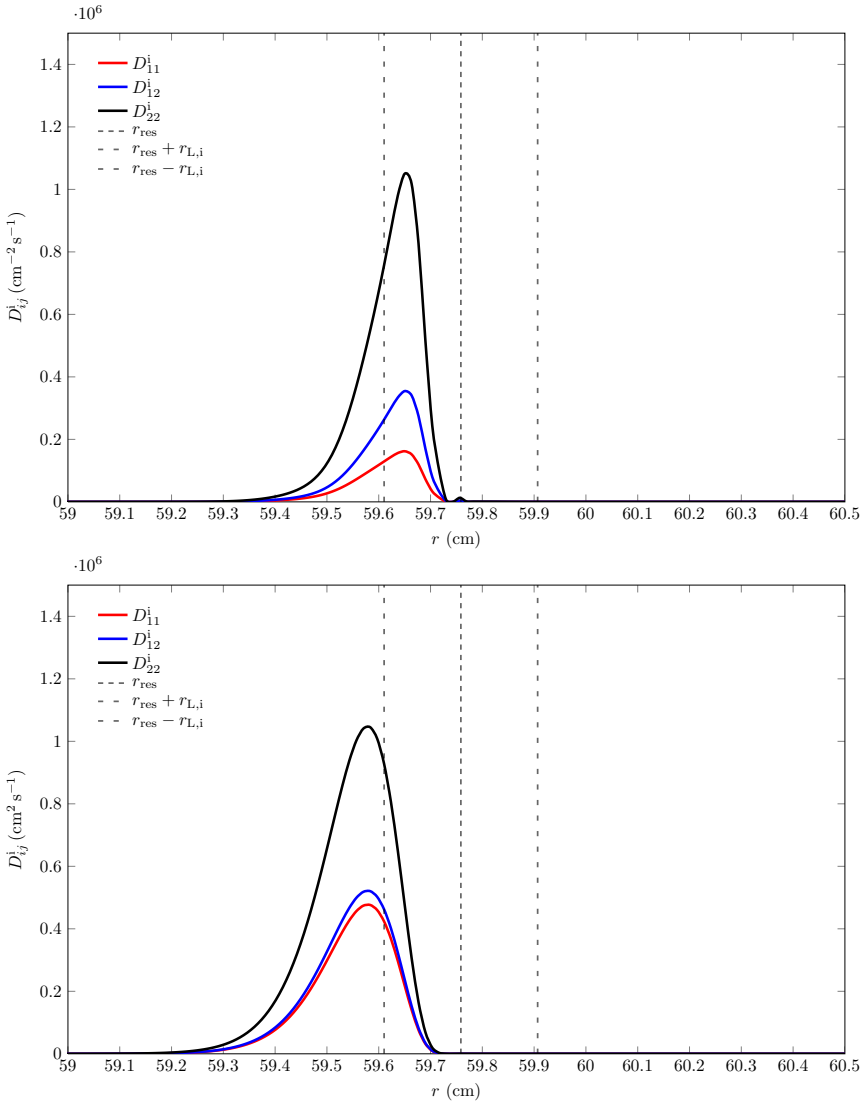

Figure 3.8: Ion Diffusion coefficients for $f = 3.65\,\mathrm{kHz}$ with (below) and without (above) momentum conservation.

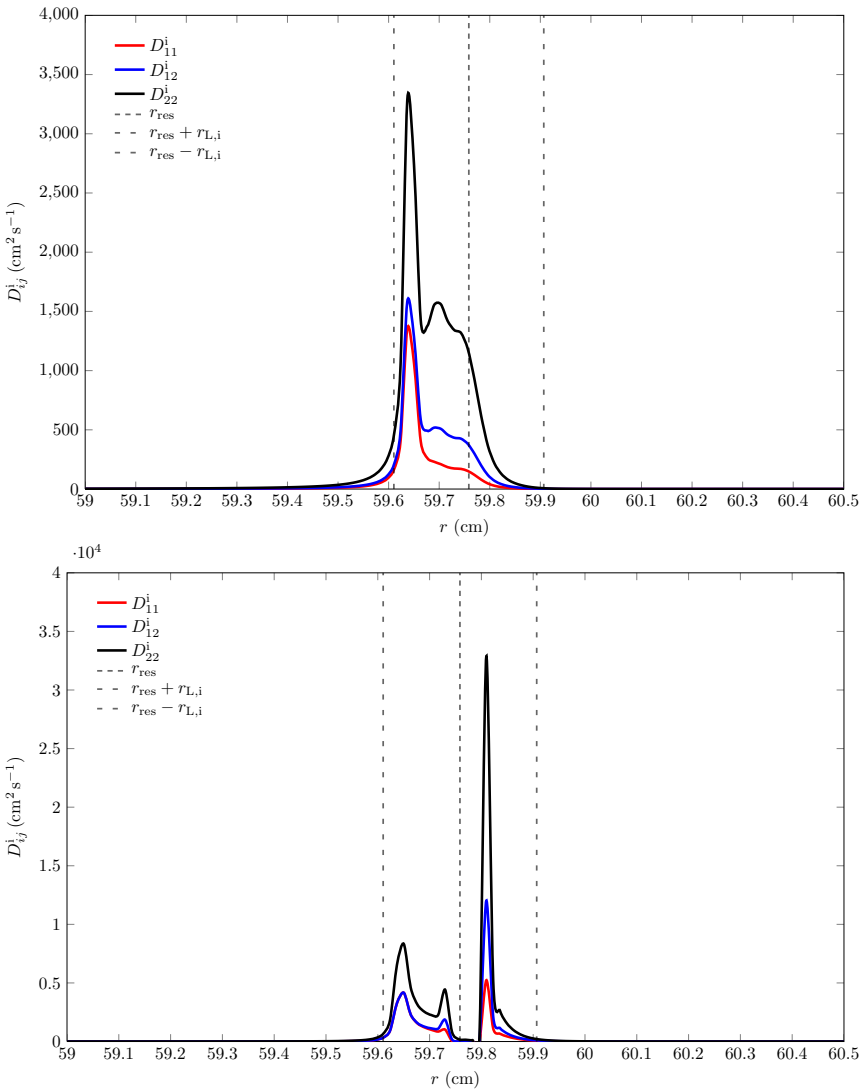

Figure 3.9: Ion diffusion coefficients for $f = 3.6\,\mathrm{kHz}$ with (below) and without (above) momentum conservation. One should notice that the scale on the vertical axis differs by an order of magnitude.

Diffusion Matrix in the collisionless limit

In the collisionless limit the kinetic equation is algebraic and solved by

$$\tilde{f}_{\boldsymbol{m}} = \frac{\mathrm{i}v^r_{\boldsymbol{m}}}{k_\parallel u + \omega_E - \omega - \mathrm{i}0^+}\left[\mathscr{A}_1 + \frac{m}{2T}\left(v_\perp^2 + u^2\right)\mathscr{A}_2 + \frac{u}{v_T}\mathscr{A}_3\right] f_0. \tag{3.108}$$

Following the same argumentation as before, the diffusion coefficients are obtained as [30]

$$D_{ij} = \frac{\pi}{2n_0}\sum_{\boldsymbol{m}}\int_{\mathbb{R}^3} \mathrm{d}^3p\ \delta(k_\parallel u + \omega_E)\left|v^r_{\boldsymbol{m}}\right|^2 a_i a_j f_0. \tag{3.109}$$

In contrast to the collisional case where one has to distinguish between primed and unprimed shifted parallel velocities u and u' in the coefficients $a_i(v_\perp, u)$, in the collisionless limit, where $G^{\mathrm{D,nc}}_{\omega\boldsymbol{m}} \propto \delta(u-u')$ the diffusion coefficients D_{ij} are immediately seen to be symmetric upon $i \leftrightarrow j$. The explicit evaluation of the diffusion coefficients is deferred to the Appendix C.2. The six independent components are given by

$$D_{11} = \frac{\sqrt{\pi}|Z|}{2|\omega_E|}\mathrm{e}^{-Z^2}\sum_{\boldsymbol{m}}|v^r_{\boldsymbol{m}}|^2_{u=-\omega_E/k_\parallel}, \tag{3.110}$$

$$D_{12} = \frac{\sqrt{\pi}|Z|}{2|\omega_E|}\mathrm{e}^{-Z^2}\sum_{\boldsymbol{m}}|v^r_{\boldsymbol{m}}|^2_{u=-\omega_E/k_\parallel}\left(1 + \frac{1}{2}\frac{\omega_E^2}{k_\parallel^2 v_T^2}\right), \tag{3.111}$$

$$D_{13} = \frac{\sqrt{\pi}|Z|}{2|\omega_E|}\mathrm{e}^{-Z^2}\sum_{\boldsymbol{m}}|v^r_{\boldsymbol{m}}|^2_{u=-\omega_E/k_\parallel}(-)\frac{\omega_E}{k_\parallel v_T}, \tag{3.112}$$

$$D_{22} = \frac{\sqrt{\pi}|Z|}{2|\omega_E|}\mathrm{e}^{-Z^2}\sum_{\boldsymbol{m}}|v^r_{\boldsymbol{m}}|^2_{u=-\omega_E/k_\parallel}\left(2 + \frac{\omega_E^2}{k_\parallel^2 v_T^2} + \frac{1}{4}\frac{\omega_E^4}{k_\parallel^4 v_T^4}\right), \tag{3.113}$$

$$D_{23} = \frac{\sqrt{\pi}|Z|}{2|\omega_E|}\mathrm{e}^{-Z^2}\sum_{\boldsymbol{m}}|v^r_{\boldsymbol{m}}|^2_{u=-\omega_E/k_\parallel}(-)\left(\frac{\omega_E}{k_\parallel v_T} + \frac{1}{2}\frac{\omega_E^3}{k_\parallel v_T^3}\right), \tag{3.114}$$

$$D_{33} = \frac{\sqrt{\pi}|Z|}{2|\omega_E|}\mathrm{e}^{-Z^2}\sum_{\boldsymbol{m}}|v^r_{\boldsymbol{m}}|^2_{u=-\omega_E/k_\parallel}\frac{\omega_E^2}{k_\parallel^2 v_T^2}, \tag{3.115}$$

with $Z = -\omega_E/\sqrt{2}k_\parallel v_T$.

Thus, the diffusion matrix reads

$$(D_{ij}) = \frac{\sqrt{\pi}|Z|}{2|\omega_E|}\mathrm{e}^{-Z^2}\sum_{\boldsymbol{m}}|v^r_{\boldsymbol{m}}|^2_{u=-\omega_E/k_\parallel} \cdot \begin{pmatrix} 1 & \frac{1}{2}\left(2+\frac{1}{v_T^2}\frac{\omega_E^2}{k_\parallel^2}\right) & -\frac{\omega_E}{k_\parallel v_T} \\ \frac{1}{2}\left(2+\frac{1}{v_T^2}\frac{\omega_E^2}{k_\parallel^2}\right) & \frac{2}{v_T^5}\left(v_T^5+\frac{\omega_E^2 v_T^3}{2k_\parallel^2}+\frac{v_T\omega_E^4}{8k_\parallel^4}\right) & \frac{1}{2v_T^3}(2uv_T^2+u^3) \\ -\frac{\omega_E}{k_\parallel v_T} & \frac{1}{2v_T^3}(2uv_T^2+u^3) & \frac{1}{v_T^2}\frac{\omega_E^2}{k_\parallel^2} \end{pmatrix} \cdot \tag{3.116}$$

3.5.2 Onsager Symmetry

In order for Onsager symmetry being satisfied the antisymmetric part of the diffusion tensor $\boldsymbol{D}^{\mathrm{as}} = \boldsymbol{D} - \boldsymbol{D}^{\mathrm{s}}$,

$$(D_{ij}^{\mathrm{as}}) = \frac{1}{2}\begin{pmatrix} 0 & D_{12}-D_{21} & D_{13}-D_{31} \\ D_{21}-D_{12} & 0 & D_{23}-D_{32} \\ D_{31}-D_{13} & D_{32}-D_{23} & 0 \end{pmatrix} \tag{3.117}$$

has to vanish. Substitution of the diffusion coefficients requires the following linear combinations of moments of the Green's function to vanish:

$$\Im(I^{12}-I^{30}) = 0 \qquad (D_{12}^{\mathrm{as}} = D_{21}^{\mathrm{as}} = 0), \tag{3.118}$$
$$\Im(I^{11}-I^{20}) = 0 \qquad (D_{13}^{\mathrm{as}} = D_{31}^{\mathrm{as}} = 0), \tag{3.119}$$
$$\Im(I^{31}-I^{22}) = 0 \qquad (D_{23}^{\mathrm{as}} = D_{32}^{\mathrm{as}} = 0). \tag{3.120}$$

In the following for all three models under consideration, i.e. *(i) energy conservation, (ii) momentum conservation* and *(iii) energy and momentum conservation* an analytic proof will be given that the particular diffusion matrix is Onsager symmetric.

Onsager symmetry for the energy conserving collision operator

According to Eq. (3.62) $I^{12} - I^{30}$ for the energy conserving collision operator is given by

$$I^{12}-I^{30} = I_{\mathrm{D}}^{12} - I_{\mathrm{D}}^{30} + \frac{1}{\Delta_1}[(I_{\mathrm{D}}^{12}-I_{\mathrm{D}}^{10})(I_{\mathrm{D}}^{22}-I_{\mathrm{D}}^{20})$$

$$- (I_{\mathrm{D}}^{32} - I_{\mathrm{D}}^{30})(I_{\mathrm{D}}^{20} - I_{\mathrm{D}}^{00})], \tag{3.121}$$

where $\Delta_1 = 1 + I_{\mathrm{D}}^{20} - I_{\mathrm{D}}^{00} + I_{\mathrm{D}}^{20} - I_{\mathrm{D}}^{22}$. Substitution of the following combinations of moments

$$I_{\mathrm{D}}^{12} - I_{\mathrm{D}}^{10} = \frac{\mathrm{i}x_2}{\mathrm{i}x_1}(I_{\mathrm{D}}^{20} - I_{\mathrm{D}}^{00}), \tag{3.122}$$

$$\begin{aligned} I_{\mathrm{D}}^{12} &= \frac{\mathrm{i}x_2}{\mathrm{i}x_1} I_{\mathrm{D}}^{20} + \frac{1}{\mathrm{i}x_1} \\ I_{\mathrm{D}}^{30} &= \frac{\mathrm{i}x_2}{\mathrm{i}x_1} I_{\mathrm{D}}^{20} - \frac{2}{\mathrm{i}x_1} I_{\mathrm{D}}^{20} + \frac{2}{\mathrm{i}x_1} I_{\mathrm{D}}^{00} + \frac{1}{\mathrm{i}x_1} \\ &\Rightarrow I_{\mathrm{D}}^{12} - I_{\mathrm{D}}^{30} = \frac{2}{\mathrm{i}x_1}(I_{\mathrm{D}}^{20} - I_{\mathrm{D}}^{00}) \end{aligned} \tag{3.123}$$

$$I_{\mathrm{D}}^{32} - I_{\mathrm{D}}^{30} = \frac{1}{\mathrm{i}x_1}[(\mathrm{i}x_2 - 2)(I_{\mathrm{D}}^{22} - I_{\mathrm{D}}^{20}) + 2 + 2(I_{\mathrm{D}}^{20} - I_{\mathrm{D}}^{00})] \tag{3.124}$$

yields

$$\begin{aligned} \Delta_1(I^{12} - I^{30}) = \frac{I_{\mathrm{D}}^{20} - I_{\mathrm{D}}^{00}}{\mathrm{i}x_1}[&2(1 + I_{\mathrm{D}}^{20} - I_{\mathrm{D}}^{00} + I_{\mathrm{D}}^{20} - I_{\mathrm{D}}^{22}) \\ &- \mathrm{i}x_2(I_{\mathrm{D}}^{20} - I_{\mathrm{D}}^{22}) + (\mathrm{i}x_2 - 2)(I_{\mathrm{D}}^{20} - I_{\mathrm{D}}^{22}) \\ &- 2 - 2(I_{\mathrm{D}}^{20} - I_{\mathrm{D}}^{00})] = 0 \end{aligned} \tag{3.125}$$

and Onsager symmetry is proven.

Onsager symmetry for the momentum conserving collision operator

In the following it will be shown that $I^{11} - I^{20} = 0$ for the momentum conserving collision operator. According to Eq. (3.61)

$$I^{11} - I^{20} = I_{\mathrm{D}}^{11} - I_{\mathrm{D}}^{20} + \frac{1}{1 - I_{\mathrm{D}}^{11}}(I_{\mathrm{D}}^{11} I_{\mathrm{D}}^{11} - I_{\mathrm{D}}^{12} I_{\mathrm{D}}^{10}).$$

After rearranging terms $(I_{\mathrm{D}}^{11})^2$ cancels and we are left with

$$(1 - I_{\mathrm{D}}^{11})(I^{11} - I^{20}) = I_{\mathrm{D}}^{11} - I_{\mathrm{D}}^{20} + I_{\mathrm{D}}^{20} I_{\mathrm{D}}^{11} - I_{\mathrm{D}}^{12} I_{\mathrm{D}}^{10}.$$

Substitution of the following identities from the recursion,

$$I_{\mathrm{D}}^{20} = \frac{\mathrm{i}x_2}{\mathrm{i}x_1} I_{\mathrm{D}}^{10} - \frac{1}{\mathrm{i}x_1} I_{\mathrm{D}}^{10}, \qquad I_{\mathrm{D}}^{11} = \frac{\mathrm{i}x_2}{\mathrm{i}x_1} I_{\mathrm{D}}^{10}, \tag{3.126}$$

$$I_{\mathrm{D}}^{12} = \frac{1}{\mathrm{i}x_1}[(\mathrm{i}x_2 - 1)I_{\mathrm{D}}^{11} + 1] = \left(\frac{\mathrm{i}x_2}{\mathrm{i}x_1}\right)^2 I_{\mathrm{D}}^{10} - \frac{1}{\mathrm{i}x_1}\frac{\mathrm{i}x_2}{\mathrm{i}x_1}I_{\mathrm{D}}^{10} + \frac{1}{\mathrm{i}x_1}, \tag{3.127}$$

this gives further

$$\begin{aligned}(1 - I_{\mathrm{D}}^{11})(I^{11} - I^{20}) = {} & \frac{\mathrm{i}x_2}{\mathrm{i}x_1}I_{\mathrm{D}}^{10} - \frac{\mathrm{i}x_2}{\mathrm{i}x_1}I_{\mathrm{D}}^{10} + \frac{1}{\mathrm{i}x_1}I_{\mathrm{D}}^{10} \\ & + \left(\frac{\mathrm{i}x_2}{\mathrm{i}x_1}I_{\mathrm{D}}^{10} + \frac{1}{\mathrm{i}x_1}I_{\mathrm{D}}^{10}\right)\frac{\mathrm{i}x_2}{\mathrm{i}x_1}I_{\mathrm{D}}^{10} \\ & - \left[\left(\frac{\mathrm{i}x_2}{\mathrm{i}x_1}\right)^2 I_{\mathrm{D}}^{10} - \frac{1}{\mathrm{i}x_1}\frac{\mathrm{i}x_2}{\mathrm{i}x_1}I_{\mathrm{D}}^{10} + \frac{1}{\mathrm{i}x_1}\right] I_{\mathrm{D}}^{10} = 0,\end{aligned} \tag{3.128}$$

and Onsager symmetry is proven again.

Onsager symmetry for the energy and momentum conserving collision operator

By application of (3.55), Eq. (3.118) is expressed as follows:

$$\begin{aligned}I^{12} - I^{30} = {} & I_{\mathrm{D}}^{12} - I_{\mathrm{D}}^{30} \\ & + \frac{1}{\Delta}(I_{\mathrm{D}}^{12} - I_{\mathrm{D}}^{10})[I_{\mathrm{D}}^{11}(I_{\mathrm{D}}^{22} - I_{\mathrm{D}}^{20}) - I_{\mathrm{D}}^{31}(I_{\mathrm{D}}^{20} - I_{\mathrm{D}}^{00})] \\ & + \frac{1}{\Delta}\Delta_1(I_{\mathrm{D}}^{11}I_{\mathrm{D}}^{12} - I_{\mathrm{D}}^{31}I_{\mathrm{D}}^{10}) \\ & + \frac{1}{\Delta}(1 - I_{\mathrm{D}}^{11})[(I_{\mathrm{D}}^{12} - I_{\mathrm{D}}^{10})(I_{\mathrm{D}}^{22} - I_{\mathrm{D}}^{20}) \\ & - (I_{\mathrm{D}}^{32} - I_{\mathrm{D}}^{30})(I_{\mathrm{D}}^{20} - I_{\mathrm{D}}^{00})] \\ & + \frac{1}{\Delta}(I_{\mathrm{D}}^{12} - I_{\mathrm{D}}^{10})[(I_{\mathrm{D}}^{12} - I_{\mathrm{D}}^{10})I_{\mathrm{D}}^{12} - (I_{\mathrm{D}}^{32} - I_{\mathrm{D}}^{30})I_{\mathrm{D}}^{10}],\end{aligned} \tag{3.129}$$

where $\Delta = \Delta_1(1 - I_{\mathrm{D}}^{11}) - \Delta_2^2$, $\Delta_1 = 1 + I_{\mathrm{D}}^{20} - I_{\mathrm{D}}^{00} + I_{\mathrm{D}}^{20} - I_{\mathrm{D}}^{22}$ and $\Delta_2 = I_{\mathrm{D}}^{12} - I_{\mathrm{D}}^{10}$. It was already shown for the energy conserving collision operator that

$$\begin{aligned}\Delta_1(I^{12} - I^{30}) = {} & \Delta_1(I_{\mathrm{D}}^{12} - I_{\mathrm{D}}^{30}) + (I_{\mathrm{D}}^{12} - I_{\mathrm{D}}^{10})(I_{\mathrm{D}}^{22} - I_{\mathrm{D}}^{20}) \\ & - (I_{\mathrm{D}}^{32} - I_{\mathrm{D}}^{30})(I_{\mathrm{D}}^{20} - I_{\mathrm{D}}^{00}) = 0,\end{aligned} \tag{3.130}$$

which serves as a major simplification for the general case, if we compare this result with the fourth line of (3.129). After substitution of the following combinations of moments

$$I_{\mathrm{D}}^{12} - I_{\mathrm{D}}^{10} = \frac{\mathrm{i}x_2}{\mathrm{i}x_1}(I_{\mathrm{D}}^{20} - I_{\mathrm{D}}^{00}), \tag{3.131}$$

$$I_{\mathrm{D}}^{12} = \frac{\mathrm{i}x_2}{\mathrm{i}x_1}I_{\mathrm{D}}^{20} + \frac{1}{\mathrm{i}x_1}, \quad I_{\mathrm{D}}^{30} = \frac{\mathrm{i}x_2}{\mathrm{i}x_1}I_{\mathrm{D}}^{20} - \frac{2}{\mathrm{i}x_1}I_{\mathrm{D}}^{20} + \frac{2}{\mathrm{i}x_1}I_{\mathrm{D}}^{00} + \frac{1}{\mathrm{i}x_1} \tag{3.132}$$

$$\Rightarrow I_{\mathrm{D}}^{12} - I_{\mathrm{D}}^{30} = \frac{2}{\mathrm{i}x_1}(I_{\mathrm{D}}^{20} - I_{\mathrm{D}}^{00}) \tag{3.133}$$

$$I_{\mathrm{D}}^{32} - I_{\mathrm{D}}^{30} = \frac{1}{\mathrm{i}x_1}[(\mathrm{i}x_2 - 2)(I_{\mathrm{D}}^{22} - I_{\mathrm{D}}^{20}) + 2 + 2(I_{\mathrm{D}}^{20} - I_{\mathrm{D}}^{00})] \tag{3.134}$$

$$I_{\mathrm{D}}^{11} = \frac{\mathrm{i}x_2}{\mathrm{i}x_1} I_{\mathrm{D}}^{10}, \quad I_{\mathrm{D}}^{31} = \frac{\mathrm{i}x_2}{\mathrm{i}x_1} I_{\mathrm{D}}^{30} \tag{3.135}$$

$$\Rightarrow I_{\mathrm{D}}^{12} I_{\mathrm{D}}^{11} - I_{\mathrm{D}}^{31} I_{\mathrm{D}}^{10} = \frac{2}{\mathrm{i}x_1}\frac{\mathrm{i}x_2}{\mathrm{i}x_1}(I_{\mathrm{D}}^{20} - I_{\mathrm{D}}^{00}) I_{\mathrm{D}}^{10} \tag{3.136}$$

$$I_{\mathrm{D}}^{12} = \frac{\mathrm{i}x_2}{\mathrm{i}x_1} I_{\mathrm{D}}^{20} + \frac{1}{\mathrm{i}x_1}, \qquad I_{\mathrm{D}}^{10} = \frac{\mathrm{i}x_2}{\mathrm{i}x_1} I_{\mathrm{D}}^{00} + \frac{1}{\mathrm{i}x_1} \tag{3.137}$$

the remaining terms of (3.129) are

$$\begin{aligned}
\Delta(I^{12} - I^{30}) = \frac{1}{\mathrm{i}x_1}(I_{\mathrm{D}}^{20} - I_{\mathrm{D}}^{00}) \Big\{ & -2\Delta_2^2 + \frac{(\mathrm{i}x_2)^2}{\mathrm{i}x_1} I_{\mathrm{D}}^{10}(I_{\mathrm{D}}^{22} - I_{\mathrm{D}}^{20}) \\
& - \frac{(\mathrm{i}x_2)^2}{\mathrm{i}x_1}\left(\frac{\mathrm{i}x_2}{\mathrm{i}x_1} I_{\mathrm{D}}^{20} + \frac{1}{\mathrm{i}x_1}\right)(I_{\mathrm{D}}^{20} - I_{\mathrm{D}}^{00}) \\
& + 2\frac{\mathrm{i}x_2}{\mathrm{i}x_1}(I_{\mathrm{D}}^{20} - I_{\mathrm{D}}^{00})\left(\frac{\mathrm{i}x_2}{\mathrm{i}x_1} I_{\mathrm{D}}^{20} + \frac{1}{\mathrm{i}x_1}\right) - 2\frac{\mathrm{i}x_2}{\mathrm{i}x_1} I_{\mathrm{D}}^{10}(I_{\mathrm{D}}^{20} - I_{\mathrm{D}}^{00}) \\
& + 2\left(\frac{\mathrm{i}x_2}{\mathrm{i}x_1}\right) I_{\mathrm{D}}^{10} + 2\left(\frac{\mathrm{i}x_2}{\mathrm{i}x_1}\right) I_{\mathrm{D}}^{10}(I_{\mathrm{D}}^{20} - I_{\mathrm{D}}^{00}) \\
& \quad + 2\left(\frac{\mathrm{i}x_2}{\mathrm{i}x_1}\right) I_{\mathrm{D}}^{10}(I_{\mathrm{D}}^{20} - I_{\mathrm{D}}^{22}) + \mathrm{i}x_2\left(\frac{\mathrm{i}x_2}{\mathrm{i}x_1} I_{\mathrm{D}}^{20} + \frac{1}{\mathrm{i}x_1}\right)(I_{\mathrm{D}}^{20} - I_{\mathrm{D}}^{00}) \\
& - \frac{(\mathrm{i}x_2)^2}{\mathrm{i}x_1} I_{\mathrm{D}}^{10}(I_{\mathrm{D}}^{22} - I_{\mathrm{D}}^{20}) + 2\frac{\mathrm{i}x_2}{\mathrm{i}x_1} I_{\mathrm{D}}^{10}(I_{\mathrm{D}}^{22} - I_{\mathrm{D}}^{20}) \\
& - 2I_{\mathrm{D}}^{10}\frac{\mathrm{i}x_2}{\mathrm{i}x_1} - 2\frac{\mathrm{i}x_2}{\mathrm{i}x_1}\left(\frac{\mathrm{i}x_2}{\mathrm{i}x_1} I_{\mathrm{D}}^{00} + \frac{1}{\mathrm{i}x_1}\right)(I_{\mathrm{D}}^{20} - I_{\mathrm{D}}^{00})\Big\} \\
= & -\frac{2}{\mathrm{i}x_1}\left(\frac{\mathrm{i}x_2}{\mathrm{i}x_1}\right)^2 (I_{\mathrm{D}}^{20} - I_{\mathrm{D}}^{00})^3 + \frac{2}{\mathrm{i}x_1}\left(\frac{\mathrm{i}x_2}{\mathrm{i}x_1}\right)^2 (I_{\mathrm{D}}^{20} - I_{\mathrm{D}}^{00})^3 = 0
\end{aligned} \tag{3.138}$$

and thus Onsager symmetry is proven,

$$\boxed{I^{30} - I^{21} = 0 \Leftrightarrow D_{12}^{\mathrm{as}} = D_{21}^{\mathrm{as}} = 0.} \tag{3.139}$$

Secondly, it is required that $D_{13}^{\mathrm{as}} = D_{31}^{\mathrm{as}} = 0$, which corresponds to

$$\begin{aligned}
I^{11} - I^{20} = & I_{\mathrm{D}}^{11} - I_{\mathrm{D}}^{20} \\
& + \frac{1}{\Delta}(I_{\mathrm{D}}^{12} - I_{\mathrm{D}}^{10})[I_{\mathrm{D}}^{11}(I_{\mathrm{D}}^{12} - I_{\mathrm{D}}^{10}) - I_{\mathrm{D}}^{12}(I_{\mathrm{D}}^{20} - I_{\mathrm{D}}^{00})]
\end{aligned}$$

$$
\begin{aligned}
&+\frac{1}{\Delta}\Delta_1((I_{\mathrm{D}}^{11})^2 - I_{\mathrm{D}}^{12}I_{\mathrm{D}}^{10}) \\
&+\frac{1}{\Delta}(1-I_{\mathrm{D}}^{11})[(I_{\mathrm{D}}^{12}-I_{\mathrm{D}}^{10})^2 - (I_{\mathrm{D}}^{22}-I_{\mathrm{D}}^{20})(I_{\mathrm{D}}^{20}-I_{\mathrm{D}}^{00})] \\
&+\frac{1}{\Delta}(I_{\mathrm{D}}^{12}-I_{\mathrm{D}}^{10})[I_{\mathrm{D}}^{11}(I_{\mathrm{D}}^{12}-I_{\mathrm{D}}^{10}) - I_{\mathrm{D}}^{10}(I_{\mathrm{D}}^{22}-I_{\mathrm{D}}^{20})]. \qquad (3.140)
\end{aligned}
$$

This time let us refer to the result for the momentum conserving collision operator, i.e.

$$
\begin{aligned}
(1-I_{\mathrm{D}}^{11})(I_{\mathrm{p}}^{11}-I_{\mathrm{p}}^{20}) = (1-I_{\mathrm{D}}^{11})(I_{\mathrm{D}}^{11}-I_{\mathrm{D}}^{20}) \\
+ (I_{\mathrm{D}}^{11})^2 - I_{\mathrm{D}}^{12}I_{\mathrm{D}}^{10} = 0. \qquad (3.141)
\end{aligned}
$$

As a consequence, after multiplication with $\Delta = \Delta_1(1-I_{\mathrm{D}}^{11}) - \Delta_2^2$, the third term together with $\Delta_1(1-I_{\mathrm{D}}^{11})(I_{\mathrm{D}}^{11}-I_{\mathrm{D}}^{20})$ of the first term of the r.h.s. of (3.140) cancels and we are left with

$$
\begin{aligned}
\Delta(I^{11}-I^{20}) &= (I_{\mathrm{D}}^{12}-I_{\mathrm{D}}^{10})^2(1+I_{\mathrm{D}}^{20}) \\
&+ (I_{\mathrm{D}}^{12}-I_{\mathrm{D}}^{10})[-I_{\mathrm{D}}^{12}(I_{\mathrm{D}}^{20}-I_{\mathrm{D}}^{00}) - I_{\mathrm{D}}^{10}(I_{\mathrm{D}}^{22}-I_{\mathrm{D}}^{20})] \\
&- (I_{\mathrm{D}}^{22}-I_{\mathrm{D}}^{20})(I_{\mathrm{D}}^{20}-I_{\mathrm{D}}^{00})(1-I_{\mathrm{D}}^{11}). \qquad (3.142)
\end{aligned}
$$

After substitution of the following linear combinations of moments from the recursion,

$$
I_{\mathrm{D}}^{20} = \frac{\mathrm{i}x_2}{\mathrm{i}x_1}I_{\mathrm{D}}^{10} - \frac{1}{\mathrm{i}x_1}I_{\mathrm{D}}^{10}, \qquad I_{\mathrm{D}}^{11} = \frac{\mathrm{i}x_2}{\mathrm{i}x_1}I_{\mathrm{D}}^{10} \qquad (3.143)
$$

$$
\Rightarrow (I_{\mathrm{D}}^{11}-I_{\mathrm{D}}^{20}) = \frac{1}{\mathrm{i}x_1}I_{\mathrm{D}}^{10} \qquad (3.144)
$$

$$
I_{\mathrm{D}}^{22}-I_{\mathrm{D}}^{20} = \frac{\mathrm{i}x_2}{\mathrm{i}x_1}(I_{\mathrm{D}}^{12}-I_{\mathrm{D}}^{10}) - \frac{1}{\mathrm{i}x_1}(I_{\mathrm{D}}^{12}-I_{\mathrm{D}}^{10}), \qquad (3.145)
$$

$$
I_{\mathrm{D}}^{12}-I_{\mathrm{D}}^{10} = \frac{\mathrm{i}x_2}{\mathrm{i}x_1}(I_{\mathrm{D}}^{20}-I_{\mathrm{D}}^{00}), \qquad (3.146)
$$

$$
I_{\mathrm{D}}^{12} = \left(\frac{\mathrm{i}x_2}{\mathrm{i}x_1}\right)^2 I_{\mathrm{D}}^{10} - \frac{1}{\mathrm{i}x_1}\frac{\mathrm{i}x_2}{\mathrm{i}x_1}I_{\mathrm{D}}^{10} + \frac{1}{\mathrm{i}x_1}, \qquad (3.147)
$$

one gets

$$
\begin{aligned}
\Delta(I^{11}-I^{20}) = \frac{\mathrm{i}x_2}{\mathrm{i}x_1}(I_{\mathrm{D}}^{20}-I_{\mathrm{D}}^{00})^2 \Bigg\{ &\frac{\mathrm{i}x_2}{\mathrm{i}x_1} + \left(\frac{\mathrm{i}x_2}{\mathrm{i}x_1}\right)^2 I_{\mathrm{D}}^{10} - \frac{1}{\mathrm{i}x_1}\frac{\mathrm{i}x_2}{\mathrm{i}x_1}I_{\mathrm{D}}^{10} \\
&- \left(\frac{\mathrm{i}x_2}{\mathrm{i}x_1}\right)^2 I_{\mathrm{D}}^{10} + \frac{1}{\mathrm{i}x_1}\frac{\mathrm{i}x_2}{\mathrm{i}x_1}I_{\mathrm{D}}^{10} - \frac{1}{\mathrm{i}x_1} - \left(\frac{\mathrm{i}x_2}{\mathrm{i}x_1}\right)^2 I_{\mathrm{D}}^{10} + \frac{1}{\mathrm{i}x_1}\frac{\mathrm{i}x_2}{\mathrm{i}x_1}I_{\mathrm{D}}^{10}
\end{aligned}
$$

$$- \frac{\mathrm{i}x_2}{\mathrm{i}x_1} + \frac{1}{\mathrm{i}x_1} + \left(\frac{\mathrm{i}x_2}{\mathrm{i}x_1}\right)^2 I_\mathrm{D}^{10} - \frac{1}{\mathrm{i}x_1}\frac{\mathrm{i}x_2}{\mathrm{i}x_1} I_\mathrm{D}^{10} \Bigg\} = 0. \tag{3.148}$$

Thus it follows

$$\boxed{I^{11} - I^{20} = 0 \Leftrightarrow D_{13}^{\mathrm{as}} = D_{31}^{\mathrm{as}} = 0.} \tag{3.149}$$

Finally, $D_{23}^{\mathrm{as}} = D_{32}^{\mathrm{as}} = 0$ requires that

$$\begin{aligned} I^{31} - I^{22} = {} & I_\mathrm{D}^{31} - I_\mathrm{D}^{22} \\ & + \frac{1}{\Delta}(I_\mathrm{D}^{12} - I_\mathrm{D}^{10})[I_\mathrm{D}^{31}(I_\mathrm{D}^{12} - I_\mathrm{D}^{10}) - I_\mathrm{D}^{21}(I_\mathrm{D}^{22} - I_\mathrm{D}^{20})] \\ & + \frac{1}{\Delta}\Delta_1(I_\mathrm{D}^{31} I_\mathrm{D}^{11} - I_\mathrm{D}^{21} I_\mathrm{D}^{21}) \\ & + \frac{1}{\Delta}(1 - I_\mathrm{D}^{11})[(I_\mathrm{D}^{32} - I_\mathrm{D}^{30})(I_\mathrm{D}^{12} - I_\mathrm{D}^{10}) \\ & - (I_\mathrm{D}^{22} - I_\mathrm{D}^{20})(I_\mathrm{D}^{22} - I_\mathrm{D}^{20})] \\ & + \frac{1}{\Delta}(I_\mathrm{D}^{12} - I_\mathrm{D}^{10})[I_\mathrm{D}^{11}(I_\mathrm{D}^{32} - I_\mathrm{D}^{30}) - I_\mathrm{D}^{21}(I_\mathrm{D}^{22} - I_\mathrm{D}^{20})] \end{aligned} \tag{3.150}$$

is zero. Substitution of (3.135), (3.145), (3.147) and

$$I_\mathrm{D}^{31} - I_\mathrm{D}^{22} = \frac{\mathrm{i}x_2}{\mathrm{i}x_1}(I_\mathrm{D}^{30} - I_\mathrm{D}^{21}) + \frac{1}{\mathrm{i}x_1} I_\mathrm{D}^{21} \tag{3.151}$$

leads to

$$\begin{aligned} \mathrm{i}x_1\Delta(I^{31} - I^{22}) = {} & \mathrm{i}x_2\Delta(I_\mathrm{p}^{30} - I_\mathrm{p}^{21}) + [\Delta_1(1 - I_\mathrm{D}^{11}) - (I_\mathrm{D}^{12} - I_\mathrm{D}^{10})^2] I_\mathrm{D}^{12} \\ & + I_\mathrm{D}^{12}(I_\mathrm{D}^{12} - I_\mathrm{D}^{10})^2 + (1 - I_\mathrm{D}^{11})(I_\mathrm{D}^{22} - I_\mathrm{D}^{20})(I_\mathrm{D}^{12} - I_\mathrm{D}^{10}) \\ & - (I_\mathrm{D}^{12} - I_\mathrm{D}^{10})(1 - I_\mathrm{D}^{11})(I_\mathrm{D}^{22} - I_\mathrm{D}^{20}) \\ & + \Delta_1(I_\mathrm{D}^{11} - 1) I_\mathrm{D}^{12} \end{aligned} \tag{3.152}$$

which is identical zero if the earlier result $I_\mathrm{p}^{30} - I_\mathrm{p}^{21} = 0$ is used:

$$\boxed{I^{31} - I^{22} = 0 \Leftrightarrow D_{23}^{\mathrm{as}} = D_{32}^{\mathrm{as}} = 0.} \tag{3.153}$$

3.5.3 Linear Plasma Response

For the discussion of shielding and penetration of RMP modes, respectively below, the linear plasma response shall now be quantified. As was discussed earlier, the RMP current density for a single spatial harmonic is linked to the RMP electric field by a differential conductivity operator, Eq. (2.235). For the details concerning the evaluation of the conductivity operator, the reader is

Resonances	
$V_{e\perp} = V_{\mathrm{dia,e}} + V_E$	Electron fluid resonance
$V_{i\perp} = V_{\mathrm{dia,i}} + V_E$	Ion fluid resonance
V_E	Electric resonance

Table 3.2: Resonances occurring where fluid velocities become zero at the resonant surface.

referred to Ivanov *et al.* (2011) [33]. It is worth mentioning however, that the conductivity operator for the improved energy and momentum conserving model is obtained by substituting the energy and momentum conserving moments W^{mn} for the original moments in Eq. (46) of that reference.

In the lowest order FLRE the parallel RMP plasma current density can be obtained from $\tilde{j}_{\omega \boldsymbol{m}\parallel} = e\int \mathrm{d}^3p\, u \tilde{f}_{\boldsymbol{m}}$. From the solution $\tilde{f}_{\boldsymbol{m}}$ of the kinetic equation it can be evaluated in terms of the moments I^{mn} of the Green's function $\tilde{G}_{\omega \boldsymbol{m}}(u, u')$,

$$\begin{aligned}\tilde{j}_{\omega \boldsymbol{m}\parallel} &= e\int \mathrm{d}^3p\, u \tilde{f}_{\boldsymbol{m}} \\ &= -\frac{n_0 e v_T}{\nu B_0}\left\{\left[(\mathscr{A}_1+\mathscr{A}_2)I^{10} + \frac{1}{2}\mathscr{A}_2 I^{21} + \mathscr{A}_3 I^{11}\right] c\tilde{E}_{\boldsymbol{m}\perp}\right. \\ &\quad \left. + \left[(\mathscr{A}_1+\mathscr{A}_2)I^{11} + \frac{1}{2}\mathscr{A}_2 I^{31} + \mathscr{A}_3 I^{21}\right] v_T \tilde{B}^r_{\boldsymbol{m}}\right\}. \end{aligned} \tag{3.154}$$

For the derivation of the response current the reader is referred to Section D in the Appendix.

The following graphs 3.10 to 3.12 show the electron and ion contributions to the linear response current as one sweeps over the electric resonance with RMP frequencies 3 kHz, 3.5 kHz, and 4 kHz. The response current flows in a thin layer around the resonant surface. Interestingly, the ion contribution to the shielding current seems to become important close to the electric resonance, Fig. 3.11 and becoming again less significant as one leaves this resonance again in the direction of higher RMP frequencies.

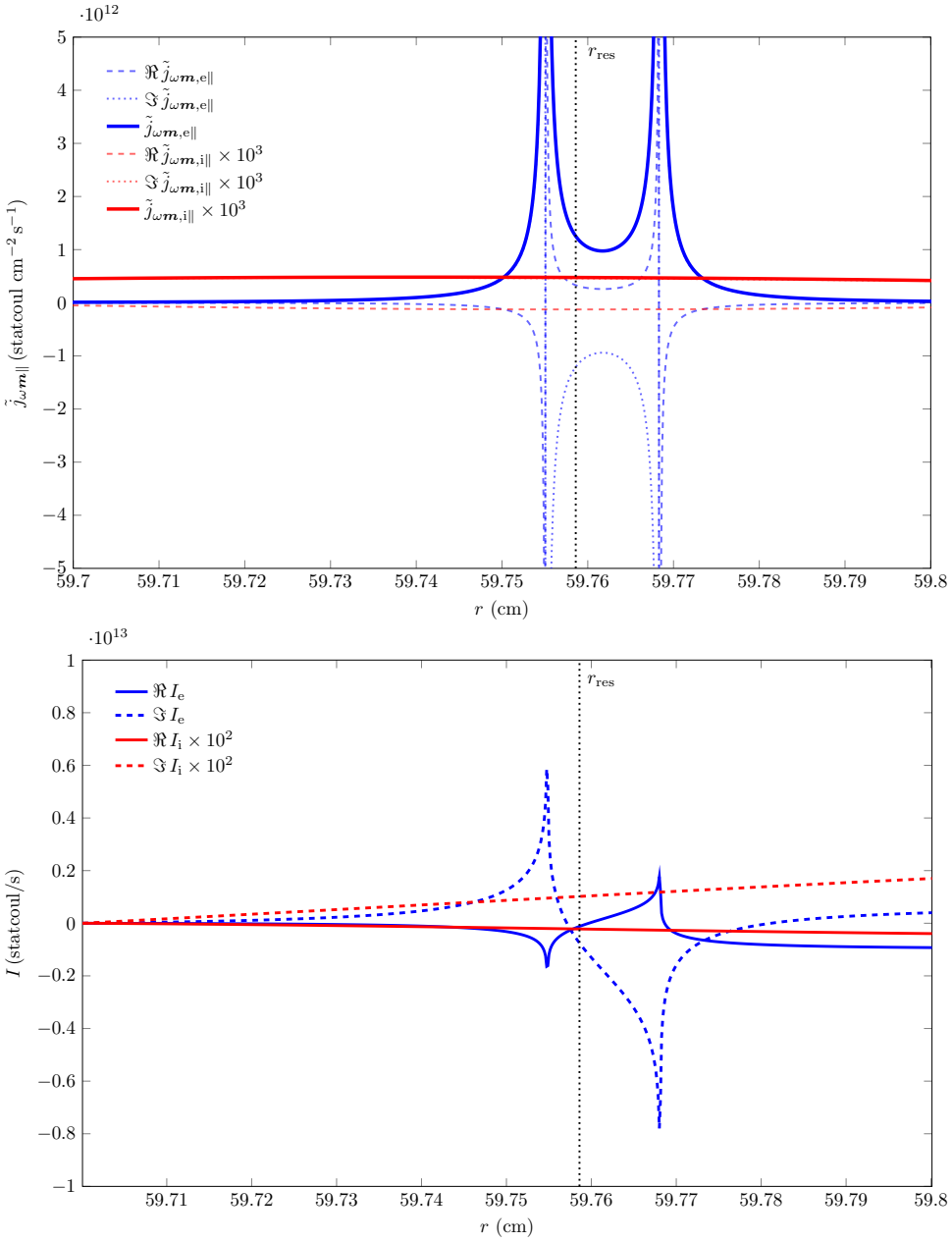

Figure 3.10: Parallel current density $\tilde{j}_{\omega\boldsymbol{m}\parallel}$ and integrated response current I for $f = 3\,\mathrm{kHz}$, i.e. just below the electric resonance, as function of radius in the vicinity of the resonant zone.

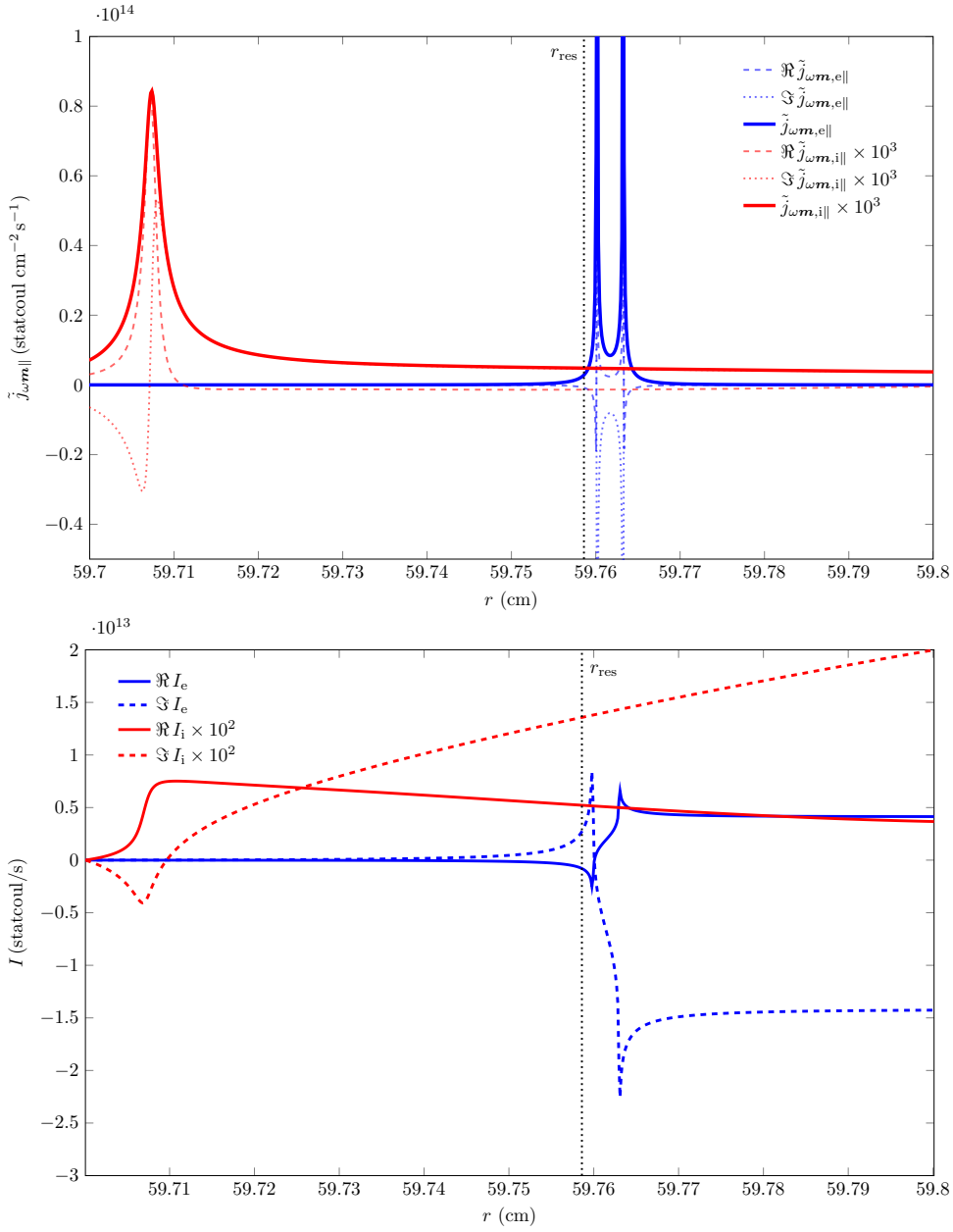

Figure 3.11: Parallel current density $\tilde{j}_{\omega\boldsymbol{m}\parallel}$ and integrated response current I for $f = 3.5\,\mathrm{kHz}$, i.e. very close to the electric resonance, as function of radius in the vicinity of the resonant zone.

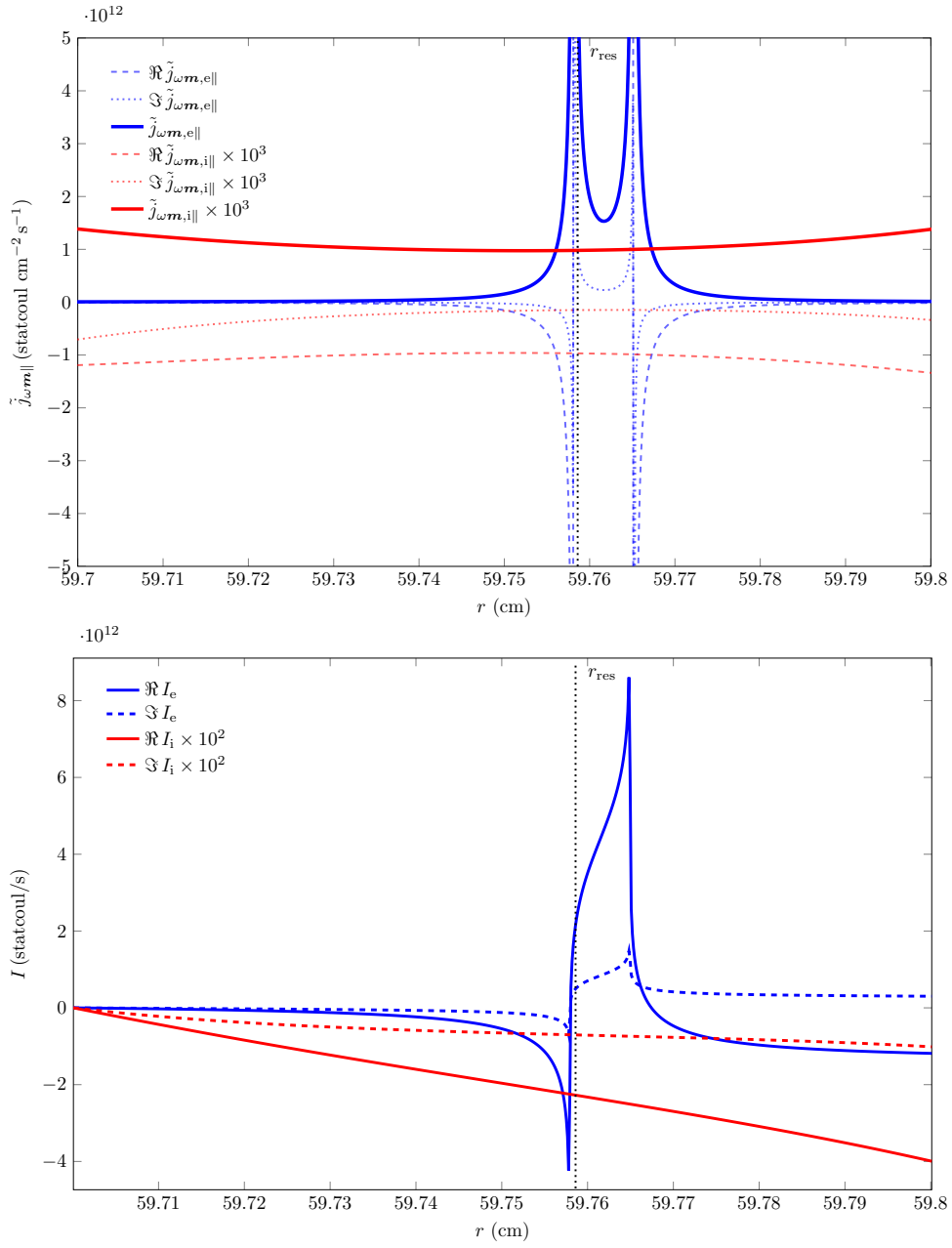

Figure 3.12: Parallel current density $\tilde{j}_{\omega\boldsymbol{m}\parallel}$ and integrated response current I for $f = 4\,\mathrm{kHz}$, i.e. after passing the electric resonance, as function of radius in the vicinity of the resonant zone.

3.6 Numerical Modelling of Plasma Shielding with and without Momentum Conservation in the Ion and Electron Collision Operators

For the numerical modelling, the linear plasma response has been computed for single modes (m, n) with poloidal mode number m and toroidal mode number $n = k_z/R_0$. The model input profiles (density, temperature of electron and ion species, q-factor and toroidal rotation velocity) are shown in Fig. 3.15. Linear temperature profiles and a cubic q-profile have been chosen since a high order FLR expansion requires high derivatives of these profiles. The profiles are typical for medium sized tokamak experiments like ASDEX-Upgrade. Further parameters used for the modelling are summarised in Table 3.3. Making use of a zero poloidal ion flow condition, the static radial electric field E_{0r} is obtained from the diamagnetic velocities of electrons and ions.

Model parameters	
Magnetic field at the magnetic axis B_0	2.12×10^4 G
Major radius R	170 cm
Plasma radius r_{plas}	68.0 cm

Table 3.3: Numerical values for the parameters used in the modelling.

In the following, solutions for the radial magnetic field perturbation amplitude are shown for different RMP frequencies $f = \omega'/2\pi$, where $\omega' = \omega - k_z V_z$. For these calculations ω was set to zero and kept constant, while scaling the toroidal velocity profile V_z. Form factors are given by the ratio $|B_{r,\mathrm{plas}}| \,/\, |B_{r,\mathrm{vac}}|$ of the radial magnetic field moduli at the resonant surface for plasma and vacuum, respectively. Form factor values larger than one indicate an amplification of the B_r field component. A basic solution of the vacuum and plasma radial magnetic field perturbation amplitude for a perturbation with $f = 10.3\,\mathrm{kHz}$ is shown in Fig. 3.16, illustrating the attenuation of the field component due to the parallel plasma response current.

Frequencies, where the perpendicular electron or ion fluid velocities $V_{\mathrm{e}\perp}$ and $V_{\mathrm{i}\perp}$ as well as the $\boldsymbol{E} \times \boldsymbol{B}$-fluid velocity V_E are zero at the mode-specific resonant surface are expected to be resonant, see Table 3.4. The significance of the electron diamagnetic fluid velocity is well known and already exploited for ELM-mitigation shots that are set-up such that the electron fluid velocity zero occurs at the top or even inside the pedestal region. For mode penetration to occur, the perturbation spectrum must consist of modes whose particular resonant surface coincides with that location. The latter resonance, occurring when the radial electric equilibrium field changes sign at the resonant surface has been discussed

in [25, 33], though its importance for RMP mode penetration has been recognised only recently [30]. These fluid velocities for mode $(-10, 2)$ as a function of radius and frequency, respectively are shown in Fig. 3.13. To the right one can read off the specific resonant frequencies, where the zeros of $V_{e\perp}$, $V_{i\perp}$ and V_E sweep over the resonant surface of mode $(-10, 2)$.

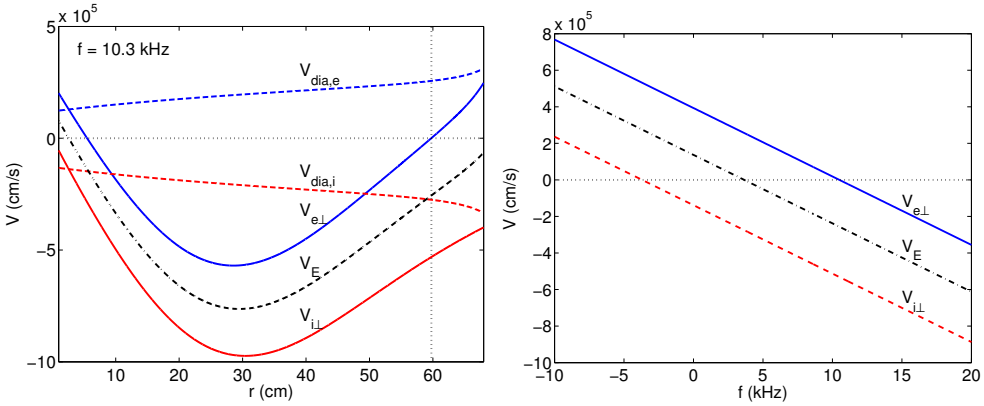

Figure 3.13: Left: Fluid velocities as a function of plasma radius for mode $(-10, 2)$. For the frequency chosen here, $V_{e\perp} = 0$ at the resonant surface. Right: Fluid velocities as a function of frequency form mode $(-10, 2)$. From Leitner *et al.* 2014 [40].

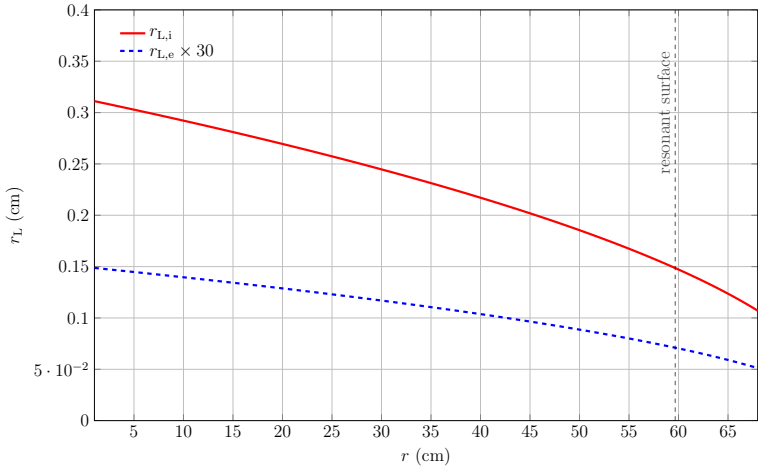

Figure 3.14: Electron- and ion Larmor radius as a function of plasma radius.

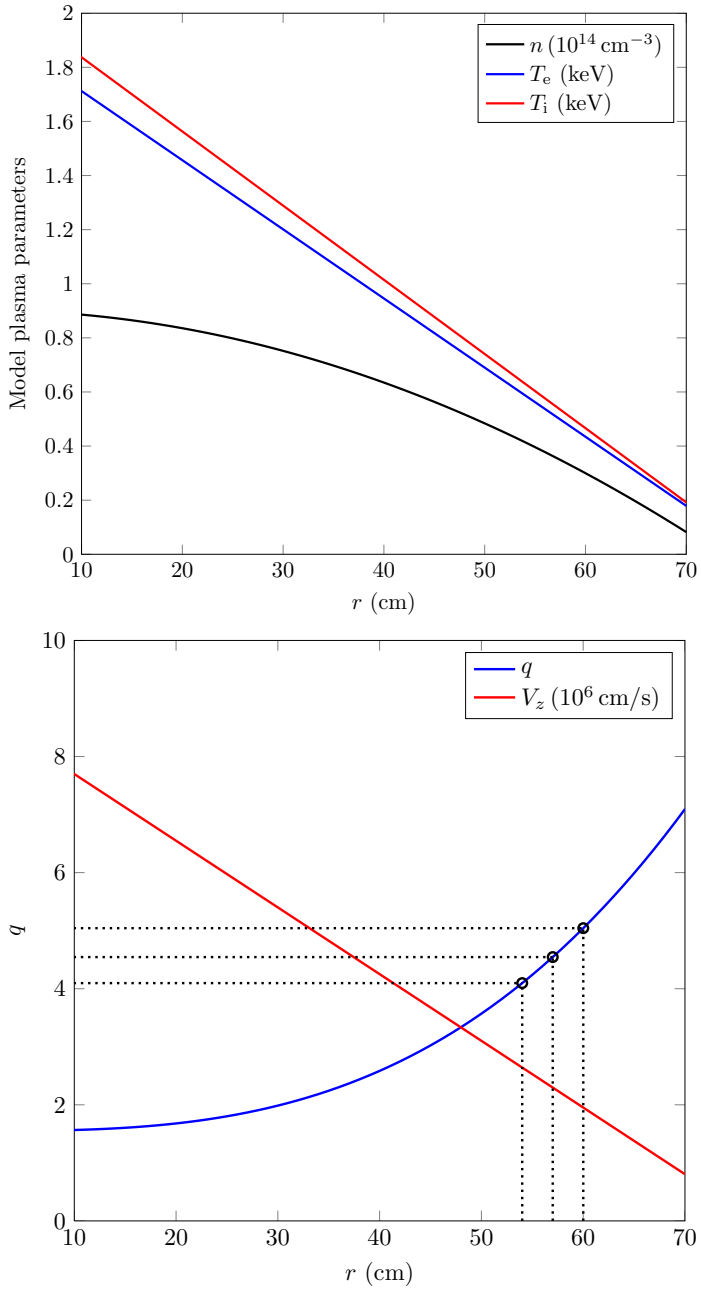

Figure 3.15: Model plasma parameter profiles. Left: Particle density n, electron and ion temperatures; Safety factor q and toroidal velocity profile. From Leitner *et al.* 2014 [40].

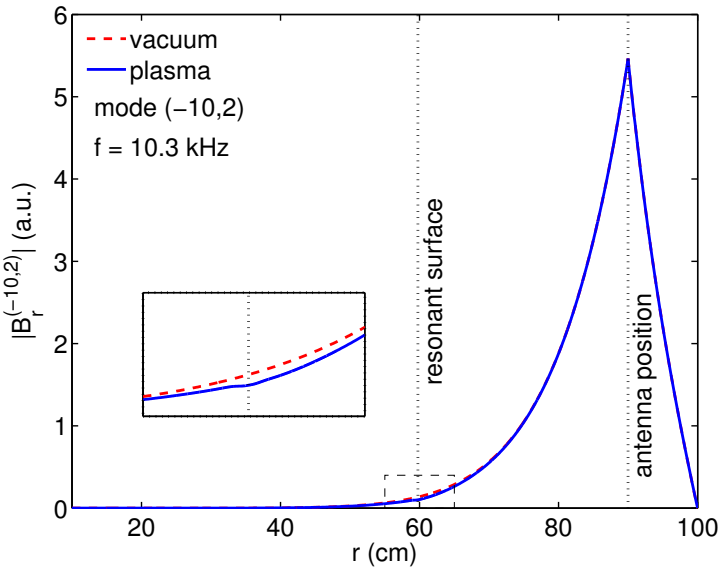

Figure 3.16: Solution of the radial magnetic field perturbation amplitude for $f = 10.3\,\mathrm{kHz}$ and mode $(-10, 2)$. Due to the plasma response current $j_\parallel$ at the resonant surface, the magnetic field becomes attenuated at that particular frequency. From Leitner *et al.* 2014 [40].

Form factors have been computed for three different collision operator models for the electron and ion species, namely (*i*) particle conservation, denoted (n), (*ii*) particle and energy conservation (n,E) and (*iii*) particle, energy and momentum conservation (n,E,M). In addition, calculations have been performed for the single perturbation modes $(-10, 2)$, $(-9, 2)$, and $(-8, 2)$ being resonant at flux surfaces with decreasing plasma radius r, see Table 3.4. Results for these calculations, specifically for collision operator models (n) and (n,E) applied to the electron component and (n), (n,E), (n,E,M) applied to the ion component, respectively are shown in Figures 3.17 and 3.18. Resonant behaviour indeed is found for the electric resonance, where E_r changes sign, i.e. zero $\boldsymbol{E} \times \boldsymbol{B}$-fluid velocity at $f \approx 3.6\,\mathrm{kHz}$ and at the electron fluid resonance, where $V_{\mathrm{e}\perp}$ changes sign at $f \approx 10.3\,\mathrm{kHz}$ but not at the ion fluid resonance. The results also show that the form factors depend sensitively on the electron collision operator model why energy conservation should be considered in the electron component when studying the plasma shielding of RMPs. On the other hand the RMP field is not significantly affected by enforcing momentum conservation on the ion component. It is the electron component that shields the RMP field for the most part, only at the electric resonance ion dynamics seems to become relevant.

Mode number	Res. surface	Resonant frequencies		
(m, n)	r_{res} (cm)	$f_{\mathrm{i}}^* + f_E$ (kHz)	f_E (kHz)	$f_{\mathrm{e}}^* + f_E$ (kHz)
$(-10, 2)$	59.76	-3.789	3.5519	10.393
$(-9, 2)$	56.72	-4.441	2.2790	8.5427
$(-8, 2)$	53.31	-5.175	0.9741	6.7056

Table 3.4: Resonant frequencies for the three modes considered in the numerical modelling.

Remarkably, neither energy nor ion momentum conservation in the ion collision operator visibly affects the RMP penetration, neither in the neighbourhood nor away from the resonances as is illustrated in Fig. 3.18. This remains true if the transition to the collisionless limit is considered, Fig. 3.19. One can see that by reducing the collisionality the exact collisionless limit is smoothly approached independently of whether momentum conservation is considered in the ion component or not. From Fig. 3.21 one can see further that the collisionless model predicts only a single resonance, namely the electron fluid resonance, that, as compared to the collisional case is shifted towards lower frequencies and has a reduced amplitude. The shift towards lower frequencies has been recognised a kinetic effect earlier, Heyn *et al.* (2006) [25]. The electric resonance is expected to disappear in the exact collisionless limit. Again, by reducing the collisionality ν, this trend can be observed in the lower panel of Fig. 3.19, although some noise results from the singular structure of the kinetic equation at that resonance.

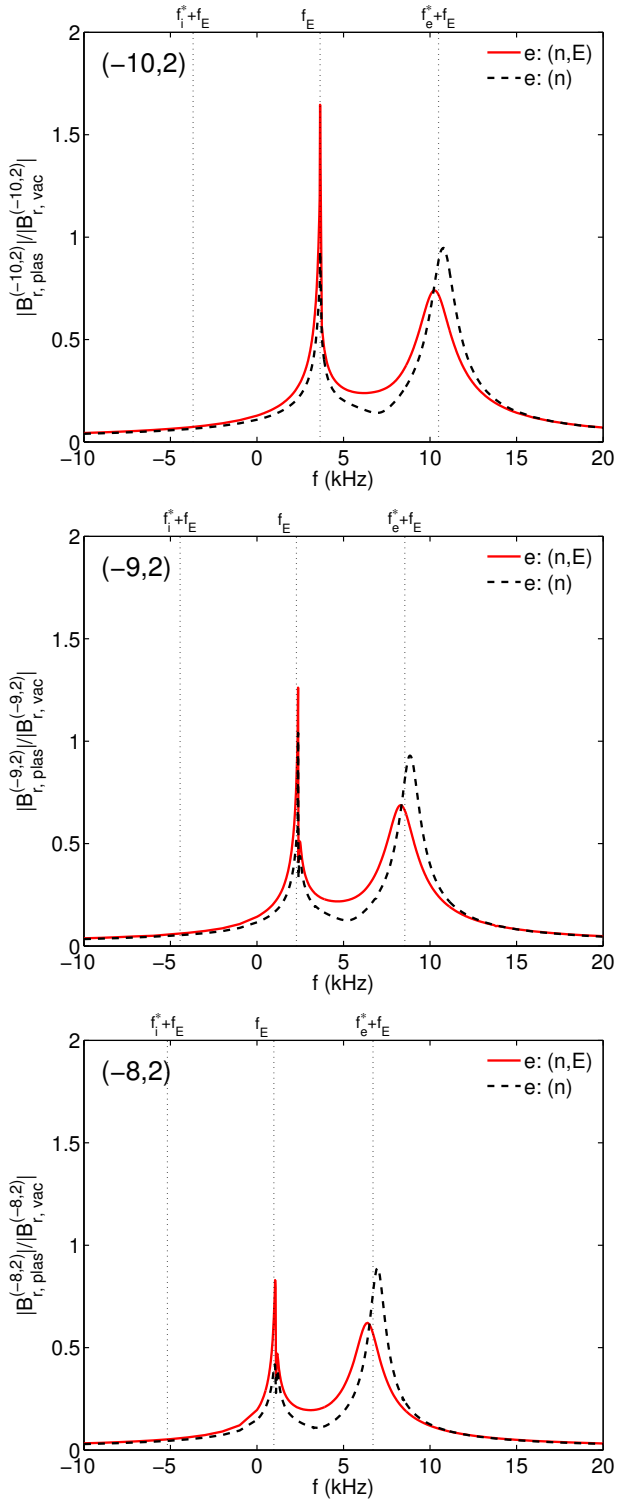

Figure 3.17: Form factors as a function of RMP frequency for modes $(m, n) = (-10, 2)$, $(-9, 2)$, and $(-8, 2)$. Different collision operator models (n), (n,E) have been applied to the electron component. From Leitner *et al.* 2014 [40].

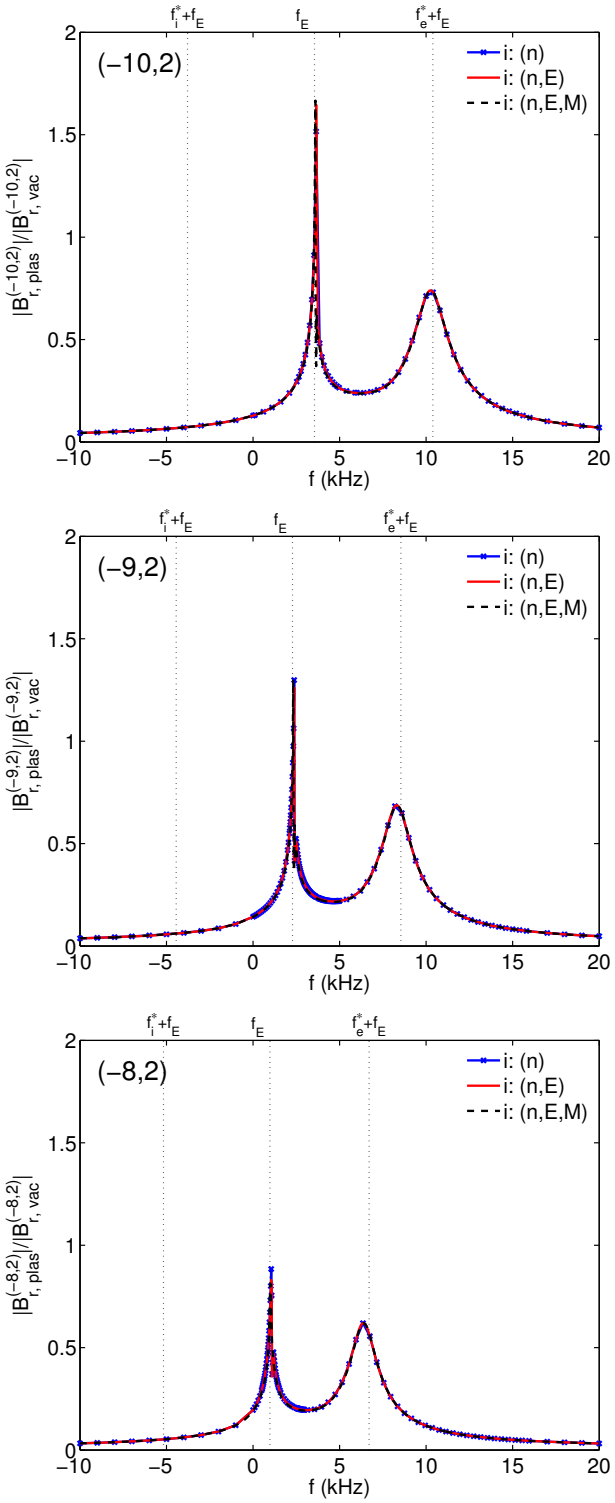

Figure 3.18: Form factors versus RMP frequency for different collision operator models (n), (n,E), (n,E,M) applied to the ion component. From Leitner *et al.* 2014 [40].

"*The position of the electron fluid resonance can be analysed with help of the lowest order current density* [. . . reference to $\tilde{j}_{\omega \boldsymbol{m}\parallel}$ as given in Eq. (3.154)] *ignoring the perpendicular electric field and the small thermodynamic force* A_3 *(it is of the next order in Larmor radius when compared to* A_1 *and* A_2*),*

$$\tilde{j}_{\omega \boldsymbol{m}\parallel} \approx -\frac{nev_T^2}{\nu B_0}\left((A_1+A_2)I^{11}+\frac{1}{2}A_2 I^{13}\right)\tilde{B}^r_{\omega \boldsymbol{m}}. \tag{30}$$

As shown in [. . . reference to Heyn *et al.* 2014 [30]] *using the "constant-psi" approximation where* $\tilde{B}^r_{\omega \boldsymbol{m}}$ *is approximately constant in the resonant layer, in the collisionless limit the total parallel current is determined by the radially integrated moments* I^{11} *and* I^{13}*. The current is proportional to* $\partial \ln(n_e T_e)/\partial r + e\partial\Phi_0/(T_e \partial r) - 0.5\partial \ln T_e/\partial r$ *and, therefore, the shielding is lost if this factor is zero. This resonance is shifted with respect to the zero of electron fluid velocity in the perturbation rest frame if a finite electron temperature gradient is present. On the other hand, it is known from fluid theory that such a shift is absent in the opposite, high collisionality limit. This can be seen as follows. In the high collisional limit,* [. . . reference to Eq. (3.63) in the limit $k = 0$] *can be integrated because* $x_1 \ll 1$*, i.e., the mean free path is much smaller than the parallel scale of the perturbation field and* $x_2 \ll 1$*, i.e., the rotation frequency is much smaller than the collision frequency. The parameter* x_1 *should be kept only in the first term in the argument of the exponent which determines the convergence of the integral. The exponent* $\mathrm{e}^{-\tau}$ *can also be ignored because the main contribution comes from* $\tau \gg 1$*. The integration then gives*

$$\begin{aligned} I_D^{mn}(x_1,x_2) &\to \frac{1}{x_1^2 - \mathrm{i}x_2}\left\{\frac{\partial^{m+n}}{\partial\alpha^m\partial\beta^n}\exp\left[\frac{(\alpha-\beta)^2}{2}\right]\right\}_{\alpha,\beta=0} \\ &= \frac{(-1)^n}{x_1^2 - \mathrm{i}x_2}\left\{\frac{\partial^{m+n}}{\partial\alpha^{m+n}}\exp\left[\frac{\alpha^2}{2}\right]\right\}_{\alpha=0}. \end{aligned} \tag{31}$$

Since all moments with odd $m + n$ *are zero, energy conservation alone (Eq. (56) of* [. . . reference to Heyn *et al.* 2014 [30]]*) does not modify the moments with odd* m *or* n*, i.e.,* $I^{11} = I_D^{11}$ *and* $I^{13} = I_D^{13}$*. Due to* $I_D^{13} = 3I_D^{11}$ *which follows from (31), we see that the current density (30) is proportional to* $\partial \ln(n_e T_e)/\partial r + e\partial\Phi_0/(T_e\partial r)$*, i.e., the current and consequently the plasma shielding vanishes if the electron fluid velocity* $V_{e\perp}$ *is zero in the rest frame of the perturbation field (dotted vertical line in* [. . . reference to upper graph in Fig. 3.19 and

Fig. 3.21]*). At the electric field resonance, the situation is different because in this case not the behaviour of the thermodynamic forces but rather the behaviour of the momenta is responsible for the resonance. In the high collisional limit it can be seen from (31) that the momenta* I_{D}^{mn} *become singular at the resonant surface in case of an electric field resonance, i.e.,* $x_2 = 0$ *at the surface where* $k_{\|} = 0$ *or, equivalently, where* $x_1 = 0$*. If one implements momentum conservation in the electron collision operator (removing resistivity but retaining parallel electron viscosity) using* [. . . reference to Eq. (3.55)]*, this singularity will vanish. Indeed, since all moments with odd* $m + n$ *are zero it follows that* $\mathcal{B} = \mathcal{B}^{\mathrm{M}} = 0$*. The only non-zero term inside the square brackets in* [. . . again referring to Eq. (3.55)] *for* I^{11} *and* I^{31} *is the second term,*

$$I^{1n} = I_{\mathrm{D}}^{1n} + \frac{1}{A^{\mathrm{M}}} I_{\mathrm{D}}^{11} I_{\mathrm{D}}^{1n} = \frac{I_{\mathrm{D}}^{1n}}{1 - I_{\mathrm{D}}^{11}} = -\frac{n I_{\mathrm{D}}^{00}}{1 + I_{\mathrm{D}}^{00}}$$
$$= -\frac{n}{1 + x_1^2 - \mathrm{i}x_2} \approx -n, \qquad n = 1, 3. \tag{32}$$

Therefore, momentum conservation in the electron collision operator will remove the singular behaviour of the momenta I^{mn} *and such the resonant behaviour of the response current at the rational surface. This correlates with the removal of the* $E_r = 0$ *resonance in the form factors (* [. . . reference to Fig. 3.21]*).*" (From Leitner *et al.* 2014 [40, p. 6f] This paragraph motivated by the referee's report originates from a discussion with my supervisor Martin Heyn and Sergei Kasilov and is intended to give a more detailed insight into the origin of the electron fluid and electric field resonance, respectively.

For the case where momentum conservation is enforced in both the electron and the ion component a large sensitivity with respect to collisionality is observed, see Fig. 3.20. Again the collisionless case is approached in the limit of low collisionality but in a non monotonic manner. Reducing the collisionality continuously, a resonant amplification of the radial magnetic field perturbation by a factor of ≈ 30 and 20, respectively at $\nu \approx 0.3$ and 0.075 is found.

Magnetic field amplification at the electric resonance

In the following the radial magnetic field amplification at the electric resonance $E_r = 0$ shall be discussed in more detail. We consider the two collision models where particles and energy for the electron component are conserved, e: (n,E), and for the ions momentum conservation is switched off i: (n,E) and

on i: (n,E,M). For a detailed examination of the resonance, the radial electric field structure and the local dispersion have been computed for three frequency points being located closely left, directly at, and closely right to the electric resonance, see Fig. 3.22. The electric field structure at the three particular frequency points is shown in Fig. 3.23 for the i: (n,E) model and in Fig. 3.24 for the i: (n,E,M) model, respectively. It can be observed that at frequency points (2) and (3) some kind of standing drift wave is formed. When moving from the low frequency point (1) to (2), the dispersion changes from an evanescent mode with $\Im\, k_r > \Re\, k_r$ to a travelling mode $\Im\, k_r < \Re\, k_r$, when passing the $E_r = 0$ resonance. Regarding the corresponding radial electric field plot, a standing wave with $\lambda = 2\pi/k_r$ is observed.

Figures 3.23 and 3.24 show the radial electric field and the local dispersion for mode $(-10, 2)$ at three consecutive frequencies located closely around the electric resonance without and with parallel momentum conservation in the ion collision operator. Comparing the two sets of figures, a significant modification with the ion collision operator model is observed, indicating that close to the electric resonance in addition to the electron also the ion dynamics gains influence. When one approaches the resonance, oscillations in the radial electric field amplitude which are of the order of the ion Larmor radius become smaller. This is even more pronounced for the model with parallel momentum conservation enforced for the ion collision operator. The tiny structures well below the ion Larmor radius that develop in the vicinity of the electric resonance and vanish as one moves farther away from $E_{0r} = 0$ can be attributed to the singularity of the kinetic equation at that resonance. Although interesting phenomena like the formation of drift waves are indicated here, strictly speaking the model assumptions break down at the resonance and no further reliable conclusions can be drawn from the present model.

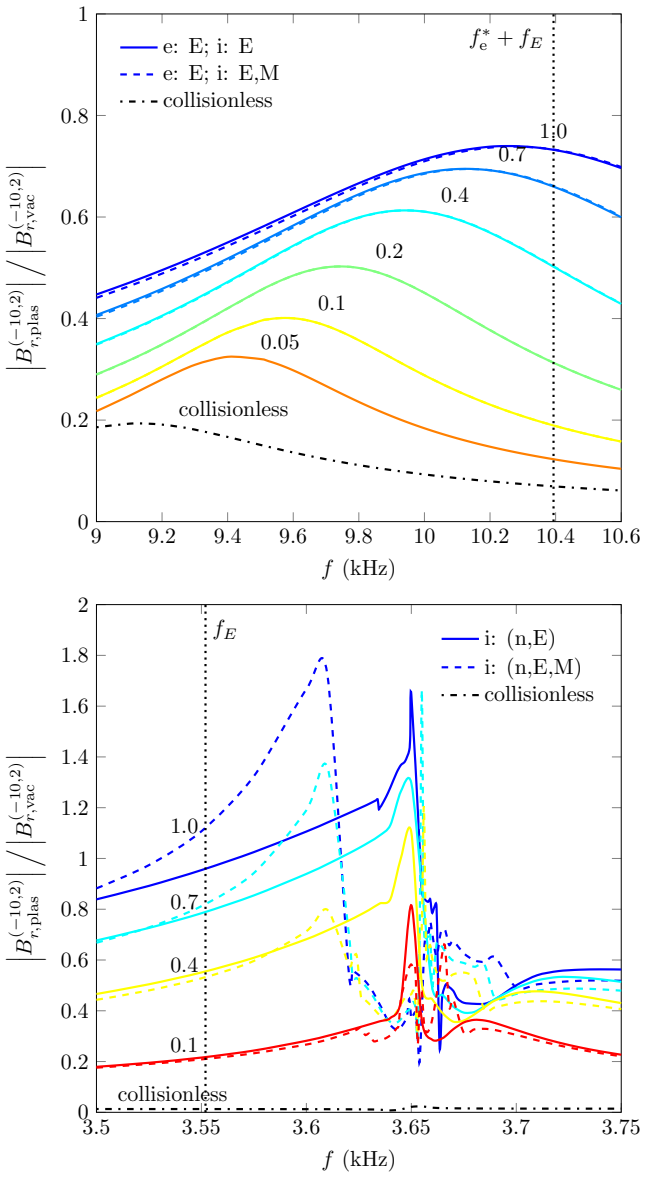

Figure 3.19: Collisionless limit for mode $(-10, 2)$ at the electron fluid resonance (top) and the electric resonance (bottom). The results have been obtained for both collision models (n,E) (solid line) and (n,E,M) (dashed line) applied to the ion component by setting the collision frequency $\nu \to \nu' = \alpha\nu$. The exact collisionless case (dashed-dotted line) is approached for continuous reduction of the collisionality ν. For the electrons the standard collision model (n,E) has been used. Upper figure from Leitner *et al.* 2014 [40].

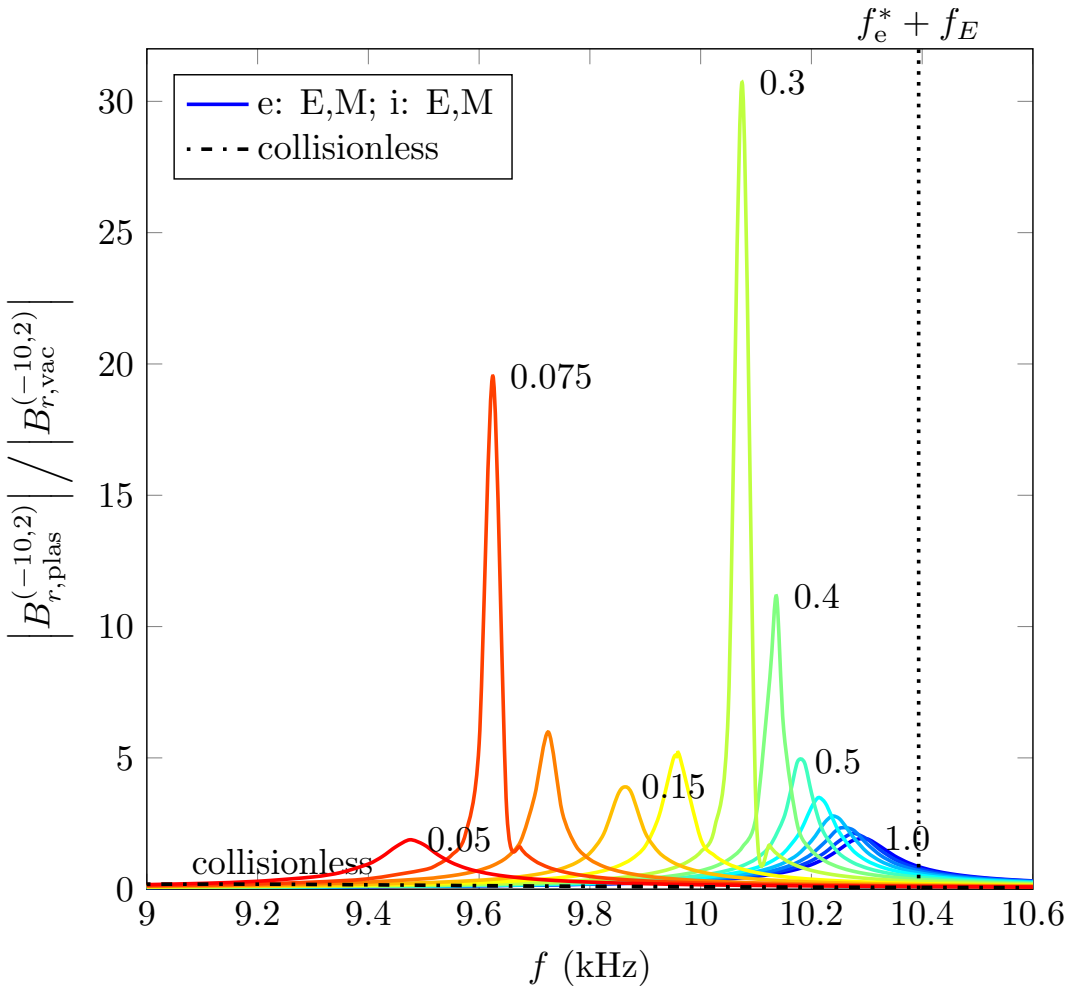

Figure 3.20: Form factors versus RMP frequency for the electron collision operator with momentum conservation.

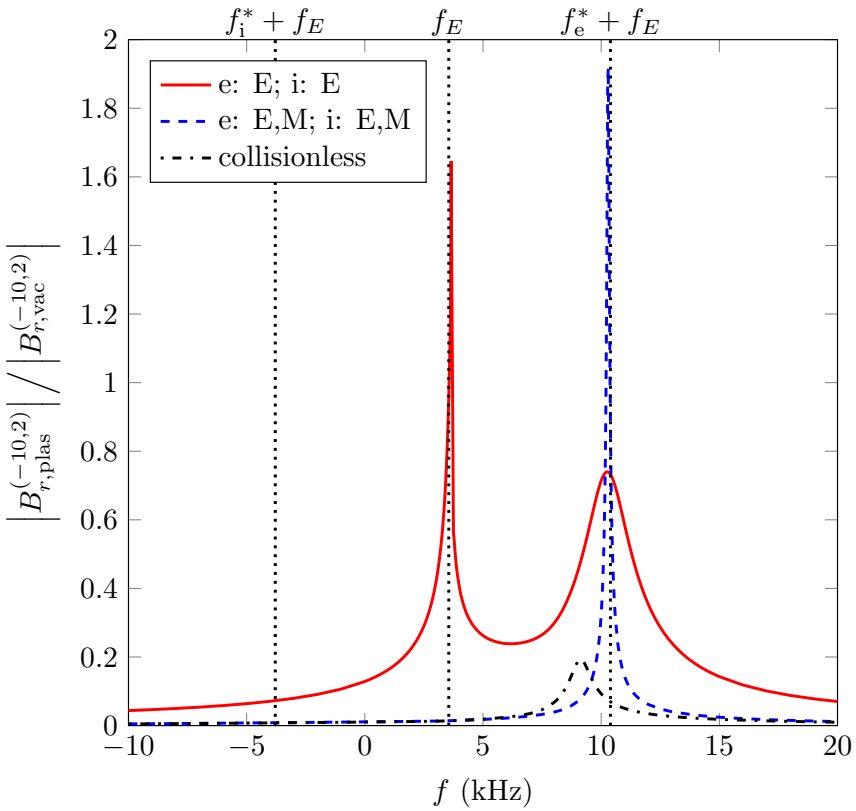

Figure 3.21: Form factors for the collision operator models (n,E) (solid line) and (n,E,M) (dashed line) in the electron component as well as for the exact collisionless limit case (dashed-dotted line) for mode $(-10, 2)$. From Leitner *et al.* 2014 [40].

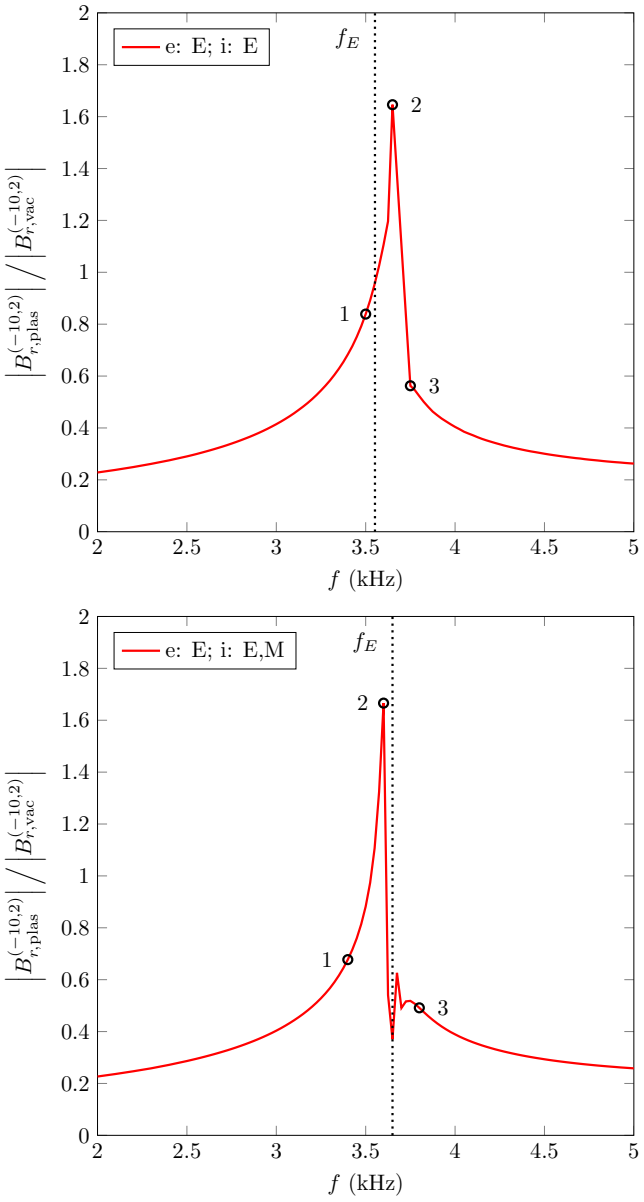

Figure 3.22: Amplification of the radial magnetic field near the electric resonance with (bottom) and without (top) momentum conserving ion collision operator. At the three indicated points, the radial electric field and the local dispersion are shown in Figs. 3.23 and 3.24. Upper figure (slightly modified) from Leitner *et al.* 2014 [40].

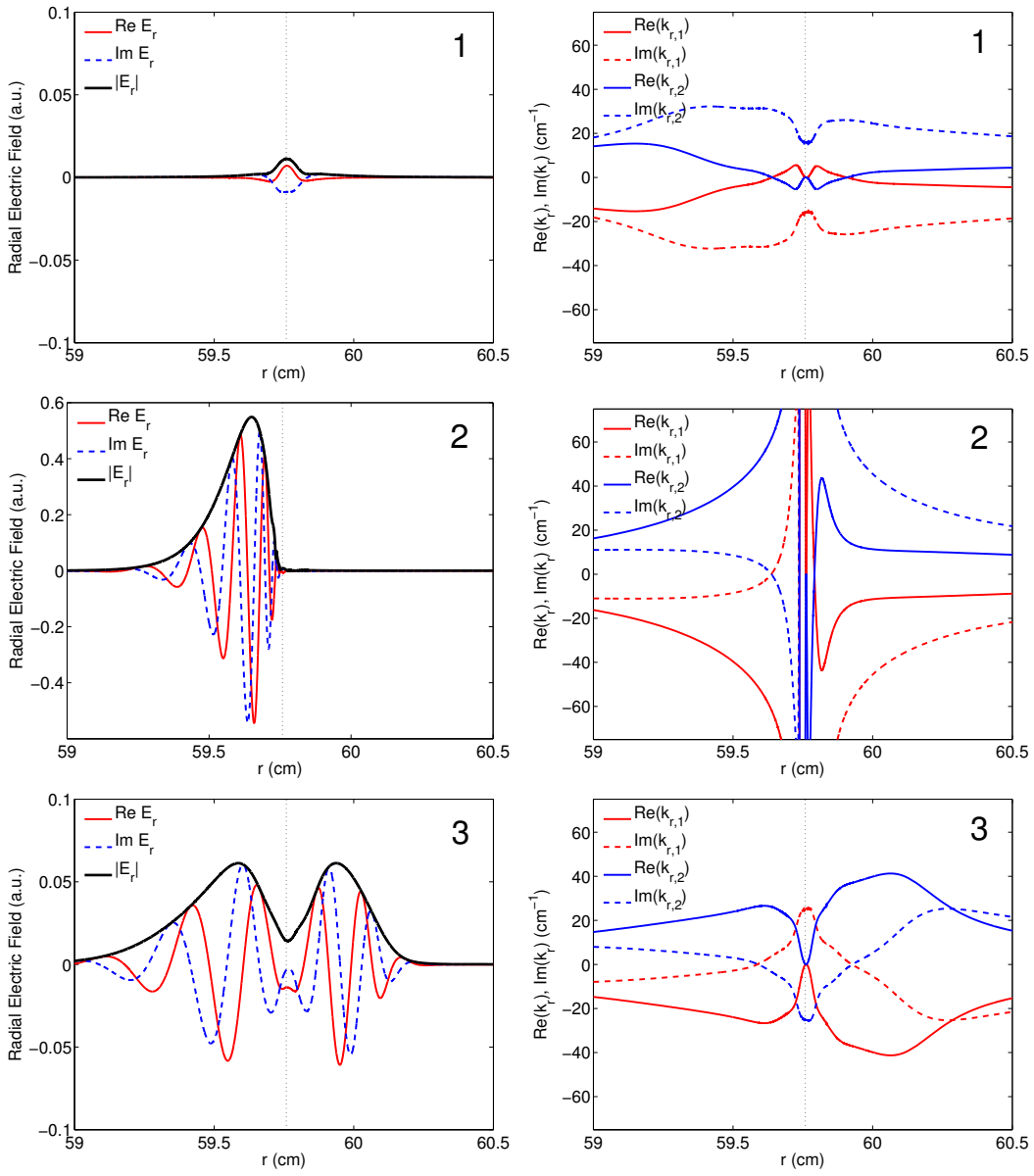

Figure 3.23: Radial electric field and local dispersion for the three frequency points in the vicinity of the electric resonance as indicated in Fig. 3.22. Lower left figure slightly modified from Leitner *et al.* (2014) [40].

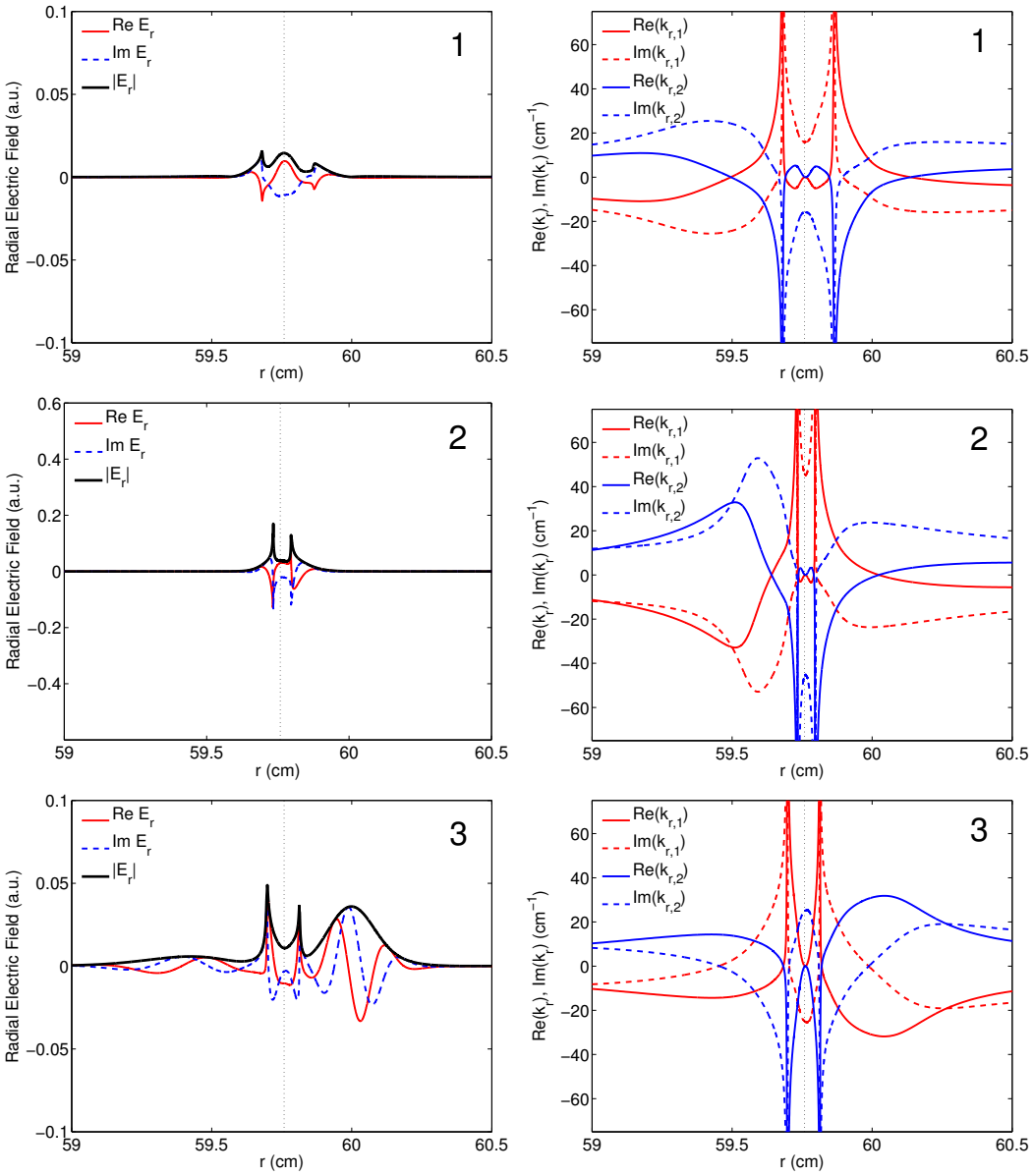

Figure 3.24: Same as Fig. 3.23 but with ion momentum conserving collision operator. Lower left figure slightly modified from Leitner *et al.* (2014) [40].

In the following it is discussed to what extent the input profiles influence the results. For this purpose the original profiles have been rescaled and their particular gradients modified according to $Q \rightarrow Q' = \alpha Q + Q_{r,\mathrm{res}}(1-\alpha)$, where Q denotes the particular quantity under consideration. For these modified inputs form factors in the vicinity of the electron fluid resonance have been recomputed, shown in Figures 3.25, 3.26 and 3.27 for the density, ion and electron temperature.

From Fig. 3.25 it is apparent that a reduction of the density shifts the fluid resonance to higher frequencies. This is due to the density reduction effecting an increase of the electron and ion diamagnetic velocity. The maximum form factor value on the other hand is not affected thereof. Rescaling the electron temperature profile and modifying its gradient leads to a shift of the fluid resonance to lower frequencies in combination with an increase of the maximum form factor values, see Fig. 3.27. In addition to the sensitivity of the form factor value on the electron temperature at the fluid resonance it also varies significantly with the collision frequency as can be seen from the form factor graphs in the upper panel of Fig. 3.19. No variation of the form factor amplitude with a reduction of the ion temperature or a modification of the ion temperature gradient could be observed, see Fig. 3.26 while the fluid resonance location is shifted to lower frequencies, considering that the varied ion diamagnetic drift velocity also affects the $\boldsymbol{E} \times \boldsymbol{B}$-velocity when the poloidal ion velocity is kept at zero. It can be concluded that at the electron fluid velocity it is the electron species that dominates the wave-particle interaction.

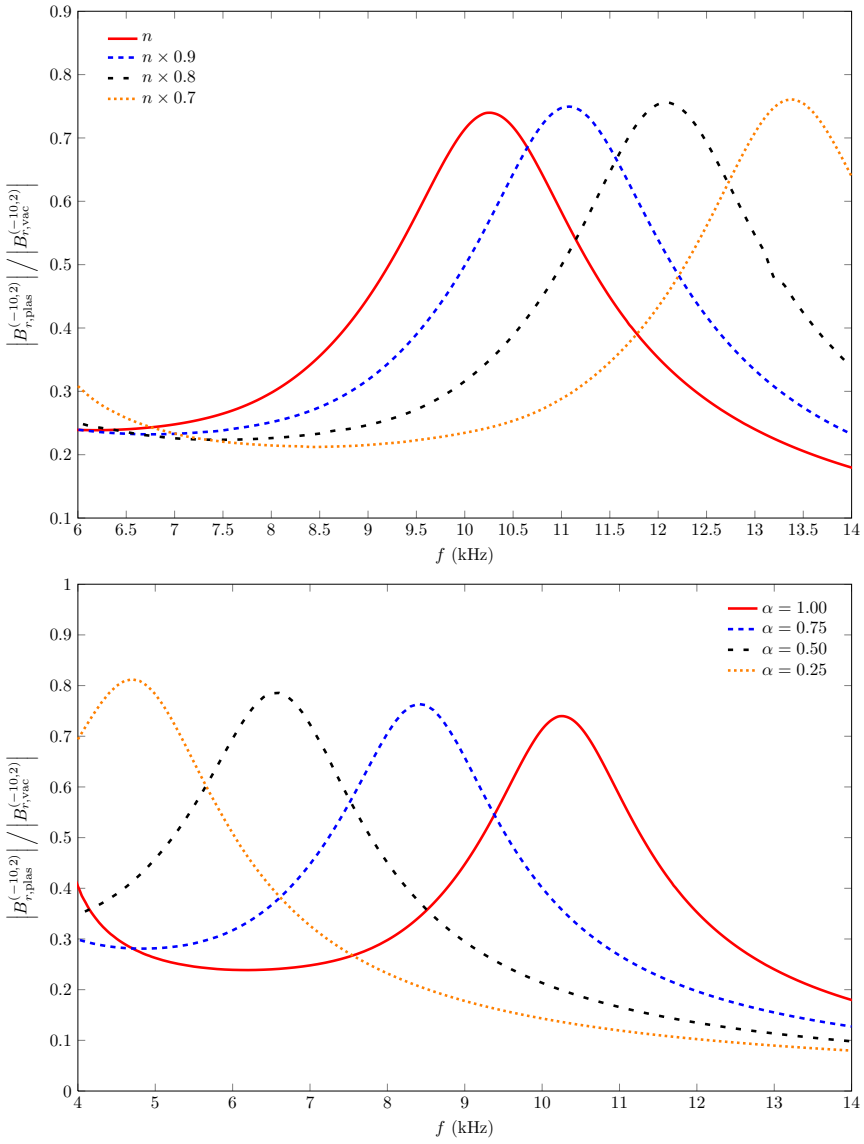

Figure 3.25: Influence of the input parameters density $n = n_\mathrm{e} + n_\mathrm{i}$ and ∇n on the form factors. For the gradient, the original profiles have been modified according to $n \to n' = \alpha n + n_{r,\mathrm{res}}(1-\alpha)$. From Leitner *et al.* 2014 [40].

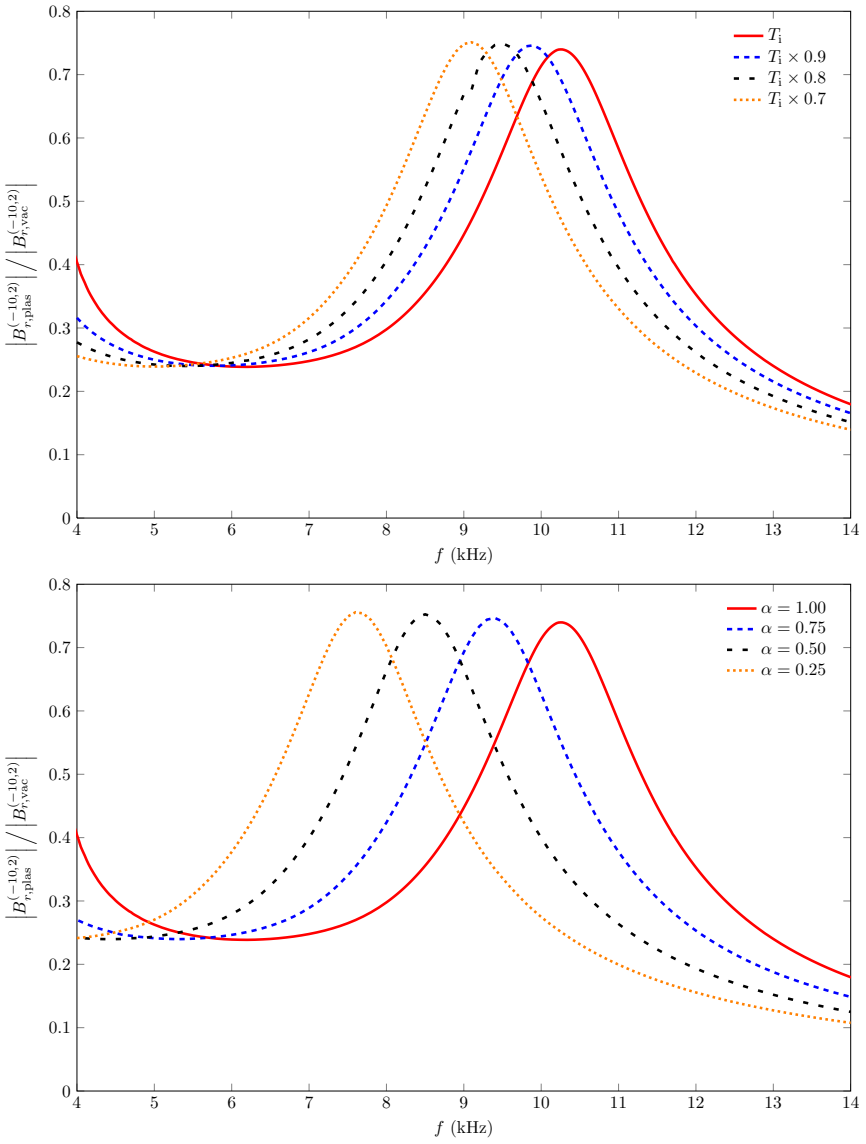

Figure 3.26: Influence of the input parameters ion temperature T_i and ∇T_i on the form factors. For the gradient the original profiles have been modified according to $T_\mathrm{i} \to T_\mathrm{i}' = \alpha T_\mathrm{i} + T_{\mathrm{i},r,\mathrm{res}}(1-\alpha)$. From Leitner *et al.* 2014 [40].

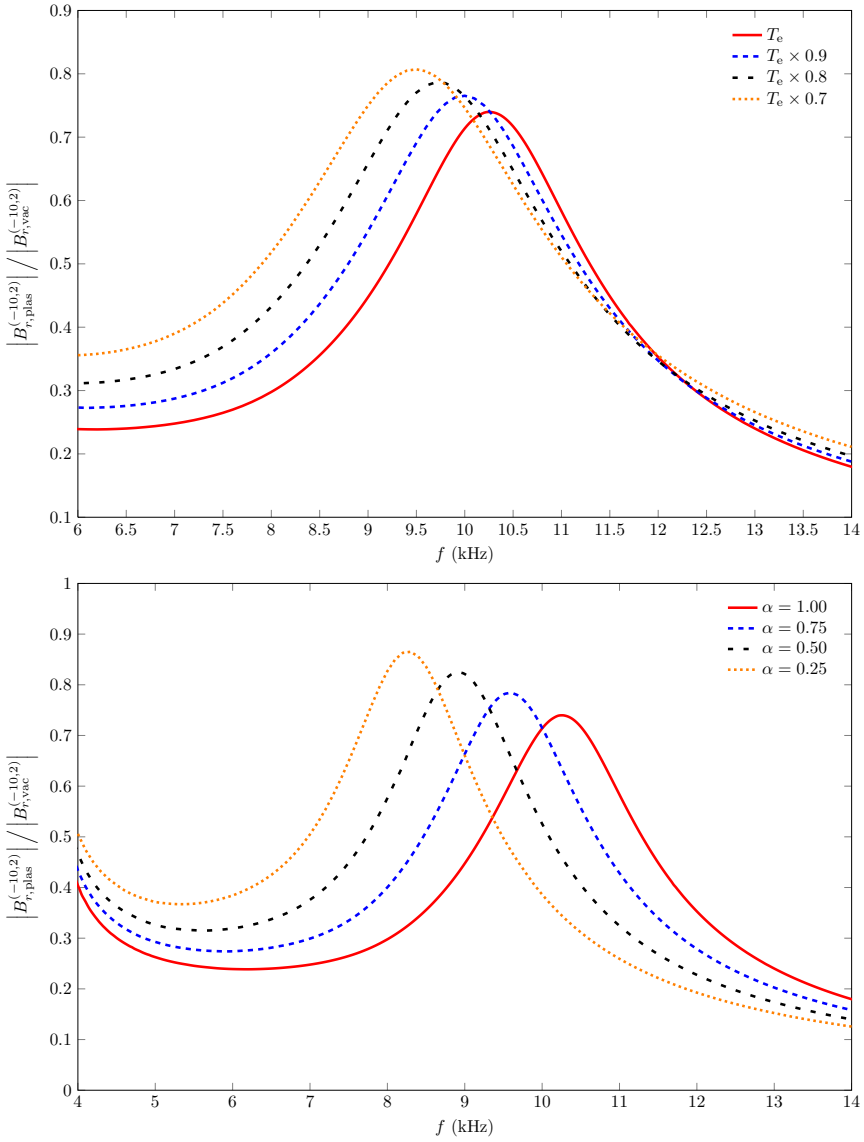

Figure 3.27: Influence of the electron temperature T_e and electron temperature gradient ∇T_e on the form factors. For the gradient the original profiles have been modified according to $T_e \to T_e' = \alpha T_e + T_{e,r,\mathrm{res}}(1-\alpha)$. From Leitner *et al.* 2014 [40].

3.7 Conclusions

The interaction of the single RMP mode $(-3, 1)$ with a JET-like tokamak plasma was studied with a self-consistent quasilinear model in kinetic approximation. RMPs are predicted to be strongly shielded within linear theory [16, 25]. From MHD-theory it is known that an RMP-generated torque on the plasma slows down the electron fluid motion across the magnetic field lines and for a certain threshold value of RMP amplitude penetration is permitted. This kinetic modelling showed that the perturbation field modifies the electron temperature profile for the most part but not so much the toroidal rotation velocity. The perpendicular electron fluid velocity was found to become zero at the resonant surface, the electron diamagnetic velocity component being the most affected. The zero of electron fluid velocity implies field penetration according to MHD theory [50], which is not the case in kinetic theory however, the radial positions of maximum radial field at the resonance zone not coinciding with zero toroidal torque. It was found that the shielding was modified, though not completely removed. The observed sensitivity of the electron temperature on RMPs in quasilinear modelling was confirmed by recent quasilinear models based on Drift-MHD theory [50].

Furthermore, an additional parallel momentum conserving integral operator was introduced and it was shown how to solve the resulting integro-differential kinetic equation. From that solution particle, momentum, and heat fluxes were computed and the corresponding diffusion matrix was obtained. A detailed analytical proof of Onsager symmetry for the full energy and momentum conserving collision model was given. For that purpose recursive relations between the moments of the Green's function of the kinetic equation were derived that proved useful for showing that the combinations of the moments occurring in the antisymmetric part of the diffusion tensor cancel each other, leaving $\boldsymbol{D}^{\mathrm{as}} = \mathbf{0}$. The recursions furthermore allow the evaluation of higher moments of the Green's function practically for free, once a set of lower moments is obtained.

In a numerical modelling of the linear plasma response for a single (but varying) perturbation mode and ASDEX-like plasma profiles several collision operator models were compared and their impact on the form factors was studied. By switching on energy conservation the induced plasma currents at the resonant surface are modified and the form factors are considerably affected. The conservation of the species' energy is therefore preferably to be considered. Enforcing parallel momentum conservation on the ions in the straight cylinder model is inconsistent with parallel flow braking occurring due to poloidal or parallel viscosity in a real toroidal tokamak geometry where parallel momentum is lost to the trapped particles at a rate of the collision frequency times the frac-

tion of trapped particles. If momentum conservation is not considered in the kinetic model, the momentum loss to trapped particles is simulated [33], while in the opposite case model results are comparable to MHD models not considering toroidal effects or shear viscosity. The fact that momentum conservation for the ion component does not have a significant effect on the RMP field inside the plasma shows that the flow braking by trapped particles can be neglected in the cylindrical tokamak model while still being a valid description for RMP shielding at the resonant surface also for a real tokamak geometry. If momentum conservation is enforced on the electrons on the other hand, a plasma with finite parallel viscosity and finite parallel heat conductivity but no resistivity is considered. For this condition the electric resonance is eliminated which is also in agreement with the collisionless model, where that resonance does not occur either. At the electron fluid resonance the amplification is highly sensitive with respect to the collisionality showing a non-monotonic limit to the collisionless case with resonant amplification up to a factor of ≈ 30.

No resonant behaviour was observed attributable to the zero of the ion perpendicular fluid velocity at the resonant surface. The plasma response, shielding RMPs in a distance of the electric resonance is caused by the electrons for the most part, while the ion dynamic seems to play an important part directly at that resonance.

A variation of density- and temperature profiles of the electrons shifts the position of the maximum form factor as well as its amplitude. For the ions, a variation of the temperature and temperature gradient profile alters the radial electric field whereby only the position of the maximum form factor is shifted.

Close to and at the electric resonance electrostatic oscillations are observed indicating the formation of drift waves. Due to the singularity of the kinetic equation at that particular resonance no further conclusions can be drawn about the phenomena occurring there within the scope of the present model.

Appendices

Appendix A

Solution of the Linearised Kinetic Equation

In this appendix it is shown how to solve the kinetic equation for the differential Fokker-Planck collision operator in Ornstein-Uhlenbeck approximation. While the solution was already found and discussed by Ivanov *et al.* [33], here a complete derivation by the method of characteristics is given due to its significant importance also for the more general integro-differential kinetic equation that is studied in this thesis.

Starting point is the kinetic equation after expansion of perturbed quantities, Eq. (2.207),

$$\left[\frac{\partial}{\partial t} + \mathrm{i}\boldsymbol{m}\cdot\boldsymbol{\Omega} - D\frac{\partial}{\partial u}\left(\frac{\partial}{\partial u} + \frac{u}{v_T^2}\right)\right]\tilde{f}_{\boldsymbol{m}}(u,t) = \tilde{Q}_{\boldsymbol{m}}(u,t), \tag{A.1}$$

where $\boldsymbol{m}\cdot\boldsymbol{\Omega} = \omega_\ell + k_\parallel u$ with the Doppler-shifted frequency ω_ℓ that can be further decomposed into a sum of the cyclotron frequency plus electric particle drift frequency, $\omega_\ell = \ell\omega_\mathrm{c} + \boldsymbol{k}\cdot\boldsymbol{V} = \ell\omega_\mathrm{c} + k_\perp V_{E\perp} + k_\parallel V_\parallel$ and $D = \nu v_T^2$, a constant diffusion coefficient. The kinetic equation

$$\left[\frac{\partial}{\partial t} + \mathrm{i}(\omega_\ell + k_\parallel u) - D\frac{\partial^2}{\partial u^2} - \frac{D}{v_T^2}\frac{\partial}{\partial u}u\right]\tilde{f}_{\boldsymbol{m}}(u,t) = \tilde{Q}_{\boldsymbol{m}}(u,t), \tag{A.2}$$

so far a partial differential equation in velocity space is transformed to k-space by consideration of the following trivial Fourier transformations,

$$\tilde{f}_{\boldsymbol{m}}(k) = \mathscr{F}\{\tilde{f}_{\boldsymbol{m}}(u)\} = \frac{1}{\sqrt{2\pi}}\int_{\mathbb{R}} \mathrm{d}u\, \tilde{f}_{\boldsymbol{m}}(u)\exp(-\mathrm{i}ku), \tag{A.3}$$

$$\begin{aligned}\mathscr{F}\left\{\frac{\mathrm{d}}{\mathrm{d}u}\tilde{f}_{\boldsymbol{m}}(u)\right\} &= \frac{1}{\sqrt{2\pi}}\int_{\mathbb{R}}\mathrm{d}u\,\left(\frac{\mathrm{d}}{\mathrm{d}u}\tilde{f}_{\boldsymbol{m}}(u)\right)\exp(-\mathrm{i}ku)\\ &= -\frac{1}{\sqrt{2\pi}}\int_{\mathbb{R}}\mathrm{d}u\,\tilde{f}_{\boldsymbol{m}}(u)\frac{\mathrm{d}}{\mathrm{d}u}\exp(-\mathrm{i}ku)\\ &= \frac{\mathrm{i}k}{\sqrt{2\pi}}\int_{\mathbb{R}}\mathrm{d}u\,\tilde{f}_{\boldsymbol{m}}(u)\exp(-\mathrm{i}ku) = \mathrm{i}k\mathscr{F}\{\tilde{f}_{\boldsymbol{m}}(u)\},\end{aligned}\tag{A.4}$$

$$\begin{aligned}\mathscr{F}\{u\tilde{f}_{\boldsymbol{m}}(u)\} &= \frac{1}{\sqrt{2\pi}}\int_{\mathbb{R}}\mathrm{d}u\,u\tilde{f}_{\boldsymbol{m}}(u)\exp(-\mathrm{i}ku)\\ &= \frac{1}{\sqrt{2\pi}}\int_{\mathbb{R}}\mathrm{d}u\,\mathrm{i}\frac{\partial}{\partial k}\exp(-\mathrm{i}ku)\tilde{f}_{\boldsymbol{m}}(u)\\ &= \mathrm{i}\frac{\partial}{\partial k}\mathscr{F}\{\tilde{f}_{\boldsymbol{m}}(u)\},\end{aligned}\tag{A.5}$$

$$\begin{aligned}\mathscr{F}\left\{\frac{\partial}{\partial u}u\tilde{f}_{\boldsymbol{m}}(u)\right\} &= \frac{1}{\sqrt{2\pi}}\int_{\mathbb{R}}\mathrm{d}u\,\frac{\partial}{\partial u}(u\tilde{f}_{\boldsymbol{m}}(u))\exp(-\mathrm{i}ku)\\ &= \frac{1}{\sqrt{2\pi}}\int_{\mathbb{R}}\mathrm{d}u\,\mathrm{i}ku\tilde{f}_{\boldsymbol{m}}(u)\exp(-\mathrm{i}ku)\\ &= \frac{1}{\sqrt{2\pi}}\int_{\mathbb{R}}\mathrm{d}u\,\mathrm{i}k\mathrm{i}\frac{\partial}{\partial k}\exp(-\mathrm{i}ku)\tilde{f}_{\boldsymbol{m}}(u)\\ &= -k\frac{\partial}{\partial k}\mathscr{F}\{\tilde{f}_{\boldsymbol{m}}(u)\}.\end{aligned}\tag{A.6}$$

For convenience the unaffected time dependence has been suppressed in the notation. The Fourier transforms of $\tilde{f}_{\boldsymbol{m}}(u,t)$ and $\tilde{Q}_{\boldsymbol{m}}(u,t)$ are denoted by their functional dependence on k, i.e. $\tilde{f}_{\boldsymbol{m}}(k,t)$ and $\tilde{Q}_{\boldsymbol{m}}(k,t)$. In k-space the equation then reads

$$\left(\frac{\partial}{\partial t}+\mathrm{i}\omega_\ell - k_\parallel\frac{\partial}{\partial k}+Dk^2+\frac{D}{v_{\mathrm{T}}^2}k\frac{\partial}{\partial k}\right)\tilde{f}_{\boldsymbol{m}}(k,t)=\tilde{Q}_{\boldsymbol{m}}(k,t).\tag{A.7}$$

A.1 Application of the Method of Characteristics

After reordering terms,

$$\frac{\partial\tilde{f}_{\boldsymbol{m}}(k,t)}{\partial t}+(\nu k-k_\parallel)\frac{\partial\tilde{f}_{\boldsymbol{m}}(k,t)}{\partial k}+\left(\mathrm{i}\omega_\ell+Dk^2\right)\tilde{f}_{\boldsymbol{m}}(k,t)=\tilde{Q}_{\boldsymbol{m}}(k,t),\tag{A.8}$$

the method of characteristics, see e.g. [14, p. 186ff], is applied by which one obtains an ordinary differential equation that is valid along the characteristics:

$$\frac{\mathrm{d}}{\mathrm{d}s}\tilde{f}_{\boldsymbol{m}}(k(s),t(s))=0 \tag{A.9}$$

$$\frac{\mathrm{d}\tilde{f}_{\boldsymbol{m}}(k)}{\mathrm{d}s}=\frac{\partial\tilde{f}_{\boldsymbol{m}}(k)}{\partial k}\frac{\mathrm{d}k}{\mathrm{d}s}+\frac{\partial\tilde{f}_{\boldsymbol{m}}(k)}{\partial t}\frac{\mathrm{d}t}{\mathrm{d}s}$$

The *characteristic equations* are:

$$\frac{\mathrm{d}t}{\mathrm{d}s}=1,\qquad \frac{\mathrm{d}k}{\mathrm{d}s}=\nu k-k_{\parallel} \tag{A.10}$$

Along the characteristic lines $k(s)$ and $t(s)$ $\mathrm{d}f_k/\,\mathrm{d}s=\text{const}$, i.e. $\tilde{f}_{\boldsymbol{m}}(k(s),t(s))=\tilde{f}_{\boldsymbol{m}}(k_0,t_0)$. Since the coefficient of $\partial f_k/\partial t$ in Eq. (A.8) is 1, the relation between t and s is trivial and together with the initial condition $t(0)=0$ one obtains

$$\frac{\mathrm{d}t}{\mathrm{d}s}=1\Rightarrow t(s)=s+\text{const},\qquad t(0)=0\Rightarrow t=s.$$

The second characteristic equation

$$\frac{\mathrm{d}k}{\mathrm{d}t}=-k_{\parallel}+\nu k \tag{A.11}$$

is easily rearranged to

$$\frac{\mathrm{d}k}{k-k_{\parallel}/\nu}=\nu\,\mathrm{d}t$$

and integrated by a change of variables $v:=k-k_{\parallel}/\nu$,

$$\int \mathrm{d}\ln v=\int \nu\ \mathrm{d}t$$

yielding

$$k(t)=\frac{k_{\parallel}}{\nu}+k_0\mathrm{e}^{\nu t}\Rightarrow k_0=\left(k-\frac{k_{\parallel}}{\nu}\right)\mathrm{e}^{-\nu t}.$$

$$\tilde{f}_{\boldsymbol{m}}(k_0,t_0)=\tilde{f}_{\boldsymbol{m}}\left(\left(k-\frac{k_{\parallel}}{\nu}\right)\mathrm{e}^{-\nu t},0\right)$$

Next $\tilde{f}_{\boldsymbol{m}}(k(t),t)$ is evaluated by integrating $\dot{\tilde{f}}_{\boldsymbol{m}}(k(t),t)$,

$$\begin{aligned}\frac{\mathrm{d}}{\mathrm{d}t}\tilde{f}_{\boldsymbol{m}}(k(t),t)&=\frac{\partial\tilde{f}_{\boldsymbol{m}}(k(t),t)}{\partial t}+\frac{\partial\tilde{f}_{\boldsymbol{m}}(k(t),t)}{\partial k}\dot{k}\\&=\frac{\partial\tilde{f}_{\boldsymbol{m}}(k(t),t)}{\partial t}-\left[\mathrm{i}\omega_\ell+Dk(t)^2\right]\tilde{f}_{\boldsymbol{m}}(k(t),t)-\frac{\partial\tilde{f}_{\boldsymbol{m}}(t,k(t))}{\partial t}\\&=-\left[\mathrm{i}\omega_\ell+Dk(t)^2\right]\tilde{f}_{\boldsymbol{m}}(k(t),t)\end{aligned}$$

$$= p(t)\tilde{f}_{\boldsymbol{m}}(k(t),t), \tag{A.12}$$

where the homogeneous equation has been used and the coefficient of $\tilde{f}_{\boldsymbol{m}}(k,t)$ in the kinetic equation (A.8) has been denoted $p(t)$. From Eq. (A.12) follows

$$\tilde{f}_{\boldsymbol{m}}(k(t),t) = \tilde{f}_{\boldsymbol{m}}(k(0),0)\exp\left\{-\int_0^t \mathrm{d}\tau\left[\mathrm{i}\omega_\ell + D\left(k_0\mathrm{e}^{\nu\tau}+\frac{k_\parallel}{\nu}\right)^2\right]\right\}. \tag{A.13}$$

The exponent, upon integration, is

$$\begin{aligned}
&-\int_0^t \mathrm{d}\tau\left[\mathrm{i}\omega_\ell + D\left(k_0^2\mathrm{e}^{2\nu t}+2k_0\mathrm{e}^{\nu t}\frac{k_\parallel}{\nu}+\frac{k_\parallel^2}{\nu^2}\right)\right]\\
&\quad= -\mathrm{i}\omega_\ell t - \frac{Dk_0^2}{2\nu}\left(\mathrm{e}^{2\nu t}-1\right) - \frac{2Dk_0k_\parallel}{\nu^2}\left(\mathrm{e}^{\nu t}-1\right) - D\frac{k_\parallel^2}{\nu^2}t\\
&\quad= -\mathrm{i}\omega_\ell t - \frac{v_T^2}{2}\left(k-\frac{k_\parallel}{\nu}\right)^2\left(1-\mathrm{e}^{-2\nu t}\right) - \frac{2v_T^2k_\parallel}{\nu}\left(k-\frac{k_\parallel}{\nu}\right)\left(1-\mathrm{e}^{-\nu t}\right)\\
&\qquad - \frac{v_T^2k_\parallel^2}{\nu}t\\
&\quad= -\tilde{a}(t)\left(k-\frac{k_\parallel}{\nu}\right)^2 - \tilde{b}(t)\left(k-\frac{k_\parallel}{\nu}\right) - c(t),
\end{aligned} \tag{A.14}$$

where in the second line $(k-k_\parallel/\nu)\mathrm{e}^{-\nu t}$ has been substituted for k_0 and the coefficients of the various powers of $(k-k_\parallel/\nu)$ have been assigned the functions

$$\tilde{a}(t) = \frac{v_T^2}{2}\left(1-\mathrm{e}^{-2\nu t}\right), \tag{A.15}$$

$$\tilde{b}(t) = \frac{2v_T^2k_\parallel}{\nu}\left(1-\mathrm{e}^{-\nu t}\right), \tag{A.16}$$

$$c(t) = \left(\mathrm{i}\omega_\ell + \frac{v_T^2k_\parallel^2}{\nu}\right)t \tag{A.17}$$

in accordance with [33]. With

$$k(0) = \frac{k_\parallel}{\nu}+k_0 = \frac{k_\parallel}{\nu}\left(1-\mathrm{e}^{-\nu t}\right) + k\mathrm{e}^{-\nu t}$$

Eq. (A.13) is further evaluated to

$$\tilde{f}_{\boldsymbol{m}}(k(t),t) = \tilde{f}_{\boldsymbol{m}}\left(\frac{k_\parallel}{\nu}\left(1-\mathrm{e}^{-\nu t}\right)+k\mathrm{e}^{-\nu t},0\right)\mathrm{e}^{-\tilde{a}(t)\left(k-\frac{k_\parallel}{\nu}\right)^2-\tilde{b}(t)\left(k-\frac{k_\parallel}{\nu}\right)-\tilde{c}(t)}. \tag{A.18}$$

Considering the initial condition $\tilde{f}_{\boldsymbol{m}}(u,0) = \delta(u-u')$ and its Fourier transform $\tilde{f}_{\boldsymbol{m}}(k,0) = (1/\sqrt{2\pi})\mathrm{e}^{-\mathrm{i}ku'}$ one finds

$$\tilde{f}_{\boldsymbol{m}}\left(\frac{k_\parallel}{\nu}\left(1-\mathrm{e}^{-\nu t}\right)+k\mathrm{e}^{-\nu t},0\right) = \frac{1}{\sqrt{2\pi}}\mathrm{e}^{-\mathrm{i}\left[k\mathrm{e}^{-\nu t}+\frac{k_\parallel}{\nu}\left(1-\mathrm{e}^{-\nu t}\right)\right]u'}$$

and hence the homogeneous solution of the kinetic equation in k-space,

$$\tilde{f}_{\boldsymbol{m}}(k(t),t) = \frac{1}{\sqrt{2\pi}}\mathrm{e}^{-\mathrm{i}\left[k\mathrm{e}^{-\nu t}+\frac{k_\parallel}{\nu}\left(1-\mathrm{e}^{-\nu t}\right)\right]u'}\mathrm{e}^{-\tilde{a}(t)\left(k-\frac{k_\parallel}{\nu}\right)^2-\tilde{b}(t)\left(k-\frac{k_\parallel}{\nu}\right)-\tilde{c}(t)}. \tag{A.19}$$

The inhomogeneous linear ODE of first order

$$\frac{\mathrm{d}\tilde{f}_{\boldsymbol{m}}}{\mathrm{d}t} - p(t)\tilde{f}_{\boldsymbol{m}} = \tilde{Q}_{\boldsymbol{m}} \tag{A.20}$$

with $p(t) = -(\mathrm{i}\omega_\ell + Dk^2)$ can be solved by the method of variation of constants, e.g. [13, p. 269], by making an ansatz out of the homogeneous solution $\tilde{f}_{\boldsymbol{m}} = \alpha\exp(\int_{t_0}^{t}\mathrm{d}t'\,p(t')) \equiv \alpha\exp P(t)$ and letting α vary with t,

$$\tilde{f}_{\boldsymbol{m}} = \alpha(t)\exp(P(t)) \tag{A.21}$$

where $\alpha(t_0)$ is set to zero. Substituting the total time derivative of $\tilde{f}_{\boldsymbol{m}}$,

$$\dot{\tilde{f}}_{\boldsymbol{m}} = \dot{\alpha}\mathrm{e}^P + \alpha\dot{P}\mathrm{e}^P = \dot{\alpha}\mathrm{e}^P + \alpha p\mathrm{e}^P$$

into the ODE (A.20) yields

$$\dot{\alpha}\mathrm{e}^P + \alpha p\mathrm{e}^P = p\alpha\mathrm{e}^P + \tilde{Q}_{\boldsymbol{m}}.$$

Isolating $\dot{\alpha} = \tilde{Q}_{\boldsymbol{m}}\mathrm{e}^{-P}$ and integrating gives

$$\alpha(t) = \int_{t_0}^{t}\mathrm{d}t'\,\tilde{Q}_{\boldsymbol{m}}(t')\mathrm{e}^{-P(t')}.$$

Inserting this function into the ansatz (A.21) one obtains the solution of the inhomogeneous equation in k-space

$$\tilde{f}_{\boldsymbol{m}}(k,t) = \int_{t_0}^{t}\mathrm{d}t'\,\tilde{Q}_{\boldsymbol{m}}(k(0),t')\mathrm{e}^{P(t)-P(t')}. \tag{A.22}$$

By taking the inverse Fourier transform of $\tilde{f}_{\boldsymbol{m}}(k,t)$, one obtains [33]

$$\boxed{\tilde{f}_{\boldsymbol{m}}(u,t) = \int_{t_0}^{t} \mathrm{d}\tau \int_{\mathbb{R}} \mathrm{d}u'\, \tilde{G}^{\mathrm{D}}_{\boldsymbol{m}}(u,u',t-\tau)\tilde{Q}_{\boldsymbol{m}}(u',\tau)} \tag{A.23}$$

with Green's function

$$\begin{aligned}
\tilde{G}^{\mathrm{D}}_{\boldsymbol{m}}(u,u',t) &= \frac{1}{\sqrt{2\pi}} \int_{\mathbb{R}} \mathrm{d}k\, \mathrm{e}^{\mathrm{i}ku} \frac{1}{\sqrt{2\pi}} \mathrm{e}^{-\mathrm{i}\left[k\mathrm{e}^{-\nu t} + \frac{k_\parallel}{\nu}\left(1-\mathrm{e}^{-\nu t}\right)\right]u'} \mathrm{e}^{-\tilde{a}(t)\left(k-\frac{k_\parallel}{\nu}\right)^2 - \tilde{b}(t)\left(k-\frac{k_\parallel}{\nu}\right) - c(t)} \\
&= \frac{1}{2\pi} \int_{\mathbb{R}} \mathrm{d}k\, \mathrm{e}^{-\tilde{a}k^2 + \left(\mathrm{i}u - \mathrm{i}u'\mathrm{e}^{-\nu t} - \tilde{b} + \frac{2\tilde{a}k_\parallel}{\nu}\right)k + \left[-c - \mathrm{i}\frac{k_\parallel}{\nu}\left(1-\mathrm{e}^{-\nu t}\right)u' - \frac{k_\parallel^2}{\nu^2}\tilde{a} + \frac{k_\parallel}{\nu}\tilde{b}\right]} \\
&= \left| \int_{\mathbb{R}} \mathrm{d}k\, \mathrm{e}^{\alpha k^2 + \beta k + \gamma} = \sqrt{\frac{\pi}{-\alpha}} \mathrm{e}^{\gamma - \beta^2/(4\alpha)} \right| \\
&= \frac{1}{2\pi}\sqrt{\frac{\pi}{\tilde{a}}} \mathrm{e}^{\left[-c - \mathrm{i}\frac{k_\parallel}{\nu}\left(1-\mathrm{e}^{-\nu t}\right)u' - \frac{k_\parallel^2}{\nu^2}\tilde{a} + \frac{k_\parallel}{\nu}\tilde{b}\right] - \left(\mathrm{i}u - \mathrm{i}u'\mathrm{e}^{-\nu t} - \tilde{b} + \frac{2\tilde{a}k_\parallel}{\nu}\right)^2/(-4\tilde{a})} \\
&= \frac{1}{\sqrt{4\pi\tilde{a}}} \mathrm{e}^{\left[-c - \mathrm{i}\frac{k_\parallel}{\nu}\left(1-\mathrm{e}^{-\nu t}\right)u' - \frac{k_\parallel^2}{\nu^2}\tilde{a} + \frac{k_\parallel}{\nu}\tilde{b}\right] - \frac{u^2}{4\tilde{a}} + \frac{uu'}{2\tilde{a}}\mathrm{e}^{-\nu t} + \frac{\mathrm{i}u'}{2\tilde{a}}\tilde{b}\mathrm{e}^{-\nu t} + \frac{\mathrm{i}uk_\parallel}{\nu} - u'^2\frac{\mathrm{e}^{-2\nu t}}{4\tilde{a}}} \\
&\quad \times \mathrm{e}^{-\frac{\mathrm{i}}{2\tilde{a}}u\tilde{b} - \mathrm{i}u'\frac{k_\parallel}{\nu}\mathrm{e}^{-\nu t} + \frac{\tilde{b}^2}{4\tilde{a}} - \frac{\tilde{b}k_\parallel}{\nu} + \frac{\tilde{a}k_\parallel^2}{\nu^2}} \\
&= \frac{1}{\sqrt{4\pi\tilde{a}}} \exp\left[-c + \mathrm{i}\frac{k_\parallel}{\nu}(u-u') - \frac{1}{4\tilde{a}}\left(u - u'\mathrm{e}^{-\nu t} + \mathrm{i}\tilde{b}\right)^2\right],
\end{aligned} \tag{A.24}$$

which corresponds to Eq. (25) of Ivanov *et al.* [33].

A.2 The Collisionless Limit

Finally, the collisionless limit case is considered. In this limit, $\nu \to 0$, the initial PDE in k-space, Eq. (A.7) reads

$$\left[\frac{\partial}{\partial t} + \mathrm{i}\omega_\ell - k_\parallel \frac{\partial}{\partial k}\right] \tilde{f}_{\boldsymbol{m}}(k,t) = \tilde{Q}_{\boldsymbol{m}}(k,t). \tag{A.25}$$

Applying again the methods of characteristics, the homogeneous equation can be written as

$$\frac{\mathrm{d}}{\mathrm{d}s}\tilde{f}_{\boldsymbol{m}}(k(s),t(s)) = -\mathrm{i}\omega_\ell \tilde{f}_{\boldsymbol{m}}(k) \tag{A.26}$$

with $\mathrm{d}\tilde{f}_{\boldsymbol{m}}(k(s),t(s))/\,\mathrm{d}s = \partial\tilde{f}_{\boldsymbol{m}}/\partial k \cdot \mathrm{d}k/\,\mathrm{d}s + \partial\tilde{f}_{\boldsymbol{m}}/\partial t \cdot \mathrm{d}t/\,\mathrm{d}s$. From Eq. (A.25) one can read off

$$\frac{\mathrm{d}t}{\mathrm{d}s} = 1, \qquad \frac{\mathrm{d}k}{\mathrm{d}s} = -k_\parallel, \tag{A.27}$$

that with initial condition $t(0) = t_0 = 0$ allows one to identify $t = s$, whereupon the second equation reads $\mathrm{d}k/\,\mathrm{d}t = -k_\parallel$ and thus

$$k = -k_\parallel t + k_0 \tag{A.28}$$

with $k_0 = k(t_0) = \text{const}$. Eq. (A.26) is integrated by separation of variables,

$$\begin{aligned} \mathrm{d}\ln \tilde{f}_{\boldsymbol{m}} &= -\mathrm{i}\omega_\ell \,\mathrm{d}t \\ \tilde{f}_{\boldsymbol{m}}(k(t),t) &= \tilde{f}_{\boldsymbol{m}}(k_0,0)\,\mathrm{e}^{-\mathrm{i}\omega_\ell t} = \tilde{f}_{\boldsymbol{m}}(k+k_\parallel t,0)\,\mathrm{e}^{-\mathrm{i}\omega_\ell t}. \end{aligned} \tag{A.29}$$

The Fourier transform $\tilde{f}_{\boldsymbol{m}}(k_0,0)$ of the initial condition $\tilde{f}_{\boldsymbol{m}}(u,0) = \delta(u-u')$ is

$$\tilde{f}_{\boldsymbol{m}}(k_0,0) = \frac{\mathrm{e}^{-\mathrm{i}k_0 u'}}{\sqrt{2\pi}} = \frac{\mathrm{e}^{-\mathrm{i}(k+k_\parallel t)u'}}{\sqrt{2\pi}}.$$

One obtains the the Green's function in the collisionless limit by taking the inverse Fourier transform

$$\begin{aligned} \tilde{G}^{\mathrm{D}}_{\boldsymbol{m}}(u,u',t) &= \frac{1}{\sqrt{2\pi}}\int_{\mathbb{R}} \mathrm{d}k\,\mathrm{e}^{\mathrm{i}ku}\frac{1}{\sqrt{2\pi}}\mathrm{e}^{-\mathrm{i}(k+k_\parallel t)u'}\mathrm{e}^{-\mathrm{i}\omega_\ell t} \\ &= \frac{1}{2\pi}\int_{\mathbb{R}} \mathrm{d}k\,\mathrm{e}^{\mathrm{i}k(u-u')}\mathrm{e}^{-\mathrm{i}(k_\parallel u'+\omega_\ell)t} \\ &= \delta(u-u')\mathrm{e}^{-\mathrm{i}(k_\parallel u'+\omega_\ell)t}. \end{aligned} \tag{A.30}$$

Letting $t_0 \to -\infty$ and Fourier transforming w.r.t. time, the solution of the kinetic equation is

$$\begin{aligned} \tilde{f}_{\boldsymbol{m}}(u,\omega) &= \lim_{h\to\infty}\frac{1}{\sqrt{2\pi}}\int_{\mathbb{R}}\mathrm{d}t\,\mathrm{e}^{\mathrm{i}\omega t}\int_0^h \mathrm{d}\tau\int_{\mathbb{R}}\mathrm{d}u'\,\tilde{G}^{\mathrm{D}}_{\boldsymbol{m}}(u,u',\tau)\tilde{Q}_{\boldsymbol{m}}(u',t-\tau) \\ &= \lim_{h\to\infty}\int_0^h \mathrm{d}\tau\int_{\mathbb{R}}\mathrm{d}u'\,\tilde{G}^{\mathrm{D}}_{\boldsymbol{m}}(u,u',\tau)\mathrm{e}^{\mathrm{i}\omega\tau}\frac{1}{\sqrt{2\pi}}\int_{\mathbb{R}}\mathrm{d}t\,\mathrm{e}^{\mathrm{i}\omega(t-\tau)}\tilde{Q}_{\boldsymbol{m}}(u',t-\tau) \\ &= \lim_{h\to\infty}\int_0^h \mathrm{d}\tau\int_{\mathbb{R}}\mathrm{d}u'\,\tilde{G}^{\mathrm{D}}_{\boldsymbol{m}}(u,u',\tau)\mathrm{e}^{\mathrm{i}\omega\tau}\tilde{Q}_{\boldsymbol{m}}(u',\omega). \end{aligned} \tag{A.31}$$

Substituting the collisionless Green's function (A.30), the solution of the kinetic equation in the collisionless limit is obtained,

$$\begin{aligned} \tilde{f}_{\boldsymbol{m}}(u,\omega) &= \lim_{h\to\infty}\int_0^h \mathrm{d}\tau\int_{\mathbb{R}}\mathrm{d}u'\,\mathrm{e}^{\mathrm{i}(\omega-\omega_\ell-k_\parallel u')\tau}\delta(u-u')\tilde{Q}_{\boldsymbol{m}}(u',\omega) \\ &= \lim_{h\to\infty}\int_0^h \mathrm{d}\tau\,\mathrm{e}^{\mathrm{i}(\omega-\omega_\ell-k_\parallel u)\tau}\tilde{Q}_{\boldsymbol{m}}(u,\omega), \end{aligned}$$

$$\boxed{\tilde{f}_{\boldsymbol{m}}(u,\omega) = \frac{\mathrm{i}}{\omega - \omega_\ell - k_\parallel u + \mathrm{i}0^+}\,\tilde{Q}_{\boldsymbol{m}}(u,\omega),} \tag{A.32}$$

where

$$\lim_{h\to\infty}\int_0^h \mathrm{d}\tau\,\mathrm{e}^{\mathrm{i}\omega\tau} = -\frac{1}{\mathrm{i}}\left[\mathrm{P}\frac{1}{\omega} - \mathrm{i}\pi\delta(\omega)\right] = \frac{\mathrm{i}}{\omega + \mathrm{i}0^+}$$

and Plemelj's formula, see e.g. [64, p. 678], has been used.

Appendix B

Momentum- and Energy Conserving Collision Operators

B.1 Construction of a Momentum Conserving Collision Operator

Here, some intermediate calculations needed for the derivation of operator $\hat{L}_{\mathrm{cI}}^{\mathrm{M}}$ in Section 3.2 are collected:

$$\begin{aligned}\frac{\partial}{\partial u}(uf_0) &= f_0 + u\frac{\partial f_0}{\partial u} \\ &= \left[1 - \frac{u^2}{v_T^2}\right] f_0 \end{aligned} \tag{B.1}$$

$$\frac{\partial}{\partial u}(u^2 f_0) = \left[2 - \frac{u^2}{v_T^2}\right] f_0 \tag{B.2}$$

$$\begin{aligned}\frac{\partial^2}{\partial u^2}(uf_0) &= \frac{\partial}{\partial u}\left[\left(1 - \frac{u^2}{v_T^2}\right) f_0\right] \\ &= \frac{\partial f_0}{\partial u}\left(1 - \frac{u^2}{v_T^2}\right) - 2f_0\frac{u}{v_T^2} \\ &= -f_0\frac{u}{v_T^2}\left(1 - \frac{u^2}{v_T^2}\right) - 2f_0\frac{u}{v_T^2} \\ &= \left(\frac{u^2}{v_T^2} - 3\right) f_0\frac{u}{v_T^2} \end{aligned} \tag{B.3}$$

$$\begin{aligned}\hat{L}_{\mathrm{cD}}(uf_0) &= \nu f_0 \frac{u^3}{v_T^2} - 3\nu f_0 + 2\nu f_0 u - \nu f_0 \frac{u^3}{v_T^2} \\ &= -\nu f_0 u \end{aligned} \tag{B.4}$$

B.2 Conservation properties of the constructed integro-differential operators

In this section, the vanishing of $\hat{L}_{\mathrm{cp}} f_0$, $\hat{L}_{\mathrm{cp}} u f_0$, and $\hat{L}_{\mathrm{cp}} u^2 f_0$ shall be proven. The Fokker-Planck operator $\hat{L}_{\mathrm{cD}}$ in the Ornstein-Uhlenbeck approximation by itself conserves the number of particles, as was already pointed out by [33]. Here, it has to be shown that also the full operator that finally is applied to the kinetic equation, $\hat{L}_{\mathrm{cp}}$, conserves the number of particles, i.e. the integral operators must not give a contribution when acting on f_0.

In a similar fashion, for momentum conservation to hold, it will be shown that $\hat{L}^{\mathrm{M}}_{\mathrm{cI}} u f_0$ compensates exactly what remains when the differential part acts on uf_0 alone, i.e. $(\hat{L}_{\mathrm{cD}} + \hat{L}^{\mathrm{M}}_{\mathrm{cI}}) u f_0 = 0$. The energy conserving operator must not contribute when acting on uf_0, such that also $\hat{L}_{\mathrm{cp}} = (\hat{L}_{\mathrm{cD}} + \hat{L}^{\mathrm{M}}_{\mathrm{cI}} + \hat{L}^{\mathrm{E}}_{\mathrm{cI}}) u f_0 = 0$.

The same argument holds for energy conservation. $\hat{L}^{\mathrm{M}}_{\mathrm{cI}}$ only compensates the term arising from $\hat{L}_{\mathrm{cD}} u f_0$, but does not give a contribution acting on $u^2 f_0$. Again, $\hat{L}_{\mathrm{cp}} = (\hat{L}_{\mathrm{cD}} + \hat{L}^{\mathrm{M}}_{\mathrm{cI}} + \hat{L}^{\mathrm{E}}_{\mathrm{cI}}) u^2 f_0$ is shown to be zero, so that energy conservation is proven to hold.

To start with, $\hat{L}_{\mathrm{cp}} f_0 = 0$ shall be shown:

$$\begin{aligned}\hat{L}_{\mathrm{cD}} f_0 &= \nu v_T^2 \frac{\partial}{\partial u}\left(\frac{\partial f_0}{\partial u} + \frac{u}{v_T^2} f_0\right) \\ &= \nu v_T^2 \frac{\partial}{\partial u}\left(-\frac{u}{v_T^2} f_0 + \frac{u}{v_T^2} f_0\right) \\ &= 0, \end{aligned} \tag{B.5}$$

$$\begin{aligned}\hat{L}^{\mathrm{M}}_{\mathrm{cI}} f_0 &= \alpha^{\mathrm{M}}(u) \int_{\mathbb{R}} \mathrm{d}u'\, \beta^{\mathrm{M}}(u') f_0(v_\perp, u') \\ &= \frac{\nu}{\sqrt{2\pi v_T^2}} \mathrm{e}^{-u^2/2v_T^2} \frac{u}{v_T} \int_{\mathbb{R}} \mathrm{d}u'\, \frac{u'}{v_T} \frac{n_0}{(2\pi v_T^2)^{3/2}} \mathrm{e}^{-v_\perp^2/2v_T^2} \mathrm{e}^{-u'^2/2v_T^2} \\ &= \frac{\nu}{\sqrt{2\pi v_T^2}} f_0 \frac{u}{v_T} \int_{\mathbb{R}} \mathrm{d}u'\, \frac{u'}{v_T} \mathrm{e}^{-u'^2/2v_T^2} \\ &= 0, \end{aligned} \tag{B.6}$$

$$\begin{aligned}
\hat{L}^{\mathrm{E}}_{\mathrm{cI}} f_0 &= \alpha^{\mathrm{E}}(u) \int_{\mathbb{R}} \mathrm{d}u'\, \beta^{\mathrm{E}}(u') f_0(v_\perp, u') \\
&= \frac{\nu}{\sqrt{2\pi v_T^2}} \mathrm{e}^{-u^2/2v_T^2} \left(\frac{u^2}{v_T^2} - 1 \right) \int_{\mathbb{R}} \mathrm{d}u' \, \left(\frac{u'^2}{v_T^2} - 1 \right) \frac{n_0}{(2\pi v_T^2)^{3/2}} \mathrm{e}^{-v_\perp^2/2v_T^2} \mathrm{e}^{-u'^2/2v_T^2} \\
&= \frac{\nu}{\sqrt{2\pi v_T^2}} f_0 \left(\frac{u^2}{v_T^2} - 1 \right) \int_{\mathbb{R}} \mathrm{d}u' \, \left(\frac{u'^2}{v_T^2} - 1 \right) \mathrm{e}^{-u'^2/2v_T^2} \\
&= \frac{\nu}{\sqrt{2\pi v_T^2}} f_0 \left(\frac{u^2}{v_T^2} - 1 \right) \left(\frac{\sqrt{2\pi} v_T^3}{v_T^2} - \sqrt{2\pi} v_T \right) \\
&= 0. \qquad \text{(B.7)}
\end{aligned}$$

Thus, the particle number is conserved for the full integro-differential operator,

$$\boxed{\hat{L}_{\mathrm{cp}} f_0 = (\hat{L}_{\mathrm{cD}} + \hat{L}^{\mathrm{M}}_{\mathrm{cI}} + \hat{L}^{\mathrm{E}}_{\mathrm{cI}}) f_0 = 0.} \qquad \text{(B.8)}$$

Secondly, also $\hat{L}_{\mathrm{cp}} u f_0 = 0$ must hold:

$$\begin{aligned}
\hat{L}_{\mathrm{cD}} u f_0 &= \nu v_T^2 \frac{\partial}{\partial u} \left(\frac{\partial u f_0}{\partial u} + \frac{u^2}{v_T^2} f_0 \right) \\
&= \nu v_T^2 \frac{\partial}{\partial u} \left(f_0 - \frac{u^2}{v_T^2} f_0 + \frac{u^2}{v_T^2} f_0 \right) \\
&= -\nu u f_0, \qquad \text{(B.9)}
\end{aligned}$$

$$\begin{aligned}
\hat{L}^{\mathrm{M}}_{\mathrm{cI}} u f_0 &= \alpha^{\mathrm{M}}(u) \int_{\mathbb{R}} \mathrm{d}u'\, \beta^{\mathrm{M}}(u') u' f(u') \\
&= \frac{\nu}{\sqrt{2\pi v_T^2}} \mathrm{e}^{-u^2/2v_T^2} \frac{u}{v_T} \int_{\mathbb{R}} \mathrm{d}u' \, \frac{u'^2}{v_T} f_0(u') \\
&= \frac{\nu}{\sqrt{2\pi v_T^2}} \frac{u}{v_T^2} f_0(v_\perp, u) \int_{\mathbb{R}} \mathrm{d}u' \, u'^2 \mathrm{e}^{-u'^2/2v_T^2} \\
&= \frac{\nu}{\sqrt{2\pi v_T^2}} \frac{u}{v_T^2} f_0 \sqrt{2\pi} v_T^3 \\
&= \nu u f_0, \qquad \text{(B.10)}
\end{aligned}$$

$$\begin{aligned}
\hat{L}^{\mathrm{E}}_{\mathrm{cI}} u f_0 &= \alpha^{\mathrm{E}}(u) \int_{\mathbb{R}} \mathrm{d}u'\, \beta^{\mathrm{E}}(u') u' f_0(v_\perp, u') \\
&= \frac{\nu}{\sqrt{2\pi v_T^2}} \left(\frac{u^2}{v_T^2} - 1 \right) \mathrm{e}^{-u^2/2v_T^2} \int_{\mathbb{R}} \mathrm{d}u' \, \left(\frac{u'^2}{v_T^2} - 1 \right) u'
\end{aligned}$$

$$
\begin{aligned}
&\times \frac{n_0}{(2\pi v_T^2)^{3/2}} \mathrm{e}^{-v_\perp^2/2v_T^2} \mathrm{e}^{-u'^2/2v_T^2} \\
&= \frac{\nu}{\sqrt{2\pi v_T^2}} \left(\frac{u^2}{v_T^2} - 1 \right) f_0(v_\perp, u) \int_{\mathbb{R}} \mathrm{d}u' \, \left(\frac{u'^2}{v_T^2} - 1 \right) u' \mathrm{e}^{-u'^2/2v_T^2} \\
&= \frac{\nu}{\sqrt{2\pi v_T^2}} \left(\frac{u'^2}{v_T^2} - 1 \right) f_0(v_\perp, u) \\
&\quad \times \left(\int_{\mathbb{R}} \mathrm{d}u' \, \frac{u'^3}{v_T^2} \mathrm{e}^{-u'^2/2v_T^2} - \int_{\mathbb{R}} \mathrm{d}u' \, u' \mathrm{e}^{-u'^2/2v_T^2} \right) = 0.
\end{aligned} \tag{B.11}
$$

So again for the full operator momentum is conserved,

$$
\boxed{\hat{L}_{\mathrm{cp}} u f_0 = (\hat{L}_{\mathrm{cD}} + \hat{L}_{\mathrm{cI}}^{\mathrm{M}} + \hat{L}_{\mathrm{cI}}^{\mathrm{E}}) u f_0 = -\nu u f_0 + \nu u f_0 + 0 = 0.} \tag{B.12}
$$

Finally, we turn towards energy conservation and determine the action of the individual operators on $u^2 f_0$:

$$
\begin{aligned}
\hat{L}_{\mathrm{cD}} u^2 f_0 &= \nu v_T^2 \frac{\partial}{\partial u} \left(\frac{\partial u^2 f_0}{\partial u} + \frac{u^3}{v_T^2} f_0 \right) \\
&= \nu v_T^2 \frac{\partial}{\partial u} \left(2u f_0 - \frac{u^3}{v_T^2} f_0 + \frac{u^3}{v_T^2} f_0 \right) \\
&= 2\nu v_T^2 \left(1 - \frac{u^2}{v_T^2} \right) f_0,
\end{aligned} \tag{B.13}
$$

$$
\begin{aligned}
\hat{L}_{\mathrm{cI}}^{\mathrm{M}} \, u^2 f_0 &= \alpha^{\mathrm{M}}(u) \int_{\mathbb{R}} \mathrm{d}u' \, \beta^{\mathrm{M}}(u') u'^2 f_0 \\
&= \frac{\nu}{\sqrt{2\pi v_T^2}} \mathrm{e}^{-u^2/2v_T^2} \frac{u}{v_T} \int_{\mathbb{R}} \mathrm{d}u' \, \frac{u'}{v_T} u'^2 \frac{n_0}{(2\pi v_T^2)^{3/2}} \mathrm{e}^{-u'^2/2v_T^2} \mathrm{e}^{-v_\perp^2/2v_T^2} \\
&= \frac{\nu}{\sqrt{2\pi v_T^2}} \frac{u}{v_T^2} f_0(v_\perp, u) \int_{\mathbb{R}} \mathrm{d}u' \, u'^3 \mathrm{e}^{-u'^2/2v_T^2} \\
&= 0,
\end{aligned} \tag{B.14}
$$

$$
\begin{aligned}
\hat{L}_{\mathrm{cI}}^{\mathrm{E}} \, u^2 f_0 &= \alpha^{\mathrm{E}}(u) \int_{\mathbb{R}} \mathrm{d}u' \, \beta^{\mathrm{E}}(u') u'^2 f_0(v_\perp, u') \\
&= \frac{\nu}{\sqrt{2\pi v_T^2}} \left(\frac{u^2}{v_T^2} - 1 \right) \mathrm{e}^{-u^2/2v_T^2} \int_{\mathbb{R}} \mathrm{d}u' \, \left(\frac{u'^2}{v_T^2} - 1 \right) u'^2 f_0(v_\perp, u') \\
&= \frac{\nu}{\sqrt{2\pi v_T^2}} \left(\frac{u^2}{v_T^2} - 1 \right) \left(\int_{\mathbb{R}} \mathrm{d}u' \, \frac{u'^4}{v_T^2} \mathrm{e}^{-u'^2/2v_T^2} - \int_{\mathbb{R}} \mathrm{d}u' \, u'^2 \mathrm{e}^{-u'^2/2v_T^2} \right) \\
&= \frac{\nu}{\sqrt{2\pi v_T^2}} \left(\frac{u^2}{v_T^2} - 1 \right) 2\sqrt{2\pi} v_T^3
\end{aligned}
$$

$$= 2\nu v_T^2 \left(\frac{u^2}{v_T^2} - 1 \right) f_0. \tag{B.15}$$

We see that also the full operator conserves energy,

$$\boxed{\hat{L}_{\rm cp} u^2 f_0 = 2\nu v_T^2 \left(1 - \frac{u^2}{v_T^2} \right) f_0 + 0 + 2\nu v_T^2 \left(\frac{u^2}{v_T^2} - 1 \right) f_0 = 0.} \tag{B.16}$$

This particle-, momentum- and energy conserving operator $\hat{L}_{\rm cp}$ is applied to the kinetic equation in Sect. 3.3.

Appendix C

Explicit Evaluation of the Diffusion Matrix

C.1 Diffusion Coefficients for the Collisional Case

In Section 3.5.1 the resulting diffusion coefficients for the collisional case are given. Here one can find their full derivation based on the general formula Eq. (3.98).

$$
\begin{aligned}
D_{11} &= \frac{1}{\sqrt{8\pi}v_T B_0^2}\,\Re\sum_{\boldsymbol{m}}\int_{-\infty}^{\infty}\mathrm{d}u\int_{-\infty}^{\infty}\mathrm{d}u'\,\tilde{G}_{\omega\boldsymbol{m}}(u,u')\exp\left(-\frac{mu'^2}{2T}\right)\\
&\quad\times\left(uu'|\tilde{B}^r_{\boldsymbol{m}}|^2+cu\tilde{E}_{\boldsymbol{m}\perp}\tilde{B}^{r*}_{\boldsymbol{m}}+cu'\tilde{E}^*_{\boldsymbol{m}\perp}\tilde{B}^r_{\boldsymbol{m}}+c^2|\tilde{E}_{\boldsymbol{m}\perp}|^2\right)\\
&= \frac{1}{\sqrt{8\pi}v_T B_0^2}\,\Re\sum_{\boldsymbol{m}}\left(\frac{\sqrt{2\pi}v_T^3}{\nu}I^{11}|\tilde{B}^r_{\boldsymbol{m}}|^2\right.\\
&\quad\left.+\frac{\sqrt{2\pi}v_T^2}{\nu}I^{10}c(\tilde{E}_{\boldsymbol{m}\perp}\tilde{B}^{r*}_{\boldsymbol{m}}+\tilde{E}^*_{\boldsymbol{m}\perp}\tilde{B}^r_{\boldsymbol{m}})+\frac{\sqrt{2\pi}v_T}{\nu}I^{00}c^2|\tilde{E}_{\boldsymbol{m}\perp}|^2\right)\\
&= \frac{1}{2\nu B_0^2}\,\Re\sum_{\boldsymbol{m}}\left[c^2I^{00}|\tilde{E}_{\boldsymbol{m}\perp}|^2+cv_T\left(\tilde{B}^{r*}_{\boldsymbol{m}}\tilde{E}_{\boldsymbol{m}\perp}+\tilde{E}^*_{\boldsymbol{m}\perp}\tilde{B}^r_{\boldsymbol{m}}\right)I^{10}\right.\\
&\quad\left.+v_T^2|\tilde{B}^r_{\boldsymbol{m}}|^2I^{11}\right],
\end{aligned}
\tag{C.1}
$$

$$
\begin{aligned}
D_{12} &= \frac{1}{\sqrt{8\pi}v_T B_0^2}\,\Re\sum_{\boldsymbol{m}}\int_{-\infty}^{\infty}\mathrm{d}u\int_{-\infty}^{\infty}\mathrm{d}u'\,\tilde{G}_{\omega\boldsymbol{m}}(u,u')\exp\left(-\frac{mu'^2}{2T}\right)\\
&\quad\times\left(uu'|\tilde{B}^r_{\boldsymbol{m}}|^2+cu\tilde{E}_{\boldsymbol{m}\perp}\tilde{B}^{r*}_{\boldsymbol{m}}+cu'\tilde{E}^*_{\boldsymbol{m}\perp}\tilde{B}^r_{\boldsymbol{m}}+c^2|\tilde{E}_{\boldsymbol{m}\perp}|^2\right)\left(1+\frac{u'^2}{2v_T^2}\right)
\end{aligned}
$$

$$
\begin{aligned}
&= D_{11} + \frac{1}{\sqrt{8\pi} v_T B_0^2} \Re \sum_{\boldsymbol{m}} \int_{-\infty}^{\infty} \mathrm{d}u \int_{-\infty}^{\infty} \mathrm{d}u' \, \tilde{G}_{\omega \boldsymbol{m}}(u, u') \exp\left(-\frac{m u'^2}{2T}\right) \\
&\quad \times \left(\frac{u u'^3 |\tilde{B}^r_{\boldsymbol{m}}|^2}{2 v_T^2} + \frac{c u u'^2 \tilde{B}^{r*}_{\boldsymbol{m}} \tilde{E}_{\boldsymbol{m}\perp}}{2 v_T^2} + \frac{c u'^3 \tilde{E}^*_{\boldsymbol{m}\perp} \tilde{B}^r_{\boldsymbol{m}}}{2 v_T^2} + \frac{c^2 u'^2 |\tilde{E}_{\boldsymbol{m}\perp}|^2}{2 v_T^2} \right) \\
&= D_{11} + \frac{1}{4\nu B_0^2} \Re \sum_{\boldsymbol{m}} \Big[v_T^2 |\tilde{B}^r_{\boldsymbol{m}}|^2 I^{31} + c v_T (\tilde{E}_{\boldsymbol{m}\perp} \tilde{B}^{r*}_{\boldsymbol{m}} I^{21} + \tilde{E}^*_{\boldsymbol{m}\perp} \tilde{B}^r_{\boldsymbol{m}} I^{30}) \\
&\quad + c^2 |\tilde{E}_{\boldsymbol{m}\perp}|^2 I^{20} \Big], \qquad \text{(C.2)}
\end{aligned}
$$

$$
\begin{aligned}
D_{13} &= \frac{1}{\sqrt{8\pi} v_T B_0^2} \Re \sum_{\boldsymbol{m}} \int_{-\infty}^{\infty} \mathrm{d}u \int_{-\infty}^{\infty} \mathrm{d}u' \, \tilde{G}_{\omega \boldsymbol{m}}(u, u') \exp\left(-\frac{m u'^2}{2T}\right) \\
&\quad \times \left(u u'' |\tilde{B}^r_{\boldsymbol{m}}|^2 + c u \tilde{E}_{\boldsymbol{m}\perp} \tilde{B}^{r*}_{\boldsymbol{m}} + c u \tilde{E}^*_{\boldsymbol{m}\perp} \tilde{B}^r_{\boldsymbol{m}} + c^2 |\tilde{E}_{\boldsymbol{m}\perp}|^2 \right) \frac{u'}{v_T} \\
&= \frac{1}{\sqrt{8\pi} v_T B_0^2} \Re \sum_{\boldsymbol{m}} \left(\frac{\sqrt{2\pi} v_T^4}{\nu v_T} I^{21} |\tilde{B}^r_{\boldsymbol{m}}|^2 + \frac{\sqrt{2\pi} v_T^3}{\nu v_T} (c \tilde{E}_{\boldsymbol{m}\perp} \tilde{B}^{r*}_{\boldsymbol{m}} I^{11} \right. \\
&\quad \left. + c \tilde{E}^*_{\boldsymbol{m}\perp} \tilde{B}^r_{\boldsymbol{m}} I^{20}) + \frac{\sqrt{2\pi} v_T^2 c^2 |\tilde{E}_{\boldsymbol{m}\perp}|^2}{\nu v_T} \right) \\
&= \frac{1}{2\nu B_0^2} \Re \sum_{\boldsymbol{m}} \Big(v_T^2 |\tilde{B}^r_{\boldsymbol{m}}|^2 I^{21} + c v_T (\tilde{E}_{\boldsymbol{m}\perp} \tilde{B}^{r*}_{\boldsymbol{m}} I^{11} + \tilde{E}^*_{\boldsymbol{m}\perp} \tilde{B}^r_{\boldsymbol{m}} I^{20}) \\
&\quad + c^2 |\tilde{E}_{\boldsymbol{m}\perp}|^2 I^{10} \Big), \qquad \text{(C.3)}
\end{aligned}
$$

$$
\begin{aligned}
D_{21} &= \frac{1}{\sqrt{8\pi} v_T B_0^2} \Re \sum_{\boldsymbol{m}} \int_{-\infty}^{\infty} \mathrm{d}u \int_{-\infty}^{\infty} \mathrm{d}u' \, \tilde{G}_{\omega \boldsymbol{m}}(u, u') \exp\left(-\frac{m u'^2}{2T}\right) \\
&\quad \times \left(u u' |\tilde{B}^r_{\boldsymbol{m}}|^2 + c u \tilde{E}_{\boldsymbol{m}\perp} \tilde{B}^{r*}_{\boldsymbol{m}} + c u' \tilde{E}^*_{\boldsymbol{m}\perp} \tilde{B}^r_{\boldsymbol{m}} + c^2 |\tilde{E}_{\boldsymbol{m}\perp}|^2 \right) \left(1 + \frac{u^2}{2 v_T^2} \right) \\
&= D_{11} + \frac{1}{\sqrt{8\pi} v_T B_0^2} \Re \sum_{\boldsymbol{m}} \int_{-\infty}^{\infty} \mathrm{d}u \int_{-\infty}^{\infty} \mathrm{d}u' \, \tilde{G}_{\omega \boldsymbol{m}}(u, u') \exp\left(-\frac{m u'^2}{2T}\right) \\
&\quad \times \left(\frac{u^3 u' |\tilde{B}^r_{\boldsymbol{m}}|^2}{2 v_T^2} + \frac{c u^3 \tilde{E}_{\boldsymbol{m}\perp} \tilde{B}^{r*}_{\boldsymbol{m}}}{2 v_T^2} + \frac{c u^2 u'^2 \tilde{E}^*_{\boldsymbol{m}\perp} \tilde{B}^r_{\boldsymbol{m}}}{2 v_T^2} + \frac{c^2 u^2 |\tilde{E}_{\boldsymbol{m}\perp}|^2}{2 v_T^2} \right) \\
&= D_{11} + \frac{1}{4\nu B_0^2} \Re \sum_{\boldsymbol{m}} \Big(v_T^2 |\tilde{B}^r_{\boldsymbol{m}}|^2 I^{31} + c v_T (\tilde{E}_{\boldsymbol{m}\perp} \tilde{B}^{r*}_{\boldsymbol{m}} I^{30} + \tilde{E}^*_{\boldsymbol{m}\perp} \tilde{B}^r_{\boldsymbol{m}} I^{21}) \\
&\quad + c^2 |\tilde{E}_{\boldsymbol{m}\perp}|^2 I^{20} \Big), \qquad \text{(C.4)}
\end{aligned}
$$

$$
\begin{aligned}
D_{22} &= \frac{1}{\sqrt{8\pi}v_T B_0^2}\,\Re\sum_{\boldsymbol{m}}\int_{-\infty}^{\infty}\mathrm{d}u\int_{-\infty}^{\infty}\mathrm{d}u'\,\tilde{G}_{\omega\boldsymbol{m}}(u,u')\exp\left(-\frac{mu'^2}{2T}\right)\\
&\quad\times\left(uu'|\tilde{B}^r_{\boldsymbol{m}}|^2+cu\tilde{E}_{\boldsymbol{m}\perp}\tilde{B}^{r*}_{\boldsymbol{m}}+cu'\tilde{E}^*_{\boldsymbol{m}\perp}\tilde{B}^r_{\boldsymbol{m}}+c^2|\tilde{E}_{\boldsymbol{m}\perp}|^2\right)\\
&\quad\times\left(2+\frac{u^2+u'^2}{2v_T^2}+\frac{u^2u'^2}{4v_T^4}\right)\\
&= 2D_{11}+\frac{1}{\sqrt{8\pi}v_T B_0^2}\,\Re\sum_{\boldsymbol{m}}\int_{-\infty}^{\infty}\mathrm{d}u\int_{-\infty}^{\infty}\mathrm{d}u'\,\tilde{G}_{\omega\boldsymbol{m}}(u,u')\exp\left(-\frac{mu'^2}{2T}\right)\\
&\quad\times\frac{1}{2v_T^2}\left(u^3u'|\tilde{B}^r_{\boldsymbol{m}}|^2+uu'^3|\tilde{B}^r_{\boldsymbol{m}}|^2+cu^3\tilde{E}_{\boldsymbol{m}\perp}\tilde{B}^{r*}_{\boldsymbol{m}}+cuu'^2\tilde{E}_{\boldsymbol{m}\perp}\tilde{B}^{r*}_{\boldsymbol{m}}\right.\\
&\quad+cu^2u'\tilde{E}^*_{\boldsymbol{m}\perp}\tilde{B}^r_{\boldsymbol{m}}+cu'^3\tilde{E}^*_{\boldsymbol{m}\perp}\tilde{B}^r_{\boldsymbol{m}}+c^2u^2|\tilde{E}_{\boldsymbol{m}}|^2+c^2|\tilde{E}_{\boldsymbol{m}\perp}|^2u'^2\\
&\quad\left.+\frac{u^3u'^3|\tilde{B}^r_{\boldsymbol{m}}|^2}{2}+\frac{cu^3u'^2\tilde{E}_{\boldsymbol{m}\perp}\tilde{B}^{r*}_{\boldsymbol{m}}}{2}+\frac{cu^2u'^3\tilde{E}^*_{\boldsymbol{m}\perp}\tilde{B}^r_{\boldsymbol{m}}}{2}+\frac{c^2u^2u'^2|\tilde{E}_{\boldsymbol{m}\perp}|^2}{2}\right)\\
&= 2D_{11}+\frac{1}{4\nu B_0^2}\,\Re\sum_{\boldsymbol{m}}\left(2v_T^2|\tilde{B}^r_{\boldsymbol{m}}|^2I^{31}+cv_T\tilde{E}_{\boldsymbol{m}\perp}\tilde{B}^{r*}_{\boldsymbol{m}}(I^{30}+I^{21})\right.\\
&\quad+cv_TE^*_{\boldsymbol{m}\perp}\tilde{B}^r_{\boldsymbol{m}}(I^{21}+I^{30})+2c^2|\tilde{E}_{\boldsymbol{m}\perp}|^2I^{20}+\frac{v_T^2|\tilde{B}^r_{\boldsymbol{m}}|^2}{2}I^{33}\\
&\quad\left.+\frac{cv_T}{2}I^{32}(\tilde{E}_{\boldsymbol{m}\perp}\tilde{B}^{r*}_{\boldsymbol{m}}+\tilde{E}^*_{\boldsymbol{m}\perp}\tilde{B}^r_{\boldsymbol{m}})+\frac{c^2|\tilde{E}_{\boldsymbol{m}\perp}|^2}{2}I^{22}\right),
\end{aligned}
\tag{C.5}
$$

$$
\begin{aligned}
D_{23} &= \frac{1}{8\pi v_T B_0^2}\,\Re\sum_{\boldsymbol{m}}\int_{-\infty}^{\infty}\mathrm{d}u\int_{-\infty}^{\infty}\mathrm{d}u'\,\tilde{G}_{\omega\boldsymbol{m}}(u,u')\exp\left(-\frac{mu'^2}{2T}\right)\\
&\quad\times\left(uu'|\tilde{B}^r_{\boldsymbol{m}}|^2+cu\tilde{E}_{\boldsymbol{m}\perp}\tilde{B}^{r*}_{\boldsymbol{m}}+cu'\tilde{E}^*_{\boldsymbol{m}\perp}\tilde{B}^r_{\boldsymbol{m}}+c^2|\tilde{E}_{\boldsymbol{m}\perp}|^2\right)\\
&\quad\times\left(\frac{u'}{v_T}+\frac{u^2u'}{2v_T^3}\right)\\
&= \frac{1}{\sqrt{8\pi}v_T B_0^2}\left[\frac{\sqrt{2\pi}v_T^4}{\nu v_T}|\tilde{B}^r_{\boldsymbol{m}}|^2I^{12}+\frac{\sqrt{2\pi}v_T^6}{2\nu v_T^3}|\tilde{B}^r_{\boldsymbol{m}}|^2I^{32}\right.\\
&\quad+\frac{cv_T}{\nu}\tilde{E}_{\boldsymbol{m}\perp}\tilde{B}^r_{\boldsymbol{m}}\left(I^{11}+\frac{I^{31}}{2}\right)+\frac{cv_T}{\nu}\tilde{E}^*_{\boldsymbol{m}\perp}\tilde{B}^r_{\boldsymbol{m}}\left(I^{20}+\frac{I^{22}}{2}\right)\\
&\quad\left.+c^2|\tilde{E}_{\boldsymbol{m}\perp}|^2\left(I^{10}+\frac{I^{21}}{2}\right)\right]\\
&= \frac{1}{2\nu B_0^2}\left[v_T^2|B^r_{\boldsymbol{m}}|^2\left(I^{21}+\frac{I^{32}}{2}\right)+cv_T\tilde{E}_{\boldsymbol{m}\perp}\tilde{B}^{r*}_{\boldsymbol{m}}\left(I^{11}+\frac{I^{31}}{2}\right)\right.
\end{aligned}
$$

$$+\ cv_T\tilde{E}^*_{\boldsymbol{m}\perp}\tilde{B}^r_{\boldsymbol{m}}\left(I^{20}+\frac{I^{22}}{2}\right)+c^2|\tilde{E}_{\boldsymbol{m}\perp}|^2\left(I^{10}+\frac{I^{21}}{2}\right)\Bigg], \tag{C.6}$$

$$\begin{aligned}
D_{31} &= \frac{1}{\sqrt{8\pi}v_TB_0^2}\,\Re\sum_{\boldsymbol{m}}\int_{-\infty}^{\infty}\mathrm{d}u\int_{-\infty}^{\infty}\mathrm{d}u'\,\tilde{G}_{\omega\boldsymbol{m}}(u,u')\exp\left(-\frac{mu'^2}{2T}\right)\\
&\quad\times\left(uu'|\tilde{B}^r_{\boldsymbol{m}}|^2+cu\tilde{E}_{\boldsymbol{m}\perp}\tilde{B}^{r*}_{\boldsymbol{m}}+cu'\tilde{E}^*_{\boldsymbol{m}\perp}\tilde{B}^r_{\boldsymbol{m}}+c^2|\tilde{E}_{\boldsymbol{m}\perp}|^2\right)\frac{u}{v_T}\\
&= \frac{1}{\sqrt{8\pi}v_TB_0^2}\,\Re\sum_{\boldsymbol{m}}\Bigg[\frac{\sqrt{2\pi}v_T^4}{\nu v_T}|\tilde{B}^r_{\boldsymbol{m}}|^2I^{21}+\frac{c\sqrt{2\pi}v_T^3}{\nu v_T}\Big(\tilde{E}_{\boldsymbol{m}\perp}\tilde{B}^{r*}_{\boldsymbol{m}}I^{20}\\
&\quad+\ \tilde{E}^*_{\boldsymbol{m}\perp}\tilde{B}^r_{\boldsymbol{m}}I^{11}\Big)+\frac{c^2\sqrt{2\pi}v_T^2}{\nu v_T}|\tilde{E}_{\boldsymbol{m}\perp}|^2I^{10}\Bigg]\\
&= \frac{1}{2\nu B_0^2}\,\Re\sum_{\boldsymbol{m}}\Big[v_T^2|\tilde{B}^r_{\boldsymbol{m}}|^2I^{21}+cv_T(\tilde{E}_{\boldsymbol{m}\perp}\tilde{B}^{r*}_{\boldsymbol{m}}I^{20}+\tilde{E}_{\boldsymbol{m}\perp}\tilde{B}^r_{\boldsymbol{m}}I^{11})\\
&\quad+\ c^2|\tilde{E}_{\boldsymbol{m}\perp}|^2I^{10}\Big],
\end{aligned} \tag{C.7}$$

$$\begin{aligned}
D_{32} &= \frac{1}{\sqrt{8\pi}v_TB_0^2}\,\Re\sum_{\boldsymbol{m}}\int_{-\infty}^{\infty}\mathrm{d}u\int_{-\infty}^{\infty}\mathrm{d}u'\,\tilde{G}_{\omega\boldsymbol{m}}(u,u')\exp\left(-\frac{mu'^2}{2T}\right)\\
&\quad\times\left(uu'|\tilde{B}^r_{\boldsymbol{m}}|^2+cu\tilde{E}_{\boldsymbol{m}\perp}\tilde{B}^{r*}_{\boldsymbol{m}}+cu'\tilde{E}^*_{\boldsymbol{m}\perp}\tilde{B}^r_{\boldsymbol{m}}+c^2|\tilde{E}_{\boldsymbol{m}\perp}|^2\right)\\
&\quad\times\left(\frac{u}{v_T}+\frac{uu'^2}{2v_T^3}\right)\\
&= \frac{1}{\sqrt{8\pi}v_TB_0^2}\,\Re\sum_{\boldsymbol{m}}\Bigg[\frac{\sqrt{2\pi}v_T^4}{\nu v_T}|\tilde{B}^r_{\boldsymbol{m}}|^2I^{21}+\frac{\sqrt{2\pi}v_T^6}{2\nu v_T^3}|\tilde{B}^r_{\boldsymbol{m}}|^2I^{23}\\
&\quad+\frac{c\sqrt{2\pi}v_T^3}{\nu v_T}\tilde{E}_{\boldsymbol{m}\perp}\tilde{B}^{r*}_{\boldsymbol{m}}I^{20}+\frac{c\sqrt{2\pi}v_T^5}{2\nu v_T^3}\tilde{E}_{\boldsymbol{m}\perp}\tilde{B}^{r*}_{\boldsymbol{m}}I^{22}+\frac{c\sqrt{2\pi}v_T^3}{\nu v_T}\tilde{E}_{\boldsymbol{m}\perp}\tilde{B}^r_{\boldsymbol{m}}I^{11}\\
&\quad+\frac{c\sqrt{2\pi}v_T^5}{2\nu v_T^3}\tilde{E}^*_{\boldsymbol{m}\perp}\tilde{B}^r_{\boldsymbol{m}}I^{13}+\frac{c^2\sqrt{2\pi}v_T^2}{\nu v_T}|\tilde{E}_{\boldsymbol{m}\perp}|^2I^{10}+\frac{c^2\sqrt{2\pi}v_T^4}{2\nu v_T^3}|\tilde{E}_{\boldsymbol{m}\perp}|^2I^{12}\Bigg]\\
&= \frac{1}{2\nu B_0^2}\,\Re\sum_{\boldsymbol{m}}\Bigg[v_T^2|\tilde{B}^r_{\boldsymbol{m}}|^2\left(I^{21}+\frac{I^{23}}{2}\right)+cv_T\tilde{E}_{\boldsymbol{m}\perp}\tilde{B}^{r*}_{\boldsymbol{m}}\left(I^{20}+\frac{I^{22}}{2}\right)\\
&\quad+cv_T\tilde{E}^*_{\boldsymbol{m}\perp}\tilde{B}^r_{\boldsymbol{m}}\left(I^{11}+\frac{I^{13}}{2}\right)+c^2|\tilde{E}_{\boldsymbol{m}\perp}|^2\left(I^{10}+\frac{I^{12}}{2}\right)\Bigg],
\end{aligned} \tag{C.8}$$

$$D_{33} = \frac{1}{\sqrt{8\pi}v_TB_0^2}\,\Re\sum_{\boldsymbol{m}}\int_{-\infty}^{\infty}\mathrm{d}u\int_{-\infty}^{\infty}\mathrm{d}u'\,\tilde{G}_{\omega\boldsymbol{m}}(u,u')\exp\left(-\frac{mu'^2}{2T}\right)$$

$$
\begin{aligned}
&\times \left(uu' |\tilde{B}^r_{\boldsymbol{m}}|^2 + cu \tilde{E}_{\boldsymbol{m}\perp} \tilde{B}^{r*}_{\boldsymbol{m}} + cu' \tilde{E}^*_{\boldsymbol{m}\perp} \tilde{B}^r_{\boldsymbol{m}} + c^2 |\tilde{E}_{\boldsymbol{m}\perp}|^2 \right) \frac{uu'}{v_T^2} \\
&= \frac{1}{\sqrt{8\pi} v_T B_0^2} \Re \sum_{\boldsymbol{m}} \left[\frac{\sqrt{2\pi} v_T^5}{\nu v_T^2} |\tilde{B}^r_{\boldsymbol{m}}|^2 I^{22} + \frac{c\sqrt{2\pi} v_T^4}{\nu v_T^2} \tilde{E}_{\boldsymbol{m}\perp} \tilde{B}^{r*}_{\boldsymbol{m}} I^{21} \right. \\
&\quad \left. + \frac{c\sqrt{2\pi} v_T^4 \tilde{E}^*_{\boldsymbol{m}\perp} \tilde{B}^r_{\boldsymbol{m}}}{\nu v_T^2} I^{12} + \frac{c^2 \sqrt{2\pi} v_T^3}{\nu v_T^2} |\tilde{E}_{\boldsymbol{m}\perp}|^2 I^{11} \right] \\
&= \frac{1}{2\nu B_0^2} \Re \sum_{\boldsymbol{m}} \left[v_T^2 |\tilde{B}^r_{\boldsymbol{m}}|^2 I^{22} + c v_T \left(\tilde{E}_{\boldsymbol{m}\perp} \tilde{B}^{r*}_{\boldsymbol{m}} I^{21} + \tilde{E}^*_{\boldsymbol{m}\perp} \tilde{B}^r_{\boldsymbol{m}} I^{12} \right) \right. \\
&\quad \left. + c^2 |\tilde{E}_{\boldsymbol{m}\perp}|^2 I^{11} \right] . \qquad \text{(C.9)}
\end{aligned}
$$

C.2 Diffusion Coefficients in the Collisionless Limit

Here, the explicit evaluation of the diffusion coefficients in the collisionless limit case, based on Eq. (3.109) and discussed in Section 3.5.1, is given.

$$
\begin{aligned}
D_{11} &= \frac{\pi}{2n_0} \sum_{\boldsymbol{m}} \int_{\mathbb{R}^3} \mathrm{d}^3 p \, \delta(k_\parallel u + \omega_E) |v^r_{\boldsymbol{m}}|^2 f_0 \\
&= \frac{\pi m^3}{2n_0} \sum_{\boldsymbol{m}} \int_{-\infty}^{\infty} \mathrm{d}u \frac{\delta(u + \omega_E/k_\parallel)}{k_\parallel} |v^r_{\boldsymbol{m}}|^2 \int_0^\infty 2\pi v_\perp \, \mathrm{d}v_\perp \\
&\quad \times \frac{n_0}{(2\pi m T)^{3/2}} \exp\left[-\frac{m(v_\perp^2 + u^2)}{2T} \right] \\
&= \frac{\sqrt{\pi}}{2^{3/2} k_\parallel v_T} \exp\left(-\frac{\omega_E^2}{2k_\parallel^2 v_T^2} \right) \sum_{\boldsymbol{m}} |v^r_{\boldsymbol{m}}|^2_{u=-\omega_E/k_\parallel} \\
&= \frac{\sqrt{\pi}|Z|}{2|\omega_E|} \mathrm{e}^{-Z^2} \sum_{\boldsymbol{m}} |v^r_{\boldsymbol{m}}|^2_{u=-\omega_E/k_\parallel}, \qquad \text{(C.10)}
\end{aligned}
$$

$$
\begin{aligned}
D_{12} &= \frac{\pi}{2n_0} \sum_{\boldsymbol{m}} \int_{\mathbb{R}^3} \mathrm{d}^3 p \, \delta(k_\parallel u + \omega_E) |v^r_{\boldsymbol{m}}|^2 \frac{m}{2T} (v_\perp^2 + u^2) \\
&\quad \times \frac{n_0}{(2\pi m T)^{3/2}} \exp\left(-\frac{v_\perp^2 + u^2}{2v_T^2} \right) \\
&= \frac{m^3}{2^{7/2} \sqrt{\pi} (mT)^{3/2} v_T^2} \sum_{\boldsymbol{m}} \int_{\mathbb{R}} \mathrm{d}u \, \frac{\delta(u + \omega_E/k_\parallel)}{k_\parallel} |v^r_{\boldsymbol{m}}|^2 \mathrm{e}^{-u^2/2v_T^2} \\
&\quad \times \int_0^\infty 2\pi v_\perp \, \mathrm{d}v_\perp \, \mathrm{e}^{-v_\perp^2/2v_T^2} \left(v_\perp^2 + u^2 \right)
\end{aligned}
$$

$$
\begin{aligned}
&= \frac{\sqrt{\pi}}{2^{5/2}k_\parallel v_T^5}\sum_{\boldsymbol{m}}\int_{\mathbb{R}}\mathrm{d}u\,\mathrm{e}^{-u^2/2v_T^2}\delta(u+\omega/k_\parallel)|v_{\boldsymbol{m}}^r|^2 v_T^2\left(2v_T^2+u^2\right)\\
&= \frac{\sqrt{\pi}}{2^{5/2}k_\parallel v_T^3}\exp\left(-\frac{\omega_E^2}{2k_\parallel^2 v_T^2}\right)\sum_{\boldsymbol{m}}|v_{\boldsymbol{m}}^r|^2_{u=-\omega_E/k_\parallel}\left(2v_T^2+\frac{\omega_E^2}{k_\parallel^2}\right)\\
&= \frac{\sqrt{\pi}|Z|}{2|\omega_E|}\mathrm{e}^{-Z^2}\sum_{\boldsymbol{m}}|v_{\boldsymbol{m}}^r|^2_{u=-\omega_E/k_\parallel}\left(1+\frac{1}{2}\frac{\omega_E^2}{k_\parallel^2 v_T^2}\right), \qquad \text{(C.11)}
\end{aligned}
$$

$$
\begin{aligned}
D_{13} &= \frac{\pi}{2n_0}\sum_{\boldsymbol{m}}\int_{\mathbb{R}^3}\mathrm{d}^3p\,\delta(k_\parallel u+\omega_E)|v_{\boldsymbol{m}}^r|^2\frac{m}{T}uv_T\\
&\quad\times\frac{n_0}{(2\pi mT)^{3/2}}\exp\left(-\frac{v_\perp^2+u^2}{2v_T^2}\right)\\
&= \frac{m^3}{2^{5/2}\sqrt{\pi}(mT)^{3/2}v_T}\sum_{\boldsymbol{m}}\int_{\mathbb{R}}\mathrm{d}u\,\frac{\delta(u+\omega_E/k_\parallel)}{k_\parallel}|v_{\boldsymbol{m}}^r|^2 u\mathrm{e}^{-u^2/2v_T^2}\\
&\quad\times\int_0^\infty 2\pi v_\perp\,\mathrm{d}v_\perp\,\mathrm{e}^{-v_\perp^2/2v_T^2}\\
&= \frac{\sqrt{\pi}}{2^{3/2}k_\parallel v_T^4}\sum_{\boldsymbol{m}}\int_{\mathbb{R}}\mathrm{d}u\,\delta(u+\omega_E/k_\parallel)|v_{\boldsymbol{m}}^r|^2 u\mathrm{e}^{-u^2/2v_T^2}v_T^2\\
&= \frac{\sqrt{\pi}|Z|}{2|\omega_E|}\mathrm{e}^{-Z^2}\sum_{\boldsymbol{m}}|v_{\boldsymbol{m}}^r|^2_{u=-\omega_E/k_\parallel}(-)\frac{\omega_E}{k_\parallel v_T}, \qquad \text{(C.12)}
\end{aligned}
$$

$$
\begin{aligned}
D_{22} &= \frac{\pi}{2n_0}\sum_{\boldsymbol{m}}\int_{\mathbb{R}^3}\mathrm{d}^3p\,\delta(k_\parallel u+\omega_E)|v_{\boldsymbol{m}}^r|^2\frac{m^2}{4T^2}\left(v_\perp^2+u^2\right)\\
&\quad\times\frac{n_0}{(2\pi mT)^{3/2}}\exp\left(-\frac{v_\perp^2+u^2}{2v_T^2}\right)\\
&= \frac{m^3}{2^{9/2}\sqrt{\pi}(mT)^{3/2}v_T^4}\sum_{\boldsymbol{m}}\int_{\mathbb{R}}\mathrm{d}u\,\frac{\delta(u+\omega_E/k_\parallel)}{k_\parallel}|v_{\boldsymbol{m}}^r|^2\mathrm{e}^{-u^2/2v_T^2}\\
&\quad\times\int_0^\infty 2\pi v_\perp\,\mathrm{d}v_\perp\left(v_\perp^4+2v_\perp^2u^2+u^4\right)\mathrm{e}^{-v_\perp^2/2v_T^2}\\
&= \frac{\sqrt{\pi}}{2^{7/2}k_\parallel v_T^7}\sum_{\boldsymbol{m}}\int_{\mathbb{R}}\mathrm{d}u\,\delta(k_\parallel u+\omega_E)|v_{\boldsymbol{m}}^r|^2\left(8v_T^6+4u^2v_T^4+u^4v_T^2\right)\mathrm{e}^{-u^2/2v_T^2}\\
&= \frac{\sqrt{\pi}|Z|}{2|\omega_E|}\mathrm{e}^{-Z^2}\sum_{\boldsymbol{m}}|v_{\boldsymbol{m}}^r|^2_{u=-\omega_E/k_\parallel}\left(2+\frac{\omega_E^2}{k_\parallel^2v_T^2}+\frac{1}{4}\frac{\omega_E^4}{k_\parallel^4v_T^4}\right), \qquad \text{(C.13)}
\end{aligned}
$$

$$
D_{23} = \frac{\pi}{2n_0}\sum_{\boldsymbol{m}}\int_{\mathbb{R}^3}\mathrm{d}^3p\,\delta(k_\parallel u+\omega_E)|v_{\boldsymbol{m}}^r|^2\frac{m^2}{2T^2}\left(v_\perp^2+u^2\right)uv_T
$$

$$
\begin{aligned}
&\times \frac{n_0}{(2\pi mT)^{3/2}} \exp\left(-\frac{v_\perp^2+u^2}{2v_T^2}\right) \\
&= \frac{m^3}{2^{7/2}\sqrt{\pi}(mT)^{3/2}v_T^3} \sum_{\boldsymbol{m}} \int_{\mathbb{R}} \mathrm{d}u\, \frac{\delta(u+\omega_E/k_\parallel)}{k_\parallel} |v_{\boldsymbol{m}}^r|^2 u \mathrm{e}^{-u^2/2v_T^2} \\
&\times \int_0^\infty 2\pi v_\perp \,\mathrm{d}v_\perp \, \left(v_\perp^2+u^2\right) \mathrm{e}^{-v_\perp^2/2v_T^2} \\
&= \frac{\sqrt{\pi}}{2^{5/2}k_\parallel v_T^6} \sum_{\boldsymbol{m}} \int_{\mathbb{R}} \mathrm{d}u\, \delta(u+\omega_E/k_\parallel) |v_{\boldsymbol{m}}^r|^2 u \mathrm{e}^{-u^2/2v_T^2} v_T^2 \left(2v_T^2+u^2\right) \\
&= \frac{\sqrt{\pi}|Z|}{2|\omega_E|} \mathrm{e}^{-Z^2} \sum_{\boldsymbol{m}} |v_{\boldsymbol{m}}^r|^2_{u=-\omega_E/k_\parallel} (-) \left(\frac{\omega_E}{k_\parallel v_T} + \frac{1}{2}\frac{\omega_E^3}{k_\parallel v_T^3}\right), \qquad \text{(C.14)}
\end{aligned}
$$

$$
\begin{aligned}
D_{33} &= \frac{\pi}{2n_0} \sum_{\boldsymbol{m}} \int_{\mathbb{R}^3} \mathrm{d}^3p\, \delta(k_\parallel u+\omega_E) |v_{\boldsymbol{m}}^r|^2 \frac{m^2}{T^2} u^2 v_T^2 f_0 \\
&= \frac{\pi m^3}{2n_0 v_T^2} \sum_{\boldsymbol{m}} \int_{\mathbb{R}} \mathrm{d}u \frac{\delta(u+\omega_E/k_\parallel)}{k_\parallel} |v_{\boldsymbol{m}}^r|^2 u^2 \exp\left(-u^2/2v_T^2\right) \\
&\quad \times \frac{n_0}{(2\pi mT)^{3/2}} \int_0^\infty 2\pi \,\mathrm{d}v_\perp \exp\left(-v_\perp^2/2v_T^2\right) \\
&= \frac{\sqrt{\pi}}{2^{3/2}k_\parallel v_T^5} \sum_{\boldsymbol{m}} \exp\left(-\frac{\omega_E^2}{2v_T^2k_\parallel^2}\right) |v_{\boldsymbol{m}}^r|^2_{u=-\omega_E/k_\parallel} \frac{\omega_E^2}{k_\parallel^2}\frac{T}{m} \\
&= \frac{\sqrt{\pi}|Z|}{2|\omega_E|} \mathrm{e}^{-Z^2} \sum_{\boldsymbol{m}} |v_{\boldsymbol{m}}^r|^2_{u=-\omega_E/k_\parallel} \frac{\omega_E^2}{k_\parallel^2 v_T^2}, \qquad \text{(C.15)}
\end{aligned}
$$

with $Z = -\omega_E/\sqrt{2}k_\parallel v_T$,

Appendix D

Linear Plasma Response

The parallel RMP plasma response current density in the lowest order FLRE as obtained from $\tilde{j}_{\omega \boldsymbol{m}\parallel} = e\int \mathrm{d}^3p\, u \tilde{f}_{\boldsymbol{m}}$ is discussed in Section 3.5.3. Here, the detailed explicit evaluation is given.

$$
\begin{aligned}
\tilde{j}_{\omega \boldsymbol{m}\parallel} &= e\int \mathrm{d}^3p\, u \tilde{f}_{\boldsymbol{m}} \\
&= 2\pi e m^3 \int_0^\infty \mathrm{d}v_\perp\, v_\perp \int_{\mathbb{R}} \mathrm{d}u\, u(-) \int_{\mathbb{R}} \mathrm{d}u'\, \tilde{G}_{\omega \boldsymbol{m}}(u,u') \\
&\quad \times \left(a_1(v_\perp,u')\mathscr{A}_1 + a_2(v_\perp,u')\mathscr{A}_2 + a_3(v_\perp,u')\mathscr{A}_3\right) f_0(v_\perp,u') v^r_{\boldsymbol{m}}(v_\perp,u') \\
&= -\frac{e n_0}{\sqrt{2\pi}B_0}\left(\frac{m}{T}\right)^{3/2} \int_0^\infty \mathrm{d}v_\perp\, v_\perp \int_{\mathbb{R}} \mathrm{d}u\, u \int_{\mathbb{R}} \mathrm{d}u'\, \tilde{G}_{\omega \boldsymbol{m}}(u,u') \\
&\quad \times \Bigg(\mathscr{A}_1 u' \tilde{B}^r_{\boldsymbol{m}} + \mathscr{A}_1 c\tilde{E}_{\boldsymbol{m}\perp} + \frac{v_\perp^2+u^2}{2v_T^2} u' \tilde{B}^r_{\boldsymbol{m}} \mathscr{A}_2 + \frac{v_\perp^2+u'^2}{2v_T^2} \mathscr{A}_2 c\tilde{E}_{\boldsymbol{m}\perp} \\
&\quad + \frac{u'}{v_T}\mathscr{A}_3 u' \tilde{B}^r_{\boldsymbol{m}} + \frac{u'}{v_T}\mathscr{A}_3 c\tilde{E}_{\boldsymbol{m}\perp} \Bigg) \mathrm{e}^{-v_\perp^2/2v_T^2} \mathrm{e}^{-u'^2/2v_T^2} \\
&= -\frac{e n_0}{\sqrt{2\pi}v_T^3 B_0} \Bigg(\mathscr{A}_1 \tilde{B}^r_{\boldsymbol{m}} v_T^2 \frac{\sqrt{2\pi}v_T^3}{\nu} I^{11} + \mathscr{A}_1 c\tilde{E}_{\boldsymbol{m}\perp} v_T^2 \frac{\sqrt{2\pi}}{\nu} v_T^2 I^{10} \\
&\quad + v_T^2 \tilde{B}^r_{\boldsymbol{m}} \mathscr{A}_2 \frac{\sqrt{2\pi}}{\nu} v_T^3 I^{11} + \frac{1}{2v_T^2} \tilde{B}^r_{\boldsymbol{m}} \mathscr{A}_2 v_T^2 \frac{\sqrt{2\pi}}{\nu} v_T^5 I^{13} \\
&\quad + v_T^2 \mathscr{A}_2 c\tilde{E}_{\boldsymbol{m}\perp} \frac{\sqrt{2\pi}}{\nu} v_T^2 I^{10} + \frac{1}{2v_T^2} \mathscr{A}_2 c\tilde{E}_{\boldsymbol{m}\perp} v_T^2 \frac{\sqrt{2\pi}}{\nu} v_T^4 I^{12} \\
&\quad + \frac{1}{v_T} \mathscr{A}_3 \tilde{B}^r_{\boldsymbol{m}} v_T^2 \frac{\sqrt{2\pi}}{\nu} v_T^4 I^{12} + \frac{1}{v_T} \mathscr{A}_3 c\tilde{E}_{\boldsymbol{m}\perp} v_T^2 \frac{\sqrt{2\pi}}{\nu} v_T^3 I^{11} \Bigg)
\end{aligned}
$$

Reordering terms one finally obtains

$$\boxed{\begin{aligned}\tilde{\dot{j}}_{\omega \boldsymbol{m}\parallel} = -\frac{n_0 e v_T}{\nu B_0}\Bigg\{&\left[(\mathscr{A}_1+\mathscr{A}_2)I^{10}+\frac{1}{2}\mathscr{A}_2 I^{21}+\mathscr{A}_3 I^{11}\right] c\tilde{E}_{\boldsymbol{m}\perp}\\ &+\left[(\mathscr{A}_1+\mathscr{A}_2)I^{11}+\frac{1}{2}\mathscr{A}_2 I^{31}+\mathscr{A}_3 I^{21}\right] v_T \tilde{B}^r_{\boldsymbol{m}}\Bigg\}.\end{aligned}} \tag{D.1}$$

List of Figures

List of Tables

Bibliography

[1] A. I. Akhiezer, I. A. Akhiezer, R. V. Polovin, A. G. Sitenko, and K. N. Stepanov. *Plasma Electrodynamics*, volume 2. Pergamon Press, Oxford, 1975.

[2] G. B. Arfken and H. J. Weber. *Mathematical Methods for Physicists*. Elsevier Academic Press, 6th edition, 2005.

[3] A. Bankhamer. Fusionsbestrebungen. *Profil – Das unabhängige Nachrichtenmagazin Österreichs*, 41, 2012.

[4] M. Becoulet, F. Orain, P. Maget, N. Mellet, X. Garbet, E. Nardon, G. T. A. Huysmans, T. Casper, A. Loarte, P. Cahyna, A. Smolyakov, F. L. Waelbroeck, M. Schaffer, T. Evans, Y. Liang, O. Schmitz, M. Beurskens, V. Rozhansky, and E. Kaveeva. Screening of resonant magnetic perturbations by flows in tokamaks. *Nucl. Fusion*, 52, 2012.

[5] P. M. Bellan. *Fundamentals of Plasma Physics*. Cambridge University Press, 2008.

[6] N. N. Bogolyubov and Y. A. Mitropolski. Asymptotic methods in the theory of nonlinear oscillations. *Gordon and Breach, New York*, 1961.

[7] A. H. Boozer. Guiding centre drift equations. *Phys. Fluids*, 23:904–908, 1980.

[8] A. H. Boozer. Onsager symmetry of transport in toroidal plasmas. *Physics of Fluids B: Plasma Physics*, 4(9):2845, 1992. ISSN 08998221. doi: 10.1063/1.860159.

[9] J. R. Cary and A. J. Brizard. Hamiltonian theory of guiding-centre motion. *Reviews of Modern Physics*, 81:693–738, 2009.

[10] W. D. D'haeseleer, W. N. G. Hitchon, J. D. Callen, and J. L. Shohet. *Flux Coordinates and Magnetic Field Structure*. Springer-Verlag, 1990.

[11] T. H. Dupree. *Kinetic Theory of Plasma and the Electromagnetic Field*, volume 6. 1963.

[12] T. E. Evans, R. A. Moyer, P. R. Thomas, J. G. Watkins, T. H. Osborne, J. A. Boedo, E. J. Doyle, M. E. Fenstermacher, K. H. Finken, R. J. Groebner, M. Groth, J. H. Harris, R. J. La Haye, C. J. Lasnier, S. Masuzaki, N. Ohyabu, D. G. Pretty, T. L. Rhodes, H. Reimerdes, D. L. Rudakov, M. J. Schaffer, G. Wang, and L. Zeng. Suppression of large edge-localized modes in high-confinement diii-d plasmas with a stochastic magnetic boundary. *Phys. Rev. Letters*, 92(23):235003–1–4, 2004.

[13] H. Fischer and H. Kaul. *Mathematik für Physiker – Band 1.* Teubner Studienbücher Mathematik, 5th edition, 2005.

[14] H. Fischer and H. Kaul. *Mathematik für Physiker – Band 2.* Teubner Studienbücher Mathematik, 3rd edition, 2008.

[15] R. Fitzpatrick. Interaction of tearing modes with external structures in cylindrical geometry (plasma). *Nuclear Fusion*, 33(7):1049–1084, July 1993. ISSN 0029-5515.

[16] R. Fitzpatrick. Bifurcated states of a rotating tokamak plasma in the presence of a static error-field. *Physics of Plasmas*, 5(9):3325–3341, 1998.

[17] R. Fitzpatrick and T. C. Hender. The interaction of resonant magnetic perturbations with rotating plasmas. *Physics of Fluids B: Plasma Physics*, 3(3):644, 1991. ISSN 08998221. doi: 10.1063/1.859863.

[18] T. Fließbach. *Mechanik.* Spektrum Akademischer Verlag, 2009.

[19] T. Fließbach. *Statistische Physik.* Spektrum Akademischer Verlag, Heidelberg, 2010.

[20] T. Fließbach. *Elektrodynamik.* Spektrum Akademischer Verlag, 2012.

[21] T. Frankel. *The Geometry of Physics.* Cambridge University Press, 3rd edition, 2012.

[22] J. Freidberg. *Plasma Physics and Fusion Energy.* Cambridge University Press, 2007.

[23] R. J. Hastie. Plasma physics. chapter Plasma particle dynamics, pages 5–28. Cambridge University Press, 1993.

[24] P. Helander. *Collisional transport in magnetized plasmas.* Cambridge University Press, 2002.

[25] M. F. Heyn, I. B. Ivanov, S. V. Kasilov, and W. Kernbichler. Kinetic modelling of the interaction of rotating magnetic fields with a radially inhomogeneous plasma. *Nuclear Fusion*, 46(4):S159, 2006. doi: 10.1088/0029-5515/46/4/S07.

[26] M. F. Heyn, I. B. Ivanov, S. V. Kasilov, W. Kernbichler, I. Joseph, R. A. Moyer, and A. M. Runov. Kinetic estimate of the shielding of resonant magnetic field perturbations by the plasma in diii-d. *Nuclear Fusion*, 48(2): 024005, 2008.

[27] M. F. Heyn, I. B. Ivanov, S. V. Kasilov, W. Kernbichler, and P. Leitner. Quasilinear response to resonant magnetic field perturbations in a tokamak. *39th EPS Conference on Plasma Physics*, 2012.

[28] M. F. Heyn, I. B. Ivanov, S. V. Kasilov, W. Kernbichler, A. Loarte, V. V. Nemov, and A. M. Runov. On the confinement of passing alpha particles in a tokamak-reactor with resonant magnetic field perturbations shielded by plasma currents. *Nucl. Fusion*, 52, 2012.

[29] M. F. Heyn, I. B. Ivanov, S. V. Kasilov, W. Kernbichler, and P. Leitner. Quasilinear modelling of RMP penetration into a tokamak plasma. *Problems of atomic science and technology/Series Plasma Physics*, 2013.

[30] M. F. Heyn, I. B. Ivanov, S. V. Kasilov, W. Kernbichler, P. Leitner, V. V. Nemov, W. Suttrop, and the ASDEX Upgrade Team. Quasilinear modelling of RMP interaction with a tokamak plasma: application to ASDEX upgrade ELM mitigation experiments. *Nuclear Fusion*, 54(6):064005, June 2014. ISSN 0029-5515, 1741-4326.

[31] F. L. Hinton and R. D. Hazeltine. Theory of plasma transport in toroidal confinement systems. *Rev. Mod. Phys.*, 48:239–308, Apr 1976. doi: 10.1103/RevModPhys.48.239.

[32] I. B. Ivanov. 2007. PhD thesis.

[33] I. B. Ivanov, M. F. Heyn, S. V. Kasilov, and W. Kernbichler. Kinetic linear model of the interaction of helical magnetic perturbations with cylindrical plasmas. *Physics of Plasmas*, 18(2):022501, 2011. doi: 10.1063/1.3551740.

[34] A. N. Kaufman. Quasilinear diffusion of an axisymmetric toroidal plasma. *Physics of Fluids*, 15(6):1063–1069, 1972. doi: 10.1063/1.1694031.

[35] P. K. Kaw and I. Bandyopadhyay. *The Case for Fusion*. International Atomic Energy Agency, 2012.

[36] M. Kikuchi, K. Lackner, and M. Q. Tran, editors. *Fusion Physics*. International Atomic Energy Agency, 2012.

[37] Y. L. Klimontovich. *The Statistical Theory of Non-equilibrium Processes in a Plasma*. M.I.T. Press, Cambridge, Mass., 1967.

[38] M. D. Kruskal and R. M. Kulsrud. Equilibrium of a magnetically confined plasma in a toroid. *Physics of Fluids (1958-1988)*, 1(4), 1958.

[39] J. D. Lawson. Some criteria for a power producing thermonuclear reactor. *Proceedings of the Physical Society. Section B*, 70(1):6–10, January 1957. ISSN 0370-1301.

[40] P. Leitner, M. F. Heyn, I. B. Ivanov, S. V. Kasilov, and W. Kernbichler. Effect of momentum conservation on fluid resonances for RMPs in a tokamak. *Physics of Plasmas*, (6):1–11, 2014.

[41] J. L. V. Lewandowski and M. Persson. Field line pitch and local magnetic shear in tokamaks. *Aust. J. Phys.*, 49:1121–33, 1996.

[42] Y. Liang, H. R. Koslowski, P. R. Thomas, E. Nardon, B. Alper, P. Andrew, Y. Andrew, G. Arnoux, Y. Baranov, M. Bécoulet, M. Beurskens, T. Biewer, M. Bigi, K. Crombe, E. De La Luna, P. de Vries, W. Fundamenski, S. Gerasimov, C. Giroud, M. P. Gryaznevich, N. Hawkes, S. Hotchin, D. Howell, S. Jachmich, V. Kiptily, L. Moreira, and V. Parail. Active control of type-i edge-localized modes with $n = 1$ perturbation fields in the jet tokamak. *Phys. Rev. Lett.*, 98(26):265004–265009, Jun 2007.

[43] R. G. Littlejohn. Hamiltonian formulation of guiding center motion. *Phys. Fluids*, 24:1730–1749, 1981.

[44] R. G. Littlejohn. Variational principles of guiding centre motion. *Journal of Plasma Physics*, 29:111–125, 1983.

[45] S. M. Mahajan and C. Y. Chen. Plasma kinetic theory in action-angle variables. *Phys. Fluids*, 28, 1985.

[46] K. Morawetz and D. Kremp. Field dependence of the collision integral and the debye-onsager relaxation effect in plasma systems. *Physical Letters A*, 173:317–325, 1992.

[47] A. I. Morozov and L. S. Solov'ev. Motion of Charged Particles in Electromagnetic Fields. *Reviews of Plasma Physics*, 2:201, 1966.

[48] M. Mulec. *Magnetohydrodynamic and kinetic modelling of resistive wall modes*. 2012. PhD thesis.

[49] M. Mulec, I. B. Ivanov, M. F. Heyn, and W. Kernbichler. Kinetic versus ideal magnetohydrodynamic modelling of the resistive wall mode in a reversed field pinch plasma. *Physics of Plasmas*, 19, 2012.

[50] E. Nardon, P. Tamain, M. Bécoulet, G. Huysmans, and F. L. Waelbroeck. Quasi-linear mhd modelling of h-mode plasma response to resonant magnetic perturbations. *Nuclear Fusion*, 50(3):034002, 2010.

[51] D. R. Nicholson. *Introduction to Plasma Theory*. John Wiley & Sons, 1983.

[52] T. G. Northrop. Adiabatic charged-particle motion. *Reviews of Geophysics and Space Physics*, 1:283–304, 1963. doi: 10.1029/RG001i003p00283.

[53] T. G. Northrop and J. A. Rome. Extensions of guiding centre motion to higher order. *Phys. Fluids*, 21:384–389, 1978.

[54] M. R. O'Brien and D. C. Robinson. Plasma physics. chapter Tokamak experiments, pages 189–208. Cambridge University Press, 1993.

[55] L. Onsager. Reciprocal relations in irreversible processes. *Phys. Rev.*, 37, 1931.

[56] J. Park, A. H. Boozer, and J. E. Menard. Nonambipolar transport by trapped particles in tokamaks. *Phys. Rev. Lett.*, 102:065002, Feb 2009. doi: 10.1103/PhysRevLett.102.065002.

[57] P. H. Rebut, R. J. Bickerton, and B. E. Keen. The joint european torus: installation, first results and prospects. *Nuclear Fusion*, 25(9):1011, 1985.

[58] A. H. Reiman and D. A. Monticello. Three-dimensional tokamak equilibria in the presence of resonant field errors. *Nuclear Fusion*, 32:1341–1350, 1992.

[59] L. Robinson and R. Beaty. Onsager phenomenological coefficients for a weakly ionized cesium plasma. *Physics of fluids*, 6:1578–1580, 1963.

[60] A. Samain and F. Nguyen. Onsager relaxation of toroidal plasmas. *Plasma Physics and Controlled Fusion*, 39:1197–1243, 1997.

[61] F. Scheck. *Theoretische Physik 1 – Mechanik. Von den Newtonschen Gesetzen zum deterministischen Chaos*. Springer Verlag, 2007.

[62] K. C. Shaing, S. A. Sabbagh, and M. S. Chu. An approximate analytic expression for neoclassical toroidal plasma viscosity in tokamaks. *Nuclear Fusion*, 50(2):025022, 2010.

[63] D. V. Sivukhin. *Reviews of Plasma Physics*, 1:1, 1965.

[64] M. Stone and P. Goldbart. *Mathematics for Physics – A Guided Tour for Graduate Students*. Cambridge University Press, 2009.

[65] H. Sugama and W. Horton. Entropy production and onsager symmetry in neoclassical transport processes of toroidal plasmas. 3:304–322, 1996.

[66] H. Sugama and W. Horton. Neoclassical electron and ion transport in toroidally rotating plasmas. *Physics of Plasmas*, 4:2215–2228, 1997.

[67] H. Sugama and S. Nishimura. Moment-equation methods for calculating neoclassical transport coefficients in general toroidal plasmas. *Physics of Plasmas*, 15, 2008.

[68] H. Sugama, M. Okamoto, W. Horton, and M. Wakatani. Transport processes and entropy production in toroidal plasmas with gyrokinetic electromagnetic turbulence. *Physics of Plasmas*, 3:2379–2394, 1996.

[69] N. G. Van Kampen. *Stochastic Processes in Physics and Chemistry*. Elsevier, Amsterdam, 1992.

[70] F. L. Waelbroeck. Shielding of resonant magnetic perturbations in the long mean-free path regime. *Physics of Plasmas*, 10(10):4040, 2003. ISSN 1070664X. doi: 10.1063/1.1607324.

[71] J. Wesson. *Tokamaks*. Clarendon Press - Oxford, 1997.